Towards Clinical Use of Engineered Tissues for Cartilage Repair

Andrea R. Tan

Submitted in partial fulfillment of the

requirements for the degree

of Doctor of Philosophy

in the Graduate School of Arts and Sciences

COLUMBIA UNIVERSITY

2014

ABSTRACT

Towards Clinical Use of Engineered Tissues for Cartilage Repair

Andrea R. Tan

Osteoarthritis (OA), the most prevalent form of joint disease, afflicts nine percent of the US population over the age of thirty and costs the economy nearly $100 billion annually in healthcare and socioeconomic costs. It is characterized by joint pain and dysfunction, though the pathophysiology remains largely unknown. The progressive loss of cartilage followed by inadequate repair and remodeling of subchondral bone are common hallmarks of this degenerative disease. Due to its avascular nature and limited cellularity, articular cartilage exhibits a poor intrinsic healing response following injury. As such, significant research efforts are aimed at producing engineered cartilage as a cell-based approach for articular cartilage repair. However, the knee joint is mechanically demanding, and during injury, also a milieu of harsh inflammatory agents. The unforgiving mechanochemical environment requires constructs that are capable of bearing such burdens.

To this end, previous work in our laboratory has explored the application of stimuli inspired by the native joint environment in attempts to create tissue with functional properties similar to native cartilage so that it may restore loading to the joint. While we have had success at producing these replacement tissues, there is little evidence in the literature that the biological functionality (i.e. response to *in vivo*-like conditions) of engineered cartilage matches native cartilage. Therefore, in an effort to provide a more complete characterization of the functional nature of developing tissues and facilitate their use clinically, the overarching motivation of the work described in this dissertation is two-fold: 1) characterize the response of engineered cartilage to chemical and mechanical injury; and 2) develop strategies for enhancing the performance and protection of engineered cartilage for

in vivo success.

Studies in the literature have extensively characterized the effects of wounding to native articular cartilage as well as the effects of an inflammatory environment. For mechanical injuries, cell death is immediate and progressive, ultimately leading to failure of the tissue. Chemical insult has been shown to promote degradation of the matrix components, also leading to failure of the tissue. Under a controlled application of injury (mechanical and chemical), it was found that engineered cartilage, in contrast to native cartilage, has the potential to repair itself following an injury event, as long as there is no catastrophic damage to the matrix. Additionally, when this matrix is intact and well-developed, engineered cartilage constructs exhibit a resistance to degradation, highlighting the potential utility of engineered cartilage as replacement tissues.

Enhancing functionality in engineered cartilage was also explored, with the aim of developing strategies to improve, repair, and protect engineered cartilage constructs for their use *in vivo*. For these purposes, the studies in this dissertation spanned both 2D migration studies to influence the limited wound repair potential of cells as well as 3D culture studies to explore the possibility of protection effects at a tissue level. Together, these models allowed us to capture the complexity needed to fully develop approaches for cartilage repair. Though it has previously been found that applied DC electric fields modulate cell migration, we have developed a novel strategy of employing this technique to screen for desirable populations of cells (those with the greatest capacity for directed migration) to use in cartilage repair. We also found that the AQP1 water channel plays a key role in mechanosensing the extracellular environment, highlighting the potential for its use in therapeutic strategies.

For tissue engineering efforts at creating functional cartilage replacement, we uncovered novel strategies to foster better tissue development via co-culture systems and promote the resistance of engineered cartilage to catabolic factors. These findings motivate their potential use in therapeutics and in tissue engineering efforts at creating clinically-relevant tissue-engineered constructs for the treatment of OA or following injury.

The research described in this dissertation has characterized the biological functionality of engi-

neered tissues and identified strategies for enhancing their use *in vivo* by modulating the subsequent response to injury, laying the foundation for their use in clinical applications.

Table of Contents

List of Figures

List of Tables

Acknowledgments

No one who achieves success does so without the help of others.
The wise and confident acknowledge this help with gratitude.
—Alfred North Whitehead

First, I would like to acknowledge and thank the funding sources that made this work possible. Funding from the National Institutes of Health and a National Science Foundation graduate research fellowship have allowed me to explore unlimited questions and extend my professional network by attending international conferences.

I am deeply grateful for the guidance and support of my committee members: Drs. Clark Hung, Gerard Ateshian, Chloe Bulinski, Helen Lu, and Jimi Cook. I have been shaped by their influences, by their leadership, by their relentless drive to answer the fundamental questions of science that define our field. Time and again, I have been humbled by their knowledge, their passion, and their generosity. I have had the extraordinary honor of learning from Gerard, and his insights have consistently challenged my thinking. I owe much thanks to Chloe; her feedback, support, encouragement, and most notably, her willingness to explain biology to a non-biology person has been invaluable. Many thanks to Helen and Jimi, whose constant support and insights have guided me throughout this journey. Above all, I am deeply appreciative of Clark for his unparalleled support and direction. His trust, encouragement, and excitement have pushed me to explore new ideas without the fear of failure. He has also been monumental in supporting my extra-laboratory efforts; for this, I could not have been luckier.

From the start, I have been privileged to be guided by those much wiser than I; Eric Lima, Kenneth Ng, Elizabeth Oswald, and Liming Bian welcomed me into the lab and shared their

wisdom, their skills, their hints at surviving this process, and their camaraderie. In particular, I owe innumerable thanks to Eric G. Lima who took me under his wing and guided my first formative years. With time, and with the addition of many more lab members, our CEL family has grown, though the core values uniting us have not changed. We are bound by the same endless pursuits of research, by the same appetite for answering that one elusive question ("Can we be the people who cure OA?"), by the friendships that extend far past our windowless lab. For this, I owe Michael Albro, Sonal Sampat, Amy Silverstein, Terri-Ann Kelly, Grace O'Connell, Elena Alegre-Aguaron, Najmuddin Gunja, Jason Fong, Alex Cigan, Bob Nims, Sevan Oungoulian, Krista Durney, Brian Jones, Adam Nover, Brendan Roach, Eben Estell, and Rob Stefani. They have helped with work, challenged ideas, and offered insights, ultimately helping to shape the course of my dissertation. I have also been fortunate in having worked with tremendous undergraduate students and orthopedic residents who have taught me as much about being a mentor as I have taught them about cartilage tissue engineering.

My deepest heartfelt appreciation goes to my family and friends who have traversed this journey with me. They have held me up, pushed me along, and cheered me on at times when I otherwise was too lost to see the path. I owe everything I am to my parents, whose love and support have been unrelenting. They instilled in me a stubbornness to strive for things far beyond what I thought was possible and reminded me gently when I fell that there was still a path to something greater. Finally, I owe my deepest gratitude to Tyler Poore, without whom this entire process would have been much harder. At every step of the way, through the late nights and long weekends in the lab, the conference deadlines and the paper submissions, he has inspired me to be better and challenged my thinking. With the patience and understanding that work so often comes before something else, Tyler has made this journey a bit easier, and for that, I could not be more appreciative.

To my parents,
without whom none of my success would be possible

Chapter 1

Introduction

Articular cartilage exhibits a poor healing response following injury due to its avascular nature and limited cellularity. The ensuing biochemical changes that accompany injurious events ultimately lead to disruption and failure of tissue function. Significant research efforts are aimed at producing engineered cartilage as a cell-based approach for articular cartilage repair. In an effort to provide a more complete characterization of the functional nature of developing tissues and facilitate their use clinically, the overarching motivation of the work described in this dissertation is two-fold: 1) characterize the response of engineered cartilage to chemical and mechanical injury; and 2) develop strategies for enhancing the performance and protection of engineered cartilage for *in vivo* success.

To guide this effort, the hypotheses and specific aims are first presented, accompanied by the significance of this work. An overview of the literature on articular cartilage and the consequences of injury, with an emphasis on potential cartilage tissue engineering repair strategies, is also provided.

1.1 Hypotheses and Specific Aims

The presented research contained in this dissertation is motivated by two interconnected themes aimed at facilitating successful replacement of engineered cartilage (Figure 1.1). By first understanding the response of engineered cartilage to various modes of injury, strategies for developing constructs, within the context of functional tissue engineering (FTE), may be facilitated. To this

end, the following hypotheses and specific aims were developed:

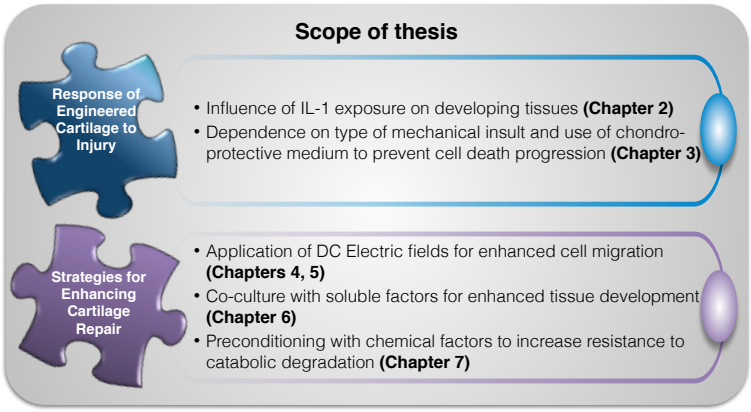

Figure 1.1: Schematic of studies described in this dissertation

Hypothesis 1: Maturity of engineered cartilage dictates response to *in vitro* mechanical insult in a manner similar to native cartilage.

> Specific Aim 1a: To impose different modes of mechanical insult mimicking iatrogenic injury (drilling, cutting, cracking) on engineered cartilage constructs of various maturity levels and monitor the long-term response through bulk mechanical and biochemical properties.
>
> Specific Aim 1b: To determine whether chondrogenic medium offers protection against imposed mechanical insult by monitoring the spread of cell death in long-term culture.

While the response of native cartilage explants - mechanical breakdown and chemical degradation - to mechanical insult has been well characterized with *in vitro* wounding studies, little is known as to the reaction of tissue engineered cartilage to the same stimuli. These studies aim to complement these explant injury studies by providing an initial characterization of the *in vitro* injury response of engineered cartilage. The use of a tissue engineering model as the surrogate tissue permits injury to be studied on engineered tissues spanning a range of mechanical and biochemical properties that reflect tissue culture maturation. The rationale of this work is that elucidation of potential failure mechanisms of engineered tissues that may occur after implantation in the defect site may be important for optimization of implantation guidelines and tissue construct design criteria.

Hypothesis 2: Applied DC electric field (EF) stimulation drives directed migration of repair cells in a manner dependent on 1) extracellular environment and 2) cell presentation. The results can be ascribed to particular populations such that galvanotaxis can be used in identifying desirable populations of cells.

Specific Aim 2a: To identify the role of AQP1 in EF-induced cell migration.

Specific Aim 2b: To elucidate the mechanotransduction of osmotic loading on cells during EF-induced migration.

Specific Aim 2c: To characterize the effect of EF on migration response for interleukin-1 (IL-1) treated-chondrocytes and synovium derived stem cells (SDSCs).

Specific Aim 2d: To characterize the passage-dependent effect of EF on migration response of potential repair cells (chondrocytes, SDSCs, bone marrow-derived stem cells (bMSCs)) from different sources (bovine, canine, human).

As field gradients exist in both wound healing and developing embryos (Robinson, 1985), understanding the effect on repair cells of changing extracellular environment in the context of EF-induced migration is crucial. The rationale of this work is two fold: First, we aimed to investigate the effects of extracellular environment on migrating cells under an applied field. As aquaporin-1 (AQP1) water channels are important mechanosensors that work to regulate cell volume, it is vital to understand their role during migration. The influence of AQP1 may be especially pronounced when cells undergo osmotic shock. Within the context of an inflammatory environment, cell migration has been reported to be limited as the addition of IL-1 to chondrocyte culture has been shown to result in a decrease in cytoskeletal components (tensin, talin, paxillin, and FAK) that is concomitant with the loss of chondrocyte phenotype as assessed by a decrease in type II collagen expression levels (Vinall et al., 2002). The alteration in expression of signaling molecules that associate with integrin-containing adhesions can adversely affect cellular motility and function (Vicente-Manzanares and Horwitz, 2011). Furthermore, it has been shown that IL-1 alters the normal volumetric response of chondrocytes to osmotic stress due to alterations to and remodeling of the F-actin cytoskeleton (Pritchard et al., 2008).

Secondly, further characterization of how factors of age, species, and cell presentation affect migration potential may allow for the possibility of using this established protocol of EF stimulation to identify potentially desirable cell populations.

Hypothesis 3: Preconditioning of engineered cartilage constructs with chemical factors affords development of functional tissue.

Specific Aim 3a: To co-culture fledgling tissue engineered cartilage constructs with metabolically active fresh chondrocytes. Measure bulk mechanical properties and biochemical content of constructs over long-term culture. Culture tissue engineered construct and 2D monolayer in contact with one another and apart to identify the mode of signaling between the two populations.

Specific Aim 3bi: To preexpose cartilage constructs to a low dose of interleukin to increase resistance against the catabolic agent. Following preexposure period, expose constructs to a dose of interleukin known to elicit tissue degradation and glycosaminoglycan breakdown. Measure bulk mechanical properties and biochemical content of constructs before preexposure, during preexposure, after preexposure, and after insult.

Specific Aim 3bii: To identify whether the activation of the hypoxia inducible factor-1α (HIF-1α) pathway is responsible for the preconditioning effects noted with low doses of IL-1. Measure bulk mechanical properties and biochemical content of cartilage constructs.

During OA and following surgical procedures, the environment of the knee is rich in proinflammatory cytokines such as IL-1 (Goldring and Goldring, 2004). Introduction of tissue engineered cartilage constructs to a chemically harsh milieu may limit the functionality of the implanted tissue over long periods. Cellular preconditioning schemes by physical (mechanical) and chemical manipulation have been used extensively in studies involving stem cells as a method to prime cells to a state in which they can withstand a harsh microenvironment (Haider and Ashraf, 2010). In particular, brief exposure to a catabolic agent afforded longer term protection against subsequent attacks and this was found to be the most effective means of cytoprotection (Murry et al., 1986). The rationale to this work, therefore, is that the application of one or more modes of preconditioning can prepare the developing tissue to withstand potential catabolic factors present in the inflammatory joint environment by providing an enhanced pericellular and extracellular matrix or by increasing or activating the cells' intrinsic survival signaling.

1.2 Significance

OA represents a substantial economic burden for patients, health care systems, and businesses (Elders, 2000; Gabriel et al., 1995; Leigh et al., 2001; Reginster, 2002). Caused by degeneration of the synovial joint, OA includes a progressive loss of articular cartilage accompanied by inadequate attempts to repair the damaged tissue, remodeling of the underlying subchondral bone, and the formation of subchondral bony lesions (Buckwalter and Martin, 2006). Primary OA develops in the absence of a known cause of joint degeneration, while secondary OA develops following joint degeneration caused by injury (Buckwalter and Mankin, 1998a).

Extensive damage to the entire joint often requires a total knee replacement to replace the articulating surface and underlying bone. These repairs, however, often require revision surgeries due to wear, subsidence, and loosening of the implant in the bony union (Ayers, 1997; Bradley et al., 1993; Mowery et al., 1987; Whiteside, 1989). For the repair of small defects such as focal lesions, more conservative approaches including autograft cell/tissue transfer via periosteal grafts (O'Driscoll et al., 2001), autologous osteochondral grafting such as mosaicplasty (Hangody et al., 1997), and the Carticel method (Brittberg et al., 1996). These options provide temporary relief from symptoms of pain and disability; however, they also introduce long-term problems. Primarily, the availability of healthy cartilage from which to harvest cells is limited for cell-based therapies or osteochondral graft harvesting. Furthermore, autologous osteochondral grafts are usually harvested from non load-bearing regions that may provide tissue of sub-optimal material properties for use in contact regions (Ahmad et al., 2001). The harvest procedure itself can induce significant cell death in the surrounding region (Lee et al., 2000a,b), leading to further structural and biochemical breakdown of the donor site tissue. As such, there have been recent attempts at developing cell-based therapies for cartilage repair, including tissue engineered constructs of cultured cells on three-dimensional scaffolds (Lima et al., 2004; Mauck et al., 2000; Pazzano et al., 2000; Vunjak-Novakovic et al., 1999).

To develop strategies to mitigate tissue injury and promote repair, culture injury models have been used to study the response of cartilage to trauma by taking advantage of the more controllable

loading environment afforded by *in vitro* systems (Loening et al., 2000; Patwari et al., 2001). While many studies have demonstrated the response of native cartilage to wounding, there exist no studies in the literature describing the effect on engineered cartilage. Towards creating functional tissue capable of withstanding the harsh mechanochemical regime present in the joint, the work contained in this dissertation attempts to narrow the gaps in the literature by focusing on modalities of injury and their subsequent responses in engineered constructs. The studies presented in Part I of this dissertation provide new insight into the response of engineered cartilage to chemical injury (**Chapter 2**) and mechanical injury (**Chapter 3**) and represent a model system from which to study further modalities of injury propagation and repair (basic science impact) as well as a guideline for *in vitro* culture (tissue engineering impact) to prepare constructs for the mechanical and chemical stresses in the native knee joint.

In Part II, the studies described in this dissertation focus on developing strategies for enhancing the performance of engineered cartilage for *in vivo* repair. First, from a basic science perspective, we reexamine the limited migration of repair cells to injured cartilage and build upon the previous literature on using electric field stimulation for directing cell migration by investigating the influence of extracellular environment under EF strengths similar to those that are known to exist during injury. By investigating the role of the AQP1 water channel, a key mechanosensor, our results offer insights into a potential mechanism by which cells sense their environment and regulate key aspects of migration, including cell volume and cytoskeletal organization (**Chapter 4**). This is then extended to specific environments in which osmotic shock and cytokines are applied. Studying cell migration in these contexts provides a new understanding for how cells may act in cartilage disease and prompts further investigation into additional cell sources that may have more potential for cartilage repair (**Chapter 5**).

Finally, for tissue engineering efforts at creating functional cartilage replacement, novel strategies are examined to both foster better tissue development via co-culture systems (**Chapter 6**) as well as enhance resistance to catabolic factors (**Chapter 7**). These results recommend the use of preconditioning with mechanical and/or chemical factors to mediate the catabolic consequence

of IL-1 exposure to produce clinically-relevant tissue-engineered constructs for treatment of OA or following injury.

1.3 Background

1.3.1 Articular Cartilage: Biology and Structure

Articular cartilage, a white, dense connective tissue that lines diarthrodial joints, serves as the load-bearing material of joints, and is characterized by excellent friction, lubrication, and wear properties (Mow and Lai, 1990). Ranging from 1 to 7 mm thick, cartilage is composed primarily of two phases, a solid matrix (collagen fibrils and proteoglycan (PG) macromolecules) (Clarke, 1971; Eyre, 1980; Muir et al., 1970) and a mobile interstitial fluid phase (mostly water) (Lipshitz et al., 1976). The polyanionic nature of the glycosaminoglycan (GAG) chains of PG draw water into the tissue, resulting in a large osmotic pressure that expands against the constraining collagen network. The interplay between swelling pressure and tension in the collagen fibers results in a highly specialized tissue that is well suited to bear compressive loads within the joint. To maintain the necessary matrix composition, chondrocytes, which make up less than 10% of the tissue volume (Stockwell, 1979), balance extracellular degradation and matrix turnover by synthesizing and secreting extracellular matrix (ECM).

The complexity of articular cartilage is evident by the changing composition, structure, and material properties this is known to vary across the tissue's depth (Guilak et al., 1995) and can be divided into three discrete zones: the superficial (SZ), middle (MZ), and deep (DZ) zones (Buckwalter and Mankin, 1998b; Donzelli et al., 1999). The SZ is a thin region at the articulating surface marked by collagen fibers that are aligned parallel to the surface and it possesses the highest concentrations of water and collagen compared to the other zones, but has the lowest level of proteoglycan. Additionally, chondrocytes in this zone are flattened in morphology. In contrast, the MZ is rich in collagen whose orientation is random, but contains the highest concentration of proteoglycans with randomly dispersed cellular bodies. In the DZ, the chondrocytes are oriented

perpendicular to the surface and arranged in a columnar structure with the lowest levels of collagen.

1.3.2 Articular Cartilage: Injury and Wound Repair

OA, the most prevalent form of joint disease, is characterized by joint pain and dysfunction (Buckwalter and Martin, 2006), though the pathophysiology remains largely unknown. The progressive loss of cartilage followed by inadequate repair and remodeling of subchondral bone are common hallmarks of this degenerative disease (Buckwalter et al., 2000).

As the only cellular component of cartilage, chondrocytes maintain tissue homeostasis, respond to injury and perform the limited remodeling process that comprises OA. Excessive mechanical insult to articular cartilage can also reduce cell viability (Chen et al., 2001; Lewis et al., 2003; Loening et al., 2000; Repo and Finlay, 1977), thereby leading to further tissue breakdown. Studies in the literature have suggested two different types of chondrocyte death, apoptosis or necrosis. Apoptosis is a form of programmed cell death and is regulated by cellular signaling systems that lead to the disintegration of individual cells into the formation of apoptotic bodies (Farber, 1994; Hockenbery, 1995). Necrosis, a form of accidental cell death, occurs as a consequence of a pathologic event. While cell death has been primarily attributed to necrosis (Stockwell, 1979), apoptosis has been identified through labeling techniques as the more likely form to elicit widespread chondrocyte death (Loening et al., 2000; Tew et al., 2000).

The biochemical factors and mechanical stress to cartilage contribute to the progression of OA by disrupting chondrocyte-matrix associations and altering the metabolic responses in the chondrocyte. This disruption in balance between anabolic and catabolic regulatory activities results in a phenotypic shift, cell death, and an increase in expression of inflammation-related genes (Goldring et al., 2011) that leads to a loss of cartilage matrix components and deterioration in the structural and functional properties of cartilage (Lee et al., 2005; Stevens et al., 2009). Catabolic cytokines may also be generated by the fibroblast- and macrophage-like cells in the synovium, the thin layer that lines the non-articulating surfaces of diarthrodial joints and maintains a synovial fluid-filled cavity (Fan et al., 2009), in response to the breakdown products from damaged cartilage. Conse-

quently, elevated levels of inflammatory cytokines such as IL-1 and tumor necrosis factor-α (TNF-α) have been measured in the synovial fluid during cartilage pathology (Pelletier et al., 1991; Sellam and Berenbaum, 2010).

Similar changes to the cell's biochemical, biophysical, and mechanical environment are elicited following mechanical injury that occurs with traumatic loading of the joint as well as during surgical procedures (Levin et al., 2005; Milentijevic et al., 2003; Tew et al., 2001). Such types of injury are known risk factors for the development of secondary OA (Buckwalter and Mankin, 1998a), as mechanical stimuli and injury regulate chondrocyte function and induce inflammatory mediators (Fermor et al., 2001; Honda et al., 2000), matrix metalloproteinases (MMP) (Millward-Sadler et al., 2000), and the release of PGs from cartilage explants (Quinn et al., 2001).

Cartilage exhibits an inability to fully repair itself following injury due to its hypocellular and avascular nature (Tew et al., 2001); articular cartilage lesions that do not penetrate the subchondral bone fail to heal due to the lack of nutrients and macrophages, endothelial cells, and mesenchymal cells that reside in bone marrow. Additionally, the lack of removal of cellular or matrix debris following trauma may confer a greater cellular response to injury (Hunziker, 1999).

Efforts to characterize the response of native behavior of cartilage in a wound environment have prompted the development of *in vitro* models of induced mechanical insult. Histologic observations of experimental wounding to articular cartilage have shown a reparative response that is marked by a region of cell death surrounding the injured area (Chen et al., 2001; Lewis et al., 2003; Tew et al., 2001, 2000). This area of cell death is apparent as soon as a few hours after and up to 7 days post injury (Chen et al., 2001), after which empty lacunae and a loss of ECM are noted (Bennett and Bauer, 1932). Adjacent to this zone of cell death is a zone of cellular proliferation (Carlson, 1957; Tew et al., 2001); ^{3}H-thymidine incorporation into the intraarticular matrix of cells suggests increased synthetic activity and altered metabolism. Disruption of the ECM, due to injury or as a downstream effect of catabolic cellular activity, may modulate the behavior of chondrocytes in situ (Fukai et al., 1998; Qi and Scully, 1998).

The extent of damage to articular cartilage following injury may then be dependent on the initial

damage to both the chondrocytes themselves and the ECM. In further support of this, experimental wounding of articular cartilage results in varying degrees of damage depending on the extent of damage to the bulk ECM due to the type of injury (compression overload, trephine insertion, scalpel cut), and the intensity and rate of loading to the bulk tissue. In addition, the maturity of the cartilage may dictate the tissue's response following injury, as the more elaborate pericellular matrix (PCM) surrounding chondrocytes from mature cartilage may offer greater protection from load-induced injury(Levin et al., 2005; Tew et al., 2001). The mechanotransduction from traumatic loading to cartilage, nonetheless, is implicated in the pathophysiology of joint degeneration and the onset of OA.

1.3.3 Cell Migration

Cell migration occurs during both physiological processes such as embryonic morphogenesis as well as pathological processes including tissue repair and inflammatory response. The process of cell migration is conceptualized as a cyclic process. Initially, cells detect a chemotactic gradient and polarize and extend protrusions in the direction of migration (Vicente-Manzanares and Horwitz, 2011). These protrusions, which can be large, broad, sheet-like lamellipodia or long, thin filopodia, are formed by actin reorganization and provide a foundation for the cell to move forward (Vicente-Manzanares and Horwitz, 2011). Extended protrusions then adhere to the extracellular matrix through integrins, generating traction forces at the site of adhesion due to the interaction of myosin II with actin. Following transient disassembly of integrin adhesions, protrusions are able to extend; reassembled adhesions then impart traction to allow the cell to pull forward on the substrate. During the formation and retraction of cell membrane protrusions, cells undergo rapid cell shape changes that are accompanied by changes in cell volume that may be due to changes in the physical properties of the cell membrane and the activity of channels and transporters (Guilak et al., 2002; Mobasheri et al., 2002). These changes in cell volume may work to propel the cell during migration; in fact, unequal rates of water entry to the front and back parts of the cell has generated forces sufficient to propel forward motion of a cell in the absence of actin (Jaeger et al., 1999). As such,

regulators of water transport across cellular membranes such as AQP1 water channels have been implicated in the mechanotransduction and regulation of cell volume (Liang et al., 2008; Mobasheri et al., 2002).

1.3.3.1 Bioelectrical Stimulation for Wound Repair

The delayed, ultimately poor healing ability of articular cartilage is thought to be due, in large part, to insufficient migration to the damage site of cells that have the potential to repair the lesion (Hehenberger et al., 1998). Thus, strategies that enhance and direct cell migration could amplify the intrinsic repair process. One approach that our lab has focused on has been the application of an applied DC electric field (Chao et al., 2000). Electric field strengths as high as 1-2 V/cm are generated at the cut surface of wounds due to the ion flux through leaky cell membranes and exist locally for days (Soong et al., 1990). Furthermore, electric fields have been suggested to play a role in regulating cellular proliferation and differentiation, as well as synthesis of growth factors and matrix proteins (Aaron et al., 2004; Hartig et al., 2000). Externally applied electric fields are already being used in orthopaedic practices to treat fracture nonunions and spinal fusions (Paterson et al., 1977), though the mechanism of the bioelectrical stimulus on the targeted cells is not well understood. *In vitro* applications of EFs have been demonstrated to elicit galvanotaxis (migration) and galvanotropism (shape change) for a number of cell types including chondrocytes, fibroblasts, meniscal cells, and keratinocytes (Chao et al., 2000, 2007; Frenkel et al., 1996; Gunja et al., 2011; Nishimura et al., 1996). In these studies, the strength of the field necessary to induce migration (1-10 V/cm) was on the order of that which has been shown to exist in developing embryos and during wound healing (Robinson, 1985). Given their potential to induce cell migration and regulate cellular biosynthetic activity, DC electric fields represent a potential tool to aid in the reparative response of wounded cartilage.

1.3.4 Functional Tissue Engineering of Articular Cartilage

Functional tissue engineering (FTE) for the regeneration of cartilage tissue damaged by disease or trauma relies on the approach of using scaffolds, cells, and exogenous factors to develop tissue constructs capable of meeting the functional (mechanical) load-bearing demands *in vivo* (Butler et al., 2000). To this end, our lab has approached this paradigm with a long-term hypothesis that by first cultivating constructs *in vitro* to match the material properties of native cartilage, prior to implantation, long-term success is improved.

Studies characterizing the contact stresses within the knee joint have found mean stress magnitudes at the articular surface range from 2MPa during daily activities, 6MPa under moderately strenuous activities, and 12MPa under vigorous, but non-traumatic conditions (Ahmed and Burke, 1983; Brown and Shaw, 1984; Fukubayashi and Kurosawa, 1980; Huberti and Hayes, 1984; Kurosawa et al., 1980; Manouel et al., 1992). Underdeveloped constructs lacking the integrity to withstand such loads, therefore, would be unsuccessful.

To this end, our lab and many others have manipulated aspects central to the themes of tissue engineering to produce engineered cartilage with functional properties. The choice of scaffold, cell type, and mechanical or chemical stimulation are major variables that influence the outcome. An overview of some of the emerging trends in cartilage tissue engineering are described below, with a particular focus on how they may be useful in human clinical translation. However, the majority of the work described in this dissertation utilizes a well-established model whereby primary or passaged juvenile bovine chondrocytes are encapsulated in an agarose hydrogel. This choice provides a relatively simple and robust system with which to study relevant phenomena.

1.3.4.1 Scaffold Choice

Hydrogels have become the scaffold material of choice for cartilage tissue engineering due to their intrinsic hydrophilic nature and high water content, similar to native soft hydrated tissues (Smetana, 1993). Hydrogels being explored include polyethylene(glycol) (Rice et al., 2008), hyaluronic acid (Burdick et al., 2005), silk (Chao et al., 2010), alginate and collagen (van Susante et al., 1995).

Agarose, a neutrally charged polysaccharide from seaweed, has been used extensively in cartilage biology for maintaining long-term chondrocyte suspension cultures due to its ability to promote and maintain the chondrocyte phenotype (Benya and Shaffer, 1982; Buschmann et al., 1995, 1992; Lee and Bader, 1995; Mauck et al., 2002, 2000), as well as being non-degradable and non-interactive with chondrocytes.

These advantages have prompted the use of agarose for cartilage tissue engineering applications, where agarose-embedded chondrocytes have been shown to successfully repair articular cartilage and tibial defects in in vivo models (Cook et al., 2003; Rahfoth et al., 1998). The properties of agarose permit application of physiologic deformational loading immediately upon encapsulation such that constructs may be physically stimulated before extensive ECM development is present. Together, these characteristics of the agarose hydrogel system have allowed for the fabrication of the most reproducible and robust cartilage tissue growth in culture (Lima et al., 2007). Furthermore, this system serves as an important tool to study tissue engineering strategies. Clinically, agarose is being used as a co-polymer with alginate as a hydrogel scaffold for ACI (Cartipatch) for cartilage defect repair and has demonstrated good 2-year clinical follow up (Selmi et al., 2007, 2008).

1.3.4.2 Cell Source

Many studies have utilized isolated juvenile bovine chondrocytes encapsulated in hydrogel systems to recreate and even surpass the properties of native bovine tissue by the temporal application of chemical (Byers et al., 2006) or physical factors (Martin et al., 2000), or a combination of the two (Lima et al., 2007). These studies capitalize on the significantly greater biosynthetic capacity of juvenile cells relative to their adult counterparts (Tran-Khanh et al., 2005), also reported for human chondrocytes (Adkisson et al., 2010). However, a juvenile cell source is limited for clinical applications due to the challenges related to tissue procurement. As such, differentiated adult chondrocytes may be obtained from a patient's own healthy, non-load bearing cartilage, although this may lead to donor site morbidity and further tissue degeneration (Gilbert, 1998). Chondrocytes from the diseased knee may be also harvested during preliminary debridement procedures.

In both cases, though, obtaining sufficient cell number to produce constructs with sufficient mechanical properties is challenging due to the reduced biosynthetic activity of cells from patients with advanced stages of the disease (Bulstra et al., 1989; Wang et al., 2003). Alternatively, due to the immunoprivileged nature of diarthrodial joints, the implantation of allogeneic cells from other patients may be expanded for use (Glenn et al., 2006), following from the clinical use of living osteochondral allografts (Garrett, 1998).

Finally, undifferentiated cartilage precursor cells, including those isolated from patient bone marrow aspirate (Tew et al., 2008), from adipose tissue (Xu et al., 2007; Zuk et al., 2002, 2001), or from the synovium (Arufe et al., 2010; Kim et al., 2011; Li and Pei, 2010) have been explored as alternative sources of cells, however, to date, constructs made with these human cells have not been capable of attaining mechanical properties at native tissue levels. Co-culture of human embryonic stem cells (hESCs) with chondrocytes and fibrochondrocytes can modulate chondrogenic expression and matrix synthesis (Hoben et al., 2009; Hwang et al., 2008). However, stem cells may have different cell density or cell-cell contact requirements than chondrocytes (Huang et al., 2009) in order to form cartilaginous tissue. Micromass, self assembled constructs (scaffold-free), and suspension in hydrogel show potential for human ESC chondrogenesis (Hoben et al., 2009; Hwang et al., 2008).

Regardless the source, the number of cells required to recreate engineered cartilage with functional properties surpasses the number that is readily available clinically. To address the limited supply of cells, one way to increase the cell number is by expanding cells through passaging under appropriate growth factors. Similar to the cocktail of growth factors used for the culture of chondrocytes encapsulated in an agarose hydrogel, these same growth factors encourage and maintain the chondrocyte phenotype. For adult chondrocytes that are less biosynthetically active, expansion in a cocktail of appropriate growth factors has been shown to rapidly expand cell number, prime the cells to reactivate rapid matrix synthesis when cultured in a 3D scaffold environment, and prevent phenotype dedifferentiation which is typically seen in monolayer culture (Benya and Shaffer, 1982; Francioli et al., 2007; Ng et al., 2010). For undifferentiated stem cells, the application of a

growth factor cocktail offers the ability to direct the differentiation of these plastic cells down the chondrocyte lineage (Guilak et al., 2004; Hwang et al., 2006; Williams et al., 2003).

1.3.4.3 Exogenous factors

Joint loading gives rise to a plethora of physical stimuli, including osmotic loading, hydrostatic pressure, electrokinetic phenomena, stress and strain (Guilak and Hung, 2005). For FTE, physiologically relevant stimuli are applied to encourage the development *in vitro* for tissues that can meet the in vivo functional demands, as well as mimic the composition of native tissue (Hung et al., 2004). The choice of scaffold material and its inherent material characteristics, therefore, dictate the nature of loading that can be applied on developing cartilage tissue constructs. Rotating wall bioreactors have been used to provide a hydrodynamic, low-shear environment supportive of enhanced nutrient transport (Gooch et al., 2001; Kaysen et al., 1999) and cartilage-like tissue growth (Freed et al., 1997; Obradovic et al., 1999; Vunjak-Novakovic et al., 1999). However, these bioreactors do not reproduce the physiologic deformational loading and hydrostatic pressure environment of the chondrocyte (Ateshian and Hung, 2003). In comparison, applying physiologic loading through a combination of applied physiologic hydrostatic pressure and perfusion (Carver and Heath, 1999) or through physiologic dynamic deformation loading (Mauck et al., 2002, 2000, 2003c) can achieve near-physiologic values for equilibrium modulus and GAG content. Such deformational loading gives rise to enhanced convection of nutrients (Albro et al., 2008; Mauck et al., 2003a), in a mechanism similar to how joint loading provides nutrients from the synovial fluid to avascular cartilage *in situ*. There is a growing body of literature suggesting that physical forces can be used to modulate chondrogenesis of mesenchymal stem cells (Elders, 2000; Huang et al., 2004; Kisiday et al., 2009; Miyanishi et al., 2006), as reviewed by Huang and co-workers (Huang et al., 2010).

In addition to mechanical loading to promote tissue growth, many groups have focused on the application of a range of chemical cues such as growth factors (transforming growth factor (TGF)-β3, TGF-β1, insulin-like growth factor (IGF), fibroblast growth factor (FGF_2) (Byers et al., 2006;

Mauck et al., 2003b, 2001; Thorp et al., 1992)), corticosteroids (Awad et al., 2003; Bian et al., 2010b), and interleukins (Aydelotte et al., 1992; Lima et al., 2008b; Ratcliffe et al., 1986). Through paracrine signaling and direct cell-cell contact, the exchange of these chemical factors has been found to promote ECM development. Physical loading may act to increase convective transport of growth factors, leading to possible synergistic interactions (Mauck et al., 2003b).

Part I

Characterizing the Injury Response in Native and Engineered Cartilage

Chapter 2

Response of Native and Tissue Engineered Cartilage to Chemical Injury

2.1 Introduction

Repair strategies for load bearing tissues such as articular cartilage have relied on tenets of functional tissue engineering (Butler et al., 2000), centering on the idea that engineered tissues will have greater success following implantation if they possess properties similar to those found in the native joint. The application of exogeneous factors such as mechanical loading (Mauck et al., 2000; Sampat et al., 2013) and chemical cues (Sampat et al., 2011) have shaped the development of tissue in an effort to create functional tissue with properties comparable to native articular cartilage (Lima et al., 2007).

Mechanical, biochemical, and histological properties have been the primary modalities to assess the integrity of these constructs when considering their potential for *in vivo* repair. We have strived, however, to understand how closely the biological response of our engineered cartilage mimics that of the native tissue, in particular, the response to cytokine exposure. To this end,

in an effort to measure how successfully our engineered cartilage mimics native cartilage, I was a significant contributor on a cohort of earlier studies by our laboratory that compared the cytokine response of engineered to native cartilage. The insights from these studies, as reviewed herein, lay the foundation for study aims of this dissertation, focusing on examination of the response of engineered cartilage to imposed injury to gain insights towards developing strategies for enhancing cartilage repair.

Engineered cartilage is initially a fragile tissue, characterized mainly by the agarose scaffold material that houses the cells. With time in culture, extracellular matrix is deposited, leading to an increased stiffness and composition. The dense matrix also may act as a chondroprotective enclosure for the encapsulated cells (Li et al., 2003), ensuring survival in the harsh mechanical loading environment of the knee joint. However, within the joint, the chemical environment is likely to contain potent catabolic mediators that stem from chronic joint inflammation (Goldring, 1999; Goldring and Goldring, 2004; Lotz, 2001; van den Berg, 2001) or the surgical intervention (Schmal et al., 2009; Smeets et al., 2003). As such, engineered cartilage must possess the fortitude to withstand these catabolic factors. Here, we review our lab's efforts in first characterizing the response of native articular cartilage to *in vitro* cytokine exposure to understand the potential effects of catabolic degradation on tissue properties. Next, we looked at whether tissue-engineered constructs exposed to a similar insult responded in a comparable manner. Finally, after noticing that engineered cartilage behaved differently than native cartilage and indeed was susceptible to IL-1-induced tissue breakdown, we explored the use of genipin as a way to permanently cross-link components of the existing extracellular matrix in an effort to protect the constructs.

A summary of the key findings of each study is described below, with full-length papers included in Appendix A.

2.1.1 Differences in interleukin-1 response between engineered and native cartilage

Articular cartilage explants exhibit a resistance *in vitro* to IL-1 induced degradation in our culture system. This may be due to the presence of a chondro-protective chemical mediator (dexamethasone) in the culture medium. The same mode of protection was noted for engineered cartilage only when properties of the tissue neared native values. However, for fledgling constructs that have not attained maturity (characterized by sufficient mechanical integrity and biochemical composition similar to native cartilage), the addition of IL-1 induced a catabolic effect that was persistent even after the removal of the cytokine. Accordingly, mature engineered cartilage constructs possess a greater potential for withstanding the harsh mechanochemical environment of the joint and should be preferentially chosen for implantation.

2.1.2 Physiologic deformational loading does not counteract the catabolic effects of interleukin-1 in long-term culture of chondrocyte seeded agarose constructs

Studies looking at short-term (Table 2.1) application of physiologic loading have found protective effects against IL-1 induced catabolic degradation, attributable to a decrease in synthesis of nitric oxide and PGE_2 as a consequence of deformational loading (Chowdhury et al., 2001, 2003; Gassner et al., 1999; Long et al., 2001). We prioritized functional properties of engineered tissues, characterized by cellular matrix output, during long-term culture, rather than temporal expression of soluble factors that many of the previous shorter studies have employed. To this end, loading over a long-term period with the addition of cytokine resulted in a decrease in material and biochemical properties, even when the concentration of IL-1 was lowered 10-fold. It is important to note, however, that the total number of cycles for our loading protocol far exceed those utilized in short-term studies and may account for the noticeable differences observed.

Table 2.1: Previous studies examining the effect of concurrent dynamic loading with cytokine exposure

Author	Loading Regime	Inflammatory Response
Chowdhury (2001,2003)	Dynamic compression: 1Hz, 15% amplitude dynamic strain, 48hr	Inhibition of NO, PGE_2
Gassner (1999), Xu (2000), Long (2001)	Cyclic tension: 0.05Hz, 6% equibiaxial strain, 24hr	Suppression of IL-1β-induced NO production
Lima (2008)	Dynamic compression: 1 Hz, 5% amplitude dynamic strain, 3hr/day for 28 days	IL-induced degradation not mitigated; decrease in material and biochemical properties

2.1.3 Genipin enhances the mechanical properties of tissue engineered cartilage and protects against inflammatory degradation when used as a medium supplement

Genipin is a naturally-derived cross-linking agent that reacts with free amine groups, such as those found on tropocollagen or proteoglycan molecules. We hypothesized that the cross-linking of extracellular matrix components would increase their resistance to catabolic degradation brought about by IL-1 exposure. Indeed, genipin-treated constructs maintained significantly higher material and biochemical properties following insult with IL-1 compared to their non genipin-treated constructs. Interestingly, while the stiffness was moderately lower in the presence of cytokine, the biochemical composition of the tissue was maintained, suggesting it is likely that the crosslinks formed between the extracellular matrix components trap degraded products.

2.2 Conclusion

Together, these studies indicate that engineered tissues, while capable of reaching native properties akin to article cartilage, are vulnerable to IL-1 exposure depending on the manner in which the cytokine is applied. However, when able to attain material and biochemical properties similar to native cartilage, these engineered tissues are better able to withstand the chemical assault, hence pointing to the importance of growing functional tissue before implantation. Furthermore, we have shown one exciting potential for mediating the effect of cytokine exposure by pretreating

constructs (such as with genipin crosslinking). The study aims of this dissertation are predicated on these insights; understanding the response of engineered cartilage to mechanical injury is examined (Chapter 3) and further modalities for enhancing cartilage repair are explored (Chapters 4-7).

Chapter 3

Response of Native and Engineered Cartilage to Mechanical Injury

3.1 Introduction

Articular cartilage exhibits a poor intrinsic healing response subsequent to injury (Tew et al., 2000) that engenders a need for cell-based therapies for repair. As the growing promise of engineered cartilage grafts is realized in clinical practice, it will be important to understand the engineered construct's response to the joint loading environment after implantation, including potential injurious loading. Mechanical injury to cartilage can occur with traumatic loading of the joint (traumatic injury) as well as in surgical procedures that include graft harvesting (iatrogenic injury, see section 3.2). In native cartilage, the mechanotransduction resulting from injury has been shown to induce chondrocyte death as early as a few hours after, and up to 7 days, post injury (Chen et al., 2001). Histologic observations of experimental wounding to articular cartilage have shown a reparative response that is marked by a region of cell death surrounding the injured area (Chen et al., 2001; Lewis et al., 2003; Tew et al., 2001, 2000). Adjacent to this zone of cell death is a zone of cellular proliferation (Carlson, 1957; Tew et al., 2001); ^{3}H-thymidine incorporation into the intraarticular matrix of cells suggests increased synthetic activity and altered metabolism. Disruption of the

ECM, due to injury or as a downstream effect of catabolic cellular activity, may modulate the behavior of chondrocytes *in situ* (Fukai et al., 1998; Qi and Scully, 1998). The extent of damage to articular cartilage following injury may then be dependent on the initial damage to both the chondrocytes themselves and the ECM.

To develop strategies that mitigate tissue injury and promote repair, culture injury models have been used to study the response of cartilage to trauma by taking advantage of the more controllable loading environment afforded by *in vitro* systems (Loening et al., 2000; Patwari et al., 2001). Experimental wounding of articular cartilage results in varying degrees of damage depending on the extent of damage to the bulk ECM due to the type of injury (compression overload, trephine insertion, scalpel cut (Amin et al., 2008b; Costouros and Kim, 2007; Tew et al., 2001)), and the intensity and rate of loading to the bulk tissue. In addition, the maturity of the cartilage may dictate the tissue's response following injury, as the more elaborate pericellular matrix (PCM) surrounding chondrocytes from mature cartilage may offer greater protection from load-induced injury (Levin et al., 2005; Tew et al., 2000). The mechanotransduction from traumatic loading to cartilage, nonetheless, is implicated in the pathophysiology of joint degeneration and the onset of OA. In this chapter, we explore the response of native and engineered cartilage to imposed mechanical injury. In the first part of this chapter, we add to the existing literature on iatrogenic injury by examining two different modes of osteochondral graft harvesting (Section 3.2). By comparing the ensuing degree of cell death, we offer some recommendations on best practices for tissue repair. Next, we examine the response of engineered cartilage to mechanical insult (Section 3.3) to offer comparisons to native cartilage. Finally, in the last part of the chapter, we discuss the impact of the use of a chondrogenic medium for prevention of cell death (Section 3.4).

3.2 Controlling Iatrogenic Injury during Graft Harvesting

3.2.1 Introduction

Removal of diseased or damaged osteochondral tissue is necessary before implantation of a replacement tissue can be performed. While the work described in this thesis focuses on an engineered cartilage tissue replacement, replacement tissue can also include autologous cartilage plugs taken from healthy non-load bearing regions of the knee. In both cases, the diseased tissue is first removed using specific instrumentation. Two methods of harvesting osteochondral grafts are common to most systems, either a hand-held power trephine (CORE, Innovasive) or a manual punch (e.g. OATS, Arthrex). Though these two modalities are commonly used, they have also been shown to cause donor site morbidity, leading to knee pain, locking, and a requirement for additional arthroscopic surgery (Huntley et al., 2005). Previous findings in the literature suggest that cutting forces are minimized when there is simultaneous pushing and rotation (Atkins et al., 2004), such as with drilling. However, when the two techniques were compared, serated hand-held power trephines were found to significantly decrease chondrocyte viability (Evans et al., 2004). We hypothesized that the damaging effect may be due to increased strains exerted on the cartilage surface at the moment of impact arising from the lack of stabilization of the tool. To this end, we explored modified versions of these two forms of iatrogenic injury under our controlled culture condition whereby the punch or drill was fixed to a solid support with only one degree of freedom and tested whether cell death continued progressing over long-term culture (weeks) compared to previous studies which looked at immediate changes (hours to days).

3.2.2 Materials and Methods

3.2.2.1 Explant Harvesting

∅6.35mm explants (full thickness cartilage with attached subchondral bone) were cored out of the carpal face of juvenile bovine wrist joints (n=2). Joints showing any contraindications were discarded. Explants were stored in chondrogenic media (serum-free DMEM supplemented with

ITS+, dexamethasone, and ascorbic acid).

3.2.2.2 Osteochondral Graft Coring

∅1mm cylindrical plugs were aseptically cored out of the center of each explant using a custom-programmed milling machine (Figure 3.1) equipped with a disposable biopsy punch. For each explant removal, cartilage plugs were extracted at varying rotational speeds (0, 60, 100, 1000, 2000 rpm) and insertion rates (30, 60, 120, 240 mm/min) with a fresh punch and then returned to culture.

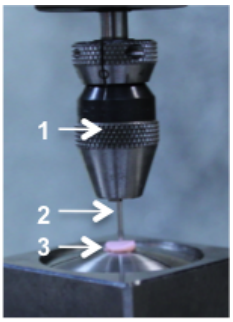

Figure 3.1: Custom drilling setup with (1) rotating collar, (2) disposable punch, and (3) ∅6.35mm collet, permitting user prescribed punch rotational speeds and insertion rates into the cartilage explant.

3.2.2.3 Cell Death Assessment

At 1, 10, and 28 days after injury, cell viability of explants was assessed with the Live/Dead viability assay (Molecular Probes, Eugene, OR) and images were acquired on a confocal microscope (Leica, Bannockburn, IL). Explants were then returned to culture to allow for assessment of the same sample at later timepoints. Overlaid images of live and dead cells were analyzed using ImageJ (NIH) to measure the area of cell death emanating away from the site of injury.

3.2.2.4 Statistics

Statistics were performed using two-way ANOVA with Tukey's HSD post-hoc tests (Statistica, Tulsa, OK), with α=0.05 and statistical significance set at $p \leq 0.05$ to compare groups across day

and treatment. All data are reported as the mean ± 95% confidence interval of 4-5 samples per time point and group.

3.2.3 Results

Cell death was mitigated depending on the harvesting extraction technique. Immediately following extraction, an area of cell death was noticeable directly adjacent to the site of the punch, regardless of harvesting technique. When punches were extracted by a straight push with zero rotation, faster insertion rates (120mm/min and 240mm/min) exhibited significantly less cell death in the surrounding region at 1 day after extraction, but with time, this trend disappeared, with all samples showing similar amounts of cell death by 28 days post extraction (Figure 3.2a). When a constant insertion rate was applied (120mm/min), the area of cell death surrounding the extracted punch varied depending on harvest conditions. Samples that were punched with the slowest rotational speeds exhibited regions of cell death that continued to grow over time; with increased rotational speeds (1000rpm, 2000rpm), cell death was contained to the original area and was significantly less than in constructs punched with zero rotation (Figure 3.2b, $p<0.05$).

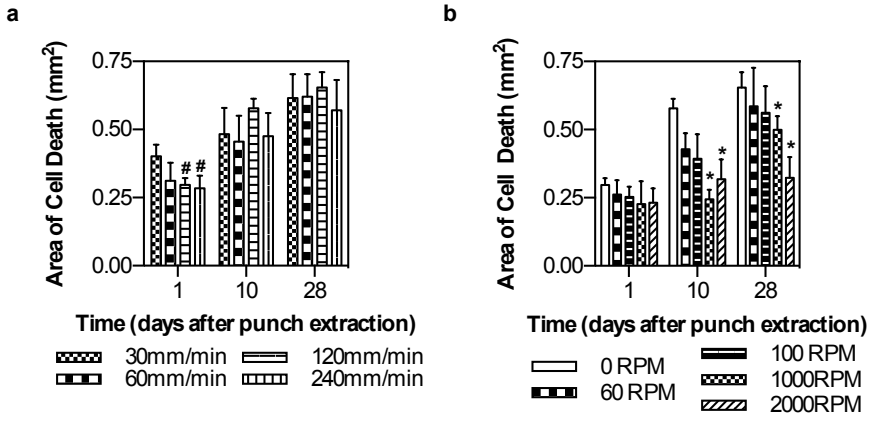

Figure 3.2: Area of cell death (mm^2) surrounding the site of graft extraction as a function of (a) insertion rate and (b) rotational speed. $^{\#}p<0.05$ vs. 30mm/min, $^{*}p<0.05$ vs. 0 RPM, n=20-25/group.

3.2.4 Discussion

Maintaining cell viability is critical to continuing proper mechanical function of the joint following osteochondral graft harvesting and reducing donor site morbidity. While grafts are typically taken from non-load bearing surfaces, it is understood that mechanical injury causing necrosis and leading to subsequent apoptosis of surrounding tissue may trigger a degenerative cascade characterized by increased collagen degradation and reduced proteoglycan synthesis, two hallmarks of the osteoarthritic pathology. Here, we demonstrate that by controlling the insertion rate and rotational speed of the punch associated with the harvesting technique, cell death in the surrounding area may be significantly reduced in half.

That varying the insertion rate of a sharp punch into the tissue had no significant effect on cell viability suggests that there may be a strain threshold, below which propagation of death does not occur. Similarly, rotating punches may minimize local strains felt by the tissue at the moment of punch insertion, thereby maintaining cell viability in the surrounding area. Interestingly, the results observed here contradict those previously reported in the literature that automated drilling is significantly more harmful than a straight punch. There may be a few reasons for the disparity. First, in traditional drills, a serrated tooth design is used on the drill bit, which may in fact tear up the surrounding tissue as it progresses through the depth of the cartilage. In our setup, a sharp, fresh biopsy punch was utilized to core out the plug. From preliminary studies, we detected that the initial point of contact of a sharp-edged punch to the articular cartilage surface is marked by minimal localized tensile strain compared to a large diffuse compressive strain produced by dull-edged punches (Figure 3.3).

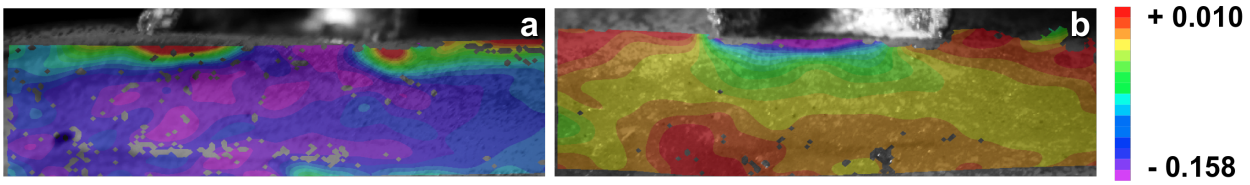

Figure 3.3: Strain (E_{YY}) maps generated from digital image correlation of the cartilage explant undergoing graft extraction with a (a) dull punch and (b) sharp punch.

These larger strains may then predispose the tissue to greater mechanical failure and subsequent cell death. Secondly, due to the constraints of a fixed system with only one degree of freedom, it is likely that the manner in which the extraction was performed was more controlled. This may have led to less peripheral damage to the tissue that might otherwise have contributed to the injury response. Finally, we must consider the specific culture conditions under which these experiments were performed. It is possible that components in the chondrogenic medium afford protection against progressive cell death. Further work exploring this possibility is described in Section 3.3.

Nonetheless, the results described here identify, for the first time, the possibility of selecting key parameters that affect cell viability, thereby making it possible to successfully reduce donor site morbidity through optimized harvesting procedures.

3.3 Engineered Tissue Construct Maturity Dictates Response to Injury

3.3.1 Introduction

Previous studies performed by our lab (Section 3.2) and others have identified native articular cartilage damage when exposed to mechanical insult. The effect on engineered cartilage, however, has not been identified. As such, the current investigation aims to complement these explant injury studies by providing an initial characterization of the *in vitro* injury response of engineered cartilage. The use of a tissue engineering model as the surrogate tissue permits injury to be studied on constructs spanning a range of mechanical and biochemical properties that reflect tissue culture maturation. Elucidation of potential failure mechanisms of engineered tissues that may occur after implantation in the defect site may be important for optimization of implantation guidelines and tissue construct design criteria.

3.3.2 Materials and Methods

3.3.2.1 Experimental Design

To understand the influence of tissue maturity at the time of applied injury on cellular response and extracellular matrix remodeling, we have developed a trauma model to induce chondrocyte death in engineered cartilage constructs of increasing culture age, in response to controlled mechanical overloading (compression-induced cracking), or sharp cutting. The cutting injury served as a method of controlling the location and extent of injury, relative to the greater uncertainty in the extent and location of cracking.

The timeline of the studies is detailed in Figure 3.4. There are two variables in the experiments: (1) the day on which trauma is imparted to the developing construct, and (2) the type of injury imposed ('crack' or 'cut'). Specifically, subsets of constructs were exposed to trauma, after which they were returned to culture conditions to study their subsequent response.

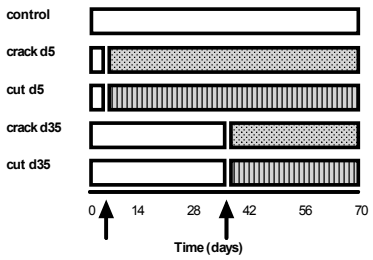

Figure 3.4: Timeline of experimental setup for different groups exposed to trauma. Arrows indicate time in culture when injury was imposed.

3.3.2.2 Tissue Isolation and Cell Culture

Articular cartilage was harvested from bovine CMC joints of freshly slaughtered 2-4-week-old calves. Four to six joints were used for each experiment and cells were pooled from all joints. Cartilage was digested in high-glucose DMEM with collagenase type V (Sigma, St. Louis, MO) for 11 hours at 37°C with shaking. Cell suspensions were filtered through a 70μm porous mesh and sedimented in a bench-top centrifuge for 15 min at 1500g. Viable cells were counted with a hemacytometer and

trypan blue. Cell suspensions (60×10^6 cells/mL) were mixed in equal parts with 4% low-gelling agarose (type VII, Sigma) at 37°C to yield a final cell concentration of 30×10^6 cells/mL in 2% agarose. The chondrocyte/agarose mixture was cast into slabs and cored using a sterile disposable punch (Miltex) to final dimensions of 4mm diameter and 2.34 mm thick. Constructs were cultured in hgDMEM supplemented with 1X PSF, 0.1μM dexamethasone, 50μg/mL ascorbate 2-phosphate, 40μg/mL L-proline, 100μg/mL sodium pyruvate, and 1X ITS+ premix (insulin, human transferrin, and selenous acid, Becton Dickinson, Franklin Lakes, NJ). Medium was further supplemented with 10ng/mL TGF-β3 (Invitrogen, Carlsbad, CA) for the first 14 days of culture. Culture media was changed every other day.

3.3.2.3 Injury

On days 5 and 35 of culture, constructs were subjected to one of two injury modes: compression-induced cracking or cutting (Figure 3.5).

Briefly, to produce cracking, constructs were loaded using a computer-controlled custom device and ramped to failure at a constant strain rate of 0.3% sec^{-1}. Mechanical failure was identified by a drop in applied load on a force-displacement plot and confirmed by gross visual inspection of each construct to ensure that constructs had sustained a fissure throughout the sample. For the cutting injury, two orthogonal cuts were made in constructs by pushing a razor blade to 50% of the construct's original thickness. Razor blades were pushed straight down to prevent the application of additional shear forces, and were replaced after every five constructs to prevent dulling of the blade. Afterwards, samples (including controls manipulated similarly to injured constructs, without actual trauma) were returned to culture in freshly supplemented media and allowed to recover in culture to day 70 for mechanical testing, or to day 85 for viability staining.

3.3.2.4 Cell Viability Assessment

Assessment of cell viability was performed using the Live/Dead cytotoxicity assay (Molecular Probes, Eugene, OR) at immediate- (1 day), short- (3, 7 days), and long- (14, 28, 50 days) time

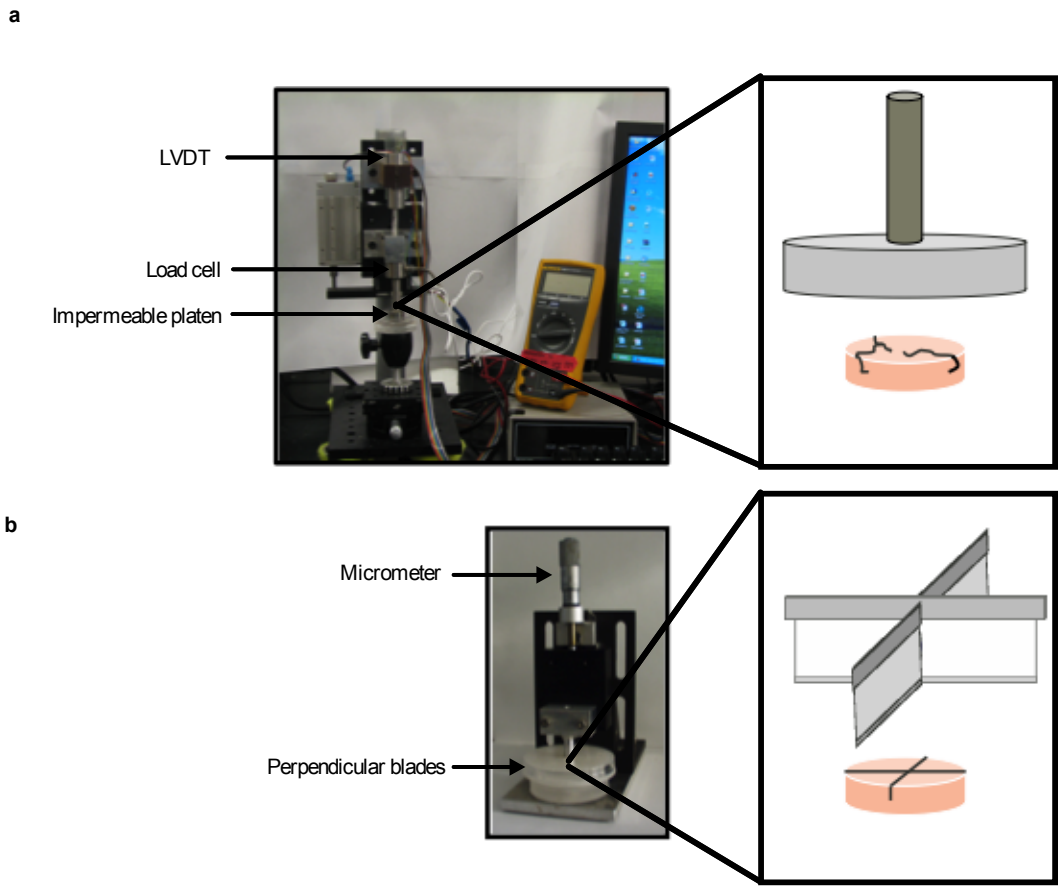

Figure 3.5: Experimental setup of the (a) cracking and (b) cutting setups with a blown up schematic of the injurious device. Compression was applied with an impermeable platen until cracking was achieved. For the cutting setup, blades were cut into the construct to a depth of 50%

points post trauma. After each viability assay, constructs were aseptically returned to culture media to allow for assessment of cell death in the same sample at later timepoints. Live and dead images were taken separately on an inverted confocal fluorescent microscope (Olympus Imaging America, Inc., Center Valley, PA) and overlaid to produce a composite image of the region (Adobe Systems Inc., San Jose, CA).

To quantify cell viability over time for an injured sample, live and dead images were processed separately for automated counting of fluorescing particles (ImageJ, NIH). The fraction of live cells present in an image was determined by calculating the area fraction of particles in a centered region

of an 8-bit, thresholded image. Live cells were characterized as those particles with sizes ranging from 0-2500 pixel^2 (approx. cell size for the given image magnification). These sizes were previously determined using other sample images by calculating average cell body sizes for multiple images. Data was collected from the ImageJ program, and the fraction of live cells reported by normalizing to respective controls.

3.3.2.5 Mechanical Testing

Samples were tested in unconfined compression to assess equilibrium modulus (E_Y) and dynamic modulus (G*) using a custom computer-controlled system (Soltz and Ateshian, 1998). An initial 0.02N tare load was applied, followed by compression to 10% strain, at a strain rate of 0.05% sec^{-1}. After stress-relaxation was achieved, a 2% peak-to-peak strain was superimposed at 0.1Hz. E_Y was measured from the stress-relaxation equilibrium response, and G* from the slope of the stress-strain response under dynamic loading.

3.3.2.6 Biochemical Content

Full constructs were used for biochemical analysis to ensure that any biochemical changes from the effect of the injury (crack or cut) would be captured. Construct swelling was quantified by measuring the gross water content of the constructs (Lima et al., 2007). Samples were dried and digested in proteinase-K buffer overnight at 56°C, as described previously (Kelly et al., 2006). An aliquot was analyzed for GAG content via the 1,9-dimethylmethylene blue dye-binding assay (Farndale et al., 1982). A further aliquot was hydrolyzed in 12N HCl at 110°C for 16 hours, dried, and resuspended in assay buffer (Kelly et al., 2006). OHP content was determined using a colorimetric assay via a reaction with chloramine T and dimethylaminobenzaldehyde , scaled for microplates. Overall collagen content was calculated by assuming a 1:7.64 OHP-to-collagen mass ratio (Stegeman and Stalder, 1967). dsDNA content was also assessed by the Picogreen assay according to the manufacturer's standard protocols. Each biochemical constituent was normalized to either tissue wet or dry weight.

3.3.2.7 Statistics

Statistics were performed using two-way ANOVA with Tukey's HSD *post hoc* tests (Statistica, Tulsa, OK), with α=0.05 and statistical significance set at $p \leq 0.05$ to compare groups across day and treatment. All data are reported as the mean ± 95% confidence interval of 4-5 samples per time point and group.

3.3.3 Results

3.3.3.1 Gross Cracking Response as a Function of Tissue Culture Maturity

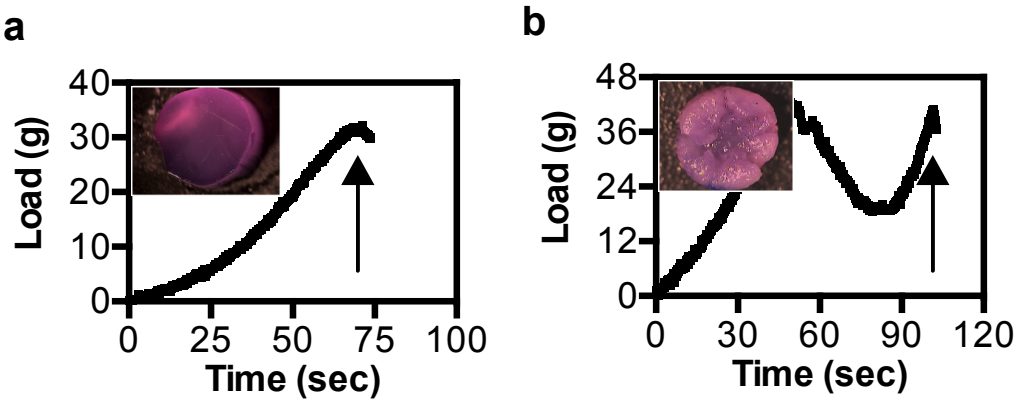

Figure 3.6: Timeline of experimental setup for different groups exposed to trauma. Arrows indicate time in culture when injury was imposed.

Using a computer-controlled system to impart strain, force-displacement profiles were generated to study the gross failure response of the constructs subjected to cracking, under controlled deformation. At early culture time points, when constructs were immature, load increased steadily to 36.1 ± 0.85% strain before cracking the construct (Figure 3.6a). In comparison, compression-induced cracking of more mature constructs produced catastrophic damage, where compaction of the extracellular matrix produced bulk tissue compression (Figure 3.6b, inset) before crack initiation at 50.3 ± 0.13% strain (Figure 3.6b).

3.3.3.2 Cell Viability and Proliferation Post Injury

Cellular viability and subsequent response after insult, as assessed by the Live/Dead cytotoxicity assay, was found to vary with mode of trauma as well as culture maturity at time of injury. For cut constructs, exposed to trauma on days 5 and 35, the area fraction of live cells within the same region of each construct increased significantly at 50 days post injury (d5 injury: 31.1 ± 2.81%, d35 injury: 59.1 ± 4.40%, Table 3.1, $p<0.001$, n=5/group) by the end of culture.

Table 3.1: Normalized area fraction of live cells in a centralized portion of cut constructs compared to control samples at different time points after early (d5) and late (d35) injury. d5 injury: 31.1±2.81%, d35 injury: 59.1±4.40%, $P<0.001$, n=5/group

	d5 injury	**d35 injury**
1 day post cut	1.02	0.44
3 days post cut	1.05	0.54
50 days post cut	1.34	0.70

At early times in culture, immediately following induced trauma on day 5, both cracked and cut constructs exhibited little cellular damage, with the only loss of cells contained to the immediate vicinity of the site of injury (Figure 3.7a,d). Over time, as early as 14 days post injury, cellular infiltration from neighboring regions into the injured space was observed, depending on the type of injury: Cellular infiltration and elongation along the site of injury was observed for constructs exposed to compression-induced cracking (Figure 3.7b). By 28 days after injury, injured sites for cracked constructs were fully infiltrated with neighboring cells (Figure 3.7c). For cut constructs, however, neighboring cells did not infiltrate the void space, leaving a clearly demarcated region of cell loss throughout the culture period (Figure 3.7e,f).

Following a longer time in culture, the response of the engineered cartilage to injury was immediately noticeable. Constructs catastrophically damaged on day 35 by compression-induced cracking exhibited a large loss of cell viability in the immediate and peripheral regions to the site of injury; these regions were not subsequently filled with neighboring cells over the remaining time in culture (Figure 3.8a-c). For constructs cut at this later time point, a larger void space demarcated the

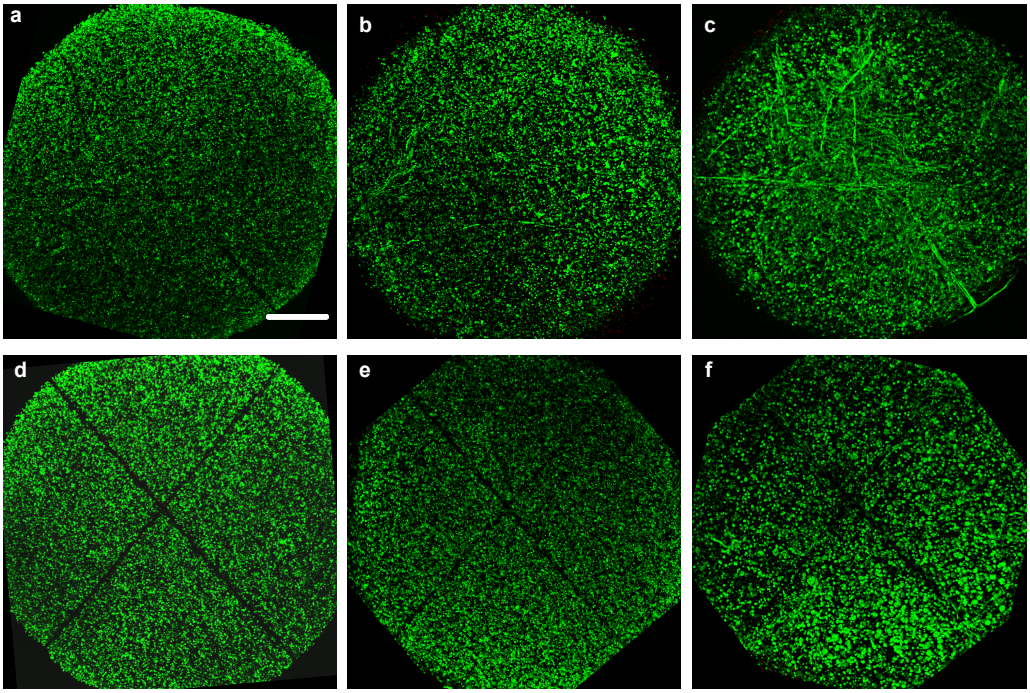

Figure 3.7: Representative superimposed live and dead images of immature cracked (top) and cut (bottom) constructs at 1 day (a, d), 14 days (b, e), and 28 days (c, f) after injury. Scalebar: 0.5 mm. With time in culture, neighboring cells infiltrate into the cracked region of constructs. For constructs injured with a scalpel cut, cells did not infiltrate the cut region, leaving a void space (represented by black space), which was still present at 28 days after injury. Dead cells are visible upon further magnification of the region only immediately (1 day) after injury.

region of injury and these constructs responded similarly to constructs cut earlier in culture (Figure 3.8d-f)

3.3.3.3 Recovery of Mechanical Response

Mechanical properties of constructs injured on day 5 of culture recovered to uninjured control values by day 14, despite the overload-cracking or cutting injury imposed on the nascent tissue (p_{E_Y}>0.999, p_{G^*}>0.999, Figure 3.9). After recovery, at the end of the culture period, constructs achieved properties similar to the Young's modulus of native bovine juvenile tissue (E_Y: 587 ± 43.9 kPa, G*: 2.4 ± 0.1 MPa, control; E_Y: 513 ± 43.8 kPa, G*: 2.2 ± 0.2 MPa, crack, p_{E_Y}=0.794, p_{G^*}=0.998; E_Y: 552 ± 74.9 kPa, G*: 2.3 ± 0.2 MPa, cut, p_{E_Y}>0.999, p_{G^*}>0.999).

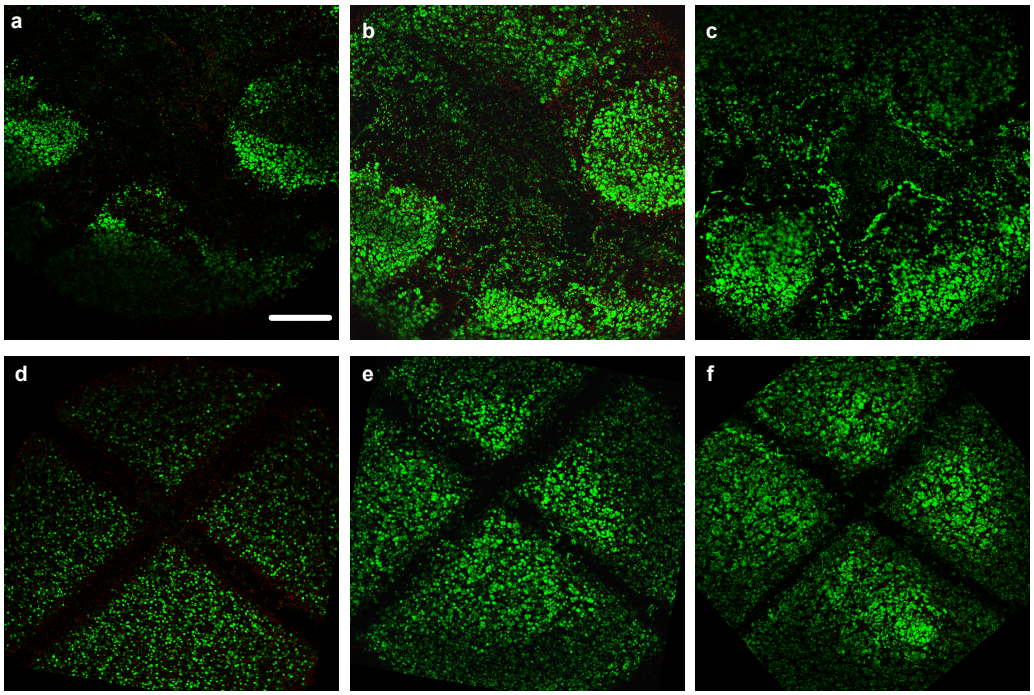

Figure 3.8: Representative superimposed live and dead images of mature cracked (top) and cut (bottom) constructs at 1 day (a, d), 28 days (b, e), and 50 days (c, f) after injury. Scalebar: 0.5 mm. Loss of cell viability (represented by black/void space) is present in the immediate and peripheral regions to the site of injury (crack or cut), which is not recovered with time in culture. Dead cells (nuclei of dead cells are stained red) are visible upon further magnification of the region at 1 day (for cut samples) and up to 28 days (for cracked samples) after injury.

When injured on day 35, however, the response of constructs depended on the mode of injury, with overloaded constructs exhibiting an immediate drop in the compressive moduli at day 42 and thereafter continually weakening, never recovering mechanical integrity even by the end of culture (E_Y: 73.9 ± 20.9 kPa, G*: 0.4 ± 0.1 MPa, $p_{E_Y}<0.001$, $p_{G*}<0.001$, Figure 3.9). Cut constructs, however, were not significantly different from uninjured samples by the end of the culture period (E_Y: 502 ± 70.1 kPa, G*: 2.2 ± 0.2 MPa, $p_{E_Y}=0.521$, $p_{G*}>0.999$, Figure 3.9).

3.3.3.4 Biochemical Composition After Injury

Water content and biochemical composition were measured at each time point following injury. Water content for injured constructs remained similar to uninjured control samples except for those

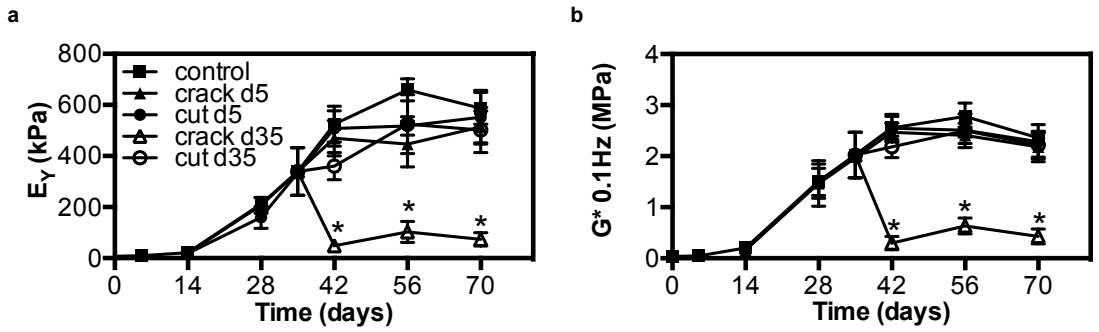

Figure 3.9: (a) Young's modulus (E_Y) and (b) Dynamic modulus (G*) of constructs with time in culture. *p<0.05 vs. control, n=5/group. Crack d35 vs. control, E_Y: p_{day42}<0.001, p_{day56}<0.001, P_{day70}<0.001. Crack d35 vs. control, G*: p_{day42}<0.001, p_{day56}<0.001, p_{day70}<0.001.

exposed to compression-induced cracking on day 35 (p_{day42}=0.020, p_{day56}<0.001, p_{day70}<0.001, Figure 3.10). For all time points, biochemical composition was normalized to construct wet weight. In cases when significant tissue swelling was noted (days 42-70), biochemical content was also normalized to construct dry weight (Figure 3.11).

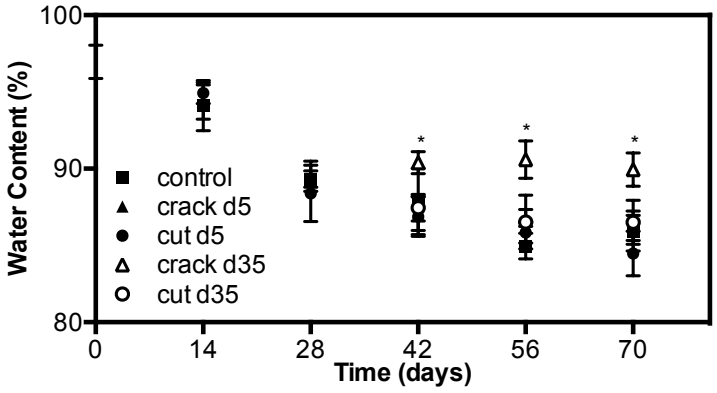

Figure 3.10: Water content of engineered constructs over time. *p<0.05 vs. control, n=5/group. p_{day42} = 0.020, p_{day56}<0.001, p_{day70}<0.001.

Regardless of culture maturity at the time of injury, constructs retained their biochemical constituents immediately following insult, as well as throughout the culture period. Specifically, constructs injured early in culture were able to recover their biochemical content with time in

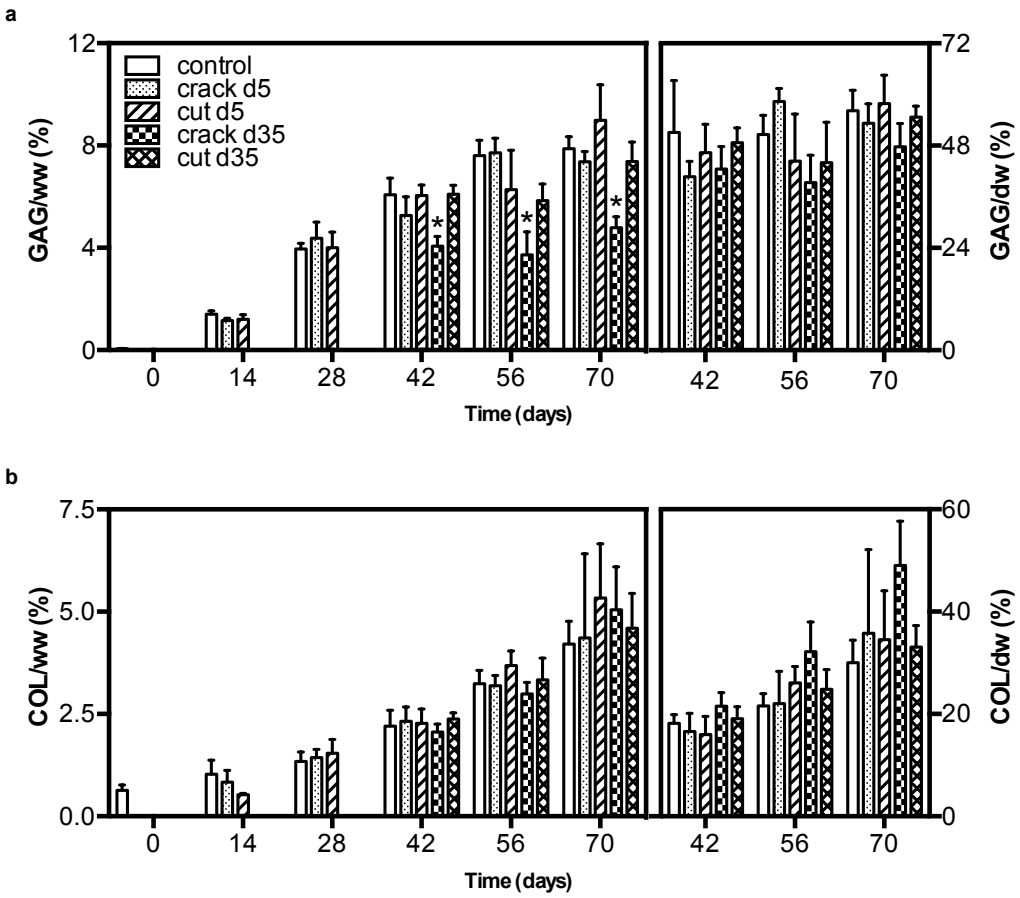

Figure 3.11: (a) GAG and (b) collagen content of control and injured constructs over time normalized to both construct wet weight (left) and dry weight (right). *p<0.05 vs. control, n=5/group. Crack d35 vs. control, GAG: $P_{day42}<0.001$, $P_{day56}<0.001$, $P_{day70}<0.001$.

culture relative to uninjured controls (GAG: 7.9 ± 0.3% ww, collagen: 4.2 ± 0.4% ww, control day 70; GAG: 7.4 ± 0.3% ww, collagen: 4.4 ± 1.5% ww, crack d5, $p_{GAG}>0.999$, $p_{COL}>0.999$; GAG: 9.0 ± 1.0% ww, collagen: 5.3 ± 0.9% ww, cut d5, $p_{GAG} = 0.208, p_{COL}=0.150$, Figure 3.11). When injured later in culture (d35), cut constructs similarly retained their biochemical makeup (GAG: 7.4 ± 0.5% ww, collagen: 4.6 ± 0.4% ww, $p_{GAG}>0.999$, $p_{COL}=0.546$, Figure 3.11). Mature constructs cracked on day 35 exhibited an apparent loss in GAG content (4.8 ± 0.3% ww, p<0.001, Figure 3.11), however, when normalized to dry weight to account for tissue swelling and increased water content, GAG content was comparable to uninjured controls (56 ± 3.4% dw, control; 48 ±

3.8% dw, crack d35, p=0.556, Figure 3.11). Collagen content was consistent for control and injured groups regardless of normalization method.

3.3.4 Discussion

Currently, the predominant approach to clinical applications of cartilage tissue engineering is to design a delivery system and scaffold that promote tissue growth *in situ* (e.g., (Caplan et al., 1997, 1993; Gao et al., 2002; Kawamura et al., 1998; Orr et al., 1999; Wakitani et al., 2007)). However, based on our understanding of the biomechanics of diarthrodial joints, we believe that the *in situ* environment is too harsh to allow a fledgling engineered tissue construct to develop a functional cartilage matrix that can withstand the native mechanical and chemical loading conditions. In particular, as the biomechanical environment is dictated by several factors including contact geometry, size of defect, and degree of load sharing, the extent of functional tissue elaboration needed to ensure the construct's survival after implantation into a joint defect remains unclear. As a first step toward predicting and characterizing the response to this harsh mechanical environment, engineered cartilage constructs of different culture maturity were exposed to either compression-induced cracking or controlled cutting.

While Young's modulus and GAG are at native levels in 8 weeks or less, the dynamic modulus (a functional measure that reflects tissue attributes such as radial tensile properties) and collagen levels remain significantly lower (native juvenile bovine: G*: ∼40MPa, %Collagen/ww: ∼10%, (Bian et al., 2008)) thereby signifying a major difference between our engineered cartilage and the native tissue. The ability to achieve native collagen levels, presumably needed to recapitulate the normal structure-function relationships of articular cartilage, continues to represent a significant challenge to the field of cartilage tissue engineering. In the current study, mature (day 35) engineered cartilage constructs exhibiting physiologic values of Young's modulus demonstrated a poor healing capacity following a cracking injury, in analogy to the known behavior of native cartilage (Kühn et al., 2004; Lewis et al., 2003; Quinn et al., 2001). In contrast, cracking of immature (day 5) constructs was followed by a complete recovery to control values by the end of the culture period.

This maturation-dependent response may be attributed to the advanced development of extracellular matrix (ECM) in the day 35 constructs. At an early stage of culture, chondrocytes embedded in the agarose hydrogel are not mechanically tethered to each other, due to the absence of a continuous collagen fibrillar matrix. The deformation applied to the construct is transduced to the cells only via the agarose hydrogel. In fact, chondrocytes deform less than the surrounding agarose because of the formation of a local pericellular matrix (PCM), which occurs around day 4 in culture (Lee and Bader, 1995), making them stiff inclusions in a soft matrix. Therefore, when cracking occurs, it is primarily a failure of the agarose hydrogel, which is known to have a limited resistance to tensile stresses, exhibiting a relatively brittle behavior (Huang et al., 2008). The chondrocytes are only subjected to a transient deformation mitigated by their pericellular matrix, and are thus able to survive the agarose cracking event (Figure 3.7) and continue to thrive by producing a functional matrix, as evident from the observed results (Figures 3.9 to 3.11).

However, as the cell-elaborated matrix begins to coalesce into tissue islands that eventually form a more contiguous ECM, the construct deformation may now be transduced to the chondrocytes via pulling of the collagen fibers (Quinn et al., 2002), and the cracking event may rip at the cells via integrin attachments. Therefore, cracking of more mature constructs leads to greater loss of cells (Figure 3.8) and poor recovery of mechanical integrity (Figure 3.9). The role of the ECM in mediating the deformation of mature constructs is directly evident in the load response at the gross level (Figure 3.6b). The biphasic load response noted in Figure 3.6b may be attributed to initial cracking of the less dense ECM inside the construct (Bian et al., 2009), followed by subsequent cracking of the denser collagenous matrix known to grow on the outer surface of the construct. Similarly, the ability of collagen fibrils to resist radial and circumferential tension is manifested in the later onset of failure in mature versus immature constructs ($\sim$50% versus $\sim$36% axial compression). Furthermore, due to the increased compressive stiffness of the GAG-laden mature constructs, chondrocytes are no longer able to resist the deformation of their surrounding matrix, so that the crack-inducing loading event may cause significantly greater cell deformation, and possibly cell death, than in immature constructs.

In contrast, sharp cutting does not exhibit the same long-term detrimental effects as cracking, analogous to native cartilage's response to partial-thickness cutting (Meachim, 1963) The response of immature constructs to cutting is similar to the cracking event: the cut primarily affects the agarose hydrogel and, other than cells that come in direct contact with the blade, chondrocytes remain unaffected by the cutting event (Figure 3.7d). Thus, the biosynthetic capacity of the surrounding cells is maintained and constructs are able to grow a functional matrix over time. In mature constructs, the blade now cuts through an elaborated ECM, causing more significant pulling of the connected network of collagen fibers and producing cell death beyond the immediate path of the blade (Figure 3.8d). However, cell death is significantly less widespread than with cracking, such that cell death is no longer observed at later time point (Figures 3.8b versus 3.8e). Since the chasms produced by the blade are not as wide as the cracks, a collagen network is apparently able to bridge these gaps over time, as evident from the measured functional properties (Figure 3.9).

The lack of pervasive and continuing cell death after injury observed in this study may also reflect the unique situation in which core biochemical constituents are maintained both immediately and long-term after imposition of trauma. In both modes of injury, overloading or cutting, transient indications of cell death were localized around crack and lesion sites. In extreme loading conditions, articular cartilage can exhibit fissuring after mechanical insult (Atkinson et al., 1998), with cell death in the proximity of tissue matrix cracks (Lewis et al., 2003). With time in culture, however, cell death is consistently seen to emanate away from the site of injury as paracrine factors are released from necrotic cells (dying from cell injury) and subsequently influence neighboring cells to undergo programmed cell death, a consequence of apoptosis (Tew et al., 2000). Similarly, in the most extreme loading condition of this study, constructs exposed to catastrophic damage exhibited prolonged cell death almost 4 weeks after injury (Figure 3.8b), suggesting that the mode of cell death is no longer necrotic, which occurs within hours or days (Chen et al., 2001), but rather in a manner consistent with apoptosis. However, in contrast to native cartilage, with further time in culture, cell death in overloaded constructs was mitigated, and further signs of continual cell death were not observed (Figure 3.8c). In comparison, for constructs injured earlier in culture or less

severely, patterns of delayed cell loss after injury were not observed, suggesting that cells either were not continually dying or new cells from cell division were repopulating injured regions and masking cell loss, as indicated by the comparable DNA content across all groups. This possibility is supported by analysis of the fraction of live cells in the center region of cut constructs which found that cells proliferated at a greater rate than uninjured control constructs and may have offset the loss in cell number stemming from the initial cell death after injury.

Explant studies have previously shown that chondrocytes close to an injury site tend to react to the imposed trauma by either dying or proliferating (Stockwell, 1979), although it is unclear what triggers one path over the other. The findings of this study suggest that while cells in engineered cartilage are immediately mechanically compromised after injury, the alternative downstream pathways of cell death or proliferation depend on the culture maturity of the construct. For constructs injured early in culture or injured less severely, rather than entering apoptotic pathways, the cells proliferate in the regions adjacent to the lesion. For engineered constructs exposed to catastrophic matrix damage, some cells enter apoptotic pathways and exhibit delayed death, but interestingly, the system seems to only reside in this state transiently with little effects on the biochemical composition of the tissue.

However, while we did not observe biochemical content degradation or continual cell death, constructs cracked late in culture were unable to recover their mechanical properties and intrinsically repair themselves, similar to that which is seen with cartilage explants in vitro and suggested to happen *in vivo*. The observed mechanical failure suggests immediate catastrophic structural damage of the construct rather than subsequent degradation cascades. This proposed mechanism of failure is further supported by the different responses seen with compression-induced cracking and cutting. Like cartilage explants exposed to scalpel injuries (Amin et al., 2008a; Tew et al., 2001), cut constructs lack the traumatic structural changes associated with other modes of injury such as compression (Chahine et al., 2004; Loening et al., 2000; Torzilli et al., 2006; Wang et al., 2002), indentation (Chen et al., 2001; Levin et al., 2001), and trephine punches (Tew et al., 2001, 2000). As such, it may be that localized structural damage from the blade is insufficient to cause

bulk structural damage of the construct that is necessary for mechanical failure.

It is important to note, however, that this response to mechanical overload as well as cutting likely reflects the conditions of the experimental setup, specifically the chosen scaffold system and the cell type used, which together define the nature of the cell-matrix interactions that develop in culture. There exist several possible mechanisms that may underscore differences in the injury response of engineered cartilage to literature reports of cartilage explant injury. First, while our engineered tissues recapitulate many of the structure-function relationships of native cartilage (Lima et al., 2007), the collagen content remains significantly lower than native levels, in contrast to GAG levels that reach native content. Collagen content is likely to affect cell-matrix coupling. Additionally, variations in engineered extracellular matrix organization may lead to differences in how dead cells and apoptotic bodies are entrapped. The avascular nature of cartilage and lack of mononuclear phagocytes *in vivo* prohibit the removal of apoptotic bodies, which subsequently become lodged in surrounding lacunae (Hashimoto et al., 1998). As such, for cartilage explants injured *in vitro*, the inherently dense extracellular matrix may act to keep apoptotic bodies bound to the tissue. The prolonged presence of these bodies has been suggested to perpetuate a degradative cascade, as is seen in osteoarthritis (Blanco et al., 1998; Kourí et al., 2000). In contrast, the less dense matrix of engineered cartilage may facilitate the removal of dead cells and apoptotic bodies; therefore, injured constructs, even in the most severe cases, do not exhibit continual cell death at 50 days post injury (Figure 3.8c).

We note that constructs having Young's modulus of approximately 300 kPa failing at 40g of force experienced a compressive stress of 0.03MPa, much lower than what is reported *in vitro* for cartilage (Milentijevic and Torzilli, 2001), but with perhaps similar failure strain levels (Ewers et al., 2001; Flachsmann et al., 2001). We attribute this disparity as a consequence of the low collagen content of our engineered cartilage as well as the unconfined compression experimental injury setup, which may exacerbate the latter by permitting free radial tissue expansion during axial compressive loading. Whether the current tissues could survive undamaged in a living joint is a complex question and would depend on the location of the focal defect on the joint being treated and its dimensions

relative to intact articulating surface, as the surrounding tissue (around the defect) would shoulder a portion of the joint loads depending on the contact geometry. Tissues grown in our laboratory with native Young's modulus have survived in focal defects (4 mm diameter) created in the canine stifle joint (trochlear groove) for 12 weeks (Ng et al., 2010). As the tissue construct gets increasingly larger, such as for replacing an entire articular surface, such as for a patella, the loading demands would increase as the contribution from surrounding tissues diminishes (Hung et al., 2003).

Furthermore, unlike native cartilage, the engineered cartilage consists of a mixed population of chondrocytes isolated from full-thickness cartilage. As such, the normal zonal (cellular, biochemical, structural and mechanical) organization of cartilage is not recapitulated. Yet, it is known that zonal cell-to-cell differences may predispose certain chondrocytes to exhibit strain-induced loss of viability (Chahine et al., 2007). In the future, the injury response of constructs with specific zonal cell populations and/or with stratified engineered hydrogel layers may need to be examined (Ng et al., 2005). To the best of our knowledge, this study represents the first attempt to model and characterize injury and the subsequent response of engineered cartilage constructs under a controlled loading environment. Unlike native cartilage explants, engineered cartilage possesses the ability to heal and repair with further time in culture as long as the bulk structural makeup of the construct is left intact. The results of this study begin to characterize the conditions under which mechanical failure occurs and provide greater insight to the behavior and response of engineered cartilage tissue grafts to mechanical insult.

3.4 Culture in Chondrogenic Medium Fosters Protection Against Propagative Cell Death

3.4.1 Introduction

The use of FBS, whose composition is highly variable and unknown, for tissue culture has been largely precluded. Instead, many groups have chosen to employ more consistent formulations of a chemically defined serum-free medium for the culture of cartilage (Dumont et al., 1999; Mauck

et al., 2006). In particular, our lab has adopted a serum-free media composition (also referred to as chondrogenic medium - CM) that has been shown to induce chondrogenesis in bone marrow-derived stem cells and promote extracellular matrix development in tissue engineered cartilage (Mauck et al., 2006). Notably, when cartilage explants were cultured in serum-supplemented medium, they exhibited significant tissue swelling degradation (Bian et al., 2008; Sah et al., 1989; Torzilli et al., 1997). In contrast, explants cultured in CM were enhanced in as little as 2 weeks and remained stable for the duration of the study (Bian et al., 2008). Hypothesized to be due to the inclusion of dexamethasone, a synthetic adrenal corticosteroid, this CM formulation contains soluble factors that promote mechanical properties of cartilage explants and protect it against catabolic factors.

In this way, we observed a potentially protective effect for cartilage explants exposed to a harsh mechanical injury (See Section 3.2). This is in contrast to reports in the literature that have consistently shown that cell death continues to emanate away from the site of injury and persist long after the initial insult. Here, we revisit that injury model and probe whether the protective effects noted earlier for explants cultured in CM translate to engineered cartilage constructs (Section 3.3: *Study 1*) and directly compare the use of CM with FBS-containing medium (Section 3.3: *Study 2*).

3.4.2 Materials and Methods

3.4.2.1 Tissue Isolation and Cell Culture

⌀6.35mm explants (full thickness cartilage with attached subchondral bone) were cored out of the carpal face of juvenile bovine wrist joints (n=2). Joints showing any contraindications were discarded. Explants were stored in chondrogenic media (serum-free DMEM supplemented with ITS+, dexamethasone, and ascorbic acid).

Articular cartilage shavings were also harvested from CMC joints of freshly slaughtered 2-4-week-old calves (n=4-6 joints). Cartilage was digested in high-glucose DMEM with collagenase type V (Sigma, St. Louis, MO) for 11 hours at 37°C with shaking. Cell suspensions were filtered through a 70μm porous mesh and sedimented in a bench-top centrifuge for 15 min at 1500g. Viable cells were counted with a hemacytometer and trypan blue. Cell suspensions (60×10^6 cells/mL)

were mixed in equal parts with 4% low-gelling agarose (type VII, Sigma) at 37°C to yield a final cell concentration of 30×10^6 cells/mL in 2% agarose. The chondrocyte/agarose mixture was cast into slabs and cored using a sterile disposable punch (Miltex) to final dimensions of 4mm diameter and 2.34 mm thick.

Constructs were cultured in hgDMEM supplemented with 1X PSF, 0.1μM dexamethasone, 50μg/mL ascorbate 2-phosphate, 40μg/mL L-proline, 100μg/mL sodium pyruvate, and 1X ITS+ premix (insulin, human transferrin, and selenous acid, Becton Dickinson, Franklin Lakes, NJ). Medium was further supplemented with 10ng/mL TGF-β3 (Invitrogen, Carlsbad, CA) for the first 14 days of culture. Culture media was changed every other day.

3.4.2.2 Injury

Study 1: On day 35 of culture, constructs exhibiting properties similar to native cartilage (Young's modulus and glycosaminoglycan content) were subjected to a cutting injury. Specifically, two orthogonal cuts were made in constructs by pushing a razor blade to 50% of the construct's original thickness (Figure 3.12). Razor blades were pushed straight down to prevent the application of additional shear forces, and were replaced after every five constructs to prevent dulling of the blade. Afterwards, samples (including controls manipulated similarly to injured constructs, without actual trauma) were returned to culture in freshly supplemented media and allowed to recover in culture to day 21 for viability staining. Explants were similarly injured by cutting 5 days after harvest.

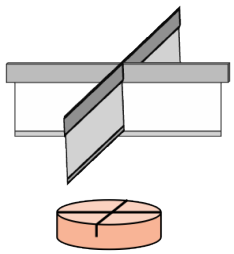

Figure 3.12: Schematic of cutting scheme. Blades were pushed straight into the sample to a depth of 50% and then removed. Blades were replaced every 5 samples to avoid dulling.

Study 2: To control whether this effect was specific to the cutting injury and the chondrogenic media formulation, a second set of explants was harvested, similarly cultured out to 5 days in the same medium, but then a ∅1mm cylindrical plug was aseptically cored out of the center of each explant using a custom-programmed milling machine (Section 3.2.2.2, Figure 3.1) equipped with a disposable biopsy punch. Post injury, samples were returned to culture in either CM media or in media supplemented with FBS.

3.4.2.3 Cell Viability Assessment

Assessment of cell viability was performed using the Live/Dead cytotoxicity assay (Molecular Probes, Eugene, OR) at immediate- (1 day), short- (10 days), and long- (21, days) time points post trauma. The assay is based on calcein AM permeating the membranes of cells with intact cell membranes, producing a green fluorescence (live), while ethidium homodimer permeates the nuclei of dead cells (with compromised cell membranes) to produce a red fluorescence (dead). An apoptosis assay (Molecular Probes, Eugene, OR) was also performed on a second set of identical constructs and explants to assess the mechanism of cell death. The assay is based on Yo-Pro©-1 (green) dye entering the permeant membrane while propidium iodide (red) dye is excluded. When used together to stain a cell population, apoptotic cells shown green fluorescence, dead cells show red and green fluorescence, and live cells show little or no fluorescence. After each viability assay, constructs were aseptically returned to culture media to allow for assessment of cell death in the same sample at later timepoints. Live and dead images were taken separately on an inverted confocal fluorescent microscope (Leica, Bannockburn, IL). Overlaid images of live and dead cells were analyzed using ImageJ (NIH) to measure the area of cell death emanating away from the site of injury (Figure 3.13).

3.4.2.4 Statistics

Statistics were performed using two-way ANOVA with Tukey's HSD post-hoc tests (Statistica, Tulsa, OK), with α=0.05 and statistical significance set at $p \leq 0.05$ to compare groups across media

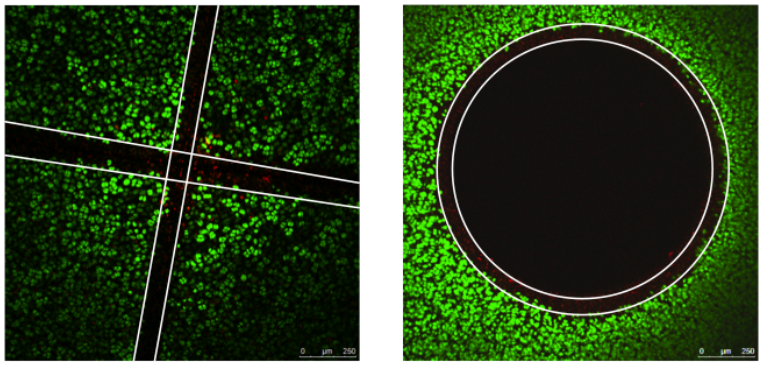

Figure 3.13: Representative overlaid live/dead stains with lines demarcating the regions of cell death adjacent to the site of injury.

type and time. All data are reported as the mean ± 95% confidence interval of 4-5 samples per time point and group.

3.4.3 Results

Study 1: Cellular viability, as assessed by the Live/Dead cytotoxicity assay and the apoptosis assay kit, was found to be maintained in both engineered constructs and cartilage explants following the cutting injury. With time in culture, the area surrounding the cut remained constant, with no infiltration of neighboring cells (Figure 3.14, $p>0.05$).

Study 2: Cored explants stored in CM exhibited similar results to the explants and tissue engineered constructs from Study 1 (Figure 3.15, $p>0.05$). Cell death area remained confined with no spreading of the paracrine factors associated with apoptosis. When FBS-containing medium was used as a storage solution, however, by day 28, cell death area was significantly increased in those constructs as compared to those stored in CM (Figure 3.15, $p<0.05$).

3.4.4 Discussion

Tissue culture storage in CM protects native and mature engineered cartilage by confining cell death to the injury site. Regardless of the mode of injury applied in these studies, cell death was

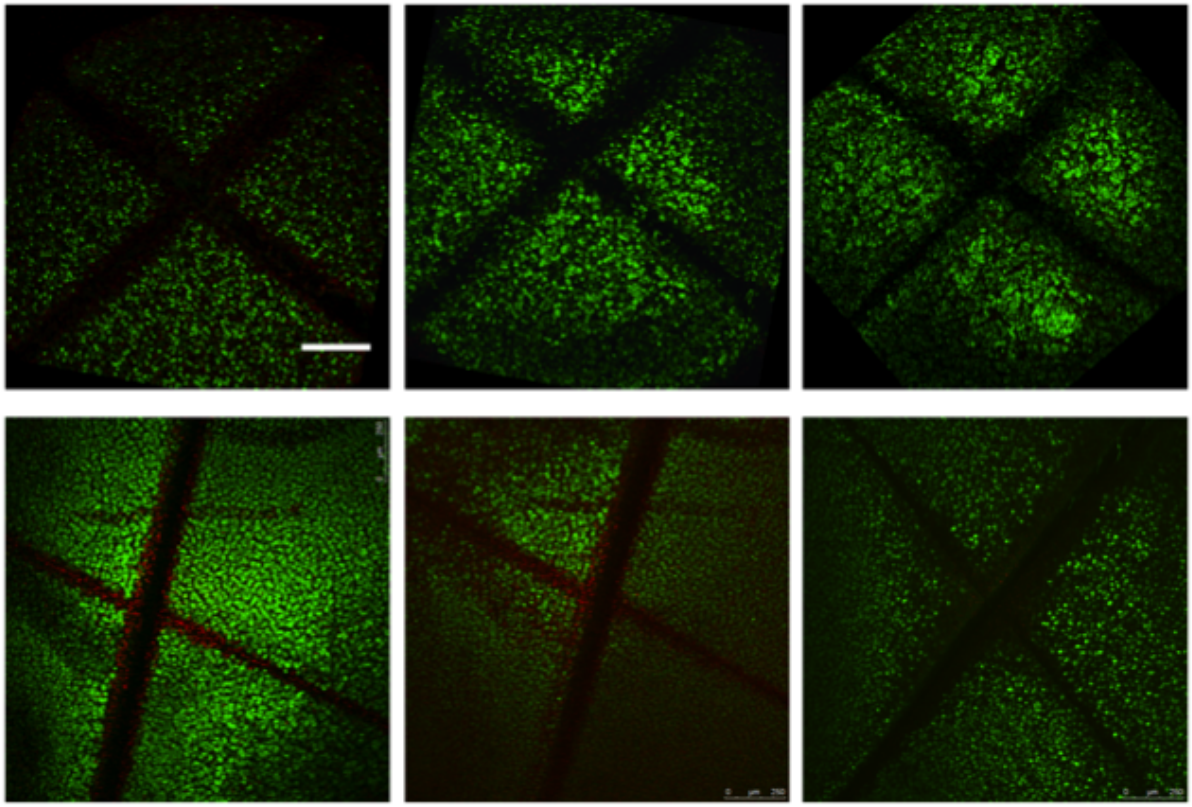

Figure 3.14: Representative overlaid live/dead images of cut (top) engineered constructs and (bottom) native cartilage with time in culture after (left) 1 day, (middle) 7 days, and (right) 21 days in culture.

mitigated and did not appear to exhibit the paracrine soluble factors that are typically associated with apoptosis after injury in cartilage (Chen et al., 2001). However, when these same explants were stored in FBS-containing medium, the area of cell death was significantly increased, agreeing with findings in the literature reporting a zone of inhibition following injury.

Though CM was observed here to prevent the progression of tissue injury, it is important to note that, as reported in Section 3.2, some modes of injury, such as stress-induced cracking, are too severe to resist the catabolic cascade that ensues following insult, no matter the culture medium formulation. However, in showing the disparity in the size of the cell death zone for constructs cultured in CM and serum-containing media for the same type of injury, as performed here, we can postulate that the protective effect against cell death propagation indeed is a direct consequence

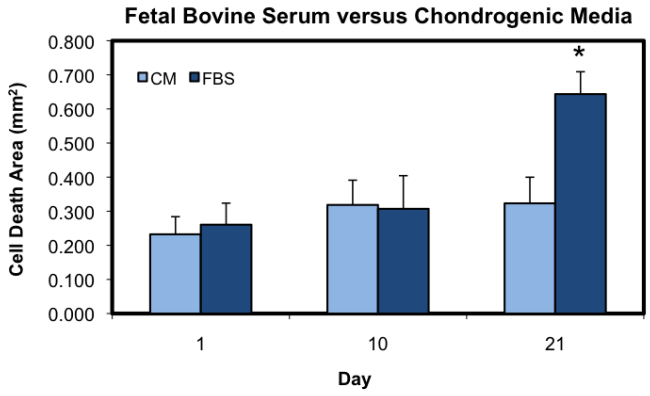

Figure 3.15: Measured cell death area for explants after punching with time in culture with different storage media. *p<0.05, n=20/group.

of soluble factors that are present in the CM formulation. Detailed high-throughput screening of the chemical mediators present in the CM formulation will be necessary, however, to elucidate the particular factor(s) responsible for this protective effect.

3.5 Conclusion

Understanding the response of cartilage, both native and engineered, to mechanical insult is crucial towards efforts in designing repair strategies. In this chapter of the dissertation, new culture systems are described, which complement existing in vitro injury model studies described in the literature. First, we assessed two common modes of iatrogenic injury stemming from graft harvesting procedures and examined whether modifications in stabilizing one degree of freedom could mitigate the spread of cell death described previously. Our results found that controlled drilling with optimized parameters of insertion rate and rotational speed were far superior to the simple punch motion, offering insights into considerations for improving graft transplantation techniques. Secondly, we characterized, for the first time, the influence of mechanical insult on engineered cartilage, and found that both the type of injury as well as construct maturity are significant factors in the consequent response. In particular, engineered cartilage, unlike native cartilage, possesses

the inherent ability to repair following injury unless catastrophic matrix failure is noted. These findings contribute to the literature on tissue engineering for cartilage replacement and strongly imply that a specific window of time exists for optimal implantation. Finally, we explored further the role of culture medium in mediating the progression of cell death. Collectively, these studies offer a more complete characterization of the response of cartilage to mechanical injury, and begin to provide insights into how the damage may be contained.

Part II

Strategies for Enhancing Cartilage Repair

Chapter 4

Influence of Extracellular Osmotic Environment during EF-Induced Cell Migration and the Role of AQP1

4.1 Introduction

As field gradients exist in both wound healing and developing embryos (Robinson, 1985), understanding osmotic challenges in the context of EF-induced migration is crucial. To this end, we examined whether changes to the osmotic extracellular environment induce cellular changes sufficient to influence cell migration patterns. As osmotic effects are highly regulated by membrane channels and transporters, we first examined the role of the AQP1 water channel during EF-induced migration (Section 4.2). Subsequently, we osmotically challenged these cells and observed their response under EF (Section 4.2). Finally, since IL-1 exposure in chondrocyte culture has been shown to result in a decrease in cytoskeletal components (tensin, talin, paxillin, and FAK, (Vinall et al., 2002)) and correspondingly volumetric response (Pritchard et al., 2008), behaviors mediated by the activity of AQP1, we examined a clinically relevant IL-1-rich environment to the examine the response of migration (Section 4.3).

4.2 Role of AQP1 in Regulating Extracellular Osmotic Environment during EF-Induced Migration

4.2.1 Introduction

Proteoglycan molecules make up 20-30% of the solid organic matrix of cartilage and their polyanionic chains bind and attract water, leading to an increase in internal swelling pressure (Buschmann et al., 1995; Lai et al., 1991). *In situ* osmolarity of cartilage tissue has been estimated to be 350-450 mOsm (Koo et al., 2010; Urban et al., 1993), depending on the zone. During osteoarthritis, degradation of matrix molecules leads to a corresponding decrease in osmolarity (Maroudas and Venn, 1977). Similarly, synovial fluid extracted from healthy knees is 400 mOsm and becomes hypotonic (∼300 mOsm) with joint injury and arthritis (Baumgarten et al., 1985; Jensen and Zachariae, 1959; Newman and Grana, 1988; Shanfield et al., 1988). Transient osmotic challenges have been shown to modulate chondrocyte intracellular signaling events and biosynthetic activities (Chao et al., 2006; Erickson et al., 2003; Yamazaki et al., 2000). Therefore, the osmotic environment and ensuing mechanotransduction events may be significant factors that influence cell migration. Previous studies have found that the extracellular osmotic environment changes membrane hydraulic permeability of chondrocytes and cell volume (Hall et al., 1996; Oswald et al., 2008; Pritchard and Guilak, 2004; Shen et al., 2002; Wang and Zhu, 2011) by alterations to the membrane structure (Borghetti et al., 1995; Erickson et al., 2001; Hopewell and Urban, 2003; Yellowley et al., 2002) and AQP1 water channels (Elmoazzen et al., 2002; Guilak et al., 2002; Jaeger et al., 1999; Mobasheri et al., 2002). These changes in cell volume may work to propel the cell during migration; in fact, unequal rates of water entry to the front and back parts of the cell has generated forces sufficient to propel forward motion of a cell even in the absence of actin (Jaeger et al., 1999). As such, AQP1 been implicated in the mechanotransduction of cell volume from theoretical principles (Liang et al., 2008; Mobasheri et al., 2002). Recently, studies have identified the presence of the AQP1 water channel in cultured human and equine articular chondrocytes (Mobasheri et al., 2004; Trujillo et al., 2004).

4.2.2 Materials and Methods

4.2.2.1 Experimental Design

Two consecutive studies are described herein that utilize our established galvanotaxis protocol. In the first study, cells were treated with an AQP1 channel inhibitor (silver sulfadiazine) and exposed to EF strengths previously shown to induce migration. In the second study, cells were first osmotically challenged before undergoing migration experiments.

4.2.2.2 Cell Harvesting and Expansion

Articular cartilage was harvested from bovine knee joints of four freshly slaughtered 2-4 week old calves and digested in high-glucose DMEM with collagenase IV (Worthington Biochemical Corporation, Lakewood, NJ) for 11 h at 37°C with shaking.

Cell suspensions were filtered through a 70μm porous mesh and sedimented in a bench-top centrifuge for 15 min at 1500g. Viable cells were counted with a hemocytometer and trypan blue and plated at high density (20×10^3 cells/cm^2). DMEM was supplemented with 10% fetal bovine serum, 100 U/mL each of penicillin, streptomycin, and fungizone, and a growth factor cocktail (1 ng/mL TGF-β1, 5 ng/mL bFGF, and 10 ng/mL PDGF-$\beta\beta$ (Ng et al., 2010; Sampat et al., 2011)). Medium was changed every three days. Chondrocytes were expanded and used after 1 passage (Chao et al., 2000).

Aquaporin-1 Inhibitor: 1mM silver sulfadiazine was dissolved in DMSO and used at a final concentration of 5μM in 0.5% DMSO.

Osmotic Solutions: Osmotic solutions were made with DMEM and water or sucrose was added to the base media (337 mOsm) to make hypo- (200 mOsm, 300 mOsm) or hypertonic (400 mOsm) solutions, respectively. Sucrose was chosen, as opposed to NaCl/KCl as previously established (Sampat et al., 2013), to maintain constant ionic content and conductivity of the bathing medium across all groups. While both sucrose and sodium chloride decrease chon-

drocyte volume, with the latter, there is an additional increase in the intracellular sodium ion concentration that may lead to altered activity of sodium-dependent membrane transporters which in turn facilitate cell migration (Schwab, 2001).

For galvanotaxis experiments, DMEM was supplemented with 5% fetal bovine serum (FBS, Atlanta Biologicals), 1% PSAM (Invitrogen, CA) and buffers. The osmolarity of the final solutions was confirmed to be ∼250, 350, and 450 mOsm using a freezing-point depression osmometer (Advanced Instruments, MA).

4.2.2.3 Galvanotaxis

Study 1: At confluence, chondrocytes were released from culture with trypsin, suspended in media for one hour to allow for equilibration, and then plated at 2.65×10^4 cells/cm^2 onto sterile glass slides using removable silicone wells. During the equilibration phase, for one subset of cells, silver sulfadiazine was added to the cell suspension.

Study 2: At confluence, chondrocytes were released from culture with trypsin, suspended in osmotic media (250 mOsm, 350 mOsm, and 450 mOsm) for at least two hours to allow for equilibration. Control studies have shown no observable differences from cells that equilibrated in osmotic media overnight or longer. Cell suspensions were then plated at 2.65×10^4 cells/cm^2 onto sterile glass slides using removable silicone wells.

For both studies, after attachment for 1 hour in a 5% CO_2 incubator at 37°C, the slide was gently rinsed to remove non-adherent cells and then positioned in the chamber. A modified parallel-plate flow chamber was used, as described previously (Chao et al., 2000). A power supply (Kiethley Instruments) delivered a current of 3.3 mA (6 V/cm EF strength) through the chamber (Figure 4.1, and experiments were performed at room temperature for 3 h. Control slides were treated similarly, except no EF was applied. Cell migration patterns were captured using an Olympus IX-70 inverted

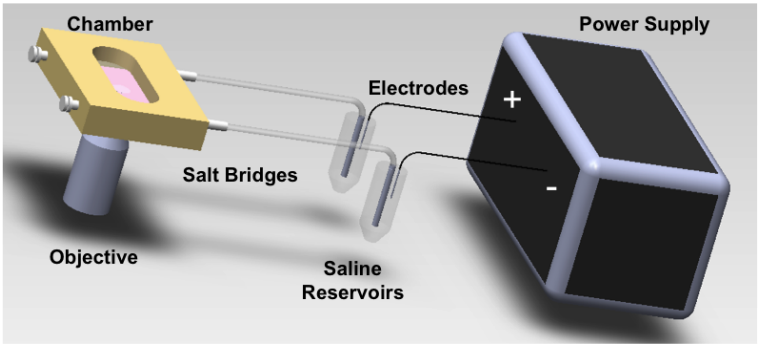

Figure 4.1: Schematic of galvanotaxis setup. Cells seeded on a glass slide were inserted into a custom chamber and exposed to an electric field gradient.

microscope equipped with a MicroMax 5-MHz interline transfer chip digital camera (Princeton Instruments, NJ) linked to a computer running Metamorph software (Universal Imaging). Using a Hoffman contrast filter and 10× objective (1 pixel = 0.68 μm), approximately 30-40 cells were observed in each field of view; images were acquired at 10 min intervals.

4.2.2.4 Cell Migration Parameters

The position of each cell was manually tracked via a custom MATLAB program that utilizes measurements of the net centroid displacement from the starting position (set as origin) to calculate overall speed of migration for each cell (the net displacement in the experiment divided by the 3 h time span of observation). Migration direction was quantified as $\sin\phi$, where ϕ is the angle between the x-coordinate axis and the migration vector, such that $\sin\phi$ was defined as the value -1 when ϕ = 4.71 rad (270°), the direction of the cathode. The directional velocity, defined as the component of the speed directed toward the negative pole (e.g. (Chao et al., 2000, 2007)), was obtained by multiplying a cell's speed by $\sin\phi$. Each data point represents the mean and standard error of the mean from 60-80 samples.

4.2.2.5 Statistics

A two-way ANOVA was performed on cell speed, directed velocity, and total displacement for factors of treatment (applied EF vs. control), and condition (either for AQP-1 inhibition (*study 1*)

or osmolarity (*study 2*)) to determine significance ($p<0.05$) of the effect of each factor and also the interaction of the factors. Tukey's honest significant difference (HSD) *post hoc* test was performed to assess significance ($p<0.05$).

4.2.2.6 Immunocytochemical Staining

Study 1: Aquaporin-1 Immunofluorescence: Following galvanotaxis, cells were fixed in ice-cold methanol for 10 minutes at -20°C, blocked with PBS containing 10% NGS for 1 hour at room temperature, and then incubated with primary polyclonal antibody to AQP1 (Millipore, diluted 1:200 in PBS containing 1% NGS) for 2 hours at room temperature and followed by Alexa Fluor 488-conjugated anti-rabbit IgG (Invitrogen) and TRITC-conjugated phalloidin. Cells were mounted in mounting medium containing a DAPI counterstain and then examined with an Olympus fluorescence microscope.

Study 2: Actin Cytoskeleton Immunofluorescence: Following galvanotaxis experiments, cells were fixed with 4% paraformaldehyde for 20 minutes at room temperature, permeabilized with 0.1% Triton X-100 (Sigma, MO), blocked with 1% BSA in PBS, and then incubated with primary antibody to Vinculin (Millipore, diluted 1:100 in 1% BSA in PBS) for 1 hour at room temperature and followed by Alexa Fluor 488-conjugated anti-goat (Invitrogen, diluted 1:50 in PBS) and TRITC-conjugated phalloidin (Millipore, diluted 1:100 in PBS). Cells were mounted in mounting medium containing a DAPI counterstain and then examined with an Olympus fluorescence microscope.

4.2.3 Results

4.2.3.1 Role of AQP1 in EF-Induced Cell Migration

Efficacy of silver sulfadiazine as an AQP1 inhibitor was first confirmed by analyzing cell volume change with a Coulter counter following osmotic loading. Addition of deionized water to a cell suspension ($\sim$380 mOsm) to create a final solution of 300mOsm yielded no volume change when chondrocytes were pretreated with silver sulfadiazine (Figure 4.2).

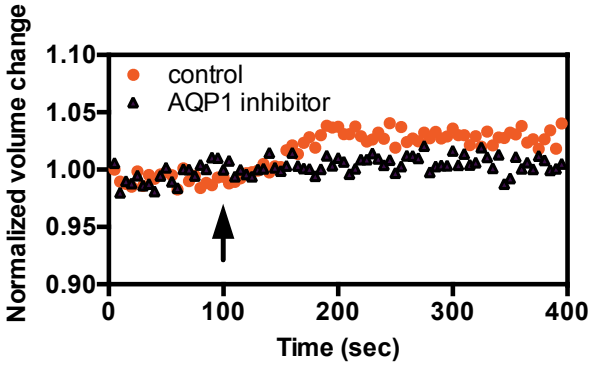

Figure 4.2: Normalized cell volume change after introduction of D.W. to 380 mOsm cell suspension to create a final osmolarity of 300mOsm. Arrow indicates point of influx, approximately 200,000 cells counted/group.

Cells treated with the AQP1 inhibitor exhibited significantly altered migration behavior; both control and electric field stimulated cells showed decreased displacement (Figure 4.3a, $p<0.05$). Furthermore, these cells exhibited less preferential migration after exposure to an electric field and showed no significant bias in direction, similar to control cells (Figure 4.3b, $p>0.05$). When these cells were stained for AQP1, actin cytoskeleton, and DAPI, differences were observed between control cells and those treated with the silver sulfadiazine (Figure 4.4). After 3 hours of electric

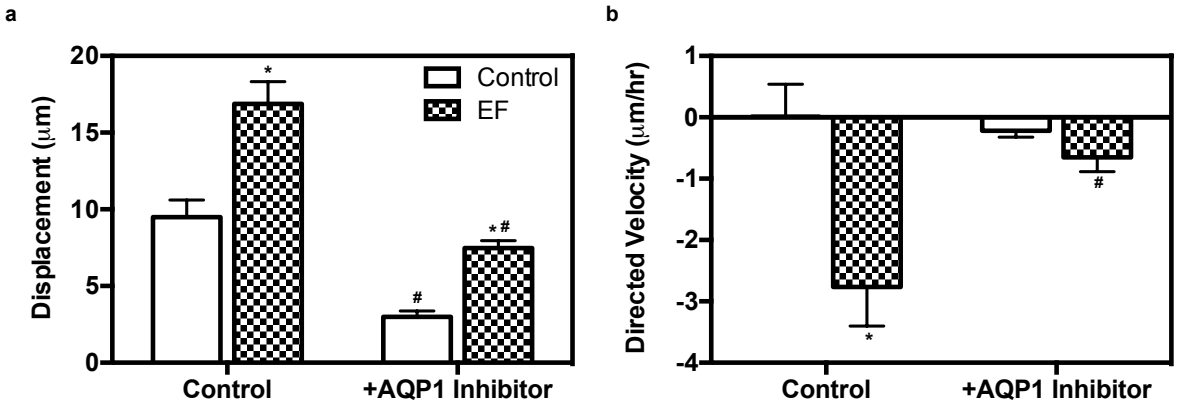

Figure 4.3: Effect of silver sulfadiazine on migration parameters ((a) displacement, (b) directed velocity) for chondrocytes after 3hr of applied DC electric field. *$p<0.05$ vs. no EF control, #$p<0.05$ vs. respective control (no inhibitor). n=50-60 cells/group.

field stimulation, control cells reoriented their long axis perpendicular to the direction of field and exhibited elongated and outstretched processes (Figure 4.4). Furthermore, AQP1 proteins localized to the periphery of the pseudopods. In contrast, cells treated with silver sulfadiazine remained spherical with diffuse AQP1 labeling.

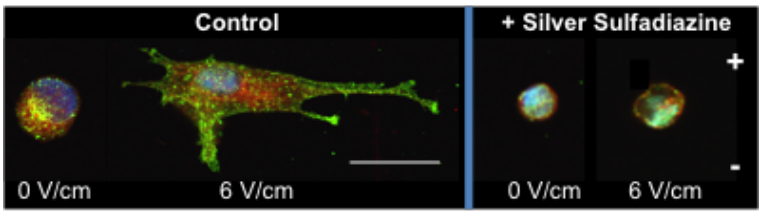

Figure 4.4: Representative immunofluorescence micrographs of cells at t=3hr after DC electric field was turned on. Alexa Fluor 488 (green): AQP1; DAPI (blue): nucleus; TRITC (red): phalloidin. Scalebar = 20 μm.

4.2.3.2 Osmotic Extracellular Environment Modulates Cell Migration Behavior

Chondrocytes exhibited a change in cell volume and shape following suspension in the chamber with the differing osmolarities. 250 mOsm-treated cells appeared stretched with spread focal adhesions (Figure 4.5). In contrast, 350 mOsm and 450 mOsm cells retained a spherical shape with minimal spreading of focal adhesions or attachment plaques. These osmolarity-dependent changes were not visible for cells that were exposed to EF; regardless of osmotic environment, all cells stretched out and oriented themselves perpendicular to the direction of field (Figure 4.5).

The baseline migration of chondrocytes was not altered with osmotic loading. Control cells moved an average of 2.64 $\pm$ 0.40 μm/hr and showed no significant differences ($p>0.05$, Figure 4.6a) across all osmolarity groups. Similarly, these cells exhibited no preferential direction of migration, resulting in an average directed velocity of 0.13 $\pm$ 0.51 μm/hr across all groups ($p>0.05$, Figure 4.6b). In contrast, when EF was applied, the migration response of chondrocytes to EF was highly dependent on osmotic environment. A parabolic trend was noted for increasing osmolarity, whereby cells traveled faster and farther at hypotonic (250 mOsm) and hypertonic (450 mOsm) osmolarities that was not significantly different from one another (12.1 $\pm$ 1.24 μm/hr vs. 10.6 $\pm$

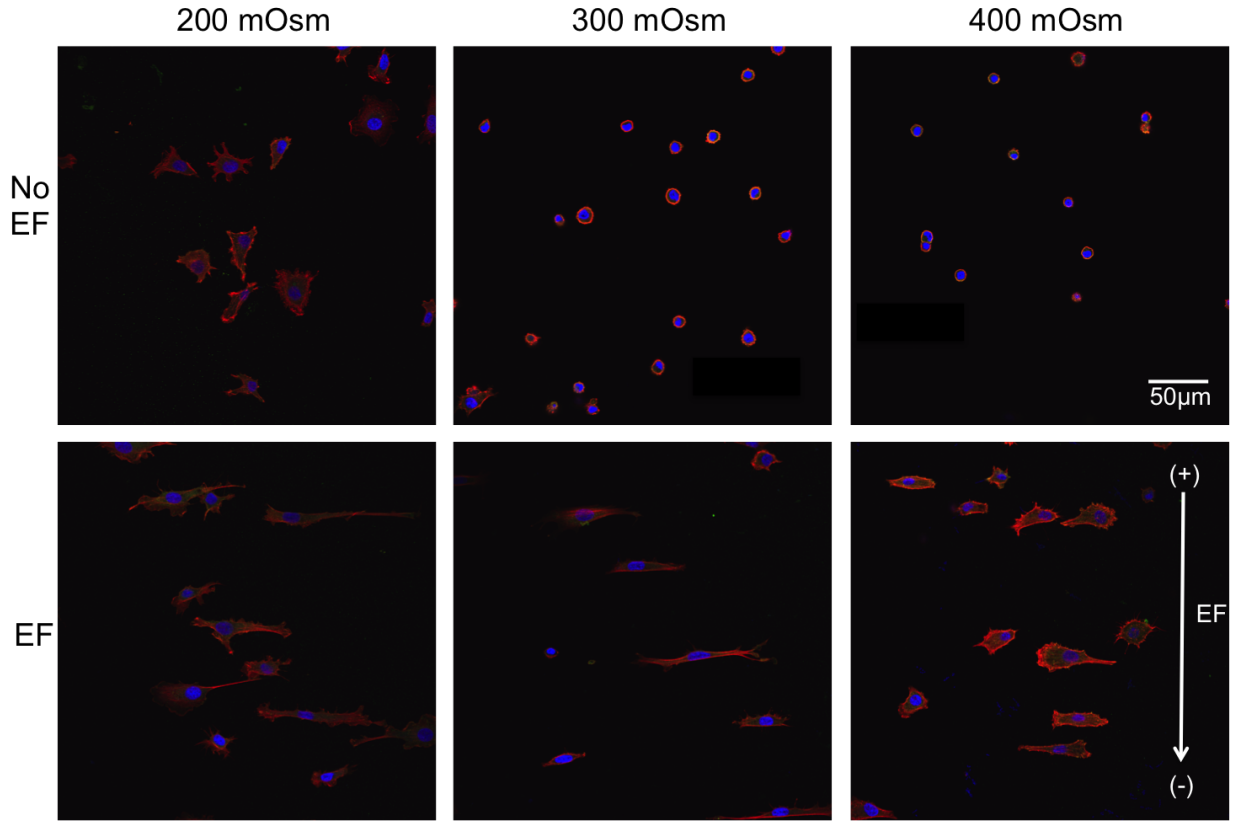

Figure 4.5: Actin cytoskeleton staining of chondrocytes exposed to various osmotic environments in the absence or presence of EF. Alexa Fluor 488 (green): vinculin; DAPI (blue): nucleus; TRITC (red): phalloidin. Scalebar = 50 μm.

0.94 μm/hr, p=0.36). Chondrocytes in isotonic medium traveled significantly slower, only reaching 7.03 $\pm$ 0.70 μm/hr ($p_{250-350}$<0.0001, $p_{350-450}$=0.0014, Figure 4.6a). The direction in which these cells traveled did not exhibit a similar parabolic trend, with hypotonic cells exceedingly traveling toward the cathode (negative pole). Meanwhile, isotonic and hypertonic cells exposed to EF were statistically similar to control cells (p=0.9999, p=0.9213, respectively, Figure 4.6b) and did not exhibit large changes in migration direction.

4.2.4 Discussion

These results showed, for the first time, that AQP1 water channels modulate chondrocyte migration with exposure to an applied DC electric field. Our findings corroborate previous studies that have

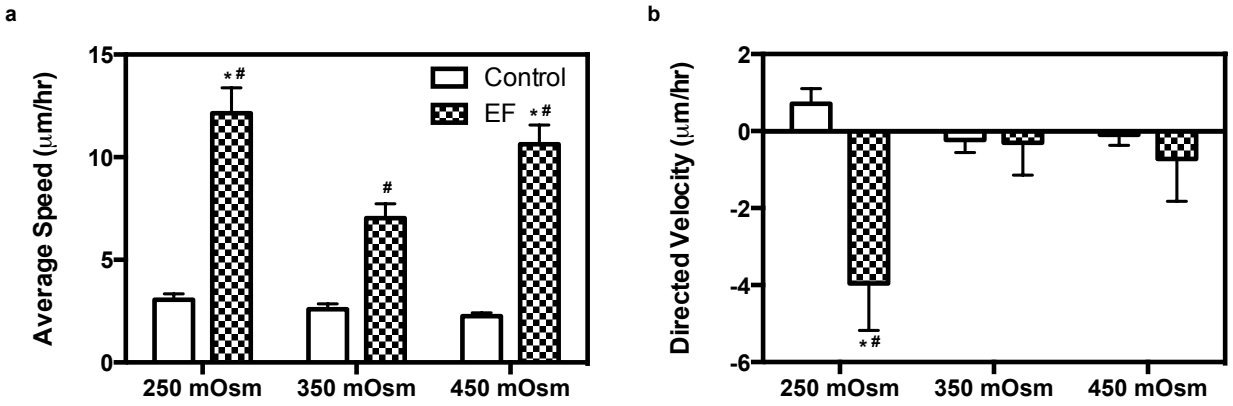

Figure 4.6: Effect of osmotic extracellular environment on migration parameters ((a) speed, (b) directed velocity) of chondrocytes. *p<0.05 vs. no EF control, #p<0.05 vs. isotonic (350 mOsm) condition.

identified AQP1 as essential for cell migration and wound healing through beta-catenin mediated cytoskeletal reorganization (Liang et al., 2008; Monzani et al., 2009; Ruiz-Ederra and Verkman, 2009). Furthermore, chondrocytes from AQP-1 knockout mice exhibit significantly reduced adhesion and migration abilities (Liang et al., 2008). Interestingly, contrary to reports in the literature that AQP1 proteins are localized to the front edge of the migrating cell (Liang et al., 2008; Monzani et al., 2009; Ruiz-Ederra and Verkman, 2009; Verkman, 2005), here we have shown that following exposure to electric field stimulation, AQP1 proteins are localized to the perimeters of the extended protrusions. This may be due to the addition of the electric field, which can redistribute surface proteins and alter reorganization of the cytoskeletal make-up.

Extracellular osmolarity has been shown to be responsible for changes in cell volume, cytoskeleton organization and gene expression (Erickson et al., 2001; Sanchez and Wilkins, 2003; Yellowley et al., 2002). We have observed that the osmotic environment significantly impacts the chondrocyte's actin cytoskeleton, and subsequently, motility in the presence of an applied EF. Hypotonic (250 mOsm) chondrocytes exhibited prominent cytoskeletal organization with dramatically enhanced cellular migration toward the cathode. In contrast, the isotonic or the more "physiologic" 350 mOsm group appeared to be smaller and exhibit a more spherical morphology. In control conditions (no EF), cells exhibited trends consistent with findings in the literature that describe

enhanced migration for cells in a hypotonic environment. In these studies, exposure to hypotonic shock led to recruitment of focal adhesion kinase (FAK) in osteoblasts via opening of large conductance calcium-and voltage-dependent potassium channels (Rezzonico et al., 2003). FAK has been shown to regulate the recruitment of key proteins necessary for stimulated cell migration (Sieg et al., 1999). With hyperosmotic environments, the opposite was found, whereby hypertonic saline in fact attenuates tumor cell migration by reducing integrin expression (Shields et al., 2006, 2004).

Interestingly, this negative trend in migration behavior was not paralleled when EF was applied. Instead, a parabolic trend was observed, whereby both hypo- and hyper-tonic cells exhibited enhanced migration. The contrasting effects noted here suggest an additional influence from the applied EF that directs migration. One possibility may be polarized redistribution of channels and transporters. The findings from Study 1 confirm that AQP channels are localized to the perimeters of the cell during EF-induced migration, contrary to their location during normal migration in the absence of EF; as a consequence, physical presentation of the cell (swollen in hypotonic conditions, shrunken in hypertonic conditions) could influence the degree of polarization and consequently the rate at which water flux occurs. This is further supported by our observations that significant directional (cathodal) migration was noted only for cells incubated in a hypotonic medium.

4.3 Characterizing Chondrocyte and SDSC Migration in an Inflammatory Environment

4.3.1 Introduction

SDSCs have shown resistance to the catabolic factors (e.g. interleukin 1β and tumor necrosis factor-α) that are present in synovial fluid during injury (Nagase et al., 2008; Zimmermann et al., 2001). Additionally, it has been speculated that in the presence of partial thickness defects in rabbits, SDSCs are recruited to the wound site (Hunziker and Rosenberg, 1996), although the mechanism of inducing their migration is unknown. While IL-1 has been widely implicated in the degradation of extracellular matrix components, less is known regarding how isolated synovium derived stem

cells (SDSCs) exposed to IL-1 behave. In studies reported in the literature, the addition of IL-1 to chondrocytes in 2D culture induced a loss of phenotype and decreased the expression of cytoskeletal components such as tensin, talin, paxillin, and focal adhesion kinase (Vinall et al., 2002), thereby altering their migration behavior. Whether the resistant nature of SDSCs extends to migration response has not been examined. Accordingly, we sought to determine the effect of cytokine exposure on the response of expanded SDSCs and chondrocytes, for comparison, to an applied DC electric field. A more complete understanding of how IL-1, a common pro inflammatory agent present during injury and disease, influences cell migration may provide new insight into the wound healing process and techniques that may be used to guide and direct the repair of articular cartilage.

4.3.2 Materials and Methods

4.3.2.1 Cell Isolation and Expansion

Articular cartilage and the intimal layer of the synovium were harvested from bovine knee joints of four freshly slaughtered 2-4 week old calves. Cartilage was digested in high-glucose DMEM with collagenase IV (Worthington Biochemical Corporation, Lakewood, NJ) for 11 h at 37°C with shaking. Synovial tissue was digested in alpha Modified Eagle's Medium (α-MEM) with collagenase type IV (Worthington, Lakewood, NJ) for only 4 h at 37°C with gentle shaking.

Cell suspensions were filtered through a 70μm porous mesh and sedimented in a bench-top centrifuge for 15 min at 1500g. Viable cells were counted with a hemocytometer and trypan blue and plated at high density (20×10^3 cells/cm^2) for chondrocytes and at low density (1.76×10^3 cells/cm^2) for SDSCs. Medium (DMEM or α-MEM for chondrocytes and SDSCs, respectively) was supplemented with 10% fetal bovine serum, 100 U/mL each of penicillin, streptomycin, and fungizone, and a growth factor cocktail (1 ng/mL TGF-β1, 5 ng/mL bFGF, and 10 ng/mL PDGF-$\beta\beta$ (Ng et al., 2010; Sampat et al., 2011)). Medium was changed every three days. Chondrocytes were expanded and used after 1 passage (Chao et al., 2000), while SDSCs were cultured for 4 passages before use, as informed by Section 4.2. A subset of each of these cell types was also

expanded in the presence of 10 ng/mL IL-1α for the passage immediately prior to their use.

4.3.2.2 Galvanotaxis

At confluence, cells were trypsinized and resuspended at 50×10^3 cells/mL in DMEM containing 5% (v/v) FBS, amino acids (0.5× minimal essential amino acids, 1× nonessential amino acids), buffers (10 mM HEPES, 10 mM sodium bicarbonate, 10 mM TES, 10 mM BES), and antibiotics (100 U/mL penicillin, 100 mg/mL streptomycin) and allowed to equilibrate for 1 h. Cells were then plated at 2.65×10^4 cells/cm^2 onto sterile glass slides (Fisher Scientific, Pittsburgh, PA) using removable silicone wells. After cells were allowed to attach for 1 h in a 5% CO_2 incubator at 37°C, the slide was rinsed with medium to remove any nonadherent cells and placed into a custom galvanotaxis chamber (described in Section 4.2.2.3) under aseptic conditions. Approximately 30-40 cells were observed in each field of view; images were acquired at 5 min intervals.

4.3.2.3 Cell Migration Parameters

The position of each cell was manually tracked via a custom MATLAB program that utilizes measurements of the net centroid displacement from the starting position (set as origin) to calculate overall speed of migration for each cell (the net displacement in the experiment divided by the 3 h time span of observation). Migration direction was quantified as $\sin\phi$, where ϕ is the angle between the x-coordinate axis and the migration vector, such that $\sin\phi$ was defined as the value -1 when ϕ = 4.71 rad (270°), the direction of the cathode. The directional velocity, defined as the component of the speed directed toward the negative pole (e.g. (Chao et al., 2000, 2007)), was obtained by multiplying a cell's speed by $\sin\phi$. Each data point represents the mean and standard deviation 60-80 samples.

4.3.2.4 Statistics

A two-way ANOVA was performed on cell speed, directed velocity, and total displacement for factors of treatment (applied EF vs. control), and interleukin exposure to determine significance

($p<0.05$) of the effect of each factor and also the interaction of the factors. Tukey's honest significant difference (HSD) *post hoc* test was performed to assess significance ($p<0.05$).

4.3.3 Results

Chondrocytes expanded in the presence of IL-1 exhibited diminished proliferative capacity, reaching confluence in 1.25x the time of normal expanded cells, perhaps due to apoptosis following IL-1 exposure. In comparison, SDSCs yielded no significantly observable differences in proliferation rate. At t=3hr following application of DC electric field, both chondrocytes and SDSCs which had been cultured in normal expansion media reoriented their long axis perpendicular to the direction of field. SDSCs exposed to IL-1 showed similar behavior following field. However, only chondrocytes exposed to IL-1 during expansion failed to elongate perpendicular to the applied field (Figure 4.7).

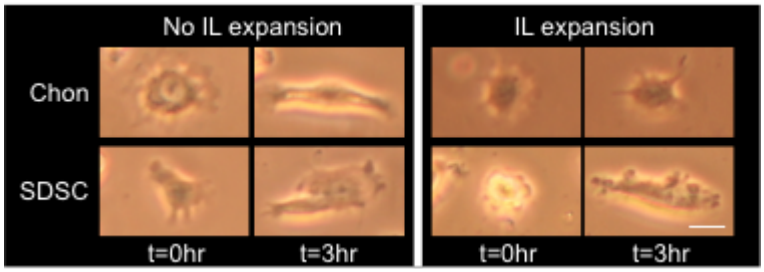

Figure 4.7: Representative images of chondrocytes and SDSCs for both expansion groups (IL-1 and no IL-1) at t=0hr and t=3hr after DC electric field was turned on. Scalebar = 20 μm.

Cell migration parameters followed these noted behaviors regarding cell proliferation and presentation; for normally expanded chondrocytes and SDSCs, cells moved faster and preferentially toward the cathode compared with no EF control cells (Figure 4.8a,b, $p<0.05$). The response of IL-expanded cells to a field depended on the specific cell type; chondrocytes exhibited a significant change in migration patterns (slower movement, reversal in migration direction, Figure 4.8c, $p<0.05$) while SDSCs showed no significant variation in speed or directed velocity (Figure 4.8d, $p>0.05$). Control cells exhibited no significant differences in speed or directed velocity regardless of expansion method.

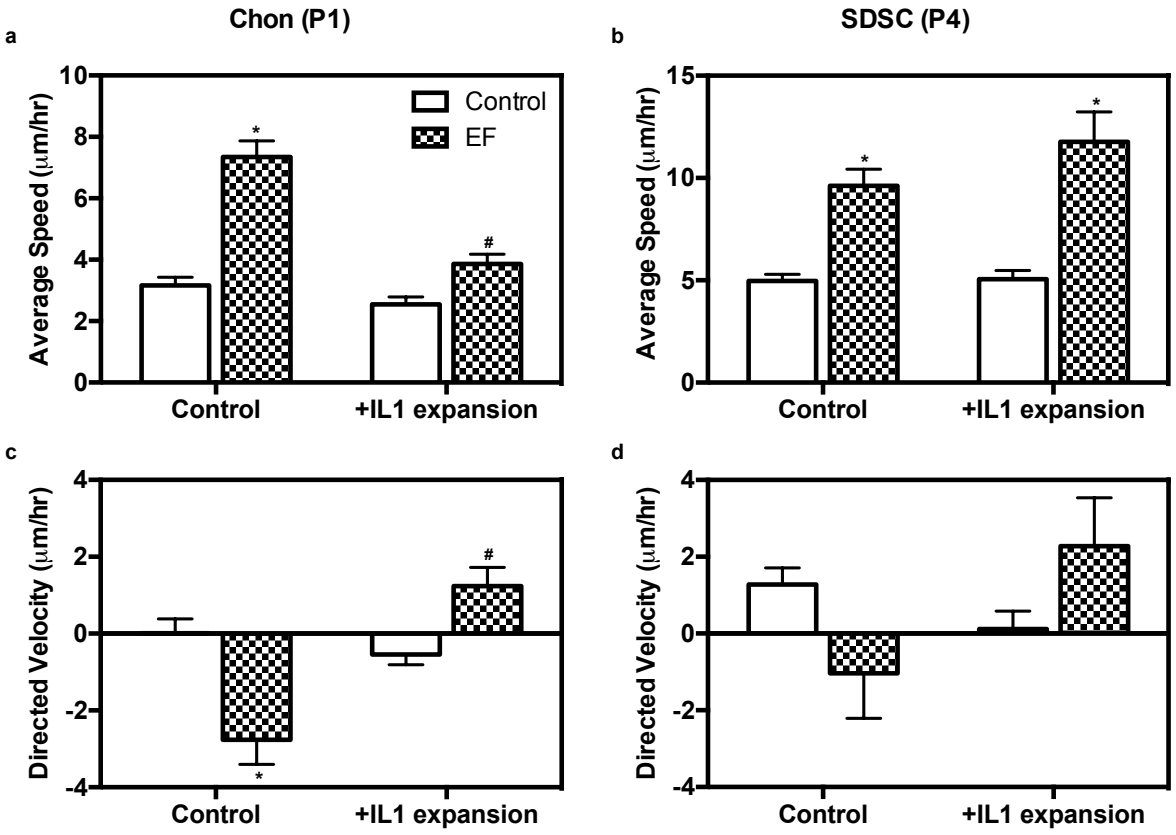

Figure 4.8: Migration parameters ((a,b) speed, (c,d) directed velocity) for chondrocytes (at P1) and SDSCs (at P4). *$p<0.05$ vs. no EF control, $^{\#}p<0.05$ vs. no IL control, n=60-70 cells/group.

4.3.4 Discussion

Our results have confirmed current literature findings that exposure to IL-1 negatively affects chondrocyte proliferation and alters and stymies migration ability, possibly due to stabilization of F-actin by a pathway of activated members of the Rho family of small GTPases (Pritchard and Guilak, 2006). Surprisingly, individually isolated SDSCs that have been primed with a growth factor cocktail, to induce chondrogenesis, appear resilient to such catabolic insult and show little change in their migration behavior. The implications of this work suggest that SDSCs may be a more favorable cell source for guided wound repair of articular cartilage, as they possess a natural ability to withstand the harsh environment of the injured joint.

4.4 Conclusion

Varying extracellular osmotic environment was noted to significantly alter cell migration patterns in a way not previously characterized by the existing literature. This dissertation provides new insights into the mechanotransduction ensuing from extracellular osmotic challenges within the context of clinically relevant electric fields, and highlights the role of AQP1 in modulating migration. Notably, the redistribution of AQP1 membrane proteins to the periphery of the pseudopods rather than to the leading edge is surprising. In injured tissues, injury potentials are created and produce electric fields that exist for days. The relative local changes in extracellular osmotic environment stemming from injury may therefore have significant influence on wound repair. Interestingly, while we noted agreement with the literature that during exposure to IL-1, chondrocytes exhibit impaired migration due to their disrupted cytoskeletal networks, the same was not true for SDSCs, suggesting that these AQP1 channels may be sensing the extracellular environment differently, leading to more effective regulation of volume changes and migration capacity.

Chapter 5

Directing Mesenchymal Stem Cell Migration using Applied Direct Current Electric Fields

5.1 Introduction

An intriguing potential for galvanotaxis studies is the use of electric fields as a procedure to identify desirable populations of cells. To establish this paradigm, detailed characterization of the response of a wide range of clinically relevant cells is needed. As such, we first focused on distinguishing favorable (defined to be responsive to EF stimulus) cell populations. Though autologous cell sources are most suitable for cartilage repair, these tissues pose a number of challenges, including a lack of viable tissue and donor site morbidity. In consideration of these limitations, we and others have investigated the use of MSCs, in particular SDSCs, as substitutes for chondrocytes (Pei et al., 2008; Sakaguchi et al., 2005; Yoshimura et al., 2007) and have successfully generated material and mechanical properties similar to native cartilage when encapsulated in agarose hydrogel (Sampat et al., 2011). Bovine SDSCs from skeletally immature animals are readily available, well characterized, and found to be capable of robust tissue growth in culture and their use facilitates comparisons

of our current findings to our earlier work with juvenile bovine SDSCs (Sampat et al., 2011) and chondrocytes (Chao et al., 2000). To facilitate translation to a canine pre-clinical model as well as potential translation in humans, the migration behavior of cells from these other sources was assessed to identify promising populations of cells for cartilage repair.

To this end, first, we performed a thorough analysis of the passage-dependent behavior of juvenile bovine SDSCs to correlate any noticeable changes in cell migration with cell makeup and presentation (Section 5.2). After observing a migration response dependency in juvenile bovine SDSCs, we expanded our exploration to see whether the effect was conditional on the particular age and species of the cells (Section 5.3). Together, these findings add to the repertoire of already performed studies and provide a baseline to use when designing strategies for guided wound repair.

5.2 Passage-Dependent Migration Behavior of SDSCs

5.2.1 Introduction

Stem cells such as SDSCs exhibit phenotypic and behavioral changes as terminal differentiation is reached. Previously, we determined via flow cytometry that changes in cell surface molecules are measurable throughout differentiation; some of these surface molecules may in fact serve as growth factor receptors or adhesion molecules that play a direct role in the differentiation process. Further, it was shown that manipulation of cell surface charges with chemical modifiers such as neuraminidase, an enzyme that removes sialic acids (Schengrund et al., 1976), or lectins (Patel and Poo, 1982), alters EF motility (Finkelstein et al., 2007), pointing to a strong influence of surface molecules in directed migration. Taken together, these results suggest the hypothesis that differentiating SDSCs exhibit markedly different behavior depending on culture expansion age.

To date, previous studies have not correlated a change in cell surface marker expression with a change in migration response to EF. It is not clear whether certain passage cells are preferentially more likely to adopt a phenotype favorable for cartilage matrix development. Thus, here, we examined the surface markers and migration characteristics of SDSCs through four passages of

culture; we hypothesized that as SDSCs reach a chondrocytic phenotype, their migration characteristics begin to resemble those reported for chondrocytes (Chao et al., 2000). In parallel, through 3D pellet cultures using cells from each passage, we attempted to elucidate the passage at which SDSCs exhibit the greatest potential to synthesize cartilaginous matrix, in order to optimize their use for tissue-engineered constructs.

5.2.2 Materials and Methods

5.2.2.1 Experimental Design

Three controlled and concurrent cell culture studies are described herein, aimed at characterizing the behavior of juvenile bovine SDSCs. Specifically, study one examined the effect of cell passage number on the expression of four cell surface markers found on MSCs. Study two characterized the cellular response of these cells at each passage to an applied DC EF of comparable magnitude as those found at the cut surface of wounds in order to identify a cell population most suitable for wound repair. Finally, study three explored the development of tissue generated from cells derived from each passage to investigate a potential correlation between cell migration behavior and matrix composition.

5.2.2.2 Cell Isolation and Expansion

The intimal layer of the synovium was harvested from bovine knee joints of four freshly slaughtered 2-4 week old calves. Synovial tissue was digested in αMEM with collagenase type IV (Worthington, Lakewood, NJ) for 4 h at 37°C with gentle shaking. Cell suspensions were filtered through 70 μm mesh filters and then retrieved from the pellet after bench-top centrifugation for 15 min at 1500 g. Viable cells were counted in a hemacytometer with trypan blue and plated at 1.76×10^3 cells/cm^2 in αMEM containing 10% fetal bovine serum, 100 U/mL each of penicillin, streptomycin, and fungizone, and a growth factor cocktail (1 ng/mL TGF-β1, 5 ng/mL bFGF, and 10 ng/mL PDGF-$\beta\beta$ (Ng et al., 2010; Sampat et al., 2011); all media components were from Invitrogen). Medium was changed every three days. At confluence, cells were trypsinized and then counted. One subset

of the cells at each passage was replated for further expansion, another subset was used for flow cytometry analysis, a third subset was used for galvanotaxis experiments, and a final subset was used for 3D micropellet culture.

5.2.2.3 Cell Surface Marker Assessment

The phenotype of bovine SDSCs at each passage was assessed by flow cytometry. At each passage (P1 to P4), cells in suspension were incubated with fluorescein isothiocyanate (FITC)- or phycoerythrin (PE)-conjugated monoclonal antibodies in phosphate-buffered saline (PBS, Invitrogen) containing 2 mM EDTA (Invitrogen). Unstained cells were used as a negative control to assess background fluorescence. Cells were stained with antibodies against CD31 (endothelial cell marker, Thermo Scientific), CD34 (hematopoietic cell marker, Abcam), and mesenchymal markers CD49c (Thermo Scientific) and CD73 (BioLegend) (Chamberlain et al., 2007; Fan et al., 2009); Positive MSC classification required the absence of CD31 and CD34 and presence of CD73 (Dominici et al., 2006), while CD49c is a marker of chondrogenic potential of MSCs. Cells were incubated in the dark at room temperature for 15 min, after which they were washed and resuspended in 0.5 mL PBS containing 2 mM EDTA for analysis. Cellular fluorescence was evaluated using a FACSCalibur flow cytometer (Becton Dickinson, Franklin Lakes, NJ) and the resulting data analyzed with FlowJo software (version 9.3.2).

5.2.2.4 Galvanotaxis

After trypsinization, cells were resuspended at 50×10^3 cells/mL in DMEM containing 5% (v/v) FBS, amino acids (0.5× minimal essential amino acids, 1× nonessential amino acids), buffers (10 mM HEPES, 10 mM sodium bicarbonate, 10 mM TES, 10 mM BES), and antibiotics (100 U/mL penicillin, 100 mg/mL streptomycin) and allowed to equilibrate for 1 h. Cells were then plated at 2.65×10^4 cells/cm^2 onto sterile glass slides (Fisher Scientific, Pittsburgh, PA) using removable silicone wells. After cells were allowed to attach for 1 h in a 5% CO_2 incubator at 37°C, the slide was rinsed with medium to remove any nonadherent cells and placed into a custom galvanotaxis

chamber under aseptic conditions, as described in Section 4.2.2.3 (Figure 4.1).

5.2.2.5 Cell Migration Parameters

The position of each cell was manually tracked via a custom MATLAB program that utilizes measurements of the net centroid displacement from the starting position (set as origin) to calculate overall speed of migration for each cell (the net displacement in the experiment divided by the 3 h time span of observation). Migration direction was quantified as $\sin\phi$, where ϕ is the angle between the x-coordinate axis and the migration vector, such that $\sin\phi$ was defined as the value -1 when ϕ = 4.71 rad (270°), the direction of the cathode. The directional velocity, defined as the component of the speed directed toward the negative pole (e.g. (Chao et al., 2000, 2007)), was obtained by multiplying a cell's speed by $\sin\phi$. Each data point represents the mean and standard deviation 60-80 samples. A two-way ANOVA was performed on cell speed, directed velocity, and total displacement for factors of treatment (applied EF vs. control), and passage number to determine significance ($p<0.05$) of the effect of each factor and also the interaction of the factors. Tukey's honest significant difference (HSD) *post hoc* test was performed to assess significance ($p<0.05$) between each treatment and passage group. Chi square tests for linear trends were used to analyze the percentage of responding cells migrating in the cathodal direction.

5.2.2.6 Micropellet Culture

Following trypsinization at each passage, cells were counted and 0.5 mL each of a 1×10^6 cell suspension was aliquotted into 1.5 mL sterile screw-top tubes. The tubes were spun in a microcentrifuge at 37°C and 2500 rpm for 20 minutes to form a visible cell pellet at the base of the tube. Micropellets were stored in an incubator maintained at 37°C and 5% CO_2 for the duration of the study (42 days). Media was prepared from high-glucose DMEM with the addition of 100 nM dexamethasone (Sigma), 100 μg/mL sodium pyruvate (Sigma), 50 μg/mL L-proline (Sigma), 1% ITS+ premix (Becton Dickinson), and 1% antibiotic-antimycotic (Invitrogen). 50 μg/mL ascorbic acid (Sigma) was added fresh to the media on each media change day and 10 ng/mL TGF-β3 (R&D Systems)

was introduced for the first 21 days in culture. At days 14, 28, and 42, micropellet samples were harvested. Media was completely removed and one subset of the micropellets was individually stored at -20°C for biochemical assaying (n=5). The other subset of micropellets was fixed in acid formalin ethanol for immunohistological analysis.

5.2.2.7 Micropellet Immunohistological Analysis

Fixed samples were paraffin embedded, sectioned (8μm thick), and stained for type I and type II collagen, as previously described (Kelly et al., 2004). Briefly, sections were digested in 0.5 mg/mL testicular hyaluronidase, swollen in 0.5M of acetic acid, blocked in 10% normal goat serum (NGS) and labeled with 10% NGS containing monoclonal primary antibody for type I and II collagens (Abcam). Alexa Fluor 488-conjugated goat anti-mouse secondary antibody labeling (Invitrogen) and TOTO-3 nuclear counterstaining (Invitrogen) were performed to visualize the collagen networks and cells, respectively. After staining, slides were coverslipped with Fluoroshield (Sigma) and sections were analyzed using an inverted microscope with an Olympus Fluoview confocal system with dual wavelengths excitation at 488 and 640 nm. Intensity profiles of the stains were generated from a line drawn through the center of the pellet and a 6^{th} order smoothing curve (32 neighbors) was superimposed to capture and characterize distribution profiles of collagen matrix formation.

5.2.2.8 Micropellet Biochemical Analysis

Samples were thawed, lyophilized, weighed dry, and digested for 16h at 56°C in proteinase K (MP Biomedicals), as described previously (Riesle et al., 1998). Aliquots of digest were analyzed for DNA content as quantified by the PicoGreen assay (Invitrogen) (McGowan et al., 2002). Glycosaminoglycan (GAG) content was measured by the 1,9 dimethylmethylene blue (Sigma) dye-binding assay (Farndale et al., 1982). A third aliquot of digest was acid hydrolyzed in 12N HCl at 110°C for 16h, dried, and resuspended in assay buffer, as previous described (Kelly et al., 2006). Ortho-hydroxyproline (OHP) content was determined via a colorimetric reaction with chloramine T (Sigma) and dimethylaminobenzaldehyde (Sigma) (Stegeman and Stalder, 1967); collagen content

was calculated using a 1:7.64 OHP-to-collagen mass ratio (Hollander et al., 1994). Each data point represents the mean and standard deviation of five samples. Groups were examined for significant differences by two-way analysis of variance (ANOVA), with GAG, DNA, or OHP as the dependent variables, and passage number as the independent variable. Tukey's honest significant difference (HSD) *post hoc* test was performed to assess significance ($p<0.05$).

5.2.3 Results

5.2.3.1 Cell Surface Marker Expression

The expression of cell surface markers in bovine SDSCs from P1 to P4 was evaluated by flow cytometry. Less than 3% of the analyzed population expressed CD31 or CD34 at any passage. Conversely, CD49c and CD73 were expressed. Expression of CD49c ($\alpha 3$ integrin) was stable and high (>93%) during all passages. However, CD73 expression (ecto-5′nucleotidase, SH3, SH4) showed a net change in expression from P1 (49.3%) to P4 (27.9%); CD73 expression initially increased from P1 to P2 ($p<0.05$) and then decreased at P3 and P4 ($p<0.01$) (Figure 5.1).

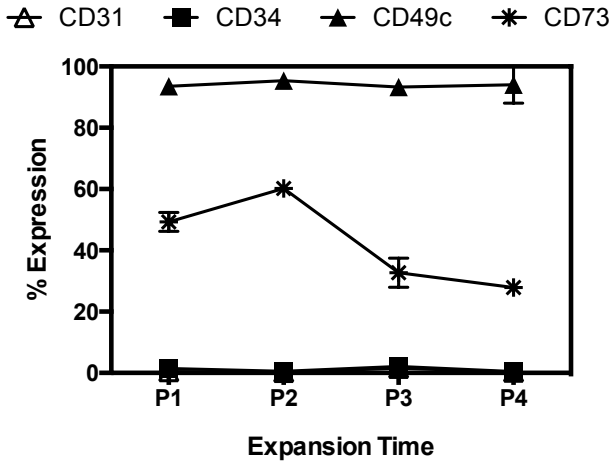

Figure 5.1: Cell surface marker expression of CD31, CD34, CD49c, and CD73 over culture passage time in a growth factor cocktail. Each data point represents the average expression of cells from three separate harvests.

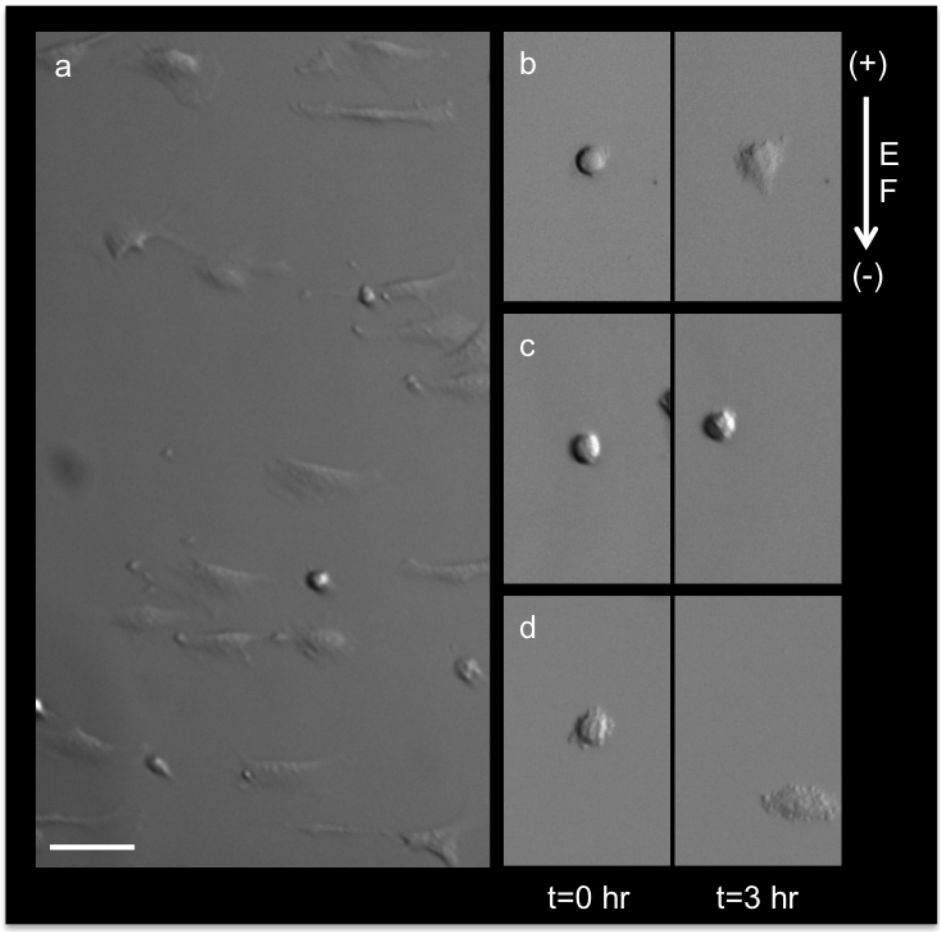

Figure 5.2: (a) Representative endpoint (t=3hr) EF cells with realignment of the long axis perpendicular to the direction of the field. Representative micrographs of (b) control cells and EF cells at (c) P1 and (d) P4. Final cell positions (images on right) were compared to initial cell positions (images on left) and used to calculate overall displacement, speed, and directed velocity. Scalebar = 50 μm.

5.2.3.2 EF-Induced Cell Realignment and Migration

Following exposure to an applied DC EF, the majority of cells reoriented their long axis perpendicular to the direction of the field; this orientation was not influenced by passage number (Figure 5.2a). The passage number of the cells, however, did directly influence the direction of induced migration. At P1, 85% of cells migrated primarily toward the positive pole (anode, Figure 5.2c); by P4, nearly 70% of SDSCs had changed their direction of migration and moved toward the negative pole (cathode, Figure 5.2d). A chi square test used to detect linear trends showed a significant de-

crease at each passage in cells migrating toward the anode (Figure 5.3b, $p<0.05$). For comparison, control cells showed little bias toward either pole at all passages, (57% $\pm$ 6.7 toward the anode) and their net displacement away from the point of origin was not significant ($p=0.13$, Figure 5.2b, Figure 5.3a).

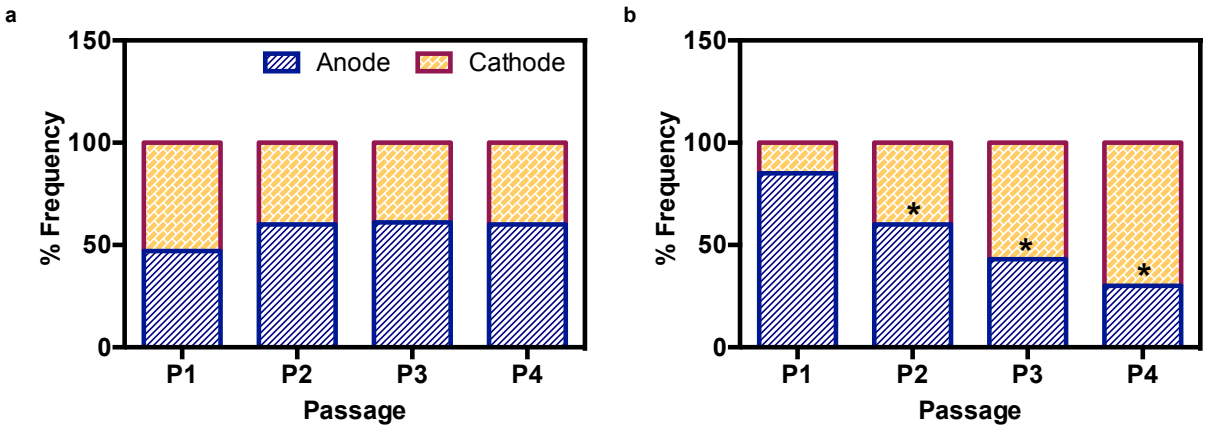

Figure 5.3: Percentage of cells migrating toward the anode (positive pole) and the cathode (negative pole). (a) Control cells showed no significant difference in migration direction across all passages. (b) EF cells significantly changed direction with increasing passage. *$p<0.0001$.

5.2.3.3 Cell Migration Parameters: Speed and Displacement depend on Passage Number

At all passages, SDSCs exposed to an applied DC EF traveled faster and migrated a further net distance than cells expanded similarly, but not exposed to a field ($p<0.05$, Table 5.1). Throughout passages P1-P4, the spontaneous migration for control cells remained similar to passage P1 ($p_{P1-P2}=0.15$; $p_{P1-P3}=0.42$; $p_{P1-P4}=0.57$), though there was a significant drop in speed ($p<0.0001$) and displacement ($p<0.0001$) following P2. Decreased motility mirrored the decrease in CD73 surface marker expression ($p<0.0001$). Similarly, under the influence of the applied EF, cells also showed a significant drop in speed following P2 ($p<0.0001$).

Table 5.1: Migration data from galvanotaxis studies performed for 3 hours

		Net displacement (μm)	**ϕ (rad)**	**Speed (μm/hr)**	**Directed Velocity (μm/hr)**
P1	Control	12.1 ± 7.13	3.12 ± 1.64	4.03 ± 2.38	-0.43 ± 3.00
	EF	20.6 ± 13.9	2.58 ± 1.70	9.18 ± 5.48	4.03 ± 4.74
P2	Control	18.7 ± 9.85	2.74 ± 2.02	6.22 ± 3.28	0.46 ± 4.98
	EF	29.1 ± 16.1	2.77 ± 1.84	9.69 ± 5.38	1.38 ± 5.65
P3	Control	6.93 ± 5.61	2.40 ± 1.81	2.31 ± 1.87	0.17 ± 1.95
	EF	14.2 ± 10.9	3.47 ± 1.76	4.75 ± 3.65	-0.93 ± 4.82
P4	Control	7.33 ± 5.42	2.40 ± 2.01	2.45 ± 1.81	0.38 ± 1.96
	EF	21.1 ± 13.7	3.91 ± 1.75	7.03 ± 4.58	-3.26 ± 6.02

5.2.3.4 Passage-Dependent Tissue Development

ECM development from SDSC pellet culture was increasingly dependent on the extent to which cells had been expanded in a growth factor cocktail and the corresponding passage number. Pellets comprised of early passage cells (P1) elaborated significantly greater amounts of GAG/dw compared to pellets containing late passage cells (P4) by day 28 (16.3 ± 1.89 %/dw vs. 10.5 ± 1.20 %/dw, $p<0.0001$) and this trend was consistent for day 42 (20.2 ± 3.64 %/dw vs. 7.35 ± 0.85 %/dw, $p<0.0001$, Figure 5.4a). In fact, P1 pellets appeared to continue elaborating GAG following day 28, while P4 pellets began losing GAG content. In comparison, an opposing trend was noticed with collagen content; P4 pellets showed significantly increased amounts of collagen at all timepoints

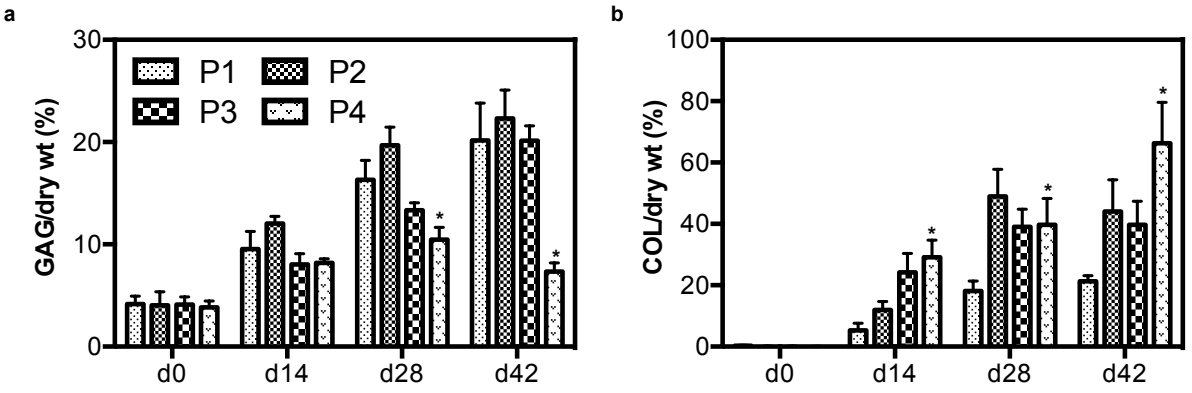

Figure 5.4: Biochemical content ((a) GAG/dry wt and (b) COL/dry wt) of SDSC pellets from cells at different passages.*$p_{P4}<0.05$ vs. P1

starting at day 14 relative to P1 pellets (day 14: 52.2 ± 7.49 %/dw vs. 11.2 ± 2.77 %/dw ($p<0.0001$); day 28: 43.5 ± 8.65 %/dw vs. 24.2 ± 4.33 %/dw ($p<0.0001$); day 42: 67.5 ± 8.56 %/dw vs. 27.1 ± 4.50 %/dw ($p<0.0001$), Figure 5.4b).

5.2.3.5 Substantial Collagen II Deposition of Late Passage SDSCs

Immunohistochemical staining revealed that collagen II deposition was more elaborate and consistent in P4 pellets than P1 pellets (Figure 5.5f vs. Figure 5.5b). Intensity profiles through the diameter of the construct confirm nonhomogenous sinusoidal distribution of collagen fibers initially at P1 (Figure 5.5d) that fills in with increasing passage number to P4, maintaining intensity across the pellet at an elevated gray value (Figure 5.5h). Collagen I deposition was localized mainly to the periphery of all pellets (Figure 6a,e), though was increasingly consistent for P4 pellets compared to their early counterparts (Figure 5.5g vs. Figure 5.5c).

5.2.4 Discussion

To our knowledge, this is the first study to characterize the changing surface marker expression and migration pattern of SDSCs over time in culture. We have reported here that at early passages (P1, P2), cultured SDSCs exhibit anodal migration under EF strengths previously used to elicit galvanotaxis in chondrocytes. SDSCs switch their direction of migration on the same timescale, moving preferentially toward the cathode, just as permanently differentiated chondrocytes do.

SDSCs show considerable plasticity over extended passages; this plasticity is sufficient to change their migration direction in response to an applied EF. The SDSCs' changes in migratory response to an applied EF may occur by one of several mechanisms. First, migration changes may be attributable to an altered differentiation state.

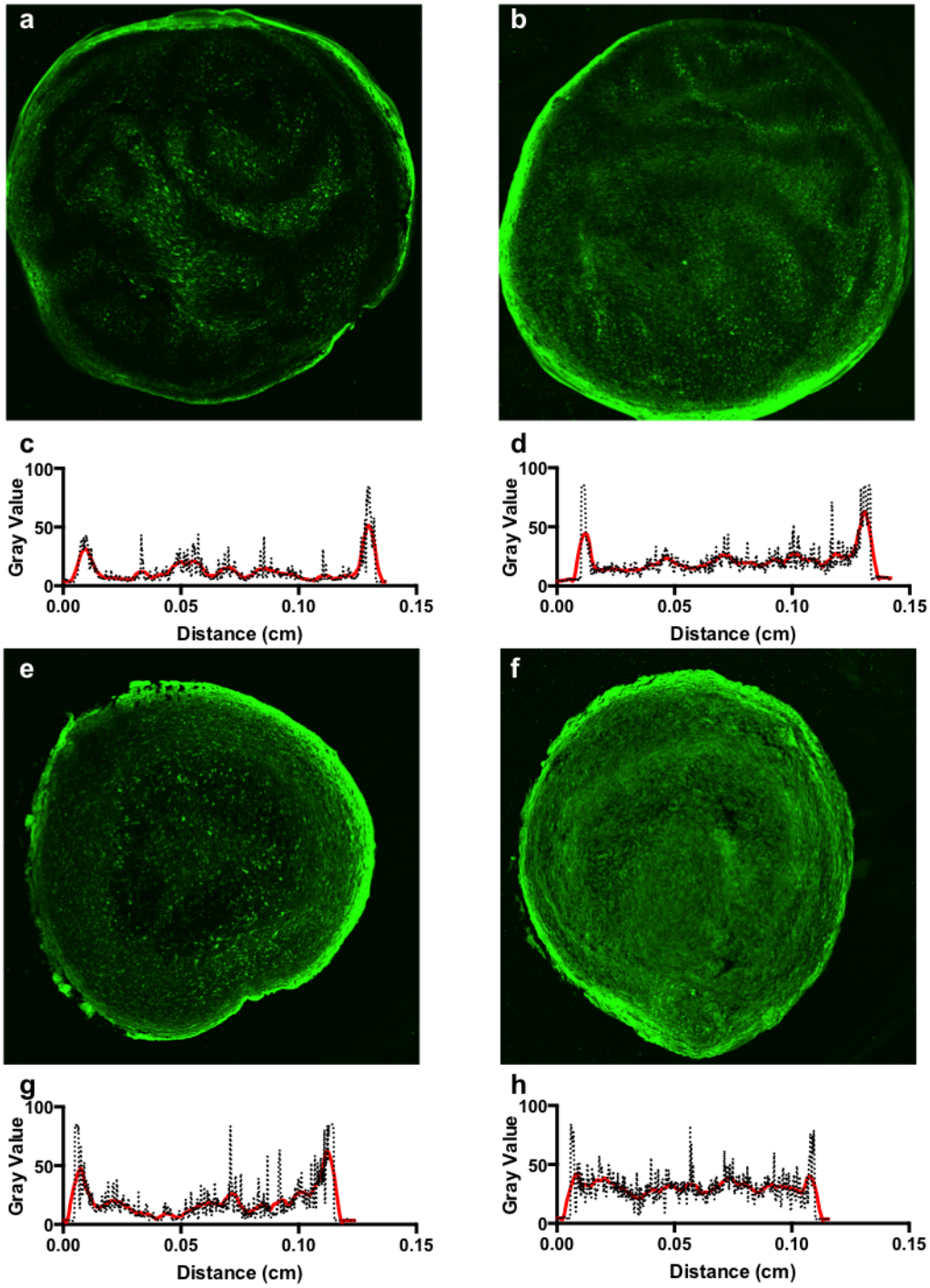

Figure 5.5: Immunohistochemical stains of collagen I (a,e) and collagen II (b,f) for pellets comprised of P1 (top row) and P4 (bottom row) expanded cells. Intensity profiles (c,d,g,h) through the center of the pellet reveal localized distribution patterns for each matrix component. Scalebar = 200 μm.

During cell culture, SDSCs are exposed to a growth factor cocktail comprised of cytokines known to be responsible for driving differentiation or redifferentiation of cells toward a chondrocyte-like state (Ng et al., 2010; Sampat et al., 2011). In particular, progressive differentiation of the SDSCs can mediate not only changes in simple physical parameters of the culture but, as we show here, also expression of cell surface molecules.

Previous studies found that early passage MSCs share morphological characteristics with fibroblasts (elongated, flat cells (Alt et al., 2011)). Further, both express N-cadherin and neural cell adhesion molecules (N-CAM) (DeLise et al., 2000), key regulators of cell-cell interaction and cell migration (Eggers et al., 2011). Additional exposure to growth factors brings about a chondrocyte differentiation process marked by distinct changes in cell morphology. Cells convert to a more spherical shape that underlies varying physical traits known to influence motility. We also note that in late passage SDSCs, actin filaments appear dense and contracted, which may limit mobility and active migration. Alternatively, extended exposure to the growth factor cocktail may induce molecular changes to the cell surface of the differentiating cells. Indeed, flow cytometry revealed changes in surface molecules, although identifying the best candidates that may mediate changes in EF responses will require further systematic study.

Expression of surface-associated proteins of chondrocytes (e.g. collagen II, keratin, sulfated proteoglycans) that are shed into the ECM surrounding the cells also increases with further expansion (Alegre-Aguaron et al., 2014). Changes in surface charge may be mediated by these surface-associated proteins, causing the cells to respond differently to the applied EF. Regulation of specific surface proteins can also change motility in EF-exposed cells. For example, upregulation of various ECM receptors for collagen and fibronectin, such as the $\alpha_2\beta_1$ integrin, have been reported to be crucial for cell migration (Etienne-Manneville and Hall, 2001); these receptors polarize the integrin and its downstream effector RhoA to influence directionality of migration (Tsai et al., 2012). Whether there are any changes in the distribution of $\alpha_2\beta_1$ integrin receptors at different passages of SDSCs and if so, whether they alter organization of the ECM receptors and their related signaling molecules have yet to be determined experimentally.

The altered migratory patterns we measured in SDSCs are likely to be initiated through changes in expression of cell surface markers, which accompanies increasing passages. We observed one such change, namely, a significant decrease in the CD73 marker for stem cell expression. In addition to bolstering our previous hypothesis that the cells have adopted a more chondrocyte-like phenotype in P4 than in P1, these observations raise the possibility that CD73 or ecto-5′-nucleotidase, an enzyme that catalyzes the conversion of extracellular nucleotides to adenosine, plays a direct role in mounting a motility response to EF. Indeed, the observed motility decreases from P1-P4 support reports implicating CD73 in directly regulating cell migration (Ode et al., 2011).

Additionally, exogenously delivered factors such as bFGF (Maniwa et al., 2001) and PDGF-$\beta\beta$ (Schmidt et al., 2006) have been found to modulate and influence cell migration, perhaps as direct chemokinetic factors, similar to the roles of receptors for epidermal growth factor and hepatocyte growth factor during tumor invasion (Wells, 2000). Alternatively, components of the growth may alter motility via their capacity to upregulate the extracellular-signal-regulated kinase (ERK) and p38 mitogen-activated kinase (MAPK) signaling pathways (Giuliani et al., 1999). Upregulation of MAPK-1 protein was indeed observed in this study. In keratinocytes and neutrophils, rapid and sustained phosphorylation of ERK, MAPK and Src is also a direct consequence of exposure to EF (Zhao et al., 2006). In fact, activated Src kinase polarizes in the migration direction and recruits phosphatidylinositol 3,4,5-triphosphate (PIP3) to the leading edge of the cell, and targets the tumor suppressor phosphatase and tensin homologue (PTEN) to the lateral and back edges.

Although the primary responder(s) to the EF are still unknown, the PIP3 and PTEN redistributions are mediated by the Phosphatidylinositol 3-OH kinase-γ (PI(3)Kγ) pathway and its upstream activators, receptor tyrosine kinases (RTK) (Zhao et al., 2006). As such, it is reasonable to expect cells at different passages, which exhibit different degrees of growth factor exposure and binding to RTKs, will also exhibit varying responses to the applied EF. For example, an alteration or attenuation in the distribution of PIP3 and PTEN that is caused by altered growth factor exposure could shift the cells' migration direction. Taken together, previous studies, along with results presented here, point to the likelihood for growth factor priming and expansion to alter the behavior and

response of the cells to external stimuli.

Late passage cells reveal the capacity to create cartilaginous-like tissue with increased expression of GAG and collagen by day 42. Surprisingly, however, these cells exhibited stunted GAG deposition that may be due to the abundance of elaborated collagen that, for the first time, nears native levels (∼60-70%/dry weight). This inverse relationship between GAG and collagen quantities follows trends noted previously for engineered cartilage (Bian et al., 2009). Confirmation of the presence of type II collagen at P4, the form predominantly found in articular cartilage, via immunohistological staining further suggests that only after multiple passages do cells possess a phenotype that resembles chondrocytes. That this phenotype is correlated with chondrocyte-like migration behavior suggests that collagen II receptors and their associated $\alpha_{10}\beta_1$ integrins may be directly involved in directed movement.

5.3 Cell Age and Species Origin Influence Migration Behavior

5.3.1 Introduction

For cartilage repair, the cells that are available may be limited and come from a variety of sources. To understand whether the trends noted in Section 4.2 hold for an older population of cells and from different species, a follow-up study was performed.

5.3.2 Materials and Methods

5.3.2.1 Cell Isolation and Expansion

The intimal layer of the synovium was harvested from juvenile and adult bovine and canine knee joints. Synovial tissue was digested in αMEM with collagenase type IV (Worthington, Lakewood, NJ) for 4 h at 37°C with gentle shaking. Cell suspensions were filtered through 70 μm mesh filters and then retrieved from the pellet after bench-top centrifugation for 15 min at 1500 g. Viable cells were counted in a hemacytometer with trypan blue and plated at 1.76×10^3 cells/cm^2 in alpha minimum essential medium containing 10% fetal bovine serum, 100 U/mL each of penicillin,

streptomycin, and fungizone, and a growth factor cocktail (1 ng/mL TGF-β1, 5 ng/mL bFGF, and 10 ng/mL PDGF-$\beta\beta$ (Ng et al., 2010; Sampat et al., 2011)). Medium was changed every three days. One subset of the cells at each passage was replated for further expansion and the other subset was used for galvanotaxis experiments.

Human bMSCs were isolated from fresh unprocessed bone marrow (Lonza) of a 22 year-old male donor. Following separation via Percoll gradient, mononucleated cells were plated (5×10^3 cells/cm^2 in DMEM); adhered MSCs were expanded until passage 4, as described above. To ensure a pure population, cells were only used starting after 2 passages.

5.3.2.2 Galvanotaxis

At confluence, cells were trypsinized and resuspended at 50×10^3 cells/mL in DMEM containing 5% (v/v) FBS, amino acids (0.5× minimal essential amino acids, 1× nonessential amino acids), buffers (10 mM HEPES, 10 mM sodium bicarbonate, 10 mM TES, 10 mM BES), and antibiotics (100 U/mL penicillin, 100 mg/mL streptomycin) and allowed to equilibrate for 1 h. Cells were then plated at 2.65×10^4 cells/cm^2 onto sterile glass slides (Fisher Scientific, Pittsburgh, PA) using removable silicone wells. After cells were allowed to attach for 1 h in a 5% CO_2 incubator at 37°C, the slide was rinsed with medium to remove any nonadherent cells and placed into a custom galvanotaxis chamber (described in Section 4.2.2.3, Figure 4.1) under aseptic conditions. Approximately 30-40 cells were observed in each field of view; images were acquired at 5 min intervals.

5.3.2.3 Cell Migration Parameters

The position of each cell was manually tracked via a custom MATLAB program that utilizes measurements of the net centroid displacement from the starting position (set as origin) to calculate overall speed of migration for each cell (the net displacement in the experiment divided by the 3 h time span of observation). Migration direction was quantified as $\sin\phi$, where ϕ is the angle between the x-coordinate axis and the migration vector, such that $\sin\phi$ was defined as the value -1 when ϕ = 4.71 rad (270°), the direction of the cathode. The directional velocity, defined as the component

of the speed directed toward the negative pole (e.g. (Chao et al., 2000, 2007)), was obtained by multiplying a cell's speed by $\sin\phi$. Each data point represents the mean and standard deviation 60-80 samples.

5.3.2.4 Statistics

A two-way ANOVA was performed on cell speed, directed velocity, and total displacement for factors of treatment (applied EF vs. control), and passage number to determine significance ($p<0.05$) of the effect of each factor and also the interaction of the factors. Tukey's honest significant difference (HSD) *post hoc* test was performed to assess significance ($p<0.05$) between each treatment and passage group.

5.3.3 Results

Although the same growth factor cocktail treatment was administered to each group, the origin of the cell strongly influenced its response to an applied DC electric field. At early passage, SDSCs from bovine synovium exhibit a more robust effect when exposed to an EF than those from canine synovium (92% and 62% of cells exhibiting significantly greater migration than control samples for adult and juvenile bovine SDSCs, respectively, $p<0.05$). In contrast, only 40% and 15% of adult and juvenile canine SDSCs register a significant cell migration compared to control samples. Even as cells were expanded in culture through passage 4, these trends remain constant with more SDSCs from bovine tissue positively responding to the EF than the canine cells (100% and 73% of adult and juvenile bovine SDSCs compared to 45% and 62% of adult and juvenile canine SDSCs).

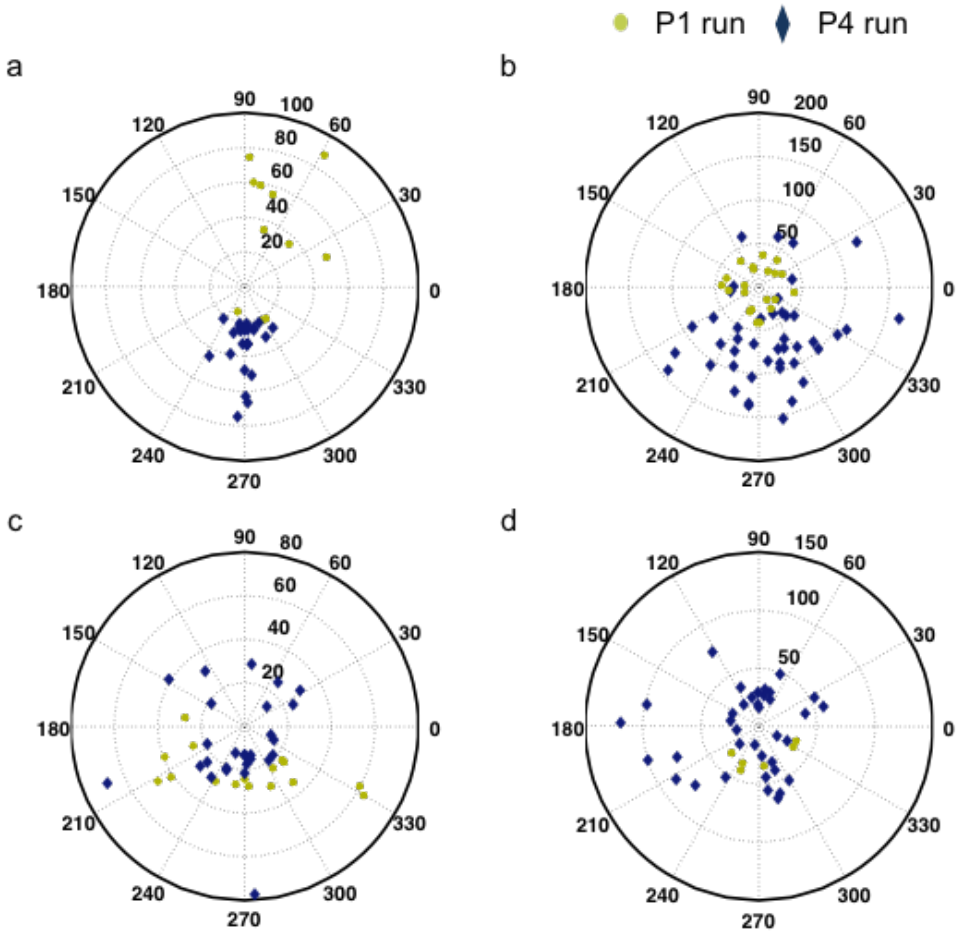

Figure 5.6: Representative polar plots of cell displacement of (a) adult and (b) juvenile bovine and (c) adult and (d) juvenile canine SDSCs at early passage (P1, yellow circle) and late passage (P4, blue diamond) subjected to EF. (0,0) represents the starting position of the cell (origin) with 90°as the anode (+) and 270°as the cathode (-). Radial distance is cell displacement (μm). n=70-80 cells/group.

For cells that responded positively to the applied EF and exhibited significantly greater migration than control cells, the direction in which they migrated was dependent on cell source and

age of tissue. The majority of adult and juvenile bovine cells migrate preferentially toward the anode (90) at early passage time (72% and 70% of responding cells, respectively, Figure 5.6). With increased passage, cells from both adult and juvenile bovine synovium exhibit a reversal in their migratory direction, preferentially traveling toward the cathode (100% and 86% of responding cells, respectively), similar to migration patterns consistent with chondrocytes (Chao et al., 2000). In contrast, SDSCs originating from canine tissue, exhibited significantly different responses to an applied EF of the same strength. At early passage time, almost all cells migrated toward the cathode (94% and 100% for adult and juvenile canine cells, respectively). Increased passage and exposure to growth factors resulted in diminished preferential migration toward the cathode (70% and 51%, respectively) that was independent of tissue age.

Interestingly, when the same protocol was applied to human bMSCs, the migration response of human bMSCs to an applied DC EF followed the same trends exhibited by bovine SDSCs. Increasing passage number revealed EF-induced migration progressively toward the cathode (Figure 5.7).

Furthermore, to investigate deeper parallels between the results seen with bovine SDSCs and human bMSCs, micropellets were formed at late passage (following the protocol of Section 5.2.2.6) and found to similarly produce cartilage-like tissue, characterized by their elevated biosynthetic activity in producing GAG and collagen (GAG/DNA = 8.32 ± 4.4 μg/μg, COL/DNA = 128 ±

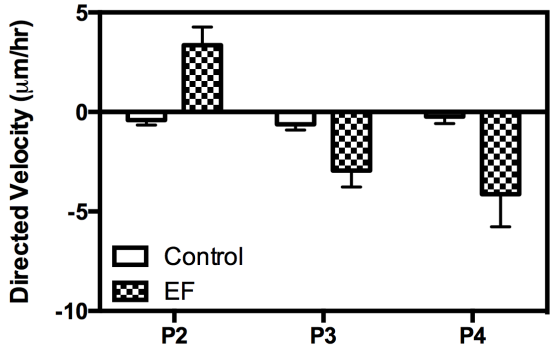

Figure 5.7: Cell migration parameters for passaged human bMSCs. Directed velocity for these cells is oriented toward the anode at P2 before changing direction toward the anode for later passages.

68.1 μg/μg).

5.3.4 Discussion

These varied findings from adult bovine and canine SDSCs as well as human bMSCs suggest that the modulators that control cell migration are specific to cells of different origin (age and species) and that it may be necessary to develop species-specific strategies for repair induction. Given the correlative findings in Section 4.2 between passage number and migration potential, it is interesting that the same trends are not consistently present across the different cell types. We can postulate that this may be due to a differential effect of the growth factors on specific cells. Furthermore, it is important to note that due to limited availability, cells from only one human donor were procured for this study. Though our observations suggest human bMSCs are compatible and capable of being shaped to behave like intended chondrocytes, intrinsic inter-donor variability warrant future studies aimed at confirming a reliable and consistent cell profile and response before this technique can be translated to clinical use.

5.4 Conclusion

The use of EFs directly controls cell migration and has the potential to influence therapeutic regimes. In this chapter of the dissertation, EF studies were performed to characterize the behavioral response of multiple cell types to use in a novel manner of identifying desirable cell populations. The results described herein contribute to the literature on the effects of applied EF and provide a greater understanding of the potential for using selected cells for guided wound repair. In particular, mesenchymal stem cells such as SDSCs offer a promising cell source for repair as they exhibit an intrinsic resistance to the chemical factors that may be present in the injured joint. By investigating the relationship between cell phenotype and surface marker expression and migration patterns, we developed a strategy to mobilize MSCs for cartilage repair. Applying growth factors during expansion produces a unique profile of surface marker expression that changes with culture. As the migration response of SDSCs mimics that seen for chondrocytes, so does their ability to produce

cartilaginous tissue. Though we observed successful translation of this work from the bovine model to human MSCs, our findings did not reflect behaviors noted for adult bovine or canine SDSCs, confirming that cell priming protocols in strategies for targeted cartilage repair must be tailored for the particular application.

Chapter 6

Coculture of Engineered Cartilage with Primary Chondrocytes Induces Expedited Growth

6.1 Introduction

Our lab and many others have investigated the use of chemical cues such as growth factors (TGF-β3, TGF-β1, insulin-like growth factor, fibroblast growth factor (Byers et al., 2006; Mauck et al., 2003b, 2001; Thorp et al., 1992), corticosteroids (Awad et al., 2003; Bian et al., 2010b), and interleukins (Aydelotte et al., 1992; Lima et al., 2008b; Ratcliffe et al., 1986)) in an effort to create engineered cartilage with functional tissue properties. When implanted into the knee joints, constructs must possess the fortitude to withstand the harsh mechanochemical environment. Though we have been successful at producing constructs that match or exceed the Young's modulus and GAG content of native tissue (Lima et al., 2007), the dynamic modulus and collagen content in engineered constructs is significantly lower than native cartilage. As such, we have continued searching for novel media supplements to cultivate this growth. Soluble chemical factors can be introduced to the culture system not only by exogenous delivery through the culture media, but also by the

addition of a second population of cells. Underlying cell monolayers, or feeder layers, introduce paracrine signaling between populations of cells and promote cell-cell interactions that have been shown to modulate cellular activity (Guillotin et al., 2004; Hwang et al., 2007; Smola et al., 1993; Solursh and Meier, 1973; Vats et al., 2006). For example, primary chondrocytes have been shown to induce chondrocyte differentiation of embryonic stem cells and cause redifferentiation of cocultured passaged chondrocytes by releasing soluble signaling factors. When cocultured, these highly plastic stem cells adopt a more rounded phenotype and show increased production of aggrecan and Type II collagen, characteristic of native chondrocytes (Bigdeli et al., 2009; Hoben et al., 2009; Vats et al., 2006). Similarly, coculture systems including primary chondrocytes with passaged chondrocytes can also induce stable redifferentiation (Ahmed et al., 2009a; Gan and Kandel, 2007; Taylor et al., 2009). Reversion in phenotype of the passaged cells toward articular chondrocytes was confirmed by increased expression of Type II collagen and cartilage oligomeric matrix protein (COMP) genes and decreased expression of the Type I collagen gene. In further support of these findings, other studies suggest articular chondrocytes expanded in monolayer cultures display characteristics similar to those of mesenchymal stem cells (Barbero et al., 2003; Tallheden et al., 2003). This may explain the ease in which passaged cells are able to reacquire their former phenotype. Taken together, these studies suggest chondrocyte feeder layers have the potential to enhance and induce chondrocyte-like behavior in populations of dedifferentiated cells (passaged cells or stem cells). It is unclear, however, what effects coculture has on already differentiated cells, such as primary chondrocytes, when they are encapsulated in a hydrogel matrix.

To investigate the use of a coculture system on engineered cartilage, we tested three hypotheses: (1) coculturing of engineered cartilage constructs in the presence of a monolayer of primary chondrocytes ("chondrocyte feeder layer") expedites and increases development of their material and biochemical properties; (2) the effects of coculture with a chondrocyte feeder layer arise from paracrine effects (soluble factors) rather than direct cell-cell contact with the feeder cells; and (3) the feeder layer effect depends on the specific morphology and expression of the two-dimensional (2D) cell monolayer.

6.2 Materials and Methods

6.2.1 Experimental Design

To investigate the effect of introducing a chondrocyte feeder layer to engineered cartilage constructs, we developed a coculture model system (Figure 6.1). Briefly, to test Hypothesis 1, the effect of culturing engineered cartilage in the presence of subconfluent (low-density) primary chondrocyte monolayers was investigated (Study 1). To test Hypothesis 2, the dependence of this effect on cell-cell contact was investigated by eliminating physical contact as a means of interaction using tissue culture Transwell® inserts (Study 2). To test Hypothesis 3, the role of the monolayer's phenotypic expression in influencing tissue development in cocultured constructs was studied (Study 3). We performed each study independently, using cell populations isolated and pooled from different animals.

6.2.2 Cell Isolation and Culture

We isolated tissue from bovine carpometacarpal joints of freshly slaughtered 2- to 4-week-old calves. Six to eight joints were used per study and cells were pooled from all joints for each study described herein. Cartilage was digested in high-glucose DMEM with collagenase Type V (Sigma-Aldrich Corp, St Louis, MO) for 11 hours at 37°C with shaking. Cell suspensions were filtered through a 70μm porous mesh and sedimented in a bench-top centrifuge for 15 minutes at 1500 g. Viable cells were counted with a hemocytometer and viability was assessed by trypan blue exclusion. Cell suspensions (60×10^6 cells/mL) were mixed in equal parts with 4% low-gelling agarose (Type VII; Sigma) to yield a final cell concentration of 30×10^6 cells/mL in 2% wt/vol agarose. We cast the chondrocyte/agarose mixture into slabs and later cored using a sterile disposable biopsy punch (Miltex Inc, York, PA) to final dimensions of 4-mm diameter and 2.34-mm thickness.

Cells from the same harvest and final suspension were plated into tissue-culture-treated 24-well plates at a density of 0.1×10^6 cells/well (5.6×10^4 cells/cm^2) in the presence of DMEM supplemented with 5% FBS to facilitate cell attachment. We exposed developing engineered cartilage constructs to different monolayer formulations in each of the three studies.

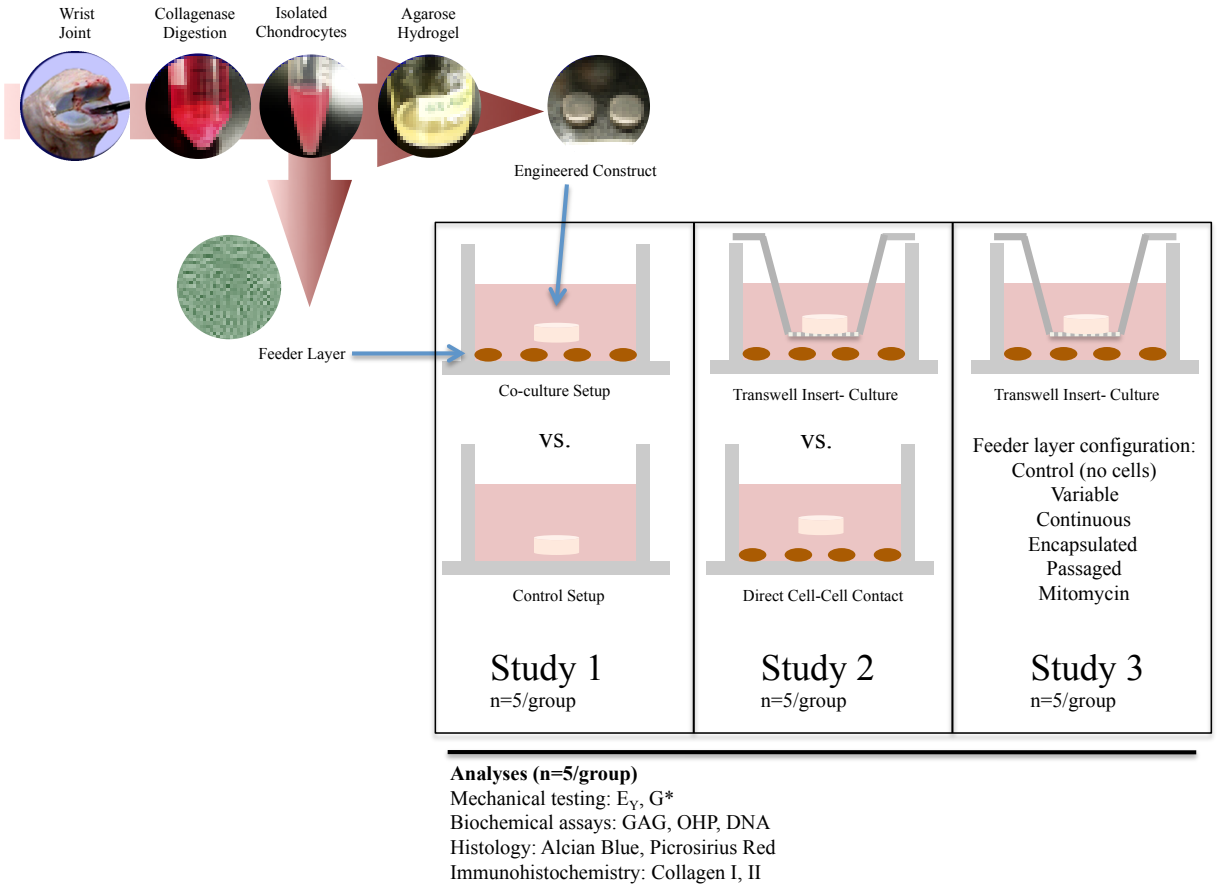

Figure 6.1: A schematic shows the experimental design of the three studies described

6.2.3 Co-Culture Setup

In Study 1, one construct was placed above the monolayer in each well and allowed to grow in culture for the duration of the study (Figure 6.2a). In Study 2, to investigate the dependence on cell-cell contact, we physically separated chondrocyte monolayers from the three-dimensional (3D) engineered tissue by a Transwell® insert (Corning, Acton, MA) (Figure 6.2b).

Tissue-culture-treated membranes with a 3.0μm pore size, which is orders of magnitude larger than the pore size of native cartilage (Mow and Ratcliffe, 1997) or 2% type VII agarose (Ng et al., 2005), were used to permit free transport of diffusible signals but not direct cell-cell contact between the chondrocytes in the engineered constructs and feeder layer. In Study 3, we established

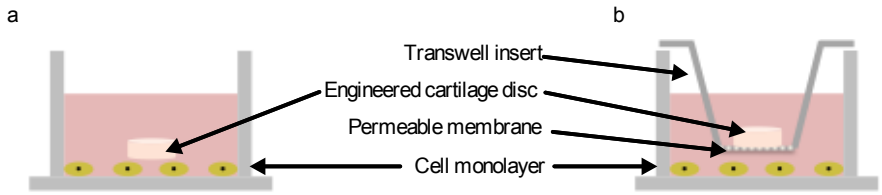

Figure 6.2: Diagram illustrating the experimental coculture setup for (a) Study 1 (direct contact between the construct and the feeder layer) and (b) studies 2 and 3 (separation between the construct and the feeder layer by a Transwell® insert).

five subgroups to examine the dependence on cell manipulation and presentation as described below. Primary chondrocyte monolayers were replated each week ("variable") to contrast with monolayers that were plated only once at the start of the study ("continuous") to assess the effect of the presentation of the feeder cells when introduced to the engineered construct. For the feeder layers in the variable group, fresh harvests and tissue digestions were performed each week to yield a new cell suspension for plating of primary cells at the same initial seeding density. Alternatively, to understand whether this effect was dependent on soluble factors released only transiently immediately after a fresh harvest, after each harvest, and tissue digestion, we plated cell suspensions in a high-density monolayer (0.4×10^6 cells/cm^2) to preserve the chondrocyte phenotype (Watt, 1988). This high-density monolayer was cultured for a week and then trypsinized and replated at a density of 0.1×10^6 cells/well (5.6×10^4 cells/cm^2) the following week and used at Passage 1 (P1, "passaged"). Then, to assess the dependence of this effect on feeder cell presentation resulting from changes in morphology, we embedded cells ("encapsulated") in low-gelling agarose at a final density of 0.5×10^6 cells/mL in 1% wt/vol agarose. An aliquot of the cell-agarose solution was then transferred to each well such that the same number of cells (0.1×10^6 cells) was entrapped in the hydrogel feeder layer to preserve cell morphology and replaced weekly to match the variable time course. Finally, to understand whether the effect was dependent on active processes of cellular division and proliferation in the feeder layer, monolayers were first treated with mitomycin C (10 μg/mL), as it inhibits cell proliferation and division, before use in the coculture setup ("mitomycin").

Two days after cell plating, we transferred one construct over to each well for all the groups

and cultured in 2 mL hgDMEM supplemented with 1X penicillin-streptomycin, 0.1 μmol/L dexamethasone, 50 μg/mL ascorbate 2-phosphate, 40 μg/mL L-proline, 100 μg/mL sodium pyruvate, and 1X ITS+ premix (insulin, human transferrin, and selenous acid; Becton Dickinson, Franklin Lakes, NJ) for the remainder of the culture period. Medium was further supplemented with 10 ng/mL TGFβ-3 (Invitrogen, Carlsbad, CA) for the first 14 days of construct culture. Culture medium was changed every other day. A minimum ratio of 1mL of medium per 1 million cells was maintained throughout the duration of the study to encourage and promote tissue growth. As the total number of cells in each well has been previously estimated to range from 1-2 million cells, 2mL of medium was used per well.

6.2.4 Mechanical Testing

We tested five whole samples from each group in unconfined compression to assess Young's equilibrium modulus (E_Y) and dynamic modulus (G^*) using a custom computer-controlled system (Soltz and Ateshian, 1998). An initial 0.02N tare load was applied, followed by compression to 10% strain, at a strain rate of 0.05% s^{-1} to measure Young's modulus after stress relaxation. Dynamic modulus was subsequently measured by superimposing a cyclical 2% peak-to-peak strain at 0.1 Hz.

6.2.5 Biochemical Analysis

After mechanical testing, we halved each sample, with one half dried and digested in proteinase K solution overnight at 56°C, as described previously (Kelly et al., 2006), preserving the other half for histology (Section 6.2.6). An aliquot was analyzed for GAG content via the 1,9-dimethylmethylene blue dye-binding assay (Farndale et al., 1982). A further aliquot was hydrolyzed in 12 N HCl at 110°C for 16 hours, dried, and resuspended in assay buffer (Kelly et al., 2006). Orthohydroxyproline (OHP) content was determined via a colorimetric assay in which chloramine T and dimethylaminobenzaldehyde reaction was quantified (Stegeman and Stalder, 1967). We calculated overall collagen content by assuming a 1:7.64 OHP-to-collagen mass ratio (Hollander et al., 1994). Double-stranded DNA content was also assessed by the PicoGreen® assay (Invitrogen) according

to the manufacturer's standard protocols. Each biochemical constituent was normalized to tissue wet weight (ww).

6.2.6 Histological Analysis

For histology, we fixed the other half of each sample in acid-formalin-ethanol (Lin et al., 1997), paraffin embedded, sectioned (8 μm thick), and stained for histology to assess both proteoglycan (alcian blue) and collagen (picrosirius red) distribution and organization. Immunohistochemistry was performed to confirm the development of collagen II in developing constructs. Briefly, tissue sections were digested in 5.0 mg/mL testicular hyaluronidase, swollen in 0.5 mol/L acetic acid, blocked in 10% normal goat serum (NGS). We labeled the sections with 10% NGS containing primary antibody for Types I and II collagen (Abcam, Cambridge, MA). Alexa Fluor® 488-conjugated goat anti-rabbit secondary antibody labeling (Molecular Probes, Eugene, OR) and counterstained with diamidino-2-phenylindole nuclear counterstaining (Molecular Probes) to visualize the extracellular matrix and cells, respectively. Three independent observers examined tissue sections on an inverted confocal microscope (Leica Microsystems, Bannockburn, IL) to assess whether constructs exposed to the feeder layer exhibited more extensive biochemical content and distribution and to confirm the type of collagen produced.

6.2.7 Statistics

All data are reported as the mean ± SD of four to five samples per time point and group. In Study 1, to assess differences in mechanical and material properties of constructs exposed to a feeder layer compared to control samples at each time point, a Student's t test was performed. Similarly, in Study 2, differences at each time point between constructs cocultured in direct contact with the monolayer and constructs cocultured in the Transwell setup were determined by a Student's t test. In Study 3, to compare the properties of control constructs to those cultured in each experimental group, a one-way ANOVA was performed, and differences were confirmed with Tukey's honest significant difference *post hoc* test. Statistica® software (StatSoft, Inc, Tulsa, OK) was used to

perform all statistical tests.

6.3 Results

Study 1 showed the feeder layer stimulated growth of differentiated chondrocytes. For constructs cocultured with a subconfluent population of primary chondrocytes, a beneficial effect was noted on cells in the constructs: constructs exhibited higher (p = 0.005) Young's modulus and greater (p = 0.019) GAG and (p = 0.001) collagen content than controls; however, this effect was only noted through Day 28 of culture (Figure 6.3). By Day 42 in culture, Young's modulus and GAG content were comparable ($p_{E_Y} = 0.176$, $p_{GAG} = 0.734$, $p_{COL} = 0.251$) whether constructs were cocultured in the presence or absence of a cell monolayer (Figure 6.3).

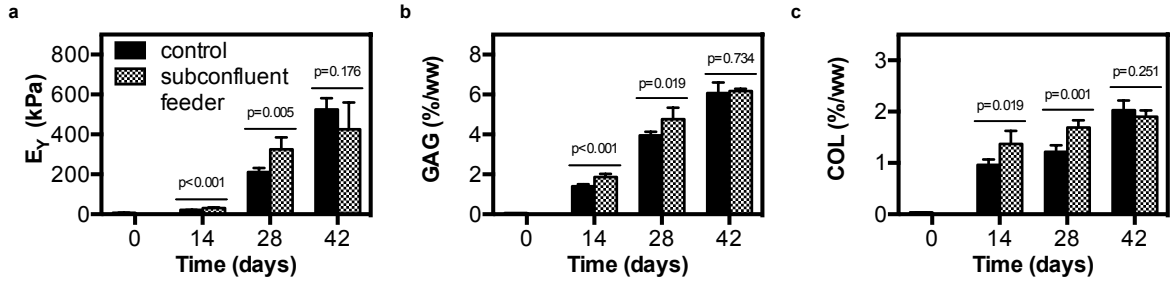

Figure 6.3: Graphs show (A) Young's modulus (E_Y), (B) GAG content, and (C) collagen (COL) content of constructs with time in culture in Study 1 (n = 5 per group). Increased mechanical properties and GAG content occurred up to Day 28 of culture.

Confirming these quantitative findings, compared to controls (Figure 6.4a), histology sections of tissue from cocultured constructs (Figure 6.4e) showed enhanced staining in alcian blue (for GAG) over time in culture, suggestive of advanced extracellular matrix development and deposition for sections exposed to a monolayer. Compared to controls (Figure 6.4b), enhanced staining for picrosirius red (for nonspecific collagen) was also present for cocultured constructs (Figure 6.4f). Similarly, when immunohistologic stains were analyzed, similar trends in Types I and II collagen distribution were observed in cocultured constructs (Figure 6.4g-h) compared to controls (Figure 6.4c-d), suggesting increased deposition of both types of collagen were present after coculture.

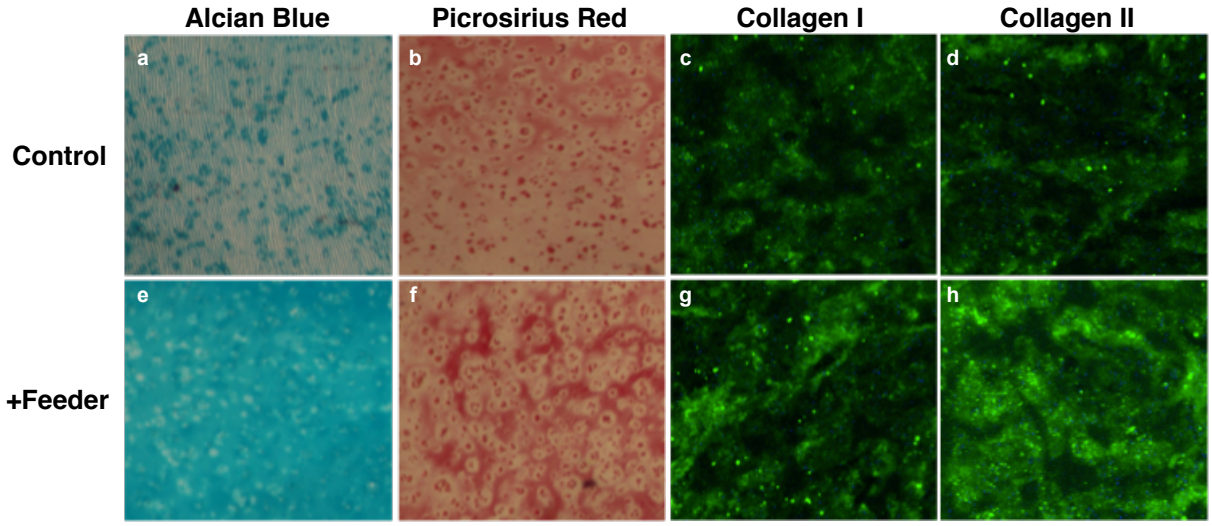

Figure 6.4: Representative constructs cocultured in the (a-d) absence and (e-h) presence of a feeder cell monolayer at day 28 of culture stained with (a,e) alcian blue, (b,f) picrosirius red, (c,g) collagen I, and (d,h) collagen II are shown. Cocultured constructs produced more extensive and organized tissue development, as assessed by staining intensity from histology and immunohistochemistry.

In Study 2, cell-cell contact was not necessary to produce the same beneficial effect of coculture as seen in Study 1, indicating the mechanism of intercellular signaling was primarily paracrine or soluble factors that can diffuse through the porous membrane. By the end of the culture period, constructs placed into Transwell® inserts and exposed to a subconfluent monolayer exhibited an increase ($p = 0.012$) in Young's modulus compared to both control and contact conditions (Figure 6.5a). This additional increase in stiffness was not paralleled in dynamic modulus; modest increases in dynamic modulus were seen compared to constructs cultured without a monolayer, but there were no differences ($p = 0.286$) between the constructs in contact with the monolayer and those separated with a Transwell® insert (Figure 6.5b).

The specific presentation of the feeder cell monolayer was crucial in affecting the development of engineered cartilage tissue (Study 3). As early as 14 days in culture, cell monolayers replaced each week with a subconfluent population of cells freshly harvested from cartilage ("variable") showed positive influences of coculture. These constructs developed superior mechanical properties and biochemical markers compared to control constructs cultured in the absence of any cells (p_{E_Y}

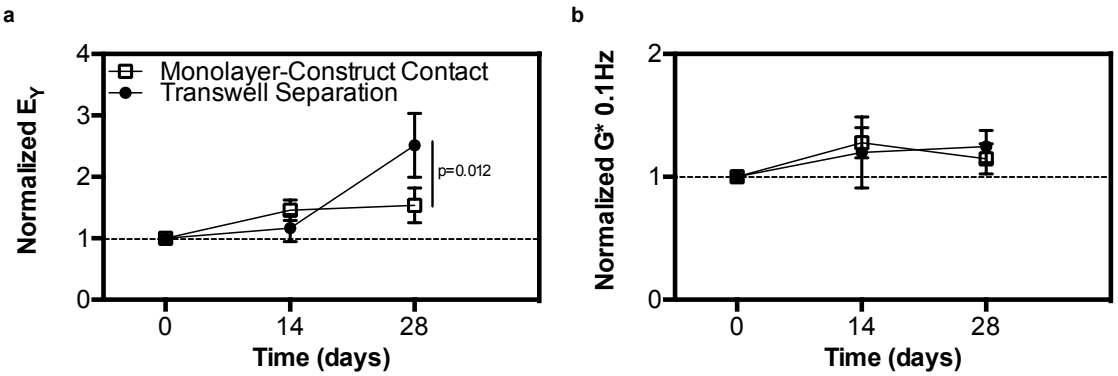

Figure 6.5: Graphs show normalized (A) Young's modulus (E_Y) and (B) dynamic modulus (G*) of constructs exposed to a feeder layer (in direct contact or with a Transwell® insert separation) compared to feeder-free controls in Study 2 (n = 5 per group). Increased mechanical properties at Day 28 are achieved when constructs are separated from the monolayer, confirming cell-cell contact is unnecessary.

<0.001, p_{G*} <0.001, p_{GAG}<0.001) or constructs cultured in the presence of a continuous monolayer (p_{E_Y}<0.001, p_{G*} = 0.014, p_{GAG}<0.001) (Figure 6.6). While collagen content for these constructs was increased over control (p = 0.020), it was comparable to levels seen in constructs exposed to the continuous monolayer (p = 0.357). The repeated replacement of the feeder layer with P1 cells did not have the same effect; constructs exposed to these monolayers developed tissue with properties comparable to control (p_{E_Y} = 0.999, p_{G*} = 1, p_{GAG} = 0.945, p_{COL} = 0.450) (Figure 6.6). In further support of the finding that replacing the cells weekly was not the sole factor responsible for producing such an effect, cells encapsulated in 1% agarose and thus forced to adopt a rounded morphology due to the hydrogel also produced results comparable to control constructs (p_{E_Y} = 0.668, p_{G*} = 1, p_{GAG} = 0.406, p_{COL} = 0.543) (Figure 6.6). Finally, when cell monolayers were mitotically inactivated by the application of mitomycin C, constructs exhibited delayed and stunted growth, yielding lower properties than controls (p_{E_Y} = 0.024, p_{G*} = 0.059, p_{GAG} <0.001, p_{COL} <0.001) (Figure 6.6). DNA content in constructs from all groups at each timepoint was comparable (DNA_{day14}: 8μg/construct; DNA_{day28} : 10μg/construct, DNA_{day42} : 12μg/construct), confirming the feeder layer did not adversely affect cellular viability.

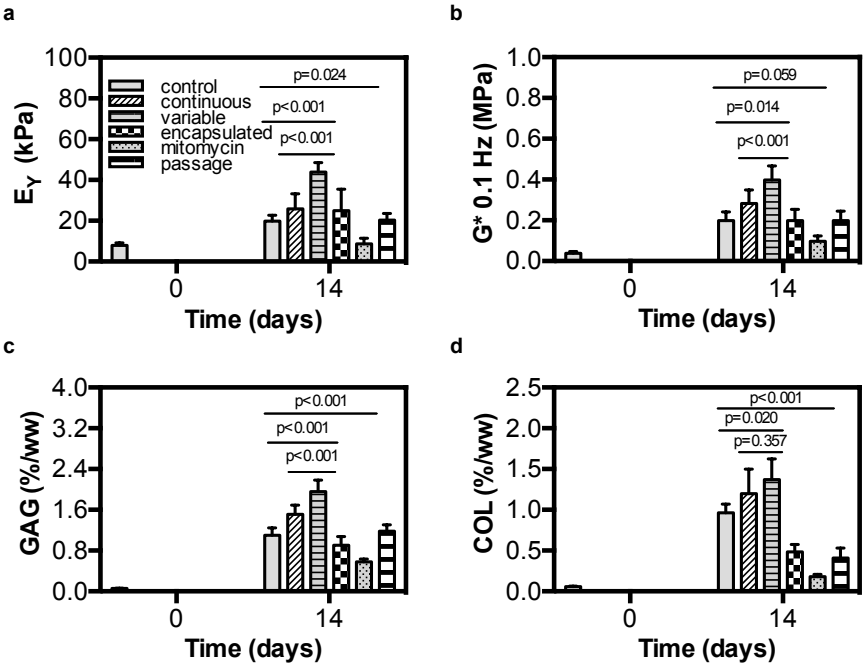

Figure 6.6: Graphs show (A) Young's modulus (E_Y), (B) dynamic modulus (G*), (C) GAG content, and (D) collagen (COL) content of constructs with time in culture in Study 3 (n = 5 per group). When the cell monolayer is replaced weekly, increased mechanical properties and biochemical content are achieved by the cocultured tissue constructs.

6.4 Discussion

The principal focus of previous studies on the effects of coculture in cartilage tissue engineering has been on the effects of primary cells on dedifferentiated chondrocytes (Ahmed et al., 2009a,b; Taylor et al., 2009) or various stem cells (Hoben et al., 2009; Hwang et al., 2006; Vats et al., 2006). Cells that have undergone dedifferentiation are believed to be more plastic, similar to stem cells, allowing them to respond more efficiently to the chemical cues present during culture. Here, by coculturing engineered cartilage constructs with a chondrocyte feeder layer, we investigated whether differentiated chondrocytes already embedded in a 3D hydrogel scaffold exhibited a similar capacity to respond to these cues, and if so, if the mechanism of cellular signaling was dependent on direct cell-cell contact. Additionally, we looked at identifying specific plating conditions of the feeder layer, which may be necessary to elicit such a response.

Our studies are subject to some limitations. First, in our study, bovine chondrocytes from skeletally immature animals were utilized, as they are readily available, well characterized, and capable of robust tissue growth in culture (relative to adult cells). While their use facilitates comparison of current findings to our earlier work (Hung et al., 2004; Lima et al., 2007) and to the extensive body of literature using bovine cartilage and chondrocytes for cartilage basic science and tissue engineering studies, it is unclear whether this technique would be applicable for an older population of cells whose release pattern of chemical factors may vary from that of younger, more robust cells. As such, further studies to identify an optimal cell source for the underlying feeder layer are warranted. Second, as the beneficial effects of a coculture system are heightened only when the feeder layer is replaced weekly with primary juvenile chondrocytes, the utility of this system in its current setup is limited due to a decreased availability of cells and may not be a clinically reasonable option. However, the data suggest soluble factors released by the underlying cell feeder layer when in a particular presentation can influence the biosynthetic activity of differentiated cells encapsulated in a 3D matrix. Our observations also suggest identifying one or more soluble mediators responsible for the beneficial feeder layer effects will be important to augmenting the coculture system and warrant future studies aimed at enhancing a chondrogenic medium formulation that could be used independent of a feeder layer.

Cell-cell communication has been identified as an important regulator in the behavior of cells and development of tissues (Bhatia et al., 1999; Gan and Kandel, 2007; Kelly et al., 2004; Watanabe et al., 2010). For the first time, we have identified the possibility for the biosynthetic activity of differentiated chondrocytes encapsulated in a 3D hydrogel matrix to be influenced by the presence of an underlying feeder chondrocyte monolayer, leading to enhanced tissue development and superior mechanical and material properties in the tissue construct (Study 1). While Young's modulus and GAG content were enhanced by the presence of a feeder layer this trend was not observed for the dynamic modulus and collagen content, however. This may be explained by the fact that the dynamic modulus is greatly influenced by the ability of collagen fibers to resist the cyclical radial and circumferential tensile strains. In our system, most likely the soluble factors released

are selectively targeting proteoglycan expression and production, exhibiting minor or no effects on collagen orientation.

In Study 2, Transwell® inserts were used to provide physical separation between the developing engineered construct and the underlying cell monolayer, allowing the effects of direct cell-cell contact to be parsed out from paracrine signaling. While some studies have suggested direct cell-cell contact provides signaling factors that upregulate the biosynthetic activity of cells compared with the transfer of soluble factors between non[neighboring populations of cells (Watanabe et al., 2010), these experimental setups generally consist of cell populations plated together on a membrane or filter. In contrast, in our experimental setup, chondrocytes in the engineered cartilage tissue were singularly embedded within the agarose hydrogel and prohibited direct contact with one another and with the cells of the monolayer, even when directly placed upon it. Therefore, it is not surprising the effects seen to facilitate this increased tissue growth and development were present even when the construct was physically separated from the feeder layer and intercellular signaling relied on the diffusible passage of chemical cues. In support of our findings, many reports in the literature already utilize setups that physically separate the different populations of cells (Jikko et al., 1999) or use conditioned media to provide chemical cues from one population of cells to another (Solursh and Meier, 1973)

While our data indicate paracrine signaling is responsible for the expedited tissue growth in a 3D scaffold system, the type and degree of soluble factors released by the monolayer appear dependent on the specific presentation of the 2D feeder cell, which may be influenced by cellular morphology, harvest freshness (eg, primary versus passaged cells), and their phase within the cell division cycle (Study 3). Cell shape has been implicated in modulating the chondrocyte phenotype (Benya and Shaffer, 1982); the feeder layers adopted in our study underwent an initial period of preconfluence where cell morphology was more stellate before reaching confluence whereupon chondrocytes assumed a more classical spherical morphology. Another factor known to influence the chondrocyte phenotype and therefore the release of particular soluble factors is passaging; with increased passage number, gene expression for collagen I increased while expression of collagen

II, aggrecan, and cartilage oligomeric matrix protein (COMP), the major biomarkers present in cartilage, were downregulated (Gunja and Athanasiou, 2007). It is feasible then downregulation of these genetic markers can adversely affect the soluble cues being emitted from the cell monolayer. Finally, mitomycin C, while used to halt the mitotic activity of cells, has been reported to induce premature aging of fibroblasts (Petri et al., 1999). Aged cells are less biosynthetically active than juvenile cells and remain in the quiescent stage of the cell cycle rather than undergoing active division (Tran-Khanh et al., 2005). Taken together, these reports in the literature support our results and indicate the presentation of the 2D feeder layer is crucial to providing the correct chemical cues to the developing tissue construct.

6.5 Conclusion

Though co-culture systems have been studied extensively and used to elicit desired changes in a population of cells, in this dissertation, by carefully and systematically manipulating the presentation of the feeder layer, we uncovered fresh insights regarding their use for tissue enhancement. In particular, these encouraging results suggest differentiated cells such as chondrocytes encapsulated in a 3D matrix have the potential to respond to soluble cues present in a coculture system and that chemical factors can prime and modulate the development of engineered cartilage constructs. Furthermore, while bovine cells were used in the engineered tissues and feeder layer of the current study, studies in the literature suggest the possibility of using cells from disparate species with beneficial effects (Ahmed et al., 2009a). In this manner, this work has the potential to be applied for donor cartilage allografts, which are currently in use clinically (Allen et al., 2005; Hennig and Abate, 2007), to increase their functional tissue properties to improve success *in vivo* after implantation.

Chapter 7

Cytokine Preconditioning on Engineered Cartilage Provides Protection Against Interleukin-1

7.1 Introduction

Articular cartilage is the connective tissue that lines the ends of diarthrodial joints and serves to bear load and provide lubrication during motion (Mow et al., 1994). When the tissue is damaged through physical injury or disease such as osteoarthritis (OA), the healing response is limited due to its avascular nature and limited cellularity (Tew et al., 2001). These types of injuries often lead to a disruption in the balance between anabolic and catabolic regulatory activities that lead to a phenotypic shift in chondrocytes, cell death, and an increase in expression of inflammation-related genes (Goldring et al., 2011) that leads to a loss of cartilage matrix components and deterioration in the structural and functional properties of cartilage (Lee et al., 2005; Stevens et al., 2009). Catabolic cytokines may also be generated by the fibroblast- and macrophage-like cells in the synovium, the thin layer that lines the non-articulating surfaces of diarthrodial joints and maintains a synovial fluid-filled cavity (Fan et al., 2009), in response to the breakdown products from damaged cartilage.

Consequently, elevated levels of inflammatory cytokines such as interluekin-1 (IL-1) and tumor necrosis factor-α (TNF-α) have been measured in the synovial fluid during cartilage pathology (Pelletier et al., 1991; Sellam and Berenbaum, 2010).

Though TNF-α is the dominant cytokine responsible for joint swelling and acute inflammation, it has been reported to be unlikely to play a role in tissue degradation (van den Berg et al., 1999). In contrast, both forms of the IL-1 isoform, IL-1α and IL-1β, are reported to be responsible for cartilage erosion and sustained cell infiltration, though their concentrations are highly dependent on the stage of osteoarthritis (van den Berg et al., 1999) and the model system. As such, our lab and others have chosen to focus on the effect of IL-1 on culture systems to better understand the mechanisms behind erosive tissue breakdown and to potentially identify strategies for repair (Aydelotte et al., 1992; Lima et al., 2008a,b; Murata et al., 2003; Temple et al., 2006; Wilusz et al., 2008).

Strategies for using engineered constructs for cartilage tissue repair have focused on the implantation of tissues possessing the mechanical integrity and chemical fortitude to withstand the potentially harsh mechanochemical environment of the joint (Lima et al., 2008b). Catabolic mediators from inflammation (Lotz, 2001) or the surgical intervention itself (Smeets et al., 2003) have been shown to be especially pronounced in underdeveloped tissues (Lima et al., 2008b; Rotter et al., 2005) in which cells are not fully embedded in the chondroprotective extracellular matrix that accompanies construct maturity. Previous studies from our lab have reported that the lingering effects of IL-1 to immature constructs remains in long-term culture, even after the cytokine has been removed (Section 2.1.1, (Lima et al., 2008b)). In order to successfully utilize these constructs for functional repair, it is important, therefore, to investigate potential strategies for preventing or mediating the effect of cytokines on the developing constructs.

In cardiovascular systems, cellular preconditioning schemes by mechanical and chemical manipulation have been used extensively to prime stem cells to a state in which they can withstand a harsh microenvironment (Haider and Ashraf, 2010; Kamota et al., 2009; Kubo et al., 2008; Pasha et al., 2008). In particular, brief exposure to a catabolic agent afforded longer term protection against

subsequent attacks, offering the most effective means of cytoprotection (Murry et al., 1986). Motivated by the reported benefits of preconditioning, we hypothesized that the catabolic effects of injurious IL-1 on engineered cartilage could be decreased by initially preconditioning them with low doses of the cytokine.

This study investigates the effects of supplementing the culture media with a low concentration of IL-1. Specifically, the effects of a 1-week preconditioning treatment on developing engineered cartilage constructs is tested against exposure to a higher concentration of the cytokine, known to elicit proteolysis as well as rapid degeneration of cartilage (Tyler, 1989). This phenomenon is investigated using a well-established juvenile bovine chondrocyte model (Hung et al., 2004), as well as an adult canine model (Ng et al., 2010) that can inform future *in vivo* studies in an established large preclinical animal model. These tissue models have both been shown to produce functional material properties (Young's modulus) and glycosaminoglycan content similar to native tissue (Bian et al., 2010a; Lima et al., 2007), providing a robust system to study potential therapies for osteoarthritis. The use of a physiologically relevant tissue to study this method of protection against cytokine exposure may shed light on the behavior of *in situ* cartilage during injury or disease.

7.2 Materials and Methods

7.2.1 Experimental Design

Three consecutive studies are described here. In study 1, we used a bovine model of chondrocytes from skeletally immature animals, as they are readily available, well characterized, and capable of growing robust tissue in culture (relative to adult cells). Additionally, use of juvenile bovine chondrocytes facilitates comparisons to our previous work , including the response of these cells to *in vitro* applications of IL-1 (10 ng/mL, (Lima et al., 2008b)). In study 2, we investigate whether results from the first study carry over to a preclinical canine model, also using chondrocytes from skeletally mature animals. For each study, the same timeline was followed (Figure 7.1).

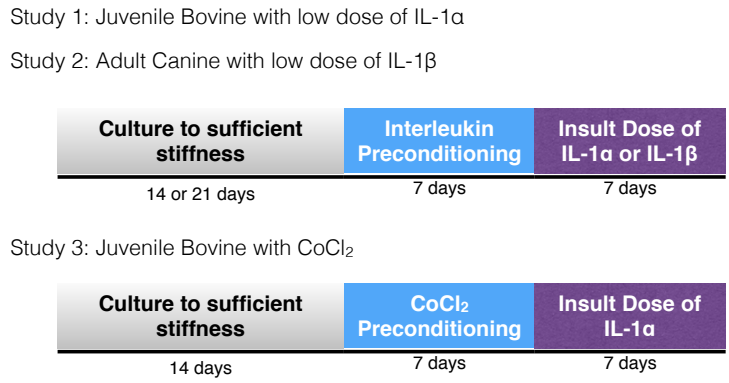

Figure 7.1: Schematic of experimental design. Studies 1 and 2 utilized low-dose IL-1 preconditioning. Study 3 examined the effect of $CoCl_2$ preconditioning to verify the mode of protection.

Briefly, constructs were allowed to elaborate a threshold amount of extracellular matrix (attaining a Young's modulus of 100kPa or 150kPa for bovine and canine tissues, respectively), exposed to a low dose concentration of IL-1α (for bovine) or IL-1β (for canine) for seven days and then subjected to an injurious level of cytokine for the final seven days. The results of these studies motivated study 3. We hypothesized that the survival signal produced by preconditioning with interleukin relied on the induction of hypoxia-inducible factor-1α (HIF-1α), similar to the mechanism suggested for hypoxic and ischemic preconditioning schemes (Hu et al., 2008; Nanduri et al., 2008). To this end, juvenile bovine constructs were preconditioned with cobalt chloride ($CoCl_2$), a chemical inducer of HIF-1α, and then exposed to an insult dose of IL-1α to investigate whether HIF-1α upregulation was sufficient to provide protection against catabolic effects.

7.2.2 Tissue Isolation and Cell Culture

Articular cartilage was harvested from knee joints of either freshly slaughtered 2-4 week old bovine calves or adult dogs. Four to six joints were used for each experiment and cells were pooled from all joints. Cartilage was digested in high-glucose DMEM with collagenase IV (Worthington Biochemical Corporation, Lakewood, NJ) for 11 h (bovine) or 8 h (canine) at 37 °C with shaking. Cell suspensions were filtered through a 70μm porous mesh and sedimented in a bench-top centrifuge for 15 min at 1500g. Viable cells were counted with a hemocytometer and trypan blue and plated at

high density (20×10^3 cells/cm^2) in a growth factor cocktail (1 ng/mL TGF-β1, 5 ng/mL bFGF, and 10 ng/mL PDGF-$\beta\beta$ (Ng et al., 2010; Sampat et al., 2011)). At confluence, cells were trypsinized, resuspended (60×10^6 cells/mL), and mixed in equal parts with 4% low-gelling agarose (type VII, Sigma) at 37°C. The chondrocyte/agarose mixture was cast into slabs and cores were produced using a sterile, disposable biopsy punch (Miltex) to yield final dimensions ($\varnothing$4mm$\times$2.34 mm thick). Constructs were cultured in DMEM supplemented with 1$\times$ penicillin, streptomycin, fungizone (PSF, Sigma), 0.1 μM dexamethasone, 40 μg/mL L-proline, 100 μg/mL sodium pyruvate, and 1$\times$ ITS+ premix (insulin, human transferrin, and selenous acid, Becton Dickinson, Franklin Lakes, NJ). Using culture protocols optimized from earlier studies of juvenile bovine and adult canine chondrocytes, respectively (Lima et al., 2004; Ng et al., 2010), medium was further supplemented with 50 μg/mL ascorbate 2-phosphate daily and 10 ng/mL TGF-β3 (Invitrogen) for the first 14 days of culture (for bovine culture) or for the entire culture (for canine culture). Media was changed every other day.

7.2.3 Preconditioning and Insult

Earlier studies have identified that constructs must comprise sufficient extracellular matrix to withstand the harsh catabolic effects of IL-1 (Lima et al., 2008b). Accordingly, for the current studies, after constructs had attained an equilibrium Young's modulus of $\sim$100 kPa (for bovine) and $\sim$150 kPa (for canine), one subset of samples was exposed transiently to a range of low dose concentrations of cytokine. For study 1, IL-1α, the more potent of the two isoforms in juvenile bovine agarose-chondrocyte constructs (Lima et al., 2008a), was administered (0.1 ng/mL, 0.5 ng/mL, 1.0 ng/mL) for seven days. In study 2, IL-1β (0.2 ng/mL, 1.0 ng/mL, 2.0 ng/mL), the more potent isoform for canine constructs was used (Cook et al., 2000; Kuroki et al., 2005). In study 3, constructs were exposed to media supplemented with 100μM $CoCl_2$ (Figure 7.1). For all studies, a negative control group was included where samples were handled similarly but no preconditioning dosage was applied. Following the preconditioning period, constructs were then exposed to an injurious level of IL-1 (10 ng/mL, isoform depending on cell species, (Cook et al., 2000; Lima et al.,

2008b)) for an additional seven days. During the period of cytokine exposure, all media was void of dexamethasone, previously shown to counter the catabolic effects of IL-1 (Lima et al., 2008b).

7.2.4 Mechanical Testing

Constructs were tested for their equilibrium Young's modulus (E_Y) and dynamic modulus (G*) in unconfined compression using a custom computer-controlled system (Soltz and Ateshian, 1998). An initial 0.02 N tare load was applied, followed by compression to 10% strain, at a strain rate of 0.05% s^{-1}. After stress relaxation was achieved, a 2% peak-to-peak strain was superimposed at 0.01Hz. E_Y was measured from the stress-relaxation equilibrium response and is used as a measure of the equilibrium behavior of cartilage after an applied load has been applied. G*, considered to be a more physiologically relevant measurement of cartilage behavior in response to applied cyclic loads, was determined from the slope of the stress-strain response under dynamic loading.

7.2.5 Biochemical Analysis

After material testing, the biochemical content of each sample was assessed by measuring the sample wet weight, lyophilizing, and then measuring the dry weight. Construct swelling was quantified by measuring the gross water content of the constructs (Lima et al., 2007). Dried samples were digested in proteinase K buffer overnight at 56 °C, as described previously (Kelly et al., 2006). One aliquot was analyzed for glycosaminoglycan (GAG) content via the 1,9 dimethylmethylene blue dye-binding assay. A second aliquot was hydrolyzed with 12 N HCl at 110 °C for 16 h, dried, and resuspended in assay buffer. Orthohydroxyproline content was determined using a colorimetric assay via a reaction with chloramine T and dimethylaminobenzaldehyde, scaled for microplates (Kelly et al., 2006). Overall collagen content was calculated using a 1:7.64 OHP-to-collagen mass ratio (Stegeman and Stalder, 1967). Total dsDNA content was assessed by the Picogreen assay.

7.2.6 Statistics

Statistical analyses were performed using two-way analysis of variance (ANOVA) with Tukey's Honest Significant Difference (HSD) *post hoc* tests (Statistica), with α=0.05 and statistical significance set at $p \leq 0.05$ to compare groups across day and treatment. Data is reported as the mean and standard deviation of 4-5 samples per time point and group.

7.3 Results

7.3.1 *Study 1*: Juvenile bovine chondrocytes - preconditioning culture

All three studies were started on constructs that had matured, i.e., elaborated sufficient ECM to resemble *in situ* cartilage. For these constructs, maturation in culture to day 21 yielded significantly greater mechanical stiffness and biochemical content compared with initial conditions ($E_{Y\,day21}$ = 96.8 ± 22.3 kPa vs. $E_{Y\,day0}$ = 2.32 ± 1.57 kPa; GAG_{day21} = 3.01 ± 0.27%/ww vs. GAG_{day0} = 0.05 ± 0.01%/ww).

Constructs were then exposed to low doses of IL-1α. At day 28, control constructs continued to elaborate matrix and increase stiffness (E_Y = 380 ± 37.0 kPa; GAG = 4.47 ± 0.69%/ww, Figure 7.2), while those exposed to low doses of IL-1α exposure showed significantly lower mechanical

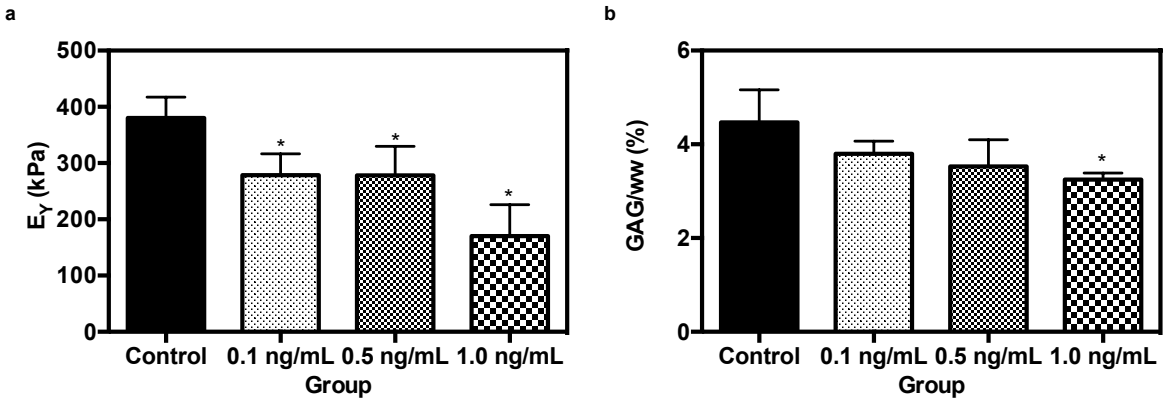

Figure 7.2: Study 1. (a) Young's modulus and (b) GAG content as a result of preconditioning with low doses of IL-1.*$p<0.05$ vs. control

stiffness and GAG composition, demonstrating a concentration-dependent degrading action of the cytokine. For example, with 0.1 ng/mL and 0.5 ng/mL doses, slight tissue degradation was noticeable, as evidenced by the 25% drop in mechanical properties compared to control samples ($E_{Y\,0.1}$ = 278 ± 38.0 kPa, $p_{0.1}$=0.02; $E_{Y\,0.5}$ = 278 ± 51.7 kPa, $p_{0.5}$=0.03, Figure 7.2a). A 15% and 22% drop in GAG content, respectively, was noted for those same low-dose concentrations, though they were not significantly lower relative to control samples ($GAG_{0.1}$ = 3.80 ± 0.27%/ww, $p_{0.1}$ = 0.10; $GAG_{0.5}$ = 3.53 ± 0.57%/ww, $p_{0.5}$=0.05, Figure 7.2b). When 1.0 ng/mL IL-1α was introduced into the culture medium, however, the catabolic effects were much more severe, lowering mechanical stiffness by nearly 55% ($E_{Y\,1.0}$ = 170 ± 55.6 kPa, $p_{1.0}$<0.001, Figure 7.2b). Interestingly, 1.0 ng/mL IL-1α did not introduce a corresponding, severe drop in GAG properties; instead only a 27% decrease was measured compared to control samples ($GAG_{1.0}$ = 3.25 ± 0.57%/ww, $p_{1.0}$ = 0.02, Figure 7.2b). Collagen content was unchanged across all groups.

7.3.2 *Study 1*: Juvenile bovine chondrocytes - insult culture

Following seven days of insult culture (10 ng/mL), positive control samples (no preconditioning dose of IL-1α, 10 ng/mL IL-1α during insult period) showed a significant degree of degradation, retaining only 23% of the construct's mechanical stiffness (E_Y = 44.7 ± 11.1 kPa) and 40% of the construct's GAG content (GAG = 1.73 ± 0.41%/ww) compared to their levels prior to cytokine insult (Figure 7.3). Preconditioning constructs with low doses of IL-1α the week prior to the insult culture afforded dose-dependent protection against catabolic degradation. With 0.1 ng/mL IL-1α preconditioning, constructs exhibited significantly greater mechanical stiffness ($E_{Y\,0.1}$ = 109 ± 11.9 kPa, p=0.16, Figure 7.3a) and GAG content ($GAG_{0.1}$ = 2.81 ± 0.48%/ww, p=0.01, Figure 7.3b) than positive control samples, retaining nearly 70% of their original properties prior to insult. 0.5 ng/mL IL-1α preconditioning provided additional protection against degradation and constructs were further enhanced ($E_{Y\,0.5}$ = 164 ± 7.59 kPa, p=0.01; $GAG_{0.5}$ = 3.29 ± 0.48%/ww, p=0.0003, Figure 7.3). However, constructs preconditioned with the high dose of IL-1α (1.0 ng/mL) showed the same degradation profile as that seen with positive control samples; they were not significantly

different in mechanical stiffness ($E_{Y\,1.0}$ = 36.8 ± 7.89 kPa, p=0.99, Figure 7.3a) or GAG content ($GAG_{1.0}$ = 1.88 ± 0.52%/ww, p=0.99, Figure 7.3b).

7.3.3 *Study 2*: Adult canine chondrocytes - preconditioning culture

Similar to bovine chondrocytes, after 14 days of culture, adult canine chondrocytes elaborated a significant amount of extracellular matrix that resulted in increased mechanical stiffness and biochemical composition by day 14 (E_Y = 191 ± 17.0 kPa; GAG = 3.01 ± 0.27%/ww). By day 21, after 7 days of low dose concentrations of IL-1β, all constructs showed continued growth that was not significantly different in the presence of the cytokine (p>0.42, Figure 7.4a). A slight, but significant, drop in DNA content per construct was noted only for the 2.0 ng/mL IL-1β group ($DNA_{control}$ = 7.30 ± 0.79 μg vs. $DNA_{2.0}$ = 5.92 ± 0.40 μg, p=0.0025, Figure 7.4b). Biochemical composition for all groups was maintained.

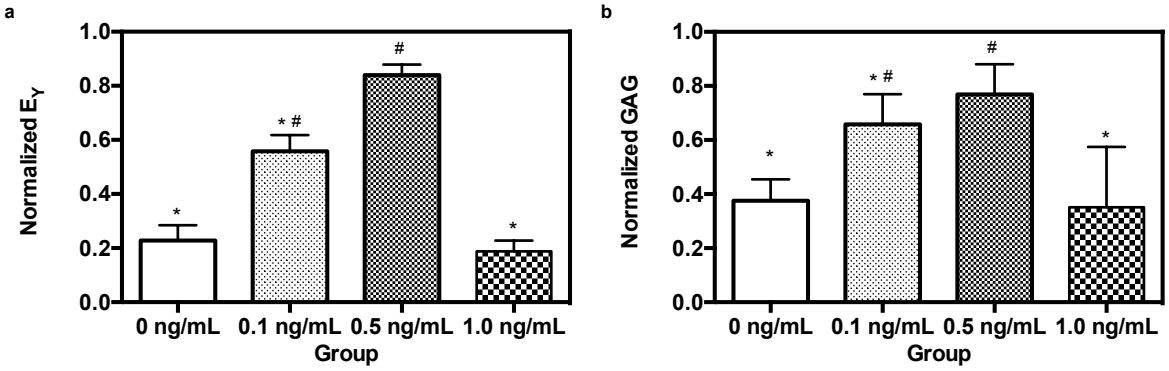

Figure 7.3: Study 1. Normalized (a) Young's modulus and (b) GAG content after insult dose of IL-1 administered. *p<0.05 vs. control, #p<0.05 vs. 0 ng/mL group (positive control)

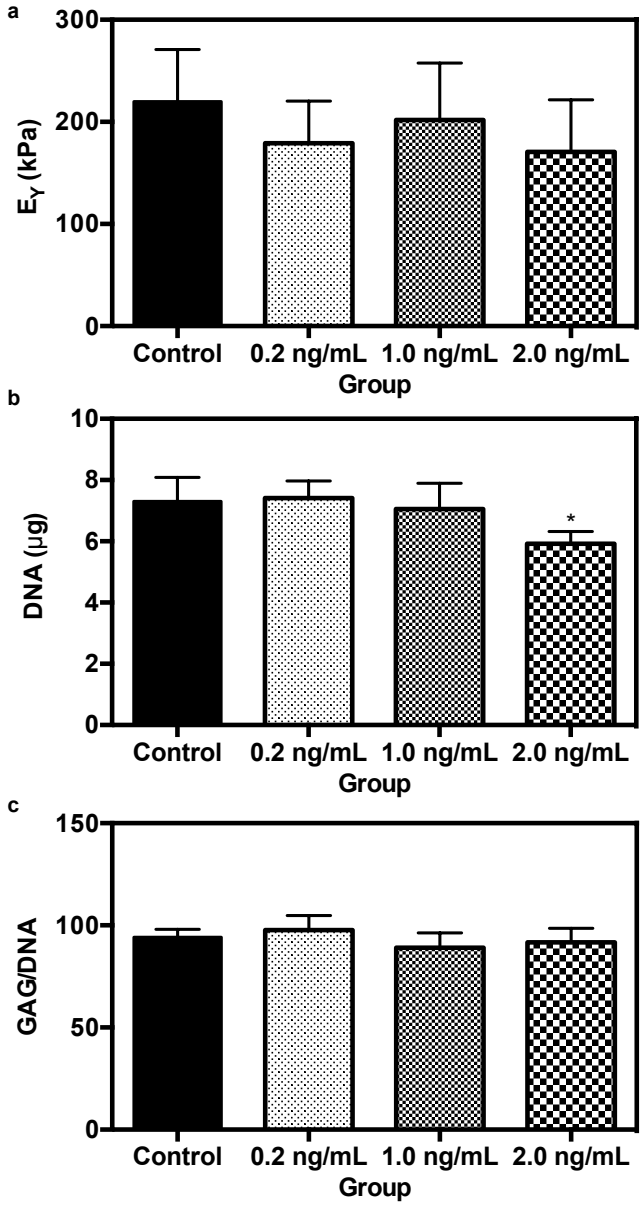

Figure 7.4: Study 2. (a) Young's modulus, (b) DNA, and (c) GAG/DNA content after low dose IL-1 preconditioning. *$p<0.05$ vs. 0 ng/mL group

7.3.4 *Study 2*: Adult canine chondrocytes - insult culture

Following cytokine insult (10 ng/mL), DNA content was significantly lower (47% and 43%, respectively) in the groups with the two highest levels of preconditioning cytokine ($p<0.0001$, Figure 7.5b). Biochemical constituents were normalized to DNA content to account for this change. Positive control samples exhibited significant decreases in mechanical properties ($E_{Y\,control} = 240 \pm 50.4$ kPa vs. $E_{Y\,poscon} = 91.3 \pm 9.10$ kPa, $p<0.0001$, Figure 7.5a) and GAG content ($GAG_{control} = 95.7 \pm 14.8\ \mu g/\mu g$ vs. $GAG_{poscon} = 55.7 \pm 5.96\ \mu g/\mu g$, $p<0.0001$, Figure 7.5c). Preconditioning with low doses of IL-1β (0.2 ng/mL) decreased catabolic degradation, as reflected in mechanical stiffness, i.e. a significantly higher Young's modulus (156 $\pm$ 13.1 kPa) was retained, compared to positive control samples (Figure 7.5a). However, the partial protection noted for mechanical stiffness was not reflected in the biochemical composition of the samples; GAG/DNA (62.9 $\pm$ 7.40 $\mu g/\mu g$, $p=0.90$, Figure 7.5c) was statistically similar to positive control samples. The reverse trend was seen for higher (1.0 and 2.0 ng/mL) preconditioning doses of IL-1β; mechanical properties were similarly affected by the insult level of cytokine as positive controls ($E_{Y\,1.0} = 109 \pm 34.4$ kPa, $p_{1.0} = 0.99$; $E_{Y\,2.0} = 98.5 \pm 27.1$ kPa, $p_{2.0}>0.99$, Figure 7.5a) though GAG content recovered and was comparable to negative control samples ($GAG_{1.0} = 88.2 \pm 2.22\ \mu g/\mu g$, $p_{1.0} = 0.87$; $GAG_{2.0} = 97.9 \pm 5.85\ \mu g/\mu g$, $p_{2.0}>0.99$, Figure 7.5c). Collagen content was unaffected for all groups.

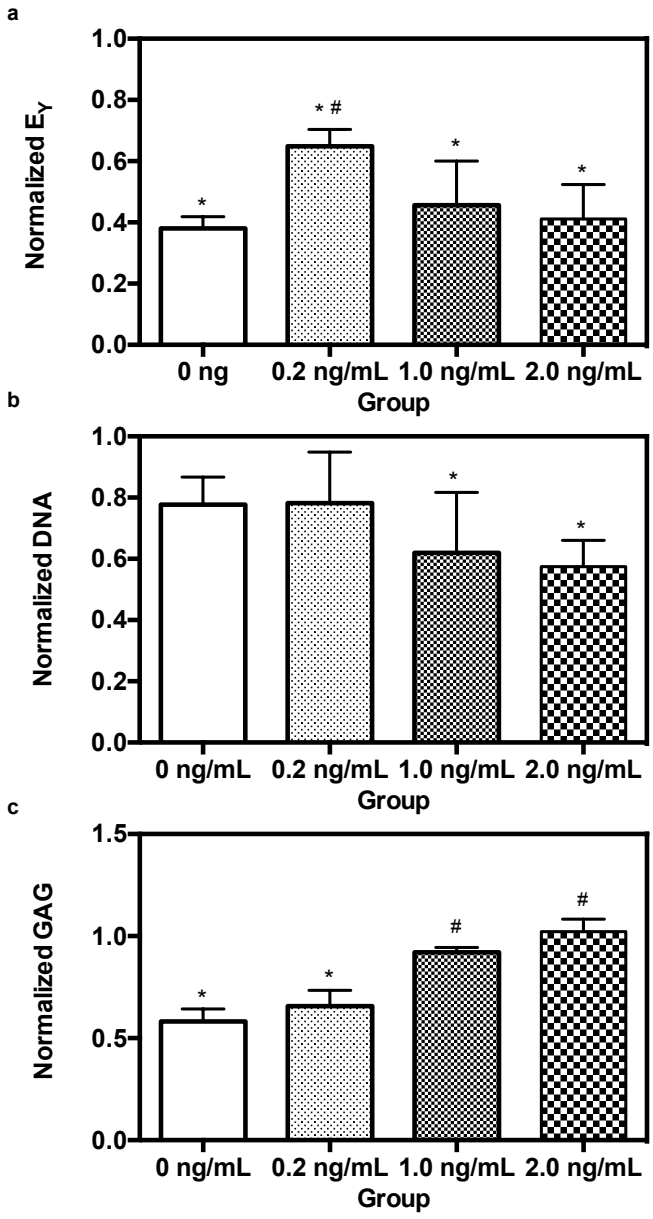

Figure 7.5: Study 2. Normalized (a) Young's modulus, (b) DNA, and (c) GAG content after insult dose of IL-1 administered. *$p<0.05$ vs. control, $^{\#}p<0.05$ vs. 0 ng/mL group (positive control)

7.3.5 *Study 3*: Juvenile bovine chondrocytes - $CoCl_2$ preconditioning

In study 3, in lieu of preconditioning with low doses of cytokine, we explored the use of $CoCl_2$ as a means of activating HIF-1α transcription. On day 14, prior to the start of $CoCl_2$ preconditioning, constructs possessed appreciable extracellular matrix deposition and associated mechanical properties similar to those in mature constructs used in studies 1 and 2 ($E_{Y\,day14}$ = 174 ± 13.8 kPa; GAG_{day14} = 3.21 ± 0.20%/ww). Following preconditioning with $CoCl_2$, constructs exhibited significantly lower stiffness (70% of control, $E_{Y\,day21CoCl2}$= 189± 21.7 kPa, p=0.0076, Figure 7.6a), but comparable dynamic modulus, GAG, and collagen content compared to control constructs (p>0.05, Figure 7.6d). Preconditioned and control constructs were next exposed to insult levels of IL-1α. Positive control samples behaved similarly to those in studies 1 and 2, degrading in mechanical properties ($E_{Y\,poscon}$ = 47.5 ± 13.8 kPa, p<0.0001; G^*_{poscon} = 0.44 ± 0.03 MPa, p=0.0019, Figure 7.7a,b) and GAG content (GAG_{poscon} = 2.41 ± 0.50%/ww, p<0.0001, Figure 7.7c) compared to control samples. Collagen content for these positive control samples was statistically similar to control samples (COL_{poscon} = 1.63 ± 0.07%/ww, p=0.55, Figure 7.7d). $CoCl_2$-preconditioned constructs showed resistance to the catabolic degradation imparted by IL-1α and were capable of retaining more of their GAG content (GAG_{CoCl2}= 3.08± 0.29%/ww, p=0.04, Figure 7.7c), leading to improved mechanical properties (E_Y = 89.7 ± 11.8 kPa, p=0.02, G* = 0.97 ± 0.01 MPa, p=0.0008, Figure 7.7a,b) as compared to positive control samples. However, unlike in studies 1 and 2, collagen content for those preconditioned with $CoCl_2$ decreased significantly (COL_{CoCl2}= 0.97± 0.07%/ww, p<0.0001, Figure 7.7d) compared to control samples and positive control samples.

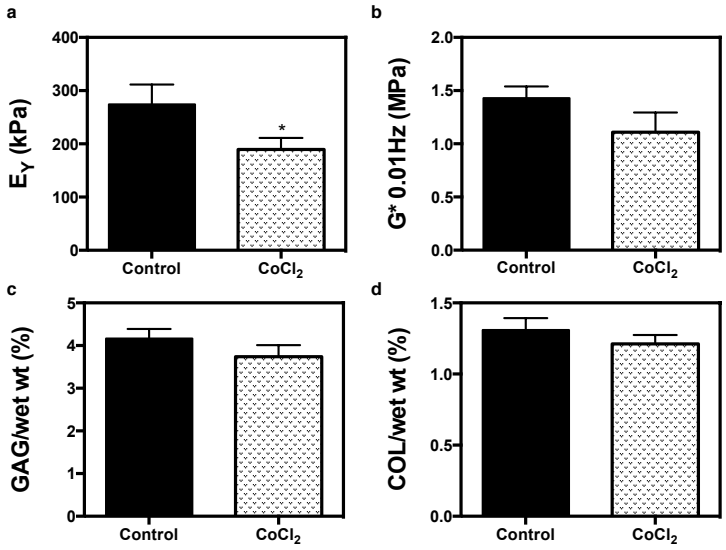

Figure 7.6: Study 3. (a) Young's modulus, (b) Dynamic modulus, (c) GAG content and (d) COL content after preconditioning with 100 μM CoCl2. *p<0.05 vs. control

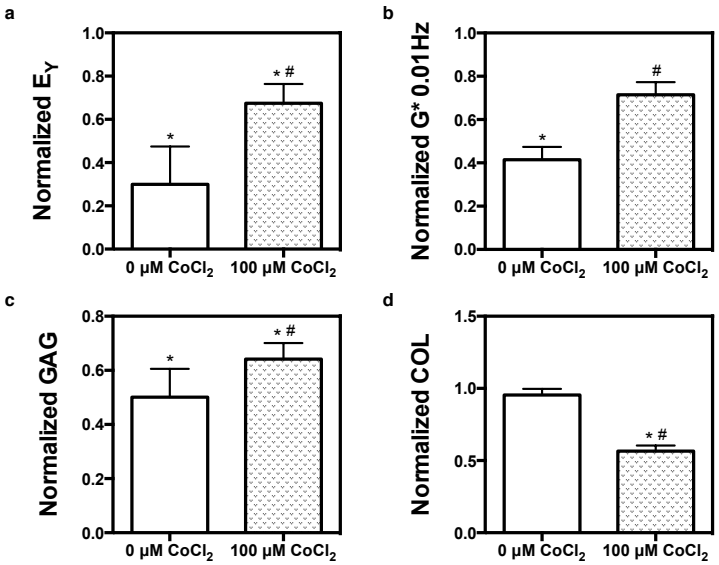

Figure 7.7: Study 3. Normalized (a) Young's modulus, (b) Dynamic modulus, (c) GAG, and (c) COL content after insult dose of IL-1 administered. *p<0.05 vs. control, #p<0.05 vs. 0 μM group (positive control)

7.4 Discussion

Cartilage grafts introduced to an injured or arthritic joint will be subjected to a cytokine-rich environment. Thus, in order to promote engineered cartilage as a clinically-relevant replacement tissue, the construct must be able to survive the chemical and mechanical loads that are imparted upon implantation. In this context, we explored a protection method by which functional engineered cartilage constructs that are capable of attaining native functional properties (bovine: ∼400-1000 kPa (Bian et al., 2008; Lima et al., 2007); canine: ∼380 kPa (Bian et al., 2010a)) can better withstand the harsh chemical environment of the joint. To our knowledge, this is the first study to show that chemical preconditioning schemes impart protection against injurious IL-1 exposure. Specifically, by varying the preconditioning dose, we were able to identify conditions under which mechanical properties and biochemical composition were retained, despite subsequent exposure to injurious levels of the cytokine. These results support our hypothesis regarding the benefits of cytokine preconditioning. The successful translation of these results from a bovine to a canine model, a large preclinical animal model system, corroborates the bovine work and provides encouragement for eventual application of this strategy to therapies for cartilage repair in the clinic.

While many studies employ a classical concept of preconditioning involving cyclical exposure to brief episodes (Haider et al., 2009; Kamota et al., 2009; Patel et al., 2005), other studies utilized a single long-term exposure (Hu et al., 2008; Kubo et al., 2008; Rosova et al., 2008; Tang et al., 2009) to initiate survival signaling that was then followed by the harmful insult. We chose to adopt the latter as the longer preconditioning time frame would increase the likelihood of the cytokine diffusing fully through the agarose construct within the preconditioning period. It is important to note, however, that while the protective effect we observed here has been previously noted with other chemical schemes to prepare individual cells against harsh conditions (Haider and Ashraf, 2010; Murry et al., 1986), this is the first time the effect has been observed for complex whole tissues that include elaborated extracellular matrix. The dense matrix in cartilage constructs confounds attempts to understand the potential mechanism(s) of protection. That is, the mode of protection may arise from an altered state of the cells themselves, or because the preconditioning has induced

the cells to develop a chondroprotective matrix that is able to mediate the effects of the cytokines.

Previous studies have supported the idea that a cell's tolerance to subsequent insult events is afforded by activation of a survival signal that depends on multiple signaling pathways or on the release of chemical activators such as adenosine or nitric oxide (Patel et al., 2005). Furthermore, other studies have found that modulation of growth factor expression either through the use of specific factors during expansion (Murry et al., 1986) or through genetic manipulation can produce similar beneficial preconditioning effects. Further studies are necessary to systematically identify which pathways are involved in the protective process, however, we can postulate that, in agreement with previous preconditioning studies (Hu et al., 2008; Nanduri et al., 2008) and as supported by the results we observed, the HIF-1α pathway has a central role in the activation of this survival signal against IL-1 catabolic degradation. Despite the protection afforded by preconditioning, however, we noted a decrease in collagen content after preconditioning with $CoCl_2$ that was not seen with IL-1 preconditioning groups. This may point to the possibility that a downstream effect of inducing hypoxia may be an upregulation of collagenases that did not occur in our other preconditioning scheme. Additionally, though we did not directly assay for HIF-1α upregulation, previous studies have found an association between hypoxia induction with the upstream activation of the p38 mitogen-activated protein (MAP) kinase pathway (Emerling et al., 2005). p38 MAP kinase has been found to upregulate cytokine production via direct phosphorylation of transcription factors (Ashwell, 2006), possibly leading to additional catabolic effects on the bulk construct. Further work will be necessary to fully elucidate this possibility. Nevertheless, preconditioning with a low dose of IL-1 had a similar effect as preconditioning with induced hypoxia, suggesting that the downstream effect of IL-1 preconditioning may be attributable to upregulation of HIF-1α or a similar effect on cellular transcription.

The heightened generation of a chondroprotective matrix is unlikely to be the only cause of the protection. Previous studies have suggested that pools of GAG in the pericellular region and inter-territorial regions change with culture time such that changes to the local environment of the cell alter the cell's function and response to external stimuli such as IL-1 (Quinn et al., 2002).

However, under our current experimental conditions, unlike previously reported studies (Lima et al., 2008b), we have observed vulnerability to IL-1 regardless of mechanical integrity or biochemical composition, thus ruling out extensive cryoprotection by matrix components. Furthermore, samples with the same composition and mechanical integrity responded differently to insult levels of IL-1 depending on their preconditioning (none vs. low dose IL-1 vs. $CoCl_2$ treatment). It is important to note, however, that our measurements of bulk properties and biochemical constituent content may not detect compositional changes to the matrix. Changes in the composition of matrix could be responsible for the protection against IL-1 that preconditioning with either low dose IL-1 or $CoCl_2$ elicits. Further analysis, however, using comprehensive proteomics gene expression arrays will be required to better understand whether changes to the matrix or subsequent cellular changes are responsible for resisting the catabolic damage brought about by IL-1 exposure.

Although the concentration of the cytokine used to inpart damage to the tissue was on par with concentrations typically utilized for *in vitro* studies (5-20 ng/mL (Li et al., 2003; Temple et al., 2006; Xu et al., 1996)), the dose we used is well above doses found *in vivo* (0.01-0.2 ng/mL (McNulty et al., 2013; Wilusz et al., 2008)). We reason that in free swelling conditions, as described here, in the absence of any mechanical loading, a higher concentration of cytokine may be necessary to elicit an injurious effect. In fact, previous studies have demonstrated that engineered cartilage is insensitive to interleukin at $\leq$0.01 ng/mL, and exhibits an all-or-nothing response at IL concentrations from 0.1 to 10 ng/mL (Lima et al., 2008a). Theoretical modeling of dynamic deformational loading of hydrogels such as agarose have predicted that loading leads to enhanced transport of soluble factors such as cytokines (Albro et al., 2008; Chahine et al., 2009; Mauck et al., 2003a,b). Accordingly, it may be possible to utilize more physiologic levels of cytokines in tandem with dynamic loading protocols in future evaluations of preconditioning schemes for tissue engineered cartilage (Lima et al., 2007).

7.5 Conclusion

In this chapter of the dissertation, a novel method for de-sensitizing engineered cartilage to cytokine exposure was discovered. Though preconditioning protocols have been investigated and are widely recognized for their use in hypoxic and ischaemic conditions, this is the first time such a protocol has been applied for protection against cytokine insult. Preconditioning with a low dose of IL-1 immediately is capable of protecting the construct against subsequent catabolic destruction from exposure to injurious levels of cytokine and offers an intriguing potential for using this technique for clinical therapeutic applicability. These findings contribute to the existing basic science literature on preconditioning mechanisms and add to a growing repertoire of methods with which to modulate cartilage injury.

Part III

Conclusions and Future Directions

Chapter 8

Conclusions and Future Directions

The overall aim of this dissertation was two-fold: 1) characterize the functional nature of developing tissues by assessing their response to induced chemical or mechanical insult and 2) develop reparative and protective strategies for enhancing the performance of engineered cartilage *in vivo*. Our lab has adopted the long-term hypothesis that engineered cartilage must possess material properties matching that of native cartilage in order to survive the harsh mechanochemical loading environment of the knee joint. Towards this goal, this dissertation uncovered new findings on these two interrelated themes and shed light on potential therapeutics for cartilage repair. The studies described here spanned both 2D migration studies to characterize the limited wound repair potential of cells as well as 3D culture studies to explore injury and protection effects at a tissue level. Together, these models allowed us to capture the complexity needed to fully understand the response of engineered constructs to injury and the potential in using it to repair wounded cartilage. We first present a summary of the findings for each study and discuss them in the context of their relevance toward our main goal. Finally, future studies motivated by the work described here are suggested.

8.1 Conclusions

To date, most studies have assessed the quality of the repair tissue by short-term factors such as gene expression or protein analysis or with material properties such as mechanical strength, biochemical composition, or histological properties. We have strived to characterize the biological functionality of our engineered constructs in response to both chemical and mechanical insult in an effort to understand the true biological functionality of our tissues and to predict how they may perform after *in vivo* implantation.

8.1.1 Characterizing the Injury Response in Native and Engineered Cartilage

In Part I, we began this dissertation examining a cohort of earlier studies, to which I contributed, that investigated the response of native and engineered cartilage to cytokine insult (**Chapter 2**). While many studies have previously described interleukin-induced degradation of articular cartilage (Chowdhury et al., 2003; Legare et al., 2002; Li et al., 2003; Rotter et al., 2005; Stabellini et al., 2003; Temple et al., 2006; Xu et al., 1996), our findings revealed that in our chondrogenic medium formulation, native cartilage was resistant to the degradative effects of IL-1. Notably, the response of engineered tissue to the same insult was reliant on the maturity of the construct; i.e. for fledgling engineered cartilage lacking a chondroprotective ECM, constructs exhibited catastrophic degradation. In comparison, ECM-rich constructs were capable of withstanding the insult without degradation of properties, similar to native tissue. Even with the application of physiologic deformational loading, underdeveloped constructs were not capable of surviving the exposure to cytokines. These results direct the use of engineered cartilage for *in vivo* implantation only when constructs have attained sufficient maturity.

The successful implantation of engineered cartilage requires the construct not only to be able to withstand the cytokine-rich environment of the joint, but also to withstand the mechanical burdens characteristic of a load-bearing joint. We explored this theme further by studying the effects of mechanical injury under a controlled loading environment (**Chapter 3**). Many studies in the literature have looked at the response of native articular cartilage to various modes of mechanical

injury; we contribute to the literature in assessing two particular modes of iatrogenic injury and offer suggestions how they may be modified to limit pervasive cell death. Our findings revealed that by manipulating and controlling particular factors (e.g. insertion rate and rotational speed) of the drill apparatus, cartilage tissue is preserved. Next, we filled a large gap in the literature by providing insights into how engineered cartilage responds to similar types of injury. Surprisingly, we found that engineered cartilage exhibited the potential for repair following injury, but that this remained largely dependent on the mode of injury (cutting vs. overload induced cracking) as well as the point in culture (early or late) at which the insult was applied. Briefly, underdeveloped constructs were able to withstand the applied injury, most likely due to the lack of cell-matrix development. As the constructs matured and ECM developed, only cut constructs were able to withstand the insult. Mature overloaded constructs demonstrated a poor healing capacity following cracking injury, analogous to the known behavior of native cartilage. Finally, our results also suggest that disparities between the behavior of our engineered cartilage to native cartilage explants may be due to the inclusion of a anabolic corticosteroid (dexamethasone) that works to not only promote cartilage development, but also protect it against propagative cell death following injury. Therefore, Hypothesis 1 was accepted. Together, these results further differentiate the response of engineered cartilage from native cartilage to mechanical injury and begin to provide insights into how the damage may be contained.

8.1.2 Strategies for Enhancing Cartilage Repair

In Part II of this dissertation work, we developed strategies for enhancing the performance of engineered cartilage for *in vivo* repair. We first analyzed the limited migration of repair cells to wound sites in cartilage and built upon the previous literature on using electric field stimulation for directing cell migration by investigating the influence of extracellular environment. We focused on one particular mechanosensor, the AQP1 water channel, and confirmed our hypothesis that it plays a significant role in migration in the presence of applied EF (**Chapter 4**). Our results highlighted a potential mechanism by which cells sense their environment and regulate key aspects

of migration, including cell volume and cytoskeletal organization. This finding was then tested in harsh environments, modulated both by extracellular medium osmolarity and cytokine exposure. Though cytoskeletal structure was different in hypotonic vs. hypertonic environments, migration capacity was not significantly different, revealing that altered cytoskeletal distribution does not exclusively control directed migration under EF exposure. When cells were cultured in the presence of IL-1, previously reported in the literature to similarly alter cytoskeletal distribution, chondrocytes exhibited stunted migration. Surprisingly, SDSCs proved resistant to the effects of the cytokine, maintaining similar migration profiles as control cells, implying that these SDSCs may be a better source for cartilage repair (**Chapter 5**). From these collective results, we accept Hypothesis 2.

For tissue engineering efforts at creating functional cartilage replacement, we uncovered novel strategies to foster better tissue development via co-culture systems (**Chapter 6**). Fresh chondrocyte feeder layers permit the transmission of soluble factors to encapsulated chondrocytes in constructs; our results showed that these soluble factors were responsible for expediting growth of engineered cartilage depending on the presentation of the feeder layer. This work revealed potential culture techniques capable of producing more functional tissue.

In a precursor study described in **Chapter 2**, we identified a potential mediator of catabolic degradation through the use of a natural cross-linker. We continued in this vein with efforts designed at enhancing the resistance of engineered cartilage to catabolic factors (**Chapter 7**). These positive results described mediated protection against cytokine insult when a preconditioning scheme was first applied. These findings ultimately recommend the use of preconditioning with mechanical and/or chemical factors to mediate the catabolic consequence of IL-1 and we accept Hypothesis 3; such findings motivate their potential use in therapeutics and for tissue engineering efforts at creating clinically-relevant tissue-engineered constructs for the treatment of OA or following injury.

8.2 Future Directions

The collective findings of this dissertation have aimed to fill the gap in knowledge in understanding how engineered cartilage responds to injury and identified potential methods by which that response

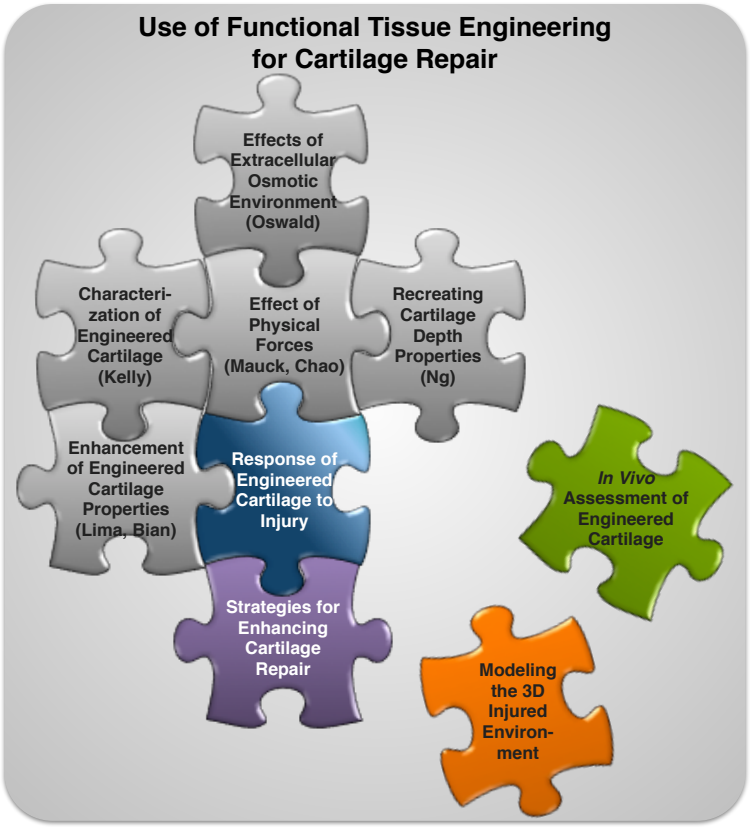

Figure 8.1: Schematic of work described in this thesis (blue, purple pieces) in the context of previous lab efforts (grey pieces). Complementary areas for future directions will add to this overall puzzle (green, orange pieces).

can be mediated. The related themes of work described in this dissertation and future studies is laid out in Figure 8.1. To date, our lab has focused on the creation and characterization of these engineered cartilage constructs, with recent efforts focused on the enhancement of tissue properties via "smart engineering": applying a combination of mechanical loading and chemical stimuli to produce functional tissues. This dissertation aimed to complement the previous studies by first characterizing the biological functionality of engineered tissues. By subjecting the constructs to conditions similar to those found in the *in vivo* environmental, we found that mature engineered cartilage has the potential to behave like native cartilage, responding similarly to both chemical and mechanical insults. These findings prompted the search into novel methods for enhancing cartilage repair with the aim of protecting them from the potentially harsh mechanochemical factors present

in the joint. These results have laid the groundwork for the next step: *in vivo* assessment of engineered constructs that have been prepared using the methodologies described herein. They also highlight areas for potential future complementary studies.

8.2.1 *In vivo* Assessment of Preconditioned Constructs

The findings described in Chapter 7 point to the ability of preconditioned engineered cartilage to partially resist the catabolic factors present in the injured joint, however *in vivo* studies assessing construct success are required to fully understand the potential of this protection scheme. The pre-clinical large animal canine model already is well established (Ng et al., 2010), and has been used to assess the biocompatibility of agarose-chondrocyte constructs.

Within the experimental conditions of our study, only one cytokine was applied during the preconditioning or insult phase. It is likely, however, that a multitude of chemical factors are present in an inflammatory environment and may render *in vivo* outcomes different from what we previously observed. This may suggest the need to reexamine the literature for measured levels of multiple cytokines (e.g. TNF-α, IL-6, leukemia inhibitory factor) found in the injured joint to guide the use of particular cytokines for *in vitro* preconditioning.

8.2.2 Creation of a 3D Injury Model

We have examined directed cell migration in the context of a 2D environment. It has been widely known, however, that the migration of cells in a 3D environment varies drastically. For example, proteolytic digestion of the extracellular matrix is an essential step for efficient migration or invasion into a tissue (Schwab et al., 2012). This is further supported by findings that SDSC migration is facilitated *in vivo* only after the degradation of GAG molecules from the surface (Hunziker and Kapfinger, 1998). To this end, while knowledge gained through the results presented in Chapters 4 and 5 is useful, further development of a 3D model may provide a more realistic view of how cells truly behave when in the joint.

We have begun to assess this potential by co-culturing a SDSC monolayer onto a Transwell

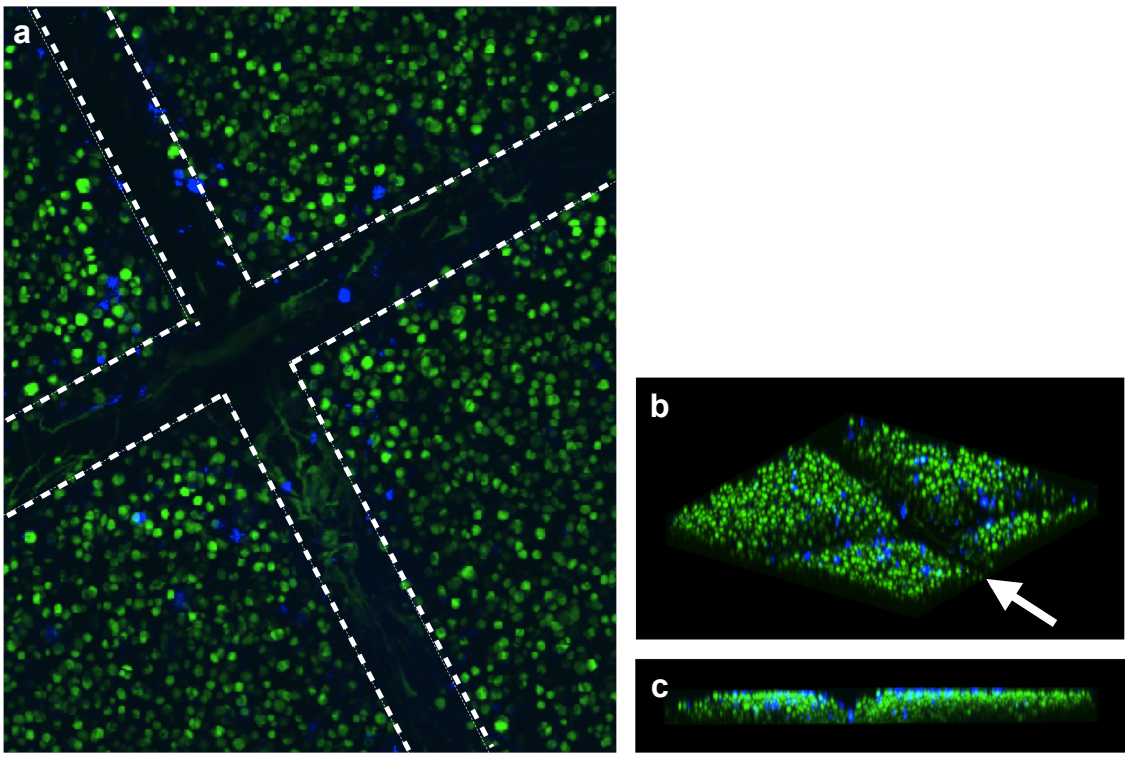

Figure 8.2: (a) 21 days after introduction of a SDSC monolayer to a wounded tissue engineered construct, a confocal stack of images of a representative construct (cartilage cells labeled green) show adhered SDSCs (labeled blue) to the superficial surface of the tissue. (b) 3D reconstruction (white arrow represents face in side view (c)) of the injured cartilage construct show SDSCs preferentially located close to and lining the surface of the cut region (cut region outlined by white dashed lines).

membrane, and positioned it in direct contact with an adjacent wounded engineered cartilage construct. Increased migration of SDSCs onto the surface and into the cut region of the injured construct was observed. As early as seven days following the initial cut injury, confocal images of the cut constructs showed significant migration of SDSCs onto the superficial surface of constructs. By day 21, adhered SDSCs appear to localize to the vicinity of the cut region (Figure 8.2a). 3D reconstruction and side views of the construct confirmed that SDSCs had begun infiltrating the depth of the cut (Figure 8.2b-c).

These results, while preliminary, demonstrate the potential for SDSCs to migrate out of a membrane into a cartilage wound site and describe a model system that can be used to study the complex interplay of multiple tissues in a diarthrodial joint in response to an injury, and to gain

further insights into the mechanisms that mediate the poor healing response of native cartilage to trauma. These results also motivate further investigation into the homing potential of SDSCs to a wound site as well as identifying modulators of cell migration that may be enhanced to increase the reparative response of cartilage.

8.2.3 Use of Pulsatile DC Electrical Stimulation for Enhanced Cell Migration

In line with the aim of creating a 3D injury model, stimulating cells to migrate to a wound site would be beneficial. While we have examined the effects of constant applied DC EF on cell migration in 2D, recent reports in the literature have reported success at generating migration in a 3D tissue under pulsatile stimulation (Yuan et al., 2014). Though the extracellular ionic currents present during wound healing constitute a relatively slow electrical phenomenon and are distinct from faster, pulsatile electrical events (generally associated with action potentials in nerve or muscle cells)(Soong et al., 1990), further investigation into the use of these fields may provide insights to guide wound repair.

In limited preliminary work, we have identified that pulsatile DC electrical stimulation effectively enhances cartilage tissue development. When human bMSC pellets were exposed to such loading, pellets exhibited a dose-dependent growth development (Figure 8.3), with stimulated tissues exhibiting greater staining for GAG and collagen distribution (Figure 8.4); parallel quantitative trends were noted for these molecules. These results point to the potential to incorporate a pulsatile EF stimulation regime during culture to enhance tissue development. Whether these effects lead to enhanced migration within engineered cartilage, however, remains to be elucidated.

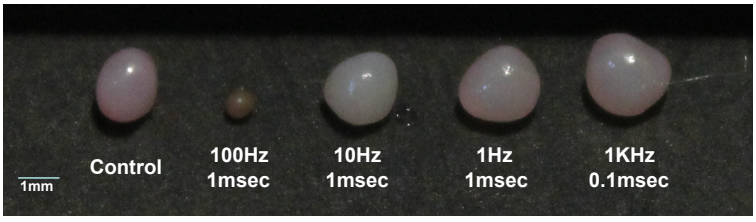

Figure 8.3: Gross morphology of human bMSC pellets exposed to a range of pulsatile DC EF strengths.

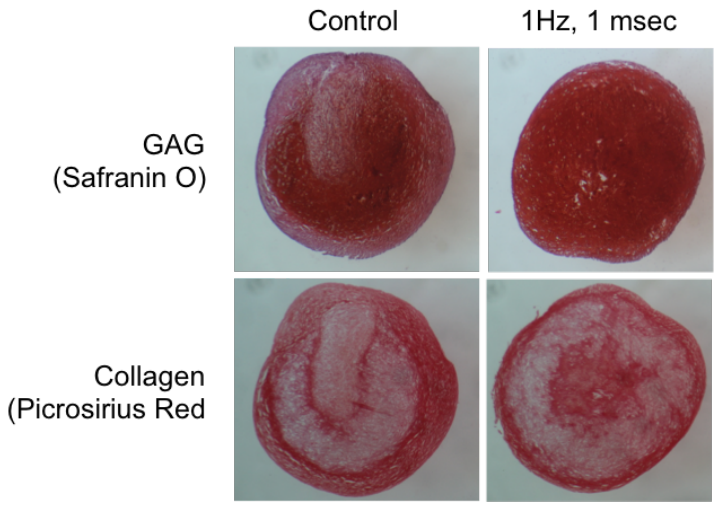

Figure 8.4: Histological analysis (GAG and COL) of human bMSC pellets exposed to pulsatile DC EF.

Part IV

References and Appendices

References

Aaron, R. K., Boyan, B. D., Ciombor, D. M., Schwartz, Z., and Simon, B. J. (2004). Stimulation of growth factor synthesis by electric and electromagnetic fields. *Clinical orthopaedics and related research*, (419):30–37.

Adkisson, H. D., Martin, J. A., Amendola, R. L., Milliman, C., Mauch, K. A., Katwal, A. B., Seyedin, M., Amendola, A., Streeter, P. R., and Buckwalter, J. A. (2010). The potential of human allogeneic juvenile chondrocytes for restoration of articular cartilage. *Am. J. Sports Med.*, 38(7):1324–1333.

Ahmad, C. S., Cohen, Z. A., Levine, W. N., Ateshian, G. A., and Mow, V. C. (2001). Biomechanical and topographic considerations for autologous osteochondral grafting in the knee. *The American journal of sports medicine*, 29(2):201–206.

Ahmed, A. M. and Burke, D. L. (1983). In-vitro measurement of static pressure distribution in synovial joints–Part I: Tibial surface of the knee. *J Biomech Eng*, 105(3):216–225.

Ahmed, N., Gan, L., Nagy, A., Zheng, J., Wang, C., and Kandel, R. A. (2009a). Cartilage tissue formation using redifferentiated passaged chondrocytes in vitro. *Tissue engineering Part A*, 15(3):665–673.

Ahmed, N., Taylor, D. W., Wunder, J., Nagy, A., Gross, A. E., and Kandel, R. A. (2009b). Passaged human chondrocytes accumulate extracellular matrix when induced by bovine chondrocytes. *Journal of tissue engineering and regenerative medicine*.

Albro, M. B., Chahine, N. O., Li, R., Yeager, K., Hung, C. T., and Ateshian, G. A. (2008). Dynamic loading of deformable porous media can induce active solute transport. *J Biomech*, 41(15):3152–3157.

Alegre-Aguaron, E., Sampat, S. R., Xiong, J. C., Colligan, R. M., Bulinski, J. C., Cook, J. L., Ateshian, G. A., Brown, L. M., and Hung, C. T. (2014). Growth Factor Priming Differentially Modulates Components of the Extracellular Matrix Proteome in Chondrocytes and Synovium-Derived Stem Cells. *PLoS ONE*.

Allen, R. T., Robertson, C. M., Pennock, A. T., Bugbee, W. D., Harwood, F. L., Wong, V. W., Chen, A. C., Sah, R. L., and Amiel, D. (2005). Analysis of stored osteochondral allografts at the time of surgical implantation. *Am. J. Sports Med.*, 33(10):11479–11484.

Alt, E., Yan, Y., Gehmert, S., Song, Y.-H., Altman, A., Gehmert, S., Vykoukal, D., and Bai, X. (2011). Fibroblasts share mesenchymal phenotypes with stem cells, but lack their differentiation and colony-forming potential. *Biology of the cell / under the auspices of the European Cell Biology Organization*, 103(4):197–208.

Amin, A. K., Huntley, J. S., Bush, P. G., Simpson, A. H. R. W., and Hall, A. C. (2008a). Chondrocyte death in mechanically injured articular cartilage—the influence of extracellular calcium. *Journal of orthopaedic research : official publication of the Orthopaedic Research Society*, 27(6):778–784.

Amin, A. K., Huntley, J. S., Bush, P. G., Simpson, A. H. R. W., and Hall, A. C. (2008b). Osmolarity influences chondrocyte death in wounded articular cartilage. *The Journal of bone and joint surgery American volume*, 90(7):1531–1542.

Arufe, M. C., De la Fuente, A., Fuentes, I., de Toro, F. J., and Blanco, F. J. (2010). Chondrogenic potential of subpopulations of cells expressing mesenchymal stem cell markers derived from human synovial membranes. *Journal of cellular biochemistry*, 111(4):834–845.

Ashwell, J. D. (2006). The many paths to p38 mitogen-activated protein kinase activation in the immune system. *Nat Rev Immunol*, 6(7):532–540.

Ateshian, G. A. and Hung, C. T. (2003). Functional properties of native articular cartilage. In *Functional Tissue Engineering*, pages p46–68. Springer-Verlag, New York.

Atkins, A. G., Xu, X., and Jeronimidis, G. (2004). Cutting, by 'pressing and slicing,' of thin floppy slices of materials illustrated by experiments on cheddar cheese and salami. *J Mater Sci*, 39:2761–2766.

Atkinson, T. S., Haut, R. C., and Altiero, N. J. (1998). Impact-induced fissuring of articular cartilage: an investigation of failure criteria. *Journal of biomechanical engineering*, 120(2):181–187.

Awad, H., Halvorsen, Y.-D. C., Gimble, J. M., and Guilak, F. (2003). Effects of transforming growth factor beta1 and dexamethasone on the growth and chondrogenic differentiation of adipose-derived stromal cells. *Tiss Eng*, 9(6):1301–1312.

Aydelotte, M. B., Raiss, R. X., Caterson, B., and Kuettner, K. (1992). Influence of interleukin-1 on the morphology and proteoglycan metabolism of cultured bovine articular chondrocytes. *Connect Tissue Res*, 28(1-2):143–159.

Ayers, D. C. (1997). Polyethylene wear and osteolysis following total knee replacement. *Instr Course Lect*, 46:205–213.

Barbero, A., Ploegert, S., Heberer, M., and Martin, I. (2003). Plasticity of clonal populations of dedifferentiated adult human articular chondrocytes. *Arthritis and rheumatism*, 48(5):1315–1325.

Baumgarten, M., Bloebaum, R. D., Ross, S. D., Campbell, P., and Sarmiento, A. (1985). Normal human synovial fluid: osmolality and exercise-induced changes. *The Journal of bone and joint surgery American volume*, 67(9):1336–1339.

Bennett, G. A. and Bauer, W. (1932). A Study of the Repair of Articular Cartilage and the Reaction of Normal Joints of Adult Dogs to Surgically Created Defects of Articular Cartilage,"Joint Mice" and Patellar Displacement. *The American journal of pathology*, 8(5):499–524.21.

Benya, P. D. and Shaffer, J. D. (1982). Dedifferentiated chondrocytes reexpress the differentiated collagen phenotype when cultured in agarose gels. *Cell*, 30(1):215–224.

Bhatia, S. N., Balis, U. J., Yarmush, M. L., and Toner, M. (1999). Effect of cell-cell interactions in preservation of cellular phenotype. Cocultivation of hepatocytes and nonparenchymal cells. *The FASEB journal : official publication of the Federation of American Societies for Experimental Biology*, 13:1883–1900.

Bian, L., Angione, S. L., Ng, K. W., Lima, E. G., Williams, D. Y., Mao, D. Q., Ateshian, G. A., and Hung, C. T. (2009). Influence of decreasing nutrient path length on the development of engineered cartilage. *Osteoarthritis and cartilage / OARS, Osteoarthritis Research Society*, 17(5):677–685.

Bian, L., Fong, J. V., Lima, E. G., Stoker, A. M., Ateshian, G. A., Cook, J. L., and Hung, C. T. (2010a). Dynamic mechanical loading enhances functional properties of tissue-engineered cartilage using mature canine chondrocytes. *Tissue engineering Part A*, 16(5):1781–1790.

Bian, L., Lima, E. G., Angione, S. L., Ng, K. W., Williams, D. Y., Xu, D., Stoker, A. M., Cook, J. L., Ateshian, G. A., and Hung, C. T. (2008). Mechanical and biochemical characterization of cartilage explants in serum-free culture. *Journal of biomechanics*, 41(6):1153–1159.

Bian, L., Stoker, A. M., Marberry, K. M., Ateshian, G. A., Cook, J. L., and Hung, C. T. (2010b). Effects of dexamethasone on the functional properties of cartilage explants during long-term culture. *Am. J. Sports Med.*, 38(1):78–85.

Bigdeli, N., Karlsson, C., Strehl, R., Concaro, S., Hyllner, J., and Lindahl, A. (2009). Coculture of human embryonic stem cells and human articular chondrocytes results in significantly altered phenotype and improved chondrogenic differentiation. *Stem Cells*, 27(8):1812–1821.

Blanco, F. J., Guitian, R., Vazquez-Martul, E., de Toro, F. J., and Galdo, F. (1998). Osteoarthritis chondrocytes die by apoptosis. A possible pathway for osteoarthritis pathology. *Arthritis and rheumatism*, 41(2):284–289.

Borghetti, P., Della Salda, L., De Angelis, E., Maltarello, M. C., Petronini, P. G., Cabassi, E., Marcato, P. S., Maraldi, N. M., and Borghetti, A. F. (1995). Adaptive cellular response to osmotic stress in pig articular chondrocytes. *Tissue Cell*, 27(2):173–183.

Bradley, G. W., Freeman, M. A., Tuke, M. A., and McKellop, H. A. (1993). Evaluation of wear in an all-polymer total knee replacement. Part 2: clinical evaluation of wear in a polyethylene on polyacetal total knee. *Clin Mater*, 14(2):127–132.

Brittberg, M., Nilsson, A., Lindahl, A., Ohlsson, C., and Peterson, L. (1996). Rabbit articular cartilage defects treated with autologous cultured chondrocytes. *Clin. Orthop.*, (326):270–283.

Brown, T. D. and Shaw, D. T. (1984). In vitro contact stress distribution on the femoral condyles. *Journal of orthopaedic research : official publication of the Orthopaedic Research Society*, 2(2):190–199.

Buckwalter, J. A. and Mankin, H. J. (1998a). Articular cartilage: degeneration and osteoarthritis, repair, regeneration, and transplantation. *Instr Course Lect*, 47:487–504.

Buckwalter, J. A. and Mankin, H. J. (1998b). Articular cartilage: tissue design and chondrocyte-matrix interactions. *Instr Course Lect*, 47:477–486.

Buckwalter, J. A., Martin, J., and Mankin, H. J. (2000). Synovial joint degeneration and the syndrome of osteoarthritis. *Instr Course Lect*, 49:481–489.

Buckwalter, J. A. and Martin, J. A. (2006). Osteoarthritis. *Advanced drug delivery reviews*, 58(2):150–167.

Bulstra, S. K., Buurman, W. A., Walenkamp, G. H., and Van der Linden, A. J. (1989). Metabolic characteristics of in vitro cultured human chondrocytes in relation to the histopathologic grade of osteoarthritis. *Clinical orthopaedics and related research*, (242):294–302.

Burdick, J. A., Chung, C., Jia, X., Randolph, M. A., and Langer, R. (2005). Controlled degradation and mechanical behavior of photopolymerized hyaluronic acid networks. *Biomacromolecules*, 6(1):386–391.

Buschmann, M. D., Gluzband, Y. A., Grodzinsky, A. J., and Hunziker, E. B. (1995). Mechanical compression modulates matrix biosynthesis in chondrocyte/agarose culture. *Journal of cell science*, 108 (Pt 4):1497–1508.

Buschmann, M. D., Gluzband, Y. A., Grodzinsky, A. J., Kimura, J. H., and Hunziker, E. B. (1992). Chondrocytes in agarose culture synthesize a mechanically functional extracellular matrix. *Journal of orthopaedic research : official publication of the Orthopaedic Research Society*, 10(6):745–758.

Butler, D. L., Goldstein, S. A., and Guilak, F. (2000). Functional tissue engineering: the role of biomechanics. *Journal of biomechanical engineering*, 122(6):570–575.

Byers, B. A., Mauck, R. L., Chiang, I., and Tuan, R. S. (2006). Temporal exposure of TGF-B3 under serum-free conditions enhances biomechanical and biochemical maturation of tissue-engineered cartilage. *Trans Orthop Res Soc*, 31:43.

Caplan, A. I., Elyaderani, M., Mochizuki, Y., Wakitani, S., and Goldberg, V. M. (1997). Principles of cartilage repair and regeneration. *Clinical orthopaedics and related research*, (342):254–269.

Caplan, A. I., Goto, T., Wakitani, S., Pineda, S. J., Haynesworth, S. E., and Goldbery, V. M. (1993). Cell-based technologies for cartilage repair. In *Biology and Biomechanics of the Traumatized Synovial Joint: The Knee as a Model.*, pages 111–122. AAOS, Rosemont.

Carlson, H. (1957). Reactions of rabbit patellary cartilage following operative defects; a morphological and autoradiographic study. *Acta orthopaedica Scandinavica. Supplementum*, 28:1–104.

Carver, S. E. and Heath, C. A. (1999). Increasing extracellular matrix production in regenerating cartilage with intermittent physiological pressure. *Biotechnology and bioengineering*, 62(2):166–174.

Chahine, N. O., Albro, M. B., Lima, E. G., Wei, V. I., DuBois, C. R., Hung, C. T., and Ateshian, G. A. (2009). Effect of dynamic loading on the transport of solutes into agarose hydrogels. *Biophysical journal*, 97(4):968–975.

Chahine, N. O., Ateshian, G. A., and Hung, C. T. (2007). The effect of finite compressive strain on chondrocyte viability in statically loaded bovine articular cartilage. *Biomechanics and modeling in mechanobiology*, 6(1-2):103–111.

Chahine, N. O., Wang, C. C.-B., Hung, C. T., and Ateshian, G. A. (2004). Anisotropic strain-dependent material properties of bovine articular cartilage in the transitional range from tension to compression. *Journal of biomechanics*, 37(8):1251–1261.

Chamberlain, G., Fox, J., Ashton, B., and Middleton, J. (2007). Concise Review: Mesenchymal Stem Cells: Their Phenotype, Differentiation Capacity, Immunological Features, and Potential for Homing. *Stem Cells*, 25(11):2739–2749.

Chao, P. H., Roy, R., Mauck, R. L., Liu, W., Valhmu, W. B., and Hung, C. T. (2000). Chondrocyte translocation response to direct current electric fields. *Journal of biomechanical engineering*, 122(3):261–267.

Chao, P.-H. G., Lu, H. H., Hung, C. T., Nicoll, S. B., and Bulinski, J. C. (2007). Effects of applied DC electric field on ligament fibroblast migration and wound healing. *Connect Tissue Res*, 48(4):188–197.

Chao, P.-H. G., West, A. C., and Hung, C. T. (2006). Chondrocyte intracellular calcium, cytoskeletal organization, and gene expression responses to dynamic osmotic loading. *American journal of physiology. Cell physiology*, 291(4):C718–25.

Chao, P.-H. G., Yodmuang, S., Wang, X., Sun, L., Kaplan, D. L., and Vunjak-Novakovic, G. (2010). Silk hydrogel for cartilage tissue engineering. *J Biomed Mater Res B Appl Biomater*, 95(1):84–90.

Chen, C. T., Burton-Wurster, N., Borden, C., Hueffer, K., Bloom, S. E., and Lust, G. (2001). Chondrocyte necrosis and apoptosis in impact damaged articular cartilage. *Journal of orthopaedic research : official publication of the Orthopaedic Research Society*, 19(4):703–711.

Chowdhury, T. T., Bader, D. L., and Lee, D. A. (2001). Dynamic compression inhibits the synthesis of nitric oxide and PGE(2) by IL-1beta-stimulated chondrocytes cultured in agarose constructs. *Biochemical and biophysical research communications*, 285(5):1168–1174.

Chowdhury, T. T., Bader, D. L., and Lee, D. A. (2003). Dynamic compression counteracts IL-1 beta-induced release of nitric oxide and PGE2 by superficial zone chondrocytes cultured in agarose constructs. *Osteoarthritis and cartilage / OARS, Osteoarthritis Research Society*, 11(9):688–696.

Clarke, I. C. (1971). Articular cartilage: a review and scanning electron microscope study. 1. The interterritorial fibrillar architecture. *The Journal of bone and joint surgery. British volume*, 53(4):732–750.

Cook, J. L., Anderson, C. C., Kreeger, J. M., and Tomlinson, J. L. (2000). Effects of human recombinant interleukin-1 beta on canine articular chondrocytes in three-dimensional culture. *American Journal of Veterinary Research*, 61(7):766–770.

Cook, J. L., Williams, N., Kreeger, J. M., Peacock, J. T., and Tomlinson, J. L. (2003). Biocompatibility of three-dimensional chondrocyte grafts in large tibial defects of rabbits. *Am. J. Vet. Res.*, 64(1):12–20.

Costouros, J. G. and Kim, H. T. (2007). Preventing chondrocyte programmed cell death caused by iatrogenic injury. *The Knee*, 14(2):107–111.

DeLise, A. M., Fischer, L., and Tuan, R. S. (2000). Cellular interactions and signaling in cartilage development. *Osteoarthritis Cartilage*, 8(5):309–334.

Dominici, M., Le Blanc, K., Mueller, I., Slaper-Cortenbach, I., Marini, F., Krause, D., Deans, R., Keating, A., Prockop, D., and Horwitz, E. (2006). Minimal criteria for defining multipotent mesenchymal stromal cells. The International Society for Cellular Therapy position statement. *Cytotherapy*, 8(4):315–317.

Donzelli, P. S., Spilker, R. L., Ateshian, G. A., and Mow, V. C. (1999). Contact analysis of biphasic transversely isotropic cartilage layers and correlations with tissue failure. *J Biomech*, 32(10):1037–1047.

Dumont, J., Ionescu, M., Reiner, A., Poole, A. R., Tran-Khanh, N., Hoemann, C. D., McKee, M. D., and Buschmann, M. D. (1999). Mature full-thickness articular cartilage explants attached to bone are physiologically stable over long-term culture in serum-free media. *Connect Tissue Res*, 40(4):259–272.

Eggers, K., Werneburg, S., Schertzinger, A., Abeln, M., Schiff, M., Scharenberg, M. A., Burkhardt, H., Muhlenhoff, M., and Hildebrandt, H. (2011). Polysialic acid controls NCAM signals at cell-cell contacts to regulate focal adhesion independent from FGF receptor activity. *Journal of cell science*, 124(Pt 19):3279–3291.

Elders, M. J. (2000). The increasing impact of arthritis on public health. *J Rheumatol Suppl*, 60:6–8.

Elmoazzen, H. Y., Elliott, J. A. W., and McGann, L. E. (2002). The effect of temperature on membrane hydraulic conductivity. *Cryobiology*, 45(1):68–79.

Emerling, B. M., Platanias, L. C., Black, E., Nebreda, A. R., Davis, R. J., and Chandel, N. S. (2005). Mitochondrial reactive oxygen species activation of p38 mitogen-activated protein kinase is required for hypoxia signaling. *Molecular and cellular biology*, 25(12):4853–4862.

Erickson, G. R., Alexopoulos, L. G., and Guilak, F. (2001). Hyper-osmotic stress induces volume change and calcium transients in chondrocytes by transmembrane, phospholipid, and G-protein pathways. *J Biomech*, 34(12):1527–1535.

Erickson, G. R., Northrup, D. L., and Guilak, F. (2003). Hypo-osmotic stress induces calcium-dependent actin reorganization in articular chondrocytes. *Osteoarthritis and cartilage / OARS, Osteoarthritis Research Society*, 11(3):187–197.

Etienne-Manneville, S. and Hall, A. (2001). Integrin-mediated activation of Cdc42 controls cell polarity in migrating astrocytes through PKCzeta. *Cell*, 106(4):489–498.

Evans, P. J., Miniaci, A., and Hurtig, M. B. (2004). Manual punch versus power harvesting of osteochondral grafts. *Arthroscopy : the journal of arthroscopic & related surgery : official publication of the Arthroscopy Association of North America and the International Arthroscopy Association*, 20(3):306–310.

Ewers, B. J., Dvoracek-Driksna, D., Orth, M. W., and Haut, R. C. (2001). The extent of matrix damage and chondrocyte death in mechanically traumatized articular cartilage explants depends on rate of loading. *Journal of orthopaedic research : official publication of the Orthopaedic Research Society*, 19(5):779–784.

Eyre, D. R. (1980). Collagen: molecular diversity in the body's protein scaffold. *Science (New York, N.Y.)*, 207(4437):1315–1322.

Fan, J., Varshney, R., Ren, L., Cai, D., and Wang, D. (2009). Synovium-Derived Mesenchymal Stem Cells: A New Cell Source for Musculoskeletal Regeneration. *Tissue engineering Part B, Reviews*.

Farber, E. (1994). Programmed cell death: necrosis versus apoptosis. *Mod Pathol*, 7(5):605–609.

Farndale, R. W., Sayers, C. A., and Barrett, A. J. (1982). A direct spectrophotometric microassay for sulfated glycosaminoglycans in cartilage cultures. *Connect Tissue Res*, 9(4):247–248.

Fermor, B., Weinberg, J. B., Pisetsky, D. S., Misukonis, M. A., Banes, A. J., and Guilak, F. (2001). The effects of static and intermittent compression on nitric oxide production in articular cartilage explants. *Journal of orthopaedic research : official publication of the Orthopaedic Research Society*, 19(4):729–737.

Finkelstein, E. I., Chao, P.-H. G., Hung, C. T., and Bulinski, J. C. (2007). Electric field-induced polarization of charged cell surface proteins does not determine the direction of galvanotaxis. *Cell motility and the cytoskeleton*, 64(11):833–846.

Flachsmann, R., Broom, N. D., and Hardy, A. E. (2001). Deformation and rupture of the articular surface under dynamic and static compression. *Journal of orthopaedic research : official publication of the Orthopaedic Research Society*, 19(6):1131–1139.

Francioli, S. E., Martin, I., Sie, C. P., Hagg, R., Tommasini, R., Candrian, C., Heberer, M., and Barbero, A. (2007). Growth factors for clinical-scale expansion of human articular chondrocytes: relevance for automated bioreactor systems. *Tissue engineering*, 13(6):1227–1234.

Freed, L. E., Langer, R., Martin, I., Pellis, N. R., and Vunjak-Novakovic, G. (1997). Tissue engineering of cartilage in space. *Proc Natl Acad Sci U S A*, 94(25):13885–13890.

Frenkel, S. R., Clancy, R. M., Ricci, J. L., Di Cesare, P. E., Rediske, J. J., and Abramson, S. B. (1996). Effects of nitric oxide on chondrocyte migration, adhesion, and cytoskeletal assembly. *Arthritis and rheumatism*, 39(11):1905–1912.

Fukai, F., Mashimo, M., Akiyama, K., Goto, T., Tanuma, S., and Katayama, T. (1998). Modulation of apoptotic cell death by extracellular matrix proteins and a fibronectin-derived antiadhesive peptide. *Experimental cell research*, 242(1):92–99.

Fukubayashi, T. and Kurosawa, H. (1980). The contact area and pressure distribution pattern of the knee. A study of normal and osteoarthrotic knee joints. *Acta orthopaedica Scandinavica*, 51(6):871–879.

Gabriel, S. E., Crowson, C. S., and O'Fallon, W. M. (1995). Costs of osteoarthritis: estimates from a geographically defined population. *J Rheumatol Suppl*, 43:23–25.

Gan, L. and Kandel, R. A. (2007). In vitro cartilage tissue formation by Co-culture of primary and passaged chondrocytes. *Tissue engineering*, 13(4):831–842.

Gao, J., Dennis, J. E., Solchaga, L. A., Goldberg, V. M., and Caplan, A. I. (2002). Repair of osteochondral defect with tissue-engineered two-phase composite material of injectable calcium phosphae and hyaluronan sponge. *Tissue engineering*, 5:827–837.

Garrett, J. C. (1998). Osteochondral allografts for reconstruction of articular defects of the knee. *AAOS Instructional Course Lectures*, 47:517–522.

Gassner, R., Buckley, M. J., Georgescu, H., Studer, R., Stefanovich-Racic, M., Piesco, N. P., Evans, C. H., and Agarwal, S. (1999). Cyclic tensile stress exerts antiinflammatory actions on chondrocytes by inhibiting inducible nitric oxide synthase. *Journal of immunology (Baltimore, Md. : 1950)*, 163(4):2187–2192.

Gilbert, J. E. (1998). Current treatment options for the restoration of articular cartilage. *The American journal of knee surgery*, 11(1):42–46.

Giuliani, R., Bastaki, M., Coltrini, D., and Presta, M. (1999). Role of endothelial cell extracellular signal-regulated kinase1/2 in urokinase-type plasminogen activator upregulation and in vitro angiogenesis by fibroblast growth factor-2. *Journal of cell science*, 112 (Pt 15):2597–2606.

Glenn, R. E., McCarty, E. C., Potter, H. G., Juliao, S. F., Gordon, J. D., and Spindler, K. P. (2006). Comparison of fresh osteochondral autografts and allografts: a canine model. *The American journal of sports medicine*, 34(7):1084–1093.

Goldring, M. B. (1999). The role of cytokines as inflammatory mediators in osteoarthritis: lessons from animal models. *Connect Tissue Res*, 40(1):1–11.

Goldring, M. B., Otero, M., Plumb, D. A., Dragomir, C., Favero, M., El Hachem, K., Hashimoto, K., Roach, H. I., Olivotto, E., Borzì, R. M., and Marcu, K. B. (2011). Roles of inflammatory and anabolic cytokines in cartilage metabolism: signals and multiple effectors converge upon MMP-13 regulation in osteoarthritis. *European cells & materials*, 21:202–220.

Goldring, S. R. and Goldring, M. B. (2004). The role of cytokines in cartilage matrix degeneration in osteoarthritis. *Clinical orthopaedics and related research*, (427 Suppl):S27–36.

Gooch, K. J., Kwon, J. H., Blunk, T., Langer, R., Freed, L. E., and Vunjak-Novakovic, G. (2001). Effects of mixing intensity on tissue-engineered cartilage. *Biotechnology and bioengineering*, 72(4):402–407.

Guilak, F., Awad, H. A., Fermor, B., Leddy, H. A., and Gimble, J. M. (2004). Adipose-derived adult stem cells for cartilage tissue engineering. *Biorheology*, 41(3-4):389–399.

Guilak, F., Erickson, G. R., and Ting-Beall, H. P. (2002). The effects of osmotic stress on the viscoelastic and physical properties of articular chondrocytes. *Biophysical journal*, 82(2):720–727.

Guilak, F. and Hung, C. T. (2005). Physical Regulation of Cartilage Metabolism. In *Basic Orthopaedic Biomechanics*, pages 179–207. Lippincott-Raven, Philadelphia.

Guilak, F., Ratcliffe, A., and Mow, V. C. (1995). Chondrocyte deformation and local tissue strain in articular cartilage: a confocal microscopy study. *Journal of orthopaedic research : official publication of the Orthopaedic Research Society*, 13(3):410–421.

Guillotin, B., Bourget, C., Remy-Zolgadri, M., Bareille, R., Fernandez, P., Conrad, V., and Amédée-Vilamitjana, J. (2004). Human primary endothelial cells stimulate human osteoprogenitor cell differentiation. *Cellular physiology and biochemistry : international journal of experimental cellular physiology, biochemistry, and pharmacology*, 14(4-6):325–332.

Gunja, N. J. and Athanasiou, K. A. (2007). Passage and reversal effects on gene expression of bovine meniscal fibrochondrocytes. *Arthritis research & therapy*, 9(5):R93.

Gunja, N. J., Dujari, D., Chen, A., Luengo, A., Fong, J. V., and Hung, C. T. (2011). Migration responses of outer and inner meniscus cells to applied direct current electric fields. *Journal of orthopaedic research : official publication of the Orthopaedic Research Society*.

Haider, H. K. and Ashraf, M. (2010). Preconditioning and stem cell survival. *Journal of cardiovascular translational research*, 3(2):89–102.

Haider, K. H., Kim, H. W., and Ashraf, M. (2009). Hypoxia-inducible factor-1alpha in stem cell preconditioning: mechanistic role of hypoxia-related micro-RNAs. *The Journal of thoracic and cardiovascular surgery*, 138(1):257.

Hall, A. C., Starks, I., Shoults, C. L., and Rashidbigi, S. (1996). Pathways for K+ transport across the bovine articular chondrocyte membrane and their sensitivity to cell volume. *The American journal of physiology*, 270(5 Pt 1):C1300–10.

Hangody, L., Kish, G., Karpati, Z., Szerb, I., and Udvarhelyi, I. (1997). Arthroscopic autogenous osteochondral mosaicplasty for the treatment of femoral condylar articular defects. A preliminary report. *Knee Surg Sports Traumatol Arthrosc*, 5(4):262–267.

Hartig, M., Joos, U., and Wiesmann, H. P. (2000). Capacitively coupled electric fields accelerate proliferation of osteoblast-like primary cells and increase bone extracellular matrix formation in vitro. *Eur. Biophys. J.*, 29(7):499–506.

Hashimoto, S., Ochs, R. L., Rosen, F., Quach, J., McCabe, G., Solan, J., Seegmiller, J. E., Terkeltaub, R., and Lotz, M. (1998). Chondrocyte-derived apoptotic bodies and calcification of articular cartilage. *Proceedings of the National Academy of Sciences of the United States of America*, 95(6):3094–3099.

Hehenberger, K., Heilborn, J. D., Brismar, K., and Hansson, A. (1998). Inhibited proliferation of fibroblasts derived from chronic diabetic wounds and normal dermal fibroblasts treated with high glucose is associated with increased formation of l-lactate. *Wound repair and regeneration : official publication of the Wound Healing Society [and] the European Tissue Repair Society*, 6(2):135–141.

Hennig, A. and Abate, J. (2007). Osteochondral allografts in the treatment of articular cartilage injuries of the knee. *Sports Med. Athrosc.*, 15:126–132.

Hoben, G. M., Willard, V. P., and Athanasiou, K. A. (2009). Fibrochondrogenesis of hESCs: growth factor combinations and cocultures. *Stem cells and development*, 18(2):283–292.

Hockenbery, D. (1995). Defining apoptosis. *The American journal of pathology*, 146(1):16–19.

Hollander, A. P., Heathfield, T. F., Webber, C., Iwata, Y., Bourne, R., Rorabeck, C., and Poole, A. R. (1994). Increased damage to type II collagen in osteoarthritic articular cartilage detected by a new immunoassay. *The Journal of clinical investigation*, 93:1722–1732.

Honda, K., Ohno, S., Tanimoto, K., Ijuin, C., Tanaka, N., Doi, T., Kato, Y., and Tanne, K. (2000). The effects of high magnitude cyclic tensile load on cartilage matrix metabolism in cultured chondrocytes. *European journal of cell biology*, 79(9):601–609.

Hopewell, B. and Urban, J. P. (2003). Adaptation of articular chondrocytes to changes in osmolality. *Biorheology*, 40(1-3):73–77.

Hu, X., Yu, S. P., Fraser, J. L., Lu, Z., Ogle, M. E., Wang, J.-A., and Wei, L. (2008). Transplantation of hypoxia-preconditioned mesenchymal stem cells improves infarcted heart function via enhanced survival of implanted cells and angiogenesis. *The Journal of thoracic and cardiovascular surgery*, 135(4):799–808.

Huang, A. H., Farrell, M. J., and Mauck, R. L. (2010). Mechanics and mechanobiology of mesenchymal stem cell-based engineered cartilage. *Journal of biomechanics*, 43(1):128–136.

Huang, A. H., Stein, A., Tuan, R. S., and Mauck, R. L. (2009). Transient exposure to transforming growth factor beta 3 improves the mechanical properties of mesenchymal stem cell-laden cartilage constructs in a density-dependent manner. *Tissue engineering Part A*, 15(11):3461–3472.

Huang, A. H., Yeger-McKeever, M., Stein, A., and Mauck, R. L. (2008). Tensile properties of engineered cartilage formed from chondrocyte- and MSC-laden hydrogels. *Osteoarthritis and cartilage / OARS, Osteoarthritis Research Society*, 16(9):1074–1082.

Huang, C.-Y. C., Hagar, K. L., Frost, L. E., Sun, Y., and Cheung, H. S. (2004). Effects of cyclic compressive loading on chondrogenesis of rabbit bone-marrow derived mesenchymal stem cells. *Stem Cells*, 22(3):313–323.

Huberti, H. H. and Hayes, W. C. (1984). Patellofemoral contact pressures. The influence of q-angle and tendofemoral contact. *J Bone Joint Surg Am*, 66(5):715–724.

Hung, C. T., Lima, E. G., Mauck, R. L., Takai, E., Taki, E., LeRoux, M. A., Lu, H. H., Stark, R. G., Guo, X. E., and Ateshian, G. A. (2003). Anatomically shaped osteochondral constructs for articular cartilage repair. *Journal of biomechanics*, 36(12):1853–1864.

Hung, C. T., Mauck, R. L., Wang, C. C. B., Lima, E. G., and Ateshian, G. A. (2004). A paradigm for functional tissue engineering of articular cartilage via applied physiologic deformational loading. *Annals of Biomedical Engineering*, 32(1):35–49.

Huntley, J. S., Bush, P. G., McBirnie, J. M., Simpson, A. H., and Hall, A. C. (2005). Chondrocyte death associated with human femoral osteochondral harvest as performed for mosaicplasty. *The Journal of bone and joint surgery American volume*, 87(2):351–360.

Hunziker, E. B. (1999). Articular cartilage repair: are the intrinsic biological constraints undermining this process insuperable? *Osteoarthritis Cartilage*, 7:15–28.

Hunziker, E. B. and Kapfinger, E. (1998). Removal of proteoglycans from the surface of defects in articular cartilage transiently enhances coverage by repair cells. *The Journal of bone and joint surgery. British volume*, 80(1):144–150.

Hunziker, E. B. and Rosenberg, L. C. (1996). Repair of partial-thickness defects in articular cartilage: cell recruitment from the synovial membrane. *The Journal of bone and joint surgery American volume*, 78(5):721–733.

Hwang, N. S., Varghese, S., and Elisseeff, J. (2008). Derivation of chondrogenically-committed cells from human embryonic cells for cartilage tissue regeneration. *PLoS ONE*, 3(6):e2498.

Hwang, N. S., Varghese, S., Puleo, C., Zhang, Z., and Elisseeff, J. (2007). Morphogenetic signals from chondrocytes promote chondrogenic and osteogenic differentiation of mesenchymal stem cells. *Journal of cellular physiology*, 212(2):281–284.

Hwang, N. S., Varghese, S., Theprungsirikul, P., Canver, A., and Elisseeff, J. (2006). Enhanced chondrogenic differentiation of murine embryonic stem cells in hydrogels with glucosamine. *Biomaterials*, 27(36):6015–6023.

Jaeger, M., Carin, M., Medale, M., and Tryggvason, G. (1999). The osmotic migration of cells in a solute gradient. *Biophysical journal*, 77(3):1257–1267.

Jensen, C. E. and Zachariae, L. (1959). The contributions from hyaluronic acid and from protein to the colloid osmotic pressure of human synovial fluid. *Acta Rheumatol Scand*, 5(1):18–28.

Jikko, A., Kato, Y., Hiranuma, H., and Fuchihata, H. (1999). Inhibition of chondrocyte terminal differentiation and matrix calcification by soluble factors released by articular chondrocytes. *Calcified tissue international*, 65(4):276–279.

Kamota, T., Li, T. S., Morikage, N., Murakami, M., Ohshima, M., Kubo, M., Kobayashi, T., Mikamo, A., Ikeda, Y., Matsuzaki, M., and Hamano, K. (2009). Ischemic pre-conditioning enhances the mobilization and recruitment of bone marrow stem cells to protect against ischemia/reperfusion injury in the late phase. *J Am Coll Cardiol*, 53(19):1814–1822.

Kawamura, S., Wakitani, S., Kimura, T., Maeda, A., Caplan, A. I., Shino, K., and Ochi, T. (1998). Articular cartilage repair. Rabbit experiments with a collagen gel-biomatrix and chondrocytes cultured in it. *Acta orthopaedica Scandinavica*, 69(1):56–62.

Kaysen, J. H., Campbell, W. C., Majewski, R. R., Goda, F. O., Navar, G. L., Lewis, F. C., Goodwin, T. J., and Hammond, T. G. (1999). Select de novo gene and protein expression during renal epithelial cell culture in rotating wall vessels is shear stress dependent. *J. Membr. Biol.*, 168(1):77–89.

Kelly, T.-A. N., Ng, K. W., Wang, C. C.-B., Ateshian, G. A., and Hung, C. T. (2006). Spatial and temporal development of chondrocyte-seeded agarose constructs in free-swelling and dynamically loaded cultures. *Journal of biomechanics*, 39(8):1489–1497.

Kelly, T.-A. N., Wang, C. C. B., Mauck, R. L., Ateshian, G. A., and Hung, C. T. (2004). Role of cell-associated matrix in the development of free-swelling and dynamically loaded chondrocyte-seeded agarose gels. *Biorheology*, 41(3-4):223–237.

Kim, J. H., Lee, M. C., Seong, S. C., Park, K. H., and Lee, S. (2011). Enhanced proliferation and chondrogenic differentiation of human synovium-derived stem cells expanded with basic fibroblast growth factor. *Tissue engineering Part A*, 17(7-8):991–1002.

Kisiday, J. D., Frisbie, D. D., McIlwraith, C. W., and Grodzinsky, A. J. (2009). Dynamic compression stimulates proteoglycan synthesis by mesenchymal stem cells in the absence of chondrogenic cytokines. *Tissue engineering Part A*, 15(10):2817–2824.

Koo, J., Kim, K.-I., Min, B.-H., and Lee, G. M. (2010). Controlling medium osmolality improves the expansion of human articular chondrocytes in serum-free media. *Tissue engineering Part C, Methods*, 16(5):957–963.

Kourí, J. B., Aguilera, J. M., Reyes, J., Lozoya, K. A., and González, S. (2000). Apoptotic chondrocytes from osteoarthrotic human articular cartilage and abnormal calcification of subchondral bone. *The Journal of rheumatology*, 27(4):1005–1019.

Kubo, M., Li, T. S., Suzuki, R., Shirasawa, B., Morikage, N., Ohshima, M., Qin, S. L., and Hamano, K. (2008). Hypoxic preconditioning increases survival and angiogenic potency of peripheral blood mononuclear cells via oxidative stress resistance. *Am. J. Physiol. Heart Circ. Physiol.*, 294(2):H590–5.

Kühn, K., D'Lima, D. D., Hashimoto, S., and Lotz, M. (2004). Cell death in cartilage. *Osteoarthritis and cartilage / OARS, Osteoarthritis Research Society*, 12(1):1–16.

Kuroki, K., Stoker, A. M., and Cook, J. L. (2005). Effects of proinflammatory cytokines on canine articular chondrocytes in a three-dimensional culture. *Am. J. Vet. Res.*, 66(7):1187–1196.

Kurosawa, H., Fukubayashi, T., and Nakajima, H. (1980). Load-bearing mode of the knee joint: physical behavior of the knee joint with or without menisci. *Clin. Orthop.*, (149):283–290.

Lai, W. M., Hou, J. S., and Mow, V. C. (1991). A triphasic theory for the swelling and deformation behaviors of articular cartilage. *Journal of biomechanical engineering*, 113(3):245–258.

Lee, C. R., Grodzinsky, A. J., Hsu, H. P., Martin, S. D., and Spector, M. (2000a). Effects of harvest and selected cartilage repair procedures on the physical and biochemical properties of articular cartilage in the canine knee. *Journal of orthopaedic research : official publication of the Orthopaedic Research Society*, 18(5):790–799.

Lee, D. A. and Bader, D. L. (1995). The development and characterization of an in vitro system to study strain-induced cell deformation in isolated chondrocytes. *In Vitro Cell Dev Biol Anim*, 31(11):828–835.

Lee, D. A., Noguchi, T., Frean, S. P., Lees, P., and Bader, D. L. (2000b). The influence of mechanical loading on isolated chondrocytes seeded in agarose constructs. *Biorheology*, 37(1-2):149–161.

Lee, J. H., Fitzgerald, J. B., DiMicco, M. A., and Grodzinsky, A. J. (2005). Mechanical injury of cartilage explants causes specific time-dependent changes in chondrocyte gene expression. *Arthritis and rheumatism*, 52(8):2386–2395.

Legare, A., Garon, M., Guardo, R., Savard, P., Poole, A. R., and Buschmann, M. D. (2002). Detection and analysis of cartilage degeneration by spatially resolved streaming potentials. *Journal of orthopaedic research : official publication of the Orthopaedic Research Society*, 20(4):819–826.

Leigh, J. P., Seavey, W., and Leistikow, B. (2001). Estimating the costs of job related arthritis. *The Journal of rheumatology*, 28(7):1647–1654.

Levin, A., Burton-Wurster, N., Chen, C. T., and Lust, G. (2001). Intercellular signaling as a cause of cell death in cyclically impacted cartilage explants. *Osteoarthritis and cartilage / OARS, Osteoarthritis Research Society*, 9(8):702–711.

Levin, A. S., Chen, C.-T. C., and Torzilli, P. A. (2005). Effect of tissue maturity on cell viability in load-injured articular cartilage explants. *Osteoarthritis and cartilage / OARS, Osteoarthritis Research Society*, 13(6):488–496.

Lewis, J. L., Deloria, L. B., Oyen-Tiesma, M., Thompson, R. C., Ericson, M., and Oegema, T. R. (2003). Cell death after cartilage impact occurs around matrix cracks. *Journal of orthopaedic research : official publication of the Orthopaedic Research Society*, 21(5):881–887.

Li, J. and Pei, M. (2010). Optimization of an in vitro three-dimensional microenvironment to reprogram synovium-derived stem cells for cartilage tissue engineering. *Tissue engineering Part A*.

Li, K. W., Wang, A. S., and Sah, R. L. (2003). Microenvironment regulation of extracellular signal-regulated kinase activity in chondrocytes: effects of culture configuration, interleukin-1, and compressive stress. *Arthritis and rheumatism*, 48(3):689–699.

Liang, H.-T., Feng, X.-C., and Ma, T.-H. (2008). Water channel activity of plasma membrane affects chondrocyte migration and adhesion. *Clinical and Experimental Pharmacology and Physiology*, 35(1):7–10.

Lima, E. G., Bian, L., Ng, K. W., Mauck, R. L., Byers, B. A., Tuan, R. S., Ateshian, G. A., and Hung, C. T. (2007). The beneficial effect of delayed compressive loading on tissue-engineered cartilage constructs cultured with TGF-beta3. *Osteoarthritis and cartilage / OARS, Osteoarthritis Research Society*, 15(9):1025–1033.

Lima, E. G., Mauck, R. L., Han, S. H., Park, S., Ng, K. W., Ateshian, G. A., and Hung, C. T. (2004). Functional tissue engineering of chondral and osteochondral constructs. *Biorheology*, 41(3-4):577–590.

Lima, E. G., Tan, A. R., Tai, T., Bian, L., Ateshian, G. A., Cook, J. L., and Hung, C. T. (2008a). Physiologic deformational loading does not counteract the catabolic effects of interleukin-1 in long-term culture of chondrocyte-seeded agarose constructs. *Journal of biomechanics*, 41(15):3253–3259.

Lima, E. G., Tan, A. R., Tai, T., Bian, L., Stoker, A. M., Ateshian, G. A., Cook, J. L., and Hung, C. T. (2008b). Differences in interleukin-1 response between engineered and native cartilage. *Tissue engineering Part A*, 14(10):1721–1730.

Lin, W., Shuster, S., Maibach, H. I., and Stern, R. (1997). Patterns of hyaluronan staining are modified by fixation techniques. *The journal of histochemistry and cytochemistry : official journal of the Histochemistry Society*, 45(8):1157–1163.

Lipshitz, H., Etheredge, R. r., and Glimcher, M. J. (1976). Changes in the hexosamine content and swelling ratio of articular cartilage as functions of depth from the surface. *J Bone Joint Surg Am*, 58(8):1149–1153.

Loening, A. M., James, I. E., Levenston, M. E., Badger, A. M., Frank, E. H., Kurz, B., Nuttall, M. E., Hung, H. H., Blake, S. M., Grodzinsky, A. J., and Lark, M. W. (2000). Injurious mechanical compression of bovine articular cartilage induces chondrocyte apoptosis. *Archives of biochemistry and biophysics*, 381(2):205–212.

Long, P., Gassner, R., and Agarwal, S. (2001). Tumor necrosis factor alpha-dependent proinflammatory gene induction is inhibited by cyclic tensile strain in articular chondrocytes in vitro. *Arthritis and rheumatism*, 44(10):2311–2319.

Lotz, M. (2001). Cytokines in cartilage injury and repair. *Clinical orthopaedics and related research*, (391 Suppl):S108–15.

Maniwa, S., Ochi, M., Motomura, T., Nishikori, T., Chen, J., and Naora, H. (2001). Effects of hyaluronic acid and basic fibroblast growth factor on motility of chondrocytes and synovial cells in culture. *Acta orthopaedica Scandinavica*, 72(3):299–303.

Manouel, M., Pearlman, H. S., Belakhlef, A., and Brown, T. D. (1992). A miniature piezoelectric polymer transducer for in vitro measurement of the dynamic contact stress distribution. *J Biomech*, 25(6):627–635.

Maroudas, A. and Venn, M. (1977). Chemical composition and swelling of normal and osteoarthrotic femoral head cartilage. II. Swelling. *Annals of the rheumatic diseases*, 36(5):399–406.

Martin, I., Obradovic, B., Treppo, S., Grodzinsky, A. J., Langer, R., Freed, L. E., and Vunjak-Novakovic, G. (2000). Modulation of the mechanical properties of tissue engineered cartilage. *Biorheology*, 37(1-2):141–147.

Mauck, R. L., Hung, C. T., and Ateshian, G. A. (2003a). Modeling of neutral solute transport in a dynamically loaded porous permeable gel: implications for articular cartilage biosynthesis and tissue engineering. *Journal of biomechanical engineering*, 125(5):602–614.

Mauck, R. L., Nicoll, S. B., Seyhan, S. L., Ateshian, G. A., and Hung, C. T. (2003b). Synergistic action of growth factors and dynamic loading for articular cartilage tissue engineering. *Tissue engineering*, 9(4):597–611.

Mauck, R. L., Seyhan, S. L., Ateshian, G. A., and Hung, C. T. (2002). Influence of seeding density and dynamic deformational loading on the developing structure/function relationships of chondrocyte-seeded agarose hydrogels. *Annals of Biomedical Engineering*, 30(8):1046–1056.

Mauck, R. L., Seyhan, S. L., Nicoll, S. B., Ateshian, G. A., and Hung, C. T. (2001). Transforming growth factor B1 increases the mechanical properties and matrix development of chondrocyte-seeded agarose hydrogels. *Adv. Bioeng.*, 50:691–692.

Mauck, R. L., Soltz, M. A., Wang, C. C., Wong, D. D., Chao, P. H., Valhmu, W. B., Hung, C. T., and Ateshian, G. A. (2000). Functional tissue engineering of articular cartilage through dynamic loading of chondrocyte-seeded agarose gels. *Journal of biomechanical engineering*, 122(3):252–260.

Mauck, R. L., Wang, C. C.-B., Oswald, E. S., Ateshian, G. A., and Hung, C. T. (2003c). The role of cell seeding density and nutrient supply for articular cartilage tissue engineering with deformational loading. *Osteoarthritis and cartilage / OARS, Osteoarthritis Research Society*, 11(12):879–890.

Mauck, R. L., Yuan, X., and Tuan, R. S. (2006). Chondrogenic differentiation and functional maturation of bovine mesenchymal stem cells in long-term agarose culture. *Osteoarthritis and cartilage / OARS, Osteoarthritis Research Society*, 14(2):179–189.

McGowan, K. B., Kurtis, M. S., Lottman, L. M., Watson, D., and Sah, R. L. (2002). Biochemical quantification of DNA in human articular and septal cartilage using PicoGreen and Hoechst 33258. *Osteoarthritis Cartilage*, 10(7):580–587.

McNulty, A. L., Rothfusz, N. E., Leddy, H. A., and Guilak, F. (2013). Synovial fluid concentrations and relative potency of interleukin-1 alpha and beta in cartilage and meniscus degradation. *Journal of orthopaedic research : official publication of the Orthopaedic Research Society*, 31(7):1039–1045.

Meachim, G. (1963). The Effect of Scarification on Articular Cartilage. *Journal of Bone and Joint Surgery*, 45B(1):150–161.

Milentijevic, D., Helfet, D. L., and Torzilli, P. A. (2003). Influence of stress magnitude on water loss and chondrocyte viability in impacted articular cartilage. *Journal of biomechanical engineering*, 125(5):594–601.

Milentijevic, D. and Torzilli, P. A. (2001). Influence of strain magnitude on water loss and chondrocyte viability in impacted cartilage. *Adv. Bioeng.*, BED-50:781–782.

Millward-Sadler, S. J., Wright, M. O., Davies, L. W., Nuki, G., and Salter, D. M. (2000). Mechanotransduction via integrins and interleukin-4 results in altered aggrecan and matrix metalloproteinase 3 gene expression in normal, but not osteoarthritic, human articular chondrocytes. *Arthritis and rheumatism*, 43(9):209–219.

Miyanishi, K., Trindade, M. C., Lindsey, D. P., Beaupre, G. S., Carter, D. R., Goodman, S. B., Schurman, D. J., and Smith, R. L. (2006). Effects of hydrostatic pressure and transforming growth factor-beta 3 on adult human mesenchymal stem cell chondrogenesis in vitro. *Tissue engineering*, 12(6):1419–1428.

Mobasheri, A., Carter, S. D., Martín-Vasallo, P., and Shakibaei, M. (2002). Integrins and stretch activated ion channels; putative components of functional cell surface mechanoreceptors in articular chondrocytes. *Cell biology international*, 26(1):1–18.

Mobasheri, A., Trujillo, E., Bell, S., Carter, S. D., Clegg, P. D., Martín-Vasallo, P., and Marples, D. (2004). Aquaporin water channels AQP1 and AQP3, are expressed in equine articular chondrocytes. *Vet. J.*, 168(2):143–150.

Monzani, E., Bazzotti, R., Perego, C., and La Porta, C. A. M. (2009). AQP1 is not only a water channel: it contributes to cell migration through Lin7/beta-catenin. *PLoS ONE*, 4(7):e6167.

Mow, V. C., Bachrach, N. M., Setton, L. A., and Guilak, F. (1994). Stress, strain, pressure, and flow fields in articular cartilage and chondrocytes. In *Cell Mechanics and Cellular Engineering*, pages 345–379. Springer-Verlag, New York.

Mow, V. C. and Lai, M. (1990). Biorheology of swelling tissue. *Biorheology*, 27(1):110–119.

Mow, V. C. and Ratcliffe, A. (1997). Structure and function of articular cartilage and meniscus. In *Basic Orthopaedic Biomechanics*, pages 113–177. Lippincott-Raven, Philadelphia.

Mowery, C., Botte, M., and Bradley, G. (1987). Fracture of polyethylene tibial component in a total knee replacement. A case report. *Orthopedics*, 10(2):309–313.

Muir, H., Bullough, P., and Maroudas, A. (1970). The distribution of collagen in human articular cartilage with some of its physiological implications. *The Journal of bone and joint surgery. British volume*, 52(3):554–563.

Murata, M., Bonassar, L. J., Wright, M., Mankin, H. J., and Towle, C. A. (2003). A role for the interleukin-1 receptor in the pathway linking static mechanical compression to decreased proteoglycan synthesis in surface articular cartilage. *Archives of biochemistry and biophysics*, 413(2):229–235.

Murry, C. E., Jennings, R. B., and Reimer, K. A. (1986). Preconditioning with ischemia: a delay of lethal cell injury in ischemic myocardium. *Circulation*, 74(5):1124–1136.

Nagase, T., Muneta, T., Ju, Y.-J., Hara, K., Morito, T., Koga, H., Nimura, A., Mochizuki, T., and Sekiya, I. (2008). Analysis of the chondrogenic potential of human synovial stem cells according to harvest site and culture parameters in knees with medial compartment osteoarthritis. *Arthritis and rheumatism*, 58(5):1389–1398.

Nanduri, J., Yuan, G., Kumar, G. K., Semenza, G. L., and Prabhakar, N. R. (2008). Transcriptional responses to intermittent hypoxia. *Respiratory physiology & neurobiology*, 164(1-2):277–281.

Newman, P. J. and Grana, W. A. (1988). The changes in human synovial fluid osmolality associated with traumatic or mechanical abnormalities of the knee. *Arthroscopy : the journal of arthroscopic & related surgery : official publication of the Arthroscopy Association of North America and the International Arthroscopy Association*, 4(3):179–181.

Ng, K. W., Lima, E. G., Bian, L., O'Conor, C. J., Jayabalan, P. S., Stoker, A. M., Kuroki, K., Cook, C. R., Ateshian, G. A., Cook, J. L., and Hung, C. T. (2010). Passaged adult chondrocytes can form engineered cartilage with functional mechanical properties: a canine model. *Tissue engineering Part A*, 16(3):1041–1051.

Ng, K. W., Wang, C. C.-B., Mauck, R. L., Kelly, T.-A. N., Chahine, N. O., Costa, K. D., Ateshian, G. A., and Hung, C. T. (2005). A layered agarose approach to fabricate depth-dependent inhomogeneity in chondrocyte-seeded constructs. *Journal of orthopaedic research : official publication of the Orthopaedic Research Society*, 23(1):134–141.

Nishimura, K. Y., Isseroff, R. R., and Nuccitelli, R. (1996). Human keratinocytes migrate to the negative pole in direct current electric fields comparable to those measured in mammalian wounds. *Journal of cell science*, 109:199–207.

Obradovic, B., Carrier, R. L., Vunjak-Novakovic, G., and Freed, L. E. (1999). Gas exchange is essential for bioreactor cultivation of tissue engineered cartilage. *Biotechnology and bioengineering*, 63(2):197–205.

Ode, A., Kopf, J., Kurtz, A., Schmidt-Bleek, K., Schrade, P., Kolar, P., Buttgereit, F., Lehmann, K., Hutmacher, D. W., Duda, G. N., and Kasper, G. (2011). CD73 and CD29 concurrently mediate the mechanically induced decrease of migratory capacity of mesenchymal stromal cells. *European cells & materials*, 22:26–42.

O'Driscoll, S. W., Saris, D. B., Ito, Y., and Fitzimmons, J. S. (2001). The chondrogenic potential of periosteum decreases with age. *Journal of orthopaedic research : official publication of the Orthopaedic Research Society*, 19(1):95–103.

Orr, T. E., Patel, A. M., Wong, B., Hatzigiannis, G. P., Minas, T., and Spector, M. (1999). Attachment of periosteal grafts to articular cartilage with fibrin sealent. *Journal of biomedical materials research*, 44(3):308–313.

Oswald, E. S., Chao, P. H., Bulinski, J. C., Ateshian, G. A., and Hung, C. T. (2008). Dependence of zonal chondrocyte water transport properties on osmotic environment. *Cell. Mol. Bioeng.*, 1(4):339–348.

Pasha, Z., Wang, Y., Sheikh, R., Zhang, D., Zhao, T., and Ashraf, M. (2008). Preconditioning enhances cell survival and differentiation of stem cells during transplantation in infarcted myocardium. *Cardiovasc Res*, 77(1):134–142.

Patel, H. H., Gross, E. R., Peart, J. N., Hsu, A. K., and Gross, G. J. (2005). Sarcolemmal KATP channel triggers delayed ischemic preconditioning in rats. *Am. J. Physiol. Heart Circ. Physiol.*, 288(1):H445–7.

Patel, N. and Poo, M. M. (1982). Orientation of neurite growth by extracellular electric fields. *J. Neurosci.*, 2(4):483–496.

Paterson, D. C., Carter, R. F., Maxwell, G. M., Hillier, T. M., Ludbrook, J., and Savage, J. P. (1977). Electrical bone-growth stimulation in an experimental model of delayed union. *Lancet*, 1(8025):1278–1281.

Patwari, P., Fay, J., Cook, M. N., Badger, A. M., Kerin, A. J., Lark, M. W., and Grodzinsky, A. J. (2001). In vitro models for investigation of the effects of acute mechanical injury on cartilage. *Clinical orthopaedics and related research*, (391 Suppl):S61–71.

Pazzano, D., Mercier, K. A., Moran, J. M., Fong, S. S., DiBiasio, D. D., Rulfs, J. X., Kohles, S. S., and Bonassar, L. J. (2000). Comparison of chondrogensis in static and perfused bioreactor culture. *Biotechnology progress*, 16(5):893–896.

Pei, M., He, F., Kish, V. L., and Vunjak-Novakovic, G. (2008). Engineering of functional cartilage tissue using stem cells from synovial lining: a preliminary study. *Clinical orthopaedics and related research*, 466(8):1880–1889.

Pelletier, J. P., Roughley, P. J., DiBattista, J., McCollum, R., and Martel-Pelletier, J. (1991). Are cytokines involved in osteoarthritic pathophysiology? *Semin Arthritis Rheum*, 20(6 Suppl 2):12–25.

Petri, J. B., Rott, O., Wetzig, T., Herrmann, K., and Haustein, U. F. (1999). The small proteoglycan fibromodulin is expressed in mitotic, but not in postmitotic fibroblasts. *Mol Cell Biol Res Commun*, 1(1):59–65.

Pritchard, S. and Guilak, F. (2004). The role of F-actin in hypo-osmotically induced cell volume change and calcium signaling in anulus fibrosus cells. *Annals of Biomedical Engineering*, 32(1):103–111.

Pritchard, S. and Guilak, F. (2006). Effects of interleukin-1 on calcium signaling and the increase of filamentous actin in isolated and in situ articular chondrocytes. *Arthritis and rheumatism*, 54(7):2164–2174.

Pritchard, S., Votta, B. J., Kumar, S., and Guilak, F. (2008). Interleukin-1 inhibits osmotically induced calcium signaling and volume regulation in articular chondrocytes. *Osteoarthritis and cartilage / OARS, Osteoarthritis Research Society*, 16(12):1466–1473.

Qi, W.-N. and Scully, S. P. (1998). Effect of type II collagen in chondrocyte response to TGF-beta1 regulation. *Experimental cell research*, 241:142–150.

Quinn, T. M., Allen, R. G., Schalet, B. J., Perumbuli, P., and Hunziker, E. B. (2001). Matrix and cell injury due to sub-impact loading of adult bovine articular cartilage explants: effects of strain rate and peak stress. *Journal of orthopaedic research : official publication of the Orthopaedic Research Society*, 19(2):242–249.

Quinn, T. M., Schmid, P., Hunziker, E. B., and Grodzinsky, A. J. (2002). Proteoglycan deposition around chondrocytes in agarose culture: construction of a physical and biological interface for mechanotransduction in cartilage. *Biorheology*, 39(1-2):27–37.

Rahfoth, B., Weisser, J., Sternkopf, F., Aigner, T., von der Mark, K., and Brauer, R. (1998). Transplantation of allograft chondrocytes embedded in agarose gel into cartilage defects of rabbits. *Osteoarthritis Cartilage*, 6(1):50–65.

Ratcliffe, A., Tyler, J. A., and Hardingham, T. E. (1986). Articular cartilage cultured with interleukin 1. Increased release of link protein, hyaluronate-binding region and other proteoglycan fragments. *The Biochemical journal*, 238(2):571–580.

Reginster, J. Y. (2002). The prevalence and burden of arthritis. *Rheumatology (Oxford)*, 41 Supp 1:3–6.

Repo, R. U. and Finlay, J. B. (1977). Survival of articular cartilage after controlled impact. *The Journal of bone and joint surgery American volume*, 59(8):1068–1076.

Rezzonico, R., Cayatte, C., Bourget-Ponzio, I., Romey, G., Belhacene, N., Loubat, A., Rocchi, S., Van Obberghen, E., Girault, J.-A., Rossi, B., and Schmid-Antomarchi, H. (2003). Focal adhesion kinase pp125FAK interacts with the large conductance calcium-activated hSlo potassium channel in human osteoblasts: potential role in mechanotransduction. *Journal of bone and mineral research : the official journal of the American Society for Bone and Mineral Research*, 18(10):1863–1871.

Rice, M. A., Homier, P. M., Waters, K. R., and Anseth, K. S. (2008). Effects of directed gel degradation and collagenase digestion on the integration of neocartilage produced by chondrocytes encapsulated in hydrogel carriers. *J Tissue Eng Regen Med*, 2(7):418–429.

Riesle, J., Hollander, A. P., Langer, R., Freed, L. E., and Vunjak-Novakovic, G. (1998). Collagen in tissue-engineered cartilage: types, structure, and crosslinks. *Journal of cellular biochemistry*, 71(3):313–327.

Robinson, K. R. (1985). The responses of cells to electrical fields: a review. *The Journal of cell biology*, 101(6):2023–2027.

Rosova, I., Dao, M., Capoccia, B., Link, D., and Nolta, J. A. (2008). Hypoxic preconditioning results in increased motility and improved therapeutic potential of human mesenchymal stem cells. *Stem Cells*, 26(8):2173–2182.

Rotter, N., Ung, F., Roy, A. K., Vacanti, M., Eavey, R. D., Vacanti, C. A., and Bonassar, L. J. (2005). Role for interleukin 1alpha in the inhibition of chondrogenesis in autologous implants using polyglycolic acid-polylactic acid scaffolds. *Tissue engineering*, 11(1-2):192–200.

Ruiz-Ederra, J. and Verkman, A. S. (2009). Aquaporin-1-facilitated keratocyte migration in cell culture and in vivo corneal wound healing models. *Experimental Eye Research*, 89(2):159–165.

Sah, R. L., Kim, Y. J., Doong, J. Y., Grodzinsky, A. J., Plaas, A. H., and Sandy, J. D. (1989). Biosynthetic response of cartilage explants to dynamic compression. *Journal of orthopaedic research : official publication of the Orthopaedic Research Society*, 7(5):619–636.

Sakaguchi, Y., Sekiya, I., Yagishita, K., and Muneta, T. (2005). Comparison of human stem cells derived from various mesenchymal tissues: superiority of synovium as a cell source. *Arthritis and rheumatism*, 52(8):2521–2529.

Sampat, S. R., Dermksian, M. V., Oungoulian, S. R., Winchester, R. J., Bulinski, J. C., Ateshian, G. A., and Hung, C. T. (2013). Applied osmotic loading for promoting development of engineered cartilage. *Journal of biomechanics*, 46(15):2674–2681.

Sampat, S. R., O'Connell, G. D., Fong, J. V., Alegre-Aguarón, E., Ateshian, G. A., and Hung, C. T. (2011). Growth factor priming of synovium-derived stem cells for cartilage tissue engineering. *Tissue engineering Part A*, 17(17-18):2259–2265.

Sanchez, J. C. and Wilkins, R. J. (2003). Effects of hypotonic shock on intracellular pH in bovine articular chondrocytes. *Comp Biochem Physiol A Mol Integr Physiol*, 135(4):575–583.

Schengrund, C. L., Rosenberg, A., and Repman, M. A. (1976). Ecto-ganglioside-sialidase activity of herpes simplex virus-transformed hamster embryo fibroblasts. *The Journal of cell biology*, 70(3):555–561.

Schmal, H., Mehlhorn, A., Stoffel, F., Kostler, W., Sudkamp, N. P., and Niemeyer, P. (2009). In vivo quantification of intraarticular cytokines in knees during natural and surgically induced cartilage repair. *Cytotherapy*, 11(8):1065–1075.

Schmidt, M. B., Chen, E. H., and Lynch, S. E. (2006). A review of the effects of insulin-like growth factor and platelet derived growth factor on in vivo cartilage healing and repair. *Osteoarthritis and cartilage / OARS, Osteoarthritis Research Society*, 14(5):403–412.

Schwab, A. (2001). Function and spatial distribution of ion channels and transporters in cell migration. *American journal of physiology. Renal physiology*, 280(5):F739–47.

Schwab, A., Fabian, A., Hanley, P. J., and Stock, C. (2012). Role of ion channels and transporters in cell migration. *Physiological reviews*, 92(4):1865–1913.

Sellam, J. and Berenbaum, F. (2010). The role of synovitis in pathophysiology and clinical symptoms of osteoarthritis. *Nat Rev Rheumatol*, 6(11):625–635.

Selmi, T. A., Neyret, P., Verdonk, P.C.M., and Barnouin, L. (2007). Autologous chondrocyte transplantation in combination with an alginate-agarose based hydrogel (Cartipatch). *Tech. Knee Surg.*, 6(4):253–258.

Selmi, T. A., Verdonk, P.C.M., Chambat, P., Dubrana, F., Potel, J. F., Barnouin, L., and Neyret, P. (2008). Autologous chondrocyte implantation in a novel alginate-agarose hydrogel: outcome at two years. *J. Bone Jt. Surg.*, 90(5):597–604.

Shanfield, S., Campbell, P., Baumgarten, M., Bloebaum, R., and Sarmiento, A. (1988). Synovial fluid osmolality in osteoarthritis and rheumatoid arthritis. *Clinical orthopaedics and related research*, (235):289–295.

Shen, M. R., Furla, P., Chou, C. Y., and Ellory, J. C. (2002). Myosin light chain kinase modulates hypotonicity-induced Ca2+ entry and Cl- channel activity in human cervical cancer cells. *Pflügers Archiv - European Journal of Physiology*, 444(1-2):276–285.

Shields, C. J., Winter, D. C., Geibel, J. P., O'Sullivan, G. C., Wang, J. H., and Redmond, H. P. (2006). Hypertonic saline attenuates colonic tumor cell metastatic potential by activating transmembrane sodium conductance. *J. Membr. Biol.*, 211(1):35–42.

Shields, C. J., Winter, D. C., Wang, J. H., Andrews, E., Laug, W. E., and Redmond, H. P. (2004). Hypertonic saline impedes tumor cell-endothelial cell interaction by reducing adhesion molecule and laminin expression. *Surgery*, 136(1):76–83.

Sieg, D. J., Hauck, C. R., and Schlaepfer, D. D. (1999). Required role of focal adhesion kinase (FAK) for integrin-stimulated cell migration. *Journal of cell science*, 112 (Pt 16):2677–2691.

Smeets, T. J. M., Barg, E. C., Kraan, M. C., Smith, M. D., Breedveld, F. C., and Tak, P. P. (2003). Analysis of the cell infiltrate and expression of proinflammatory cytokines and matrix metalloproteinases in arthroscopic synovial biopsies: comparison with synovial samples from patients with end stage, destructive rheumatoid arthritis. *Annals of the rheumatic diseases*, 62(7):635–638.

Smetana, K. J. (1993). Cell biology of hydrogels. *Biomaterials*, 14(14):1046–1050.

Smola, H., Thiekötter, G., and Fusenig, N. E. (1993). Mutual induction of growth factor gene expression by epidermal-dermal cell interaction. *The Journal of cell biology*, 122(2):417–429.

Soltz, M. A. and Ateshian, G. A. (1998). Experimental verification and theoretical prediction of cartilage interstitial fluid pressurization at an impermeable contact interface in confined compression. *Journal of biomechanics*, 31(10):927–934.

Solursh, M. and Meier, S. (1973). A conditioned medium (CM) factor produced by chondrocytes that promotes their own differentiation. *Developmental biology*, 30(2):279–289.

Soong, H. K., Parkinson, W. C., Bafna, S., Sulik, G. L., and Huang, S. C. (1990). Movements of cultured corneal epithelial cells and stromal fibroblasts in electric fields. *Investigative ophthalmology & visual science*, 31(11):2278–2282.

Stabellini, G., De Mattei, M., Calastrini, C., Gagliano, N., Moscheni, C., Pasello, M., Pellati, A., Bellucci, C., and Gioia, M. (2003). Effects of interleukin-1beta on chondroblast viability and extracellular matrix changes in bovine articular cartilage explants. *Biomedicine & pharmacotherapy = Biomédecine & pharmacothérapie*, 57(7):314–319.

Stegeman, H. and Stalder, K. (1967). Determination of hydroxyproline. *Clin. Chim. Acta.*, 19:267–273.

Stevens, A. L., Wishnok, J. S., White, F. M., Grodzinsky, A. J., and Tannenbaum, S. R. (2009). Mechanical injury and cytokines cause loss of cartilage integrity and upregulate proteins associated with catabolism, immunity, inflammation, and repair. *Molecular & cellular proteomics : MCP*, 8(7):1475–1489.

Stockwell, R. A. (1979). *Biology of cartilage cells*. Cambridge University Press, Cambridge ; New York.

Tallheden, T., Dennis, J. E., Lennon, D. P., Sjögren-Jansson, E., Caplan, A. I., and Lindahl, A. (2003). Phenotypic plasticity of human articular chondrocytes. *J. Bone Joint Surg.*, 85A(Supp. 2):93–100.

Tang, Y. L., Zhu, W., Cheng, M., Chen, L., Zhang, J., Sun, T., Kishore, R., Phillips, M. I., Losordo, D. W., and Qin, G. (2009). Hypoxic preconditioning enhances the benefit of cardiac progenitor cell therapy for treatment of myocardial infarction by inducing CXCR4 expression. *Circ. Res.*, 104(10):1209–1216.

Taylor, D. W., Ahmed, N., Gan, L., Gross, A. E., and Kandel, R. (2009). Proteoglycan and Collagen Accumulation by Passaged Chondrocytes Can Be Enhanced Through Side-by-Side Culture with Primary Chondrocytes. *Tissue engineering Part A*.

Temple, M. M., Xue, Y., Chen, M. Q., and Sah, R. L. (2006). Interleukin-1alpha induction of tensile weakening associated with collagen degradation in bovine articular cartilage. *Arthritis and rheumatism*, 54(10):3267–3276.

Tew, S., Redman, S., Kwan, A., Walker, E., Khan, I., Dowthwaite, G., Thomson, B., and Archer, C. W. (2001). Differences in repair responses between immature and mature cartilage. *Clinical orthopaedics and related research*, (391 Suppl):S142–52.

Tew, S. R., Kwan, A. P., Hann, A., Thomson, B. M., and Archer, C. W. (2000). The reactions of articular cartilage to experimental wounding: role of apoptosis. *Arthritis and rheumatism*, 43(1):215–225.

Tew, S. R., Murdoch, A. D., Rauchenberg, R. P., and Hardingham, T. E. (2008). Cellular methods in cartilage research: primary human chondrocytes in culture and chondrogenesis in human bone marrow stem cells. *Methods (San Diego, Calif.)*, 45(1):2–9.

Thorp, B. H., Anderson, I., and Jakowlew, S. B. (1992). Transforming growth factor-beta1, -beta2 and -beta3 in cartilage and bone cells during endochondral ossification in the chick. *Development (Cambridge, England)*, 114(4):907–911.

Torzilli, P. A., Deng, X.-H., and Ramcharan, M. (2006). Effect of compressive strain on cell viability in statically loaded articular cartilage. *Biomechanics and modeling in mechanobiology*, 5(2-3):123–132.

Torzilli, P. A., Grigiene, R., Huang, C., Friedman, S. M., Doty, S. B., Boskey, A. L., and Lust, G. (1997). Characterization of cartilage metabolic response to static and dynamic stress using a mechanical explant test system. *J Biomech*, 30(1):1–9.

Tran-Khanh, N., Hoemann, C. D., McKee, M. D., Henderson, J. E., and Buschmann, M. D. (2005). Aged bovine chondrocytes display a diminished capacity to produce a collagen-rich, mechanically functional cartilage extracellular matrix. *Journal of orthopaedic research : official publication of the Orthopaedic Research Society*, 23(6):1354–1362.

Trujillo, E., González, T., Marín, R., Martín-Vasallo, P., Marples, D., and Mobasheri, A. (2004). Human articular chondrocytes, synoviocytes and synovial microvessels express aquaporin water channels; upregulation of AQP1 in rheumatoid arthritis. *Histology and histopathology*, 19(2):435–444.

Tsai, C.-H., Lin, B.-J., and Chao, P.-H. G. (2012). $\alpha 2\beta 1$ integrin and RhoA mediates electric field-induced ligament fibroblast migration directionality. *Journal of orthopaedic research : official publication of the Orthopaedic Research Society*.

Tyler, J. A. (1989). Insulin-like growth factor 1 can decrease degradation and promote synthesis of proteoglycan in cartilage exposed to cytokines. *The Biochemical journal*, 260(2):543–548.

Urban, J. P., Hall, A. C., and Gehl, K. A. (1993). Regulation of matrix synthesis rates by the ionic and osmotic environment of articular chondrocytes. *Journal of cellular physiology*, 154(2):262–270.

van den Berg, W. B. (2001). Anti-cytokine therapy in chronic destructive arthritis. *Arthritis research*, 3(1):18–26.

van den Berg, W. B., Joosten, L. A., and van de Loo, F. A. (1999). TNF alpha and IL-1 beta are separate targets in chronic arthritis. *Clin Exp Rheumatol*, 17(6 Suppl 18):S105–14.

van Susante, J. L., Buma, P., van Osch, G. J., Versleyen, D., van der Kraan, P. M., van der Berg, W. B., and Homminga, G. N. (1995). Culture of chondrocytes in alginate and collagen carrier gels. *Acta orthopaedica Scandinavica*, 66(6):549–556.

Vats, A., Bielby, R. C., Tolley, N., Dickinson, S. C., Boccaccini, A. R., Hollander, A. P., Bishop, A. E., and Polak, J. M. (2006). Chondrogenic differentiation of human embryonic stem cells: the effect of the micro-environment. *Tissue engineering*, 12(6):1687–1697.

Verkman, A. S. (2005). More than just water channels: unexpected cellular roles of aquaporins. *Journal of cell science*, 118(Pt 15):3225–3232.

Vicente-Manzanares, M. and Horwitz, A. R. (2011). Cell Migration: An Overview. *Methods in molecular biology (Clifton, N.J.)*, 769:1–24.

Vinall, R. L., Lo, S. H., and Reddi, A. H. (2002). Regulation of articular chondrocyte phenotype by bone morphogenetic protein 7, interleukin 1, and cellular context is dependent on the cytoskeleton. *Experimental cell research*, 272(1):32–44.

Vunjak-Novakovic, G., Martin, I., Obradovic, B., Treppo, S., Grodzinsky, A. J., Langer, R., and Freed, L. E. (1999). Bioreactor cultivation conditions modulate the composition and mechanical properties of tissue-engineered cartilage. *Journal of orthopaedic research : official publication of the Orthopaedic Research Society*, 17(1):130–138.

Wakitani, S., Nawata, M., Tensho, K., Okabe, T., Machida, H., and Ohgushi, H. (2007). Repair of articular cartilage defects in the patello-femoral joint with autologous bone marrow mesenchymal cell transplantation: three case reports involving nine defects in five knees. *J Tissue Eng Regen Med*, 1(1):74–79.

Wang, C. C.-B., Guo, X. E., Sun, D., Mow, V. C., Ateshian, G. A., and Hung, C. T. (2002). The functional environment of chondrocytes within cartilage subjected to compressive loading: theoretical and experimental approach. *Biorheology*, 39(1-2):39–45.

Wang, F. and Zhu, Y. (2011). Aquaporin-1: a potential membrane channel for facilitating the adaptability of rabbit nucleus pulposus cells to an extracellular matrix environment. *Journal of orthopaedic science : official journal of the Japanese Orthopaedic Association*, 16(3):304–312.

Wang, J., Verdonk, P., Elewaut, D., Veys, E. M., and Verbruggen, G. (2003). Homeostasis of the extracellular matrix of normal and osteoarthritic human articular cartilage chondrocytes in vitro. *Osteoarthritis and cartilage / OARS, Osteoarthritis Research Society*, 11(11):801–809.

Watanabe, T., Sakai, D., Yamamoto, Y., Iwashina, T., Serigano, K., Tamura, F., and Mochida, J. (2010). Human nucleus pulposus cells significantly enhanced biological properties in a coculture system with direct cell-to-cell contact with autologous mesenchymal stem cells. *Journal of orthopaedic research : official publication of the Orthopaedic Research Society*, 28(5):623–630.

Watt, F. M. (1988). Effect of seeding density on stability of the differentiated phenotype of pig articular chondrocytes in culture. *Journal of cell science*, 89 (Pt 3):373–378.

Wells, A. (2000). Tumor invasion: role of growth factor-induced cell motility. *Adv Cancer Res*, 78:31–101.

Whiteside, L. A. (1989). Clinical results of Whiteside Ortholoc total knee replacement. *Orthop Clin North Am*, 20(1):113–124.

Williams, C. G., Kim, T. K., Taboas, A., Malik, A., Manson, P., and Elisseeff, J. (2003). In vitro chondrogenesis of bone marrow-derived mesenchymal stem cells in a photopolymerizing hydrogel. *Tissue engineering*, 9(4):679–688.

Wilusz, R. E., Weinberg, J. B., Guilak, F., and McNulty, A. L. (2008). Inhibition of integrative repair of the meniscus following acute exposure to interleukin-1 in vitro. *Journal of orthopaedic research : official publication of the Orthopaedic Research Society*, 26(4):504–512.

Xu, C., Oyajobi, B. O., Frazer, A., Kozaci, L. D., Russell, R. G., and Hollander, A. P. (1996). Effects of growth factors and interleukin-1 alpha on proteoglycan and type II collagen turnover in bovine nasal and articular chondrocyte pellet cultures. *Endocrinology*, 137(8):3557–3565.

Xu, Y., Balooch, G., Chiou, M., Bekerman, E., Ritchie, R. O., and Longaker, M. T. (2007). Analysis of the material properties of early chondrogenic differentiated adipose-derived stromal cells (ASC) using an in vitro three-dimensional micromass culture system. *Biochemical and biophysical research communications*, 359(2):311–316.

Yamazaki, N., Browning, J. A., and Wilkins, R. J. (2000). Modulation of Na(+) x H(+) exchange by osmotic shock in isolated bovinearticular chondrocytes. *Acta Physiol Scand*, 169(3):221–228.

Yellowley, C. E., Hancox, J. C., and Donahue, H. J. (2002). Effects of cell swelling on intracellular calcium and membrane currents in bovine articular chondrocytes. *Journal of cellular biochemistry*, 86(2):290–301.

Yoshimura, H., Muneta, T., Nimura, A., Yokoyama, A., Koga, H., and Sekiya, I. (2007). Comparison of rat mesenchymal stem cells derived from bone marrow, synovium, periosteum, adipose tissue, and muscle. *Cell and tissue research*, 327(3):449–462.

Yuan, X., Arkonac, D. E., Chao, P.-H. G., and Vunjak-Novakovic, G. (2014). Electrical stimulation enhances cell migration and integrative repair in the meniscus. *Scientific reports*, 4:3674.

Zhao, M., Song, B., Pu, J., Wada, T., Reid, B., Tai, G., Wang, F., Guo, A., Walczysko, P., Gu, Y., Sasaki, T., Suzuki, A., Forrester, J. V., Bourne, H. R., Devreotes, P. N., McCaig, C. D., and Penninger, J. M. (2006). Electrical signals control wound healing through phosphatidylinositol-3-OH kinase-gamma and PTEN. *Nature*, 442(7101):457–460.

Zimmermann, T., Kunisch, E., Pfeiffer, R., Hirth, A., Stahl, H. D., Sack, U., Laube, A., Liesaus, E., Roth, A., Palombo-Kinne, E., Emmrich, F., and Kinne, R. W. (2001). Isolation and characterization of rheumatoid arthritis synovial fibroblasts from primary culture–primary culture cells markedly differ from fourth-passage cells. *Arthritis research*, 3(1):72–76.

Zuk, P. A., Zhu, M., Ashjian, P., De Ugarte, D. A., Huang, J. I., Mizuno, H., Alfonso, Z. C., Fraser, J. K., Benhaim, P., and Hedrick, M. H. (2002). Human adipose tissue is a source of multipotent stem cells. *Molecular biology of the cell*, 13(12):4279–4295.

Zuk, P. A., Zhu, M., Mizuno, H., Huang, J., Futrell, J. W., Katz, A. J., Benhaim, P., Lorenz, H. P., and Hedrick, M. H. (2001). Multilineage cells from human adipose tissue: implications for cell-based therapies. *Tissue engineering*, 7(2):211–228.

Appendix A

Preliminary Findings on the Effect of IL-1 on Engineered Cartilage

A.1 Differences in Interleukin-1 Response between Engineered and Native Cartilage

Eric G. Lima, Andrea R. Tan, Timon Tai, Liming Bian, Aaron M. Stoker, Gerard A. Ateshian, James L. Cook, Clark T. Hung

TISSUE ENGINEERING: Part A
Volume 14, Number 10, 2008

DOI: 10.1089/ten.tea.2007.0347

Differences in Interleukin-1 Response between Engineered and Native Cartilage

ERIC G. LIMA, Ph.D.,[1] ANDREA R. TAN, B.S.,[1] TIMON TAI, M.P.H.,[1] LIMING BIAN, M.S.,[1] AARON M. STOKER, Ph.D.,[2] GERARD A. ATESHIAN, Ph.D.,[1,3] JAMES L. COOK, D.V.M., Ph.D.,[2] and CLARK T. HUNG, Ph.D.[1]

ABSTRACT

Unlike native cartilage explants that are used in autologous tissue transfer procedures, engineered cartilage constructs are typically highly fragile when first formed and must rely on cellular activity to develop over time. However, inflammatory cytokines such as interleukin-1α (IL-1α) are often present in target joints and may interfere with this development process. Herein we examine to what extent nascent engineered tissue is susceptible to chemical perturbations by IL-1α (10 ng/mL), especially when compared to native explants, and whether *in vitro* preconditioning may promote sufficient integrity to lessen this impact. The studies were carried out using a chemically defined medium supplemented with or without the anti-inflammatory steroid dexamethasone. We find that engineered tissue (bovine chondrocytes in agarose hydrogel) at early time points (days 0 and 14) does not grow when exposed to the cytokine even temporarily, but both bovine explants and more developed engineered tissue (day 28) are able to withstand the same exposure without degradation of properties. We argue therefore that some *in vitro* preconditioning may be necessary to promote both sufficient mechanical integrity and the chemical fortitude without which insufficiently developed engineered constructs will not survive the harsh mechanochemical environment within the joint.

INTRODUCTION

A CENTRAL TENET OF CARTILAGE tissue engineering is to replace damaged or diseased cartilage with new tissue composed of isolated, living cells embedded in a scaffold carrier.[1–8] Typically, this engineered tissue is highly fragile when first formed, but over time it matures, depositing a cartilaginous extracellular matrix and growing in stiffness until, ideally, it possesses the same mechanical and biochemical properties of native cartilage. Consequently, clinicians have a choice of developmental states available to them when using engineered tissue that would otherwise be unavailable when using native cartilage. Some tissue engineering strategies capitalize on the different states of maturity by designing a system where the tissue matures entirely *in vivo*, while other strategies implant the tissue only after it has had a chance to partially mature *in vitro*. A successful *in vivo* maturation system presents clear advantages in terms of speed and convenience over an *in vitro* cultivation system; however, some preconditioning may be necessary to promote both sufficient mechanical integrity and, as we will argue here, the chemical fortitude without which insufficiently developed engineered constructs will not survive the harsh mechanochemical environment within the joint.

After implantation, engineered tissue, unlike native tissue, must continue to grow in a chemical environment that is likely to contain potent catabolic mediators stemming

[1]Department of Biomedical Engineering, Columbia University, New York, New York.
[2]Comparative Orthopaedic Laboratory, University of Missouri, Columbia, Missouri.
[3]Department of Mechanical Engineering, Columbia University, New York, New York.

from chronic joint inflammation or even from the surgical intervention itself.[9–12] Proinflammatory cytokines and their receptors are present in increased concentrations in the synovial fluid of human subjects with cartilage pathology.[13–15] The catabolic effects of these mediators may be especially pronounced in underdeveloped tissues[16–18] whose cells are not yet fully embedded in the potentially chondroprotective enclosure of a cartilaginous extracellular matrix.[19] Therefore, treatments aimed at restoring damaged or diseased cartilage must account for continued exposure to chemical mediators. Animal studies testing tissue engineering strategies are usually carried out using healthy animals, but this is unlikely to be the case clinically. It is therefore important to establish a system for predicting the functionality of engineered tissue. We chose long-term cultures of chondrocyte-seeded agarose constructs as our *in vitro* model, a system with clear tissue engineering applications in which both chemical and mechanical stimuli can be carefully controlled. The culture system preserves the chondrocyte phenotype by maintaining a physiologic three-dimensional environment and produces a functional extracellular matrix[20,21] with a proteoglycan composition more similar to that of native cartilage than that produced using other scaffold materials.[22]

Using this model, our laboratory has been able to develop engineered constructs with functional material properties similar to those of the native tissue, exhibiting both physiologic levels of glycosaminoglycans (GAG) and Young's modulus.[23] In the current study, the effects of interleukin-1α (IL-1α), a chemical mediator, on the mechanical and biochemical properties of engineered tissue at different developmental states were compared to those effects on the native tissue. This interleukin isoform was studied because it is a potent enhancer of transcription and translation of metalloproteinases that leads to increased proteolysis *in vitro* and *in vivo*.[24] *In vitro*, IL-1α has been shown to inhibit synthesis of core proteins at low concentrations,[25] and increase proteolysis of cartilage (as well as rapid degradation) at high concentrations.[26] We hypothesized that the catabolic effects of IL-1α decrease with construct maturation in culture.

MATERIALS AND METHODS

Experimental design

Three consecutive studies carried out are discussed in this manuscript: study 1 directly compared the effects of IL-1α on immature (day 14) engineered cartilage and freshly harvested (day 0) native cartilage cultured in a chemically defined (CD) medium. The results of this study (the cytokine had deleterious effects only on engineered cartilage and not on native explants) were unexpected, and motivated studies 2 and 3.

The engineered cartilage as used in study 1 had not yet developed the extracellular matrix present in native explants. We hypothesized that this matrix, in conjunction with an antiinflammatory chemical mediator in the culture medium (dexamethasone), was necessary to mitigate the effects of the cytokine. Thus, study 2 examined the possible mitigating effects of an accumulated extracellular matrix on engineered constructs that were precultured in CD medium for different durations and challenged with IL-1α. Study 3 examined the culture media for antiinflammatory chemical mediators. For convenience of presentation, it was split into two parts: study 3a specifically tested whether it was the inclusion of dexamethasone in the CD medium that counteracted the catabolic effects of IL-1α on native explants in study 1; study 3b extended these findings to engineered cartilage at different levels of maturity, testing whether the inclusion or exclusion of dexamethasone counteracts the catabolic effects of IL-1α on engineered cartilage precultured for different durations. Each study was performed independently using explants from different animals or individual cell isolations pooled across several different animals, and repeated at least once to ensure repeatability.

The timelines of all three studies are detailed in Figure 1. For study 1 ($n = 6$ per group) freshly harvested native cartilage explants (mid-zone only) or immature engineered tissue (day 14) was cultured in a CD medium and challenged for 14 days with IL-1α (10 ng/mL) (Fig. 1, study 1). For study 2 ($n = 5$–8 per group) engineered constructs were maintained in CD medium and challenged with IL-1α at different developmental stages in culture. Specifically, at 14-day intervals the control group was divided and a subset was exposed to 10 ng/mL IL-1α for 14 days. Similarly, half the previous IL-1α group was tested and the remainder cultured in CD medium without IL-1α for an additional 14 days (recovery group) (Fig. 1, study 2). For study 3a ($n = 10$–18 per group) native explants were cultured for 14 days in CD medium (+/−) dexamethasone and (+/−) IL-1α. For study 3b ($n = 8$ per group) engineered constructs were precultured for 14 days with transforming growth factor beta-3 (TGF-β3) and exposed thereafter to IL-1α at various times in culture (days 14 and 28) as in study 2 but with the modification that the culture medium did or did not include dexamethasone.

Cell isolation

Articular cartilage was harvested from bovine carpometacarpal (CMC) joints of freshly slaughtered 1–3-week-old calves. Three to five joints were used for each study, and cells were pooled from all joints. Explants (studies 1 and 3a) were cored using a sterile disposable punch (Ø 4 mm; Miltex, York, PA) and then sectioned using a custom device to a final thickness of 2.3 mm, keeping the mid zone only. For engineered tissue (studies 1, 2, and 3b), chunks of cartilage were harvested, combined, and digested in Dulbecco's modified Eagle's medium (DMEM) with 390 U/mL collagenase type VI (Sigma, St. Louis, MO) for 11 h at 37°C with stirring. The resulting cell suspension was then filtered through a 70-μm-pore-size mesh and sedimented in a

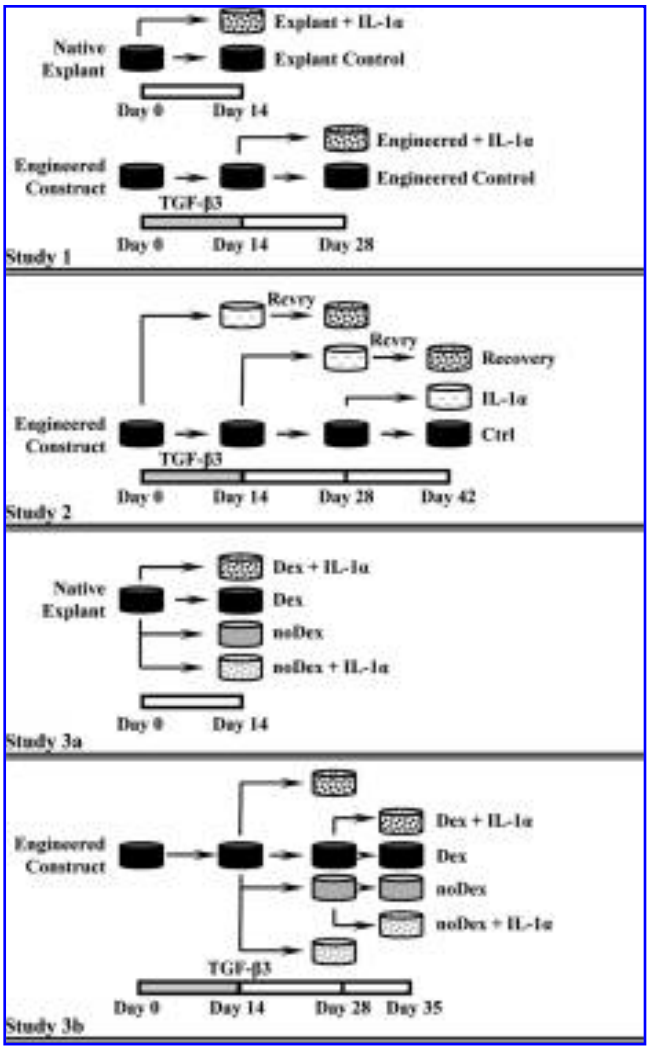

FIG. 1. (**Study 1**) Either freshly harvested explants (day 0) or engineered constructs (initially at day 14) were cultured for 14 days in CD medium (+/−) IL-1α. (**Study 2**) Engineered constructs were cultured in CD medium for 42 days. The control group was divided at 14-day intervals, and a subset exposed to IL-1α for 14 days. These constructs were then maintained without IL-1α for an additional 14 days recovery group (Revry). (**Study 3a**) Explants were cultured for 14 days in CD medium (+/−) IL-1α (as in study 1) but also (+/−) dexamethasone. (**Study 3b**) Engineered constructs were exposed to IL-1α at various times in culture as in study 2 but with the additional modification that the culture medium did or did not include dexamethasone.

bench-top centrifuge for 10 min at 1000 *g*. Viable cells were counted using a hemacytometer and trypan blue. One volume of chondrocyte suspension (at 60×10^6 cells/mL) was then mixed with an equal volume of 4% low-melt agarose (type VII, Sigma) at 37°C to yield a final cell concentration of 30×10^6 cells/mL in 2% agarose. The chondrocyte/agarose mixture was cast into slabs and cored using a sterile disposable punch (Miltex) to final dimensions of 4 mm diameter and 2.3 mm thickness.

Growth medium

The growth medium was changed every other day and consisted of high-glucose DMEM supplemented with 1×PSF (100 units/mL Penicillin, 100 µg/mL Streptomycin, and 0.25 µg/mL Fungizone), 0.1 µM dexamethasone, 50 µg/mL ascorbate 2-phosphate, 40 µg/mL L-proline, 100 µg/mL sodium pyruvate, and 1×ITS + premix (insulin, human transferrin, and selenous acid; Becton Dickinson, Franklin Lakes, NJ). For studies using engineered-tissue (studies 1, 2, and 3b), CD medium was further supplemented with 10 ng/mL of TGF-β3 (R&D Systems, Minneapolis, MN) for the first 14 days of culture.

Material testing

Cylindrical constructs were tested for both their equilibrium Young's modulus (E_Y) and their dynamic modulus (G^*) in unconfined compression using a custom computer-controlled testing system.[27] The equilibrium E_Y is commonly used as a measure of the behavior of cartilage that has been allowed to reach equilibrium after a known load or displacement has been applied. The dynamic modulus is considered to be a more physiologically relevant measurement as it measures the behavior of the tissue during the application of cyclic loads and better captures fluid pressurization within the biphasic tissue. To measure E_Y an initial 0.02 N tare load was applied, followed by a compression to 10% strain, at a strain rate of 0.05%/s. E_Y was calculated from the equilibrium stress at 10% strain. Previous studies have shown E_Y to remain invariant across strain magnitudes ranging from 0% to 20% for cartilage explants. G^* was measured after achieving stress-relaxation equilibrium by superimposing a 2% peak-to-peak sinusoidal strain at 0.01 Hz.

Biochemical content

The biochemical content of each sample was assessed by first measuring sample wet weight, lyophilizing for 24 h, and then measuring the sample dry weight. Gross water content was determined from the difference. Once dry, the samples were digested in proteinase-K overnight at 56°C, as described previously.[28] Aliquots of digest were analyzed for GAG content using the 1,9-dimethylmethylene blue dye-binding assay.[29] A further aliquot was acid hydrolyzed in 12 N HCl at 110°C for 16 h, dried over NaOH, and resuspended in assay buffer.[28] Ortho-hydroxyproline (OHP) content was then determined via a colorimetric assay by reaction with chloramine T and dimethylaminobenzaldehyde,[30] scaled for microplates. OHP content was converted to total collagen content using the conversion of 1:7.64 ratio of OHP:collagen.[31] Each biochemical constituent (GAG and collagen) was normalized to tissue wet weight. For study 3, media samples were retained and tested for matrix metalloproteinases-1 (MMP-1) and MMP-3 by the Luminex assay (R&D systems) according to manufacturer's protocol.

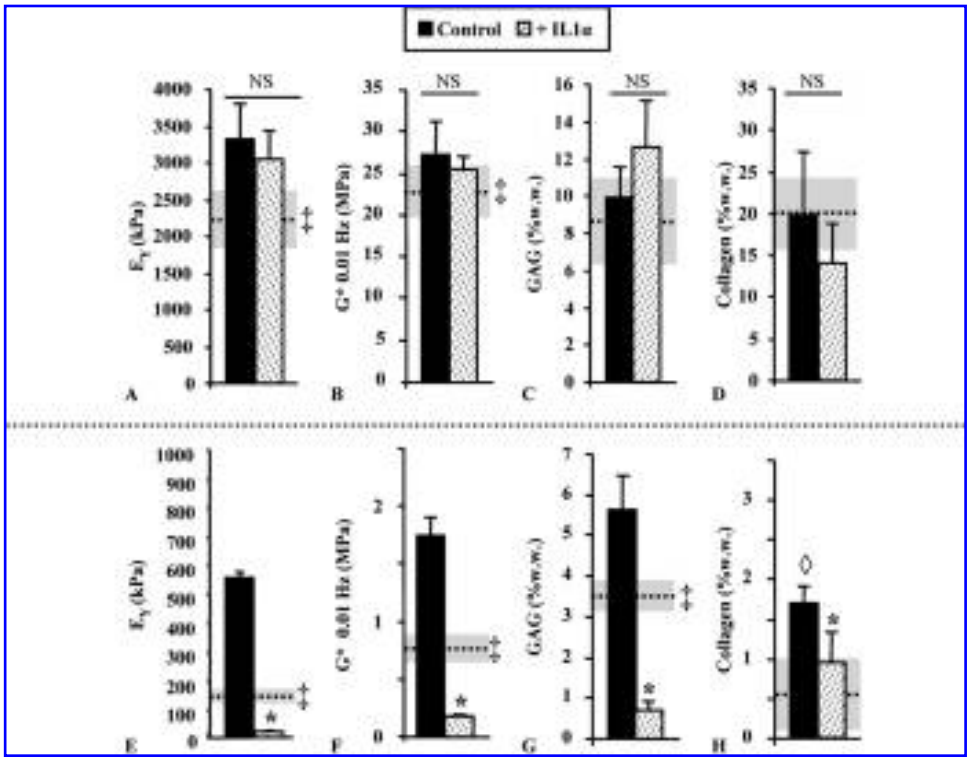

FIG. 2. (**A, E**) Equilibrium Young's modulus, (**B, F**) dynamic modulus at 0.01 Hz, (**C, G**) GAG (% wet weight), and (**D, H**) collagen (% wet weight) for explants (top row) or engineered constructs (bottom row) cultured for 14 days in CD medium (+/−) IL-1α. Dotted line indicates initial value (day 0 for explants; day 14 for engineered constructs); horizontal shaded bar indicates standard deviation. $^{\ddagger}p \leq 0.05$ for day 0 versus all other groups; $^{*}p \leq 0.05$ versus control; $^{\diamond}p \leq 0.05$ versus day 0; NS, not significant.

Statistics

Statistics were performed with the Statistica (Statsoft, Tulsa, OK) software package. Each data point represents the mean and standard deviation. Groups were examined for significant differences by analysis of variance ($\alpha = 0.05$), with E_Y, G^*, GAG, or OHP as the dependent variable. Tukey's honest significant difference *post hoc* tests were carried out with a statistical significance set at $p = 0.05$.

RESULTS

Study 1

The effects of IL-1α on cartilage explants were different from the effects of the same cytokines on immature engineered cartilage (Study 1, Fig. 2). Whereas the mechanical and biochemical properties of immature engineered cartilage degraded swiftly in the presence of IL-1α, there was no such degradation in explants cultured in the same chemical conditions.

Explants. All explant groups (regardless of cytokine treatment) cultured in CD medium developed significantly higher E_Y (Fig. 2A) and G^* (Fig. 2B) but not GAG (Fig. 2C) or collagen (Fig. 2D) by day 14 of culture compared to day 0 values ($E_Y = 2247 \pm 447$ kPa, $G^* = 23 \pm 3$ MPa, GAG = $8.3 \pm 2.4\%$ wet weight [%ww], and collagen = 21.2 ± 4.4%ww). Further, on day 14 there were no significant differences between the control and the cytokine-treated group ($E_Y = 3411 \pm 335$ kPa, $G^* = 31 \pm 3$ MPa, GAG = 12.4 ± 1.4%ww, and collagen = 21.1 ± 10%ww).

Engineered constructs. For engineered constructs the control group developed significantly higher E_Y (Fig. 2E), G^* (Fig. 2F), GAG (Fig. 2G), and collagen (Fig. 2H) by day 28 of culture ($E_Y = 547 \pm 14$ kPa, $G^* = 1.75 \pm 0.25$ MPa, GAG = 5.64 ± 0.83%ww, and collagen = 1.70 ± 0.22%ww) compared to day 14 values ($E_Y = 144 \pm 8$ kPa, $G^* = 0.8 \pm 0.1$ MPa, GAG = 3.5 ± 0.46%ww, and collagen = 0.56 ± 0.53%ww). Contrary to the explant results detailed above, cytokine treatment to engineered constructs resulted in significant differences from the control and from the initial day 14 values. By day 28 the IL-1α group ($E_Y = 20 \pm 2$ kPa, $G^* = 0.19 \pm 0.02$ MPa, GAG = 0.71 ± 0.19%ww, and collagen = 0.94 ± 0.38%ww) had significantly lower E_Y, G^*, GAG, and collagen compared to the control. These values were also significantly lower than initial day 14 values in E_Y, G^*, and GAG.

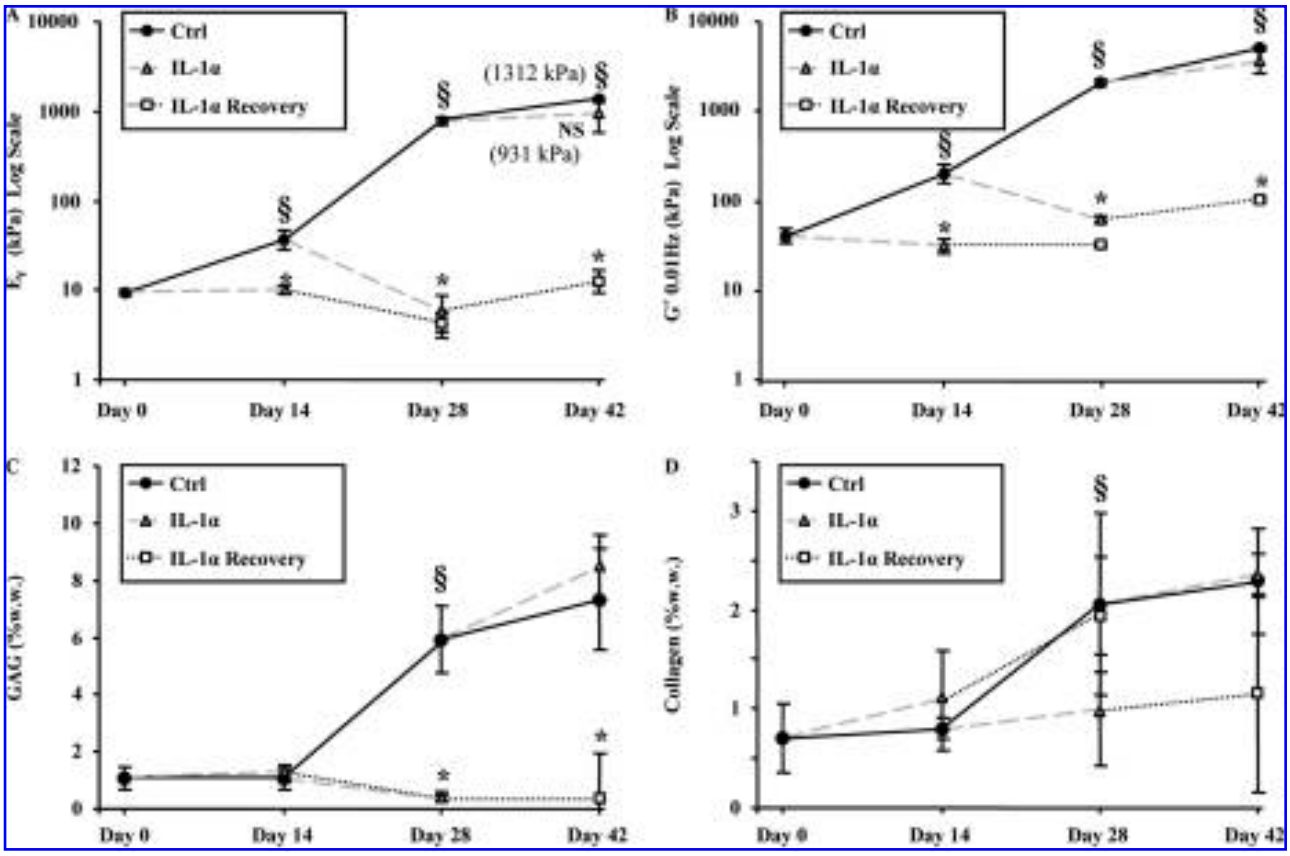

FIG. 3. (**A**) Equilibrium Young's modulus, (**B**) dynamic modulus at 0.01 Hz, (**C**) GAG (% wet weight), and (**D**) collagen (% wet weight) for engineered constructs. Subsets of control (solid lines) were challenged at each time point with IL-1α (dashed lines) and subsequently allowed to recover without IL-1α (dotted lines). $^{*}p \leq 0.05$ versus control group at all time points other than day 0; $^{\S}p \leq 0.05$ versus previous time points within same group; NS, not significant.

Study 2

Engineered constructs subjected to IL-1α at early time cultures (days 0 and 14) exhibited tissue degradation and GAG loss that was not present in tissue subjected to IL-1α at later time points (day 28) (Fig. 3). These degradative effects appeared to be long term: discontinuation of IL-1α treatment on engineered constructs (day 14 or 28) did not lead to recovery of tissue properties 14 days later (Fig. 3, recovery group).

Engineered constructs cultured under control conditions grew significantly in all values measured over the 42 day culture period, increasing from day 0 values ($E_Y = 9 \pm 1$ kPa, $G^* = 0.04 \pm 0.01$ MPa, GAG $= 1.1 \pm 0.4\%$ww, and collagen $= 0.7 \pm 0.4\%$ww) to day 42 values ($E_Y = 1312 \pm 70$ kPa, $G^* = 5 \pm 0.01$ MPa, GAG $= 7.3 \pm 1.8\%$ww, and collagen $= 2.2 \pm 0.5\%$ww) for the control group. The day 14 IL-1α group had no significant differences to day 0 and was significantly lower than the day 14 control group in all values except collagen. The day 28 IL-1α group also had no significant differences to day 0 and was significantly lower than both day 14 and day 28 control in all values except collagen. The day 42 IL-1α group, however, was significantly higher than the day 28 control and further had no significantly differences to the day 42 control group in all values. The IL-1α recovery groups had no significant differences to day 0 or to their preceding IL-1α groups at all times measured (Fig. 3).

Study 3a

Explants (+/−) dexamethasone (+/−) IL-1α. Explants cultured in the absence of dexamethasone (Fig. 4, nodex) maintained initial day 0 values throughout the culture period for all measurements assessed. Explants cultured in the presence of dexamethasone (Fig. 4, dex) developed significantly higher G^*, but not E_Y, GAG, or collagen, than day 0 and nodex groups. These constructs also had significantly higher E_Y and G^* than the nodex + α group.

Explants challenged with IL-1α in the presence of dexamethasone (Fig. 4, dex + α) did not develop any significant differences from the dex-only group and similarly displayed significantly higher properties when compared to the nodex

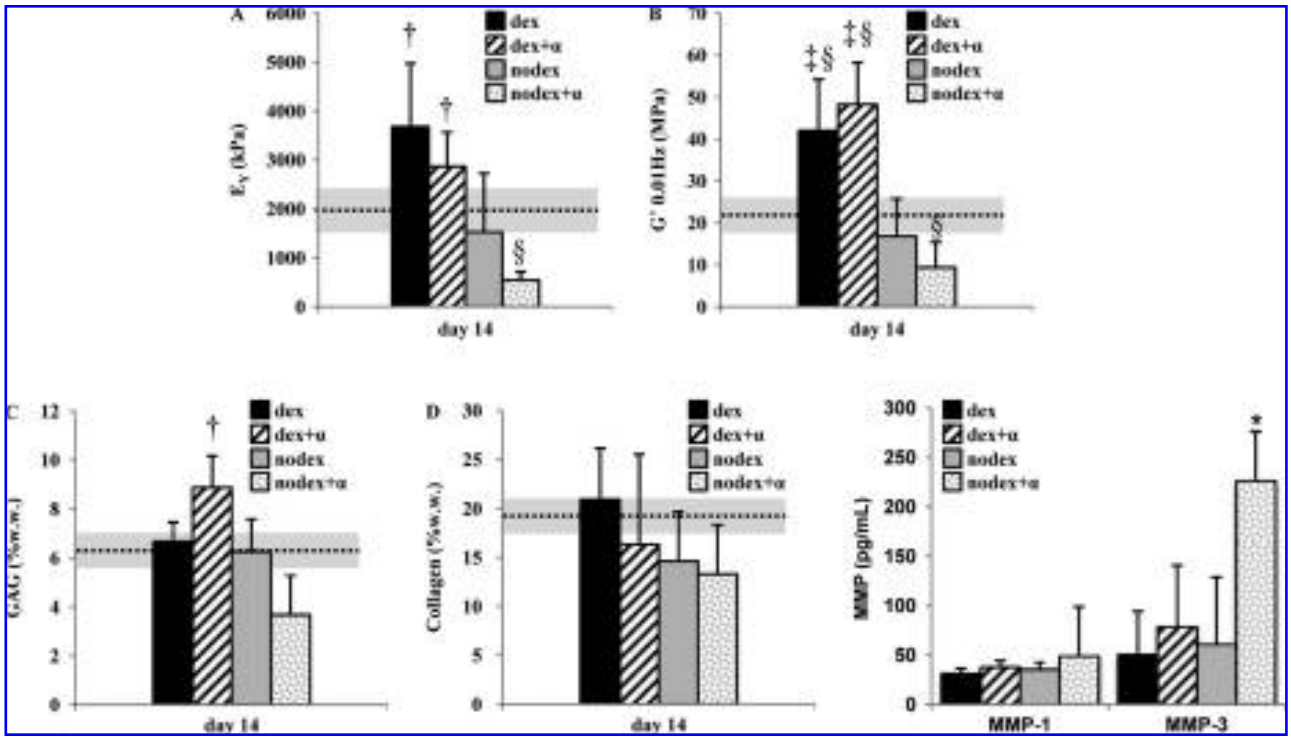

FIG. 4. (**A**) Equilibrium Young's modulus, (**B**) dynamic modulus at 0.01 Hz, (**C**) GAG, and (**D**) collagen (% wet weight) for explants cultured for 14 days in CD medium (+/−) dexamethasone and (+/−) IL-1α. Dotted line indicates day 0 time point; horizontal shaded bar indicates standard deviation. (**E**) MMP-1 and MMP-3 response in spent media with or without dexamethasone. $^{\dagger}p < 0.05$ vs. nodex + α; $^{\ddagger}p < 0.05$ for groups with dex vs. groups without dex; $^{\S}p < 0.05$ vs. day 0; $^{*}p < 0.05$ for nodex + α vs. other groups.

and nodex + α groups. Explants challenged with IL-1α in the absence of dexamethasone (Fig. 4, nodex + α), however, degraded significantly over the 14 days of culture, dropping to 27% of the E_Y (Fig. 4A), 42% of the G^* (Fig. 4B), and 58% of the GAG (Fig. 4C), but with no significant differences in collagen (Fig. 4D) when compared to initial values. Examination of the spent growth medium for matrix metallopeptidase proteins revealed significantly higher MMP-3 but not MMP-1 in the nodex + α group compared to all other groups.

Study 3b

Engineered constructs (+/−) dexamethasone (+/−) IL-1α over time. Engineered constructs cultured with dexamethasone grew significantly in all values measured over the culture period, increasing from day 0 values $E_Y = 10 \pm 5$ kPa, $G^* = 0.05 \pm 0.02$ MPa, GAG = 0.6 ± 0.2%ww, and collagen = 0.0 ± 0.2%ww, to $E_Y = 678 \pm 37$ kPa, $G^* = 2.8 \pm 0.08$ MPa, GAG = 7.2 ± 0.3%ww, and collagen = 3.0 ± 0.6%ww by day 35 in culture (Fig. 5, dex control group). Unlike native explants, engineered constructs cultured without dexamethasone did not differ significantly from the dex group at any time tested during culture, reaching the following values by day 35 in culture (Fig. 5, nodex control group): $E_Y = 692 \pm 71$ kPa, $G^* = 2.6 \pm 0.28$ MPa, GAG = 5.2 ± 0.7%ww, and collagen = 5.2 ± 1.9%ww.

The effect of IL-1α on engineered constructs was dependent on both the amount of preculture time and the presence or absence of dexamethasone in the culture medium. Engineered constructs subjected to IL-1α starting on day 14 of culture exhibited tissue degradation and GAG loss by day 28 regardless of whether the culture medium contained dexamethasone. Engineered constructs subjected to IL-1α starting on day 28, however, exhibited tissue degradation and GAG loss only when dexamethasone was absent from the culture medium; in the presence of dexamethasone these constructs did not differ significantly from IL-1α–free controls (Fig. 5).

DISCUSSION

For the current studies, we adopted a CD medium that has been used extensively by our laboratory for the culture of chondrocyte-seeded agarose constructs; using this medium formulation, we have been able to develop engineered constructs with functional material properties similar to

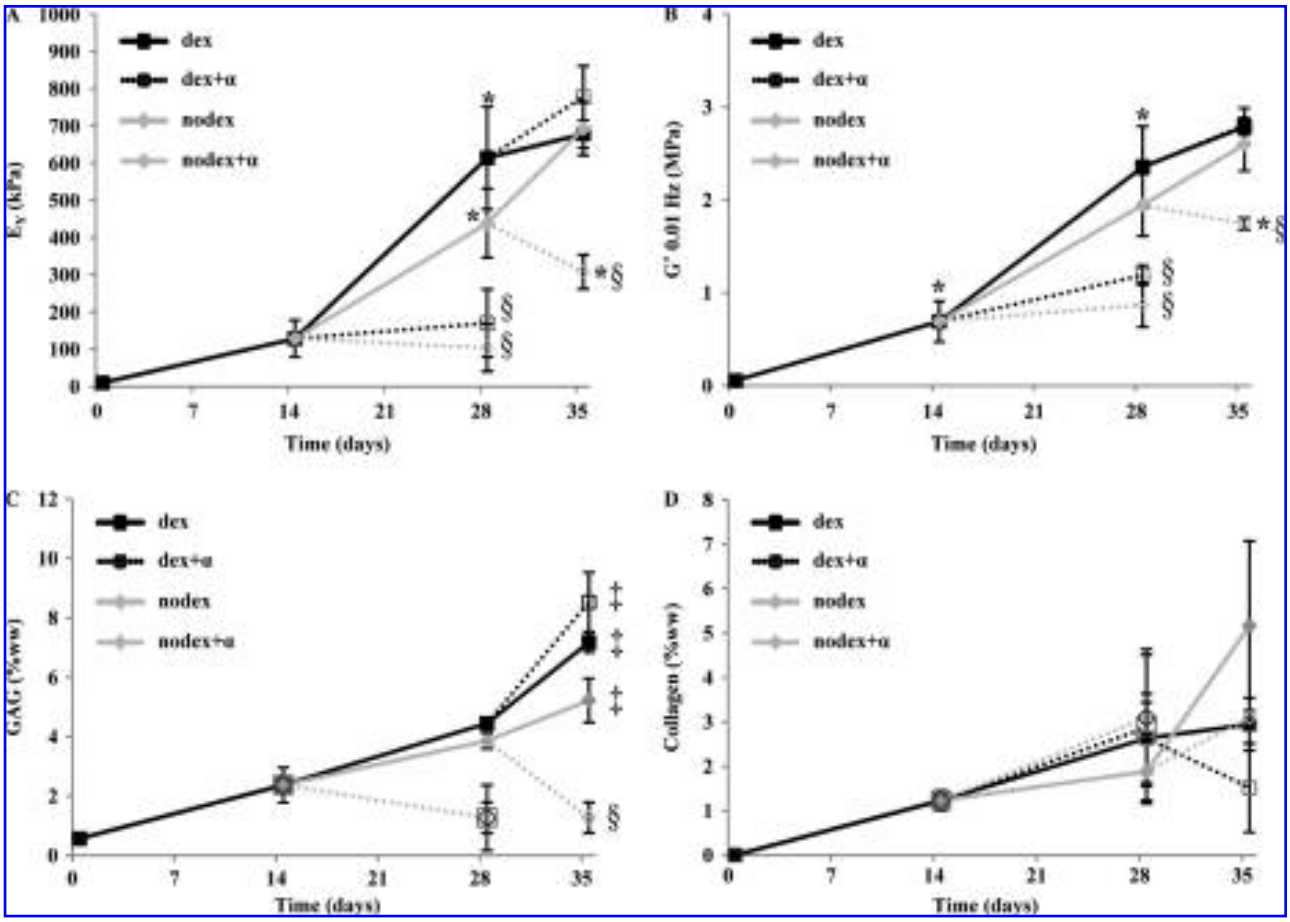

FIG. 5. (**A**) Equilibrium Young's modulus, (**B**) dynamic modulus at 0.01 Hz, (**C**) GAG (% wet weight), and (**D**) collagen for engineered constructs cultured in CD medium with (dex) or without (nodex) dexamethasone. Subsets of control were challenged at each time point with IL-1α (dex + α or nodex + α). $^{*}p < 0.05$ vs. all groups in previous time point; $^{\S}p < 0.05$ vs. IL-1α free controls; $^{\ddagger}p < 0.05$ vs. day 35 dex + α.

those of the native tissue. To our knowledge, this is the first study that has examined the effects of an interleukin cytokine on engineered cartilage constructs exhibiting both physiologic levels of GAG and Young's modulus.

Despite the varied experimental conditions in the literature, including differences in species and age and media type, most studies have reported interleukin-induced degradation of articular cartilage.[16,17,19,32–37] However, under the culture conditions of the current studies, we observed the presence of a chondro-protective soluble mediator in the culture medium that was able to suppress the interleukin-induced matrix degradation effects, the most likely of which was insulin or dexamethasone. Interestingly, the protective effects of this mediator were realized only for engineered cartilage constructs that were mature and exhibited native levels of GAG content and corresponding material properties (Figs. 3 and 5). It should be noted that in discussing maturity of engineered tissue we are not referring to cell age, but rather to the development of functional properties and extracellular matrix components relative to the native tissue. In our studies both explants and cells were harvested from immature tissue. Examining the effect of cell age on our findings could be an interesting and clinically relevant future study.

Explant studies in the literature have reported IL-1α–induced tissue degradation in culture media that do not include insulin or dexamethasone in their composition.[16,17,19,32–37] Dexamethasone has been found to be a potent antiinflammatory corticosteroid that has been well documented to modulate the anabolic–catabolic activities of explants. It was used here at a dose typically used for the culture of mesenchymal stem cells and at the lower range of that used clinically.[14,38] The dose of interleukin was typical for what is used *in vitro*,[16,17,19,32–37] and high for what is used *in vivo*.[39–41] The results of studies 3a and 3b clearly identify dexamethasone as the chondro-protective chemical mediator

in our culture medium, as both explants and engineered constructs subjected to interleukin cytokine insult degrade in the absence of dexamethasone (while in the continued presence of insulin). While the dependence on dexamethasone in protection against interleukin appears similar for cartilage explants and mature engineered constructs, the mechanism affording this protection is unclear and may be different for each. A case for differing mechanisms is supported by findings that explants cultured in CD medium maintained stiffness without dexamethasone or increased stiffness with dexamethasone over the same free-swelling culture period (study 3a), whereas engineered constructs exhibited similar increases in stiffness in the absence or presence of dexamethasone. As such, disparities in the behavior of explants and engineered cartilage to interleukin (with dexamethasone-supplemented media) should be considered in the context of this underlying difference.

The steric exclusion of interleukin from mature constructs due to decreasing permeability with culture time associated with increasing extracellular matrix density is unlikely to be a key mechanism behind our maturation-dependent findings, as the engineered tissues exhibit hydraulic permeabilities that are still much higher than that for native cartilage (as noted from the disparity in dynamic modulus); further, interleukin has been shown to degrade explant tissue in the absence of dexamethasone. Future studies will be required to better understand whether cellular changes or changes to the elaborated matrix with culture time, or both, are responsible for this protective effect. One may speculate that freshly digested cells are hypersensitive to interleukin and become increasingly less so as constructs mature. Alternatively, one can argue that changes in the extracellular environment offer protection to interleukin in conjunction with dexamethasone or insulin. From the current series of studies we can comment on the latter.

In the field of cartilage tissue engineering, the ability to generate constructs possessing native levels of collagen has eluded researchers. Interestingly, the relatively low collagen levels achieved in our studies ($\sim$10% of native levels with long-term culture), while on par with the highest levels reported in the literature for engineered cartilage, does not generally appear to be the underlying cause for the lack of protection afforded to engineered constructs compared to native explants by dexamethasone. There is the possibility of course that a requisite amount of collagen is necessary to trigger the protection, or that the location and not the quantity of collagen is the determining factor, especially if the collagen is concentrated in and around the pericellular matrix. We have previously reported local pericellular matrix development with positive type VI collagen staining in our chondrocyte-seeded constructs.[42] Interleukin-1 treated agarose cultures have been reported to respond with increased sequestration and retention of type VI collagen in an expanded microenvironment surrounding the chondrocytes, suggesting a role for type VI collagen in the differentiation of the pericellular microenvironment *in vitro*.[43] The presence of this pericellular matrix may affect how dexamethasone functions in apposition to the inflammatory cytokine.

It is also possible that the dexamethasone effect is related to tissue GAG levels present on the day the cytokine was introduced. For example, in study 1 these levels were only 12% of the native tissue values on day 14 but already 70% of those values on day 28; conversely, the collagen levels on those 2 days were only 4% of the native tissue on day 14 and still 10% on day 35. The mechanism behind the protective effects of GAG in conjunction with dexamethasone might be related to chondrocyte volume changes. Quinn *et al.*[44] have reported chondrocyte volume changes with culture time (as well as GAG deposition) suggestive of alterations in volume regulatory mechanisms. Additionally, the pools of GAGs in the pericellular region and inter-territorial regions change with culture time. We may therefore speculate that changes to the local physical environment of the cell with matrix elaboration that alter cell function may be important in our observations. While our engineered tissues grow to resemble native cartilage by its appearance, Young's modulus, and GAG levels, they begin with little or no extracellular matrix. However, cell matrix elaboration is likely governed by a negative feedback mechanism, where tissue metabolism decreases as the amount of existing matrix surrounding the cell increases.[45] As such, there is the potential therefore that the IL-1α effects observed are mediated in part by variations in the level of cell metabolism with culture. In this scenario, it would be difficult to delineate if it is matrix amount or cell metabolism or both that govern the culture time–dependent variations in interleukin-induced effects.

By examining the response of the engineered tissue to IL-1α at different levels of maturity as we have defined it, we have drawn attention to important differences in engineered cartilage and native cartilage that can have significant impact on clinical success after implantation. The results of study 1 show that engineered constructs subjected to IL-1α at early culture time will not develop functional mechanical properties even if IL-1α is removed from their culture environment (Study 1, Fig. 2). This implies that even transitory exposure to chemical factors, which may arise from inflammatory responses resulting from surgery as an example, could have long-lasting effects on the development of immature tissue within the joint. The findings of this study support the contention that engineered cartilage constructs should be implanted when the tissue is more functionally mature because the presence of an extracellular matrix may not only protect cells mechanically, allowing the constructs to better withstand the load bearing demands of the joint, but also play a role in protecting the cells from chemical assault such as the presence of inflammatory agents such as IL-1α. Further, they point toward a need to assess engineered tissue on multiple functional levels—both mechanically to assess load-bearing capabilities in comparison to native tissue, as well as biologically to assess chemical sensitivity in comparison to native tissue.

ACKNOWLEDGMENTS

This work was funded by NIH Grants AR46568 and AR53530.

REFERENCES

1. Capito, R.M., and Spector, M. Scaffold-based articular cartilage repair. IEEE Eng Med Biol Mag **22,** 42, 2003.
2. Cima, L.G., Vacanti, J.P., Vacanti, C., Ingber, D., Mooney, D., and Langer, R. Tissue engineering by cell transplantation using degradable polymer substrates. J Biomech Eng **113,** 143, 1991.
3. Giannoni, P., and Cancedda, R. Articular chondrocyte culturing for cell-based cartilage repair: needs and perspectives. Cells Tissues Organs **184,** 1, 2006.
4. Giannoudis, P.V., and Pountos, I. Tissue regeneration. The past, the present and the future. Injury **36 Suppl 4,** S2, 2005.
5. Habibovic, P., Woodfield, T., de Groot, K., and van Blitterswijk, C. Predictive value of *in vitro* and *in vivo* assays in bone and cartilage repair—what do they really tell us about the clinical performance? Adv Exp Med Biol **585,** 327, 2006.
6. Hung, C.T., Mauck, R.L., Wang, C.C., Lima, E.G., and Ateshian, G.A. A paradigm for functional tissue engineering of articular cartilage via applied physiologic deformational loading. Ann Biomed Eng **32,** 35, 2004.
7. Raghunath, J., Rollo, J., Sales, K.M., Butler, P.E., and Seifalian, A.M. Biomaterials and scaffold design: key to tissue-engineering cartilage. Biotechnol Appl Biochem **46,** 73, 2007.
8. Schulz, R.M., and Bader, A. Cartilage tissue engineering and bioreactor systems for the cultivation and stimulation of chondrocytes. Eur Biophys J **36,** 539, 2007.
9. Lotz, M. Cytokines in cartilage injury and repair. Clin Orthop Relat Res **391 Suppl,** S108, 2001.
10. Schiff, M.H. Role of interleukin 1 and interleukin 1 receptor antagonist in the mediation of rheumatoid arthritis. Ann Rheum Dis **59 Suppl 1,** i103, 2000.
11. Smeets, T.J., Barg, E.C., Kraan, M.C., Smith, M.D., Breedveld, F.C., and Tak, P.P. Analysis of the cell infiltrate and expression of proinflammatory cytokines and matrix metalloproteinases in arthroscopic synovial biopsies: comparison with synovial samples from patients with end stage, destructive rheumatoid arthritis. Ann Rheum Dis **62,** 635, 2003.
12. van den Berg, W.B., and Bresnihan, B. Pathogenesis of joint damage in rheumatoid arthritis: evidence of a dominant role for interleukin-I. Baillieres Best Prac Res **13,** 577, 1999.
13. Towle, C.A., Hung, H.H., Bonassar, L.J., Treadwell, B.V., and Mangham, D.C. Detection of interleukin-1 in the cartilage of patients with osteoarthritis: a possible autocrine/paracrine role in pathogenesis. Osteoarthritis Cartilage **5,** 293, 1997.
14. Pelletier, J.P., Roughley, P.J., DiBattista, J.A., McCollum, R., and Martel-Pelletier, J. Are cytokines involved in osteoarthritic pathophysiology? Semin Arthritis Rheum **20,** 12, 1991.
15. Martel-Pelletier, J., McCollum, R., DiBattista, J., Faure, M.P., Chin, J.A., Fournier, S., Sarfati, M., and Pelletier, J.P. The interleukin-1 receptor in normal and osteoarthritic human articular chondrocytes. Identification as the type I receptor and analysis of binding kinetics and biologic function. Arthritis Rheum **35,** 530, 1992.
16. Xu, C., Oyajobi, B.O., Frazer, A., Kozaci, L.D., Russell, R.G., and Hollander, A.P. Effects of growth factors and interleukin-1 alpha on proteoglycan and type II collagen turnover in bovine nasal and articular chondrocyte pellet cultures. Endocrinology **137,** 3557, 1996.
17. Rotter, N., Ung, F., Roy, A.K., Vacanti, M., Eavey, R.D., Vacanti, C.A., and Bonassar, L.J. Role for interleukin 1alpha in the inhibition of chondrogenesis in autologous implants using polyglycolic acid-polylactic acid scaffolds. Tissue Eng **11,** 192, 2005.
18. Cook, J.L., Anderson, C.C., Kreeger, J.M., and Tomlinson, J.L. Effects of human recombinant interleukin-1beta on canine articular chondrocytes in three-dimensional culture. Am J Vet Res **61,** 766, 2000.
19. Li, K.W., Wang, A.S., and Sah, R.L. Microenvironment regulation of extracellular signal-regulated kinase activity in chondrocytes: effects of culture configuration, interleukin-1, and compressive stress. Arthritis Rheum **48,** 689, 2003.
20. Buschmann, M.D., Gluzband, Y.A., Grodzinsky, A.J., Kimura, J.H., and Hunziker, E.B. Chondrocytes in agarose culture synthesize a mechanically functional extracellular matrix. J Orthop Res **10,** 745, 1992.
21. Buschmann, M.D., Gluzband, Y.A., Grodzinsky, A.J., and Hunziker, E.B. Mechanical compression modulates matrix biosynthesis in chondrocyte/agarose culture. J Cell Sci **108 (Pt 4),** 1497, 1995.
22. Mouw, J.K., Case, N.D., Guldberg, R.E., Plaas, A.H., and Levenston, M.E. Variations in matrix composition and GAG fine structure among scaffolds for cartilage tissue engineering. Osteoarthritis Cartilage **13,** 828, 2005.
23. Lima, E.G., Bian, L., Ng, K.W., Mauck, R.L., Byers, B.A., Tuan, R.S., Ateshian, G.A., and Hung, C.T. The beneficial effect of delayed compressive loading on tissue-engineered cartilage constructs cultured with TGF-beta3. Osteoarthritis Cartilage **15,** 1025, 2007.
24. Poole, S., Cunha, F.Q., Selkirk, S., Lorenzetti, B.B., and Ferreira, S.H. Cytokine-mediated inflammatory hyperalgesia limited by interleukin-10. Br J Pharmacol **115,** 684, 1995.
25. Benton, H.P., and Tyler, J.A. Inhibition of cartilage proteoglycan synthesis by interleukin I. Biochem Biophys Res Commun **154,** 421, 1988.
26. Tyler, J.A. Insulin-like growth factor 1 can decrease degradation and promote synthesis of proteoglycan in cartilage exposed to cytokines. Biochem J **260,** 543, 1989.
27. Soltz, M.A., and Ateshian, G.A. Experimental verification and theoretical prediction of cartilage interstitial fluid pressurization at an impermeable contact interface in confined compression. J Biomech **31,** 927, 1998.
28. Kelly, T.A., Ng, K.W., Wang, C.C., Ateshian, G.A., and Hung, C.T. Spatial and temporal development of chondrocyte-seeded agarose constructs in free-swelling and dynamically loaded cultures. J Biomech **39,** 1489, 2006.
29. Farndale, R.W., Sayers, C.A., and Barrett, A.J. A direct spectrophotometric microassay for sulfated glycosaminoglycans in cartilage cultures. Connect Tissue Res **9,** 247, 1982.
30. Stegemann, H., and Stalder, K. Determination of hydroxyproline. Clin Chim Acta **18,** 267, 1967.
31. Vunjak-Novakovic, G., Martin, I., Obradovic, B., Treppo, S., Grodzinsky, A.J., Langer, R., and Freed, L.E. Bioreactor cultivation conditions modulate the composition and mechanical

properties of tissue-engineered cartilage. J Orthop Res **17,** 130, 1999.
32. Temple, M.M., Xue, Y., Chen, M.Q., and Sah, R.L. Interleukin-1alpha induction of tensile weakening associated with collagen degradation in bovine articular cartilage. Arthritis Rheum **54,** 3267, 2006.
33. Bonassar, L.J., Sandy, J.D., Lark, M.W., Plaas, A.H., Frank, E.H., and Grodzinsky, A.J. Inhibition of cartilage degradation and changes in physical properties induced by IL-1beta and retinoic acid using matrix metalloproteinase inhibitors. Arch Biochem Biophys **344,** 404, 1997.
34. Legare, A., Garon, M., Guardo, R., Savard, P., Poole, A.R., and Buschmann, M.D. Detection and analysis of cartilage degeneration by spatially resolved streaming potentials. J Orthop Res **20,** 819, 2002.
35. Chowdhury, T.T., Bader, D.L., and Lee, D.A. Dynamic compression counteracts IL-1 beta-induced release of nitric oxide and PGE2 by superficial zone chondrocytes cultured in agarose constructs. Osteoarthritis Cartilage **11,** 688, 2003.
36. Homandberg, G.A., Ummadi, V., and Kang, H. High molecular weight hyaluronan promotes repair of IL-1 beta-damaged cartilage explants from both young and old bovines. Osteoarthritis Cartilage **11,** 177, 2003.
37. Stabellini, G., de Mattei, M., Calastrini, C., Gagliano, N., Moscheni, C., Pasello, M., Pellati, A., Bellucci, C., and Gioia, M. Effects of interleukin-1beta on chondroblast viability and extracellular matrix changes in bovine articular cartilage explants. Biomed Pharmacother **57,** 314, 2003.
38. Stove, J., Schoniger, R., Huch, K., Brenner, R., Gunther, K.P., Puhl, W., and Scharf, H.P. Effects of dexamethasone on proteoglycan content and gene expression of IL-1beta-stimulated osteoarthrotic chondrocytes *in vitro*. Acta Orthop Scand **73,** 562, 2002.
39. Cambray, G.J., Murphy, G., and Reynolds, J.J. The effects of dexamethasone *in vitro* on the production of collagenase and inhibitor by synovial and cartilage explants from the joints of rabbits with a proliferative arthritis. Rheumatol Int **1,** 69, 1981.
40. Tessler, R.H., and Salmon, W.D., Jr. Glucocorticoid inhibition of sulfate incorporation by cartilage of normal rats. Endocrinology **96,** 898, 1975.
41. Yang, Y.H., Morand, E.F., Getting, S.J., Paul-Clark, M., Liu, D.L., Yona, S., Hannon, R., Buckingham, J.C., Perretti, M., and Flower, R.J. Modulation of inflammation and response to dexamethasone by Annexin 1 in antigen-induced arthritis. Arthritis Rheum **50,** 976, 2004.
42. Kelly, T.A., Wang, C.C., Mauck, R.L., Ateshian, G.A., and Hung, C.T. Role of cell-associated matrix in the development of free-swelling and dynamically loaded chondrocyte-seeded agarose gels. Biorheology **41,** 223, 2004.
43. Chang, J., and Poole, C.A. Sequestration of type VI collagen in the pericellular microenvironment of adult chondrocytes cultured in agarose. Osteoarthritis Cartilage **4,** 275, 1996.
44. Quinn, T.M., Schmid, P., Hunziker, E.B., and Grodzinsky, A.J. Proteoglycan deposition around chondrocytes in agarose culture: construction of a physical and biological interface for mechanotransduction in cartilage. Biorheology **39,** 27, 2002.
45. Quinn, T.M., and Hunziker, E.B. Controlled enzymatic matrix degradation for integrative cartilage repair: effects on viable cell density and proteoglycan deposition. Tissue Eng **8,** 799, 2002.

Address reprint requests to:
Clark T. Hung, Ph.D.
351 Engineering Terrace MC8904
Department of Biomedical Engineering
Columbia University
1210 Amsterdam Ave.
New York, NY 10027

E-mail: cth6@columbia.edu

Received: October 24, 2007
Accepted: February 27, 2008

A.2 Physiologic deformational loading does not counteract the catabolic effects of interleukin-1 in long-term culture of chondrocyte-seeded agarose constructs

Eric G. Lima, Andrea R. Tan, Timon Tai, Liming Bian, Gerard A. Ateshian, James L. Cook, Clark T. Hung

Journal of Biomechanics ▮ (▮▮▮▮) ▮▮▮–▮▮▮

Contents lists available at ScienceDirect

Journal of Biomechanics

journal homepage: www.elsevier.com/locate/jbiomech
www.JBiomech.com

Physiologic deformational loading does not counteract the catabolic effects of interleukin-1 in long-term culture of chondrocyte-seeded agarose constructs

Eric G. Lima [a], Andrea R. Tan [b], Timon Tai [b], Liming Bian [b], Gerard A. Ateshian [c], James L. Cook [d], Clark T. Hung [b,*]

[a] Materials Characterization Laboratory, Cooper Union, 51 Astor Place, New York, NY 10003, USA
[b] Department of Biomedical Engineering, Columbia University, 351 Engineering Terrace MC8904, 1210 Amsterdam Avenue, New York, NY 10027, USA
[c] Department of Mechanical Engineering, Columbia University, 500 West 120th Street, Mail Code 4703, 220 S.W. Mudd, New York, NY 10027, USA
[d] Comparative Orthopaedic Laboratory, University of Missouri, 900 East Campus Drive, Columbia, MO 65211, USA

ARTICLE INFO

Article history:
Accepted 12 June 2008

Keywords:
Cartilage tissue engineering
Inflammatory cytokines
Interlukin-1
Physical stimulus

ABSTRACT

An interplay of mechanical and chemical factors is integral to cartilage maintenance and/or degeneration. Interleukin-1 (IL-1) is a pro-inflammatory cytokine that is present at elevated concentrations in osteoarthritic joints and initiates the rapid degradation of cartilage when cultured *in vitro*. Several short-term studies have suggested that applied dynamic deformational loading may have a protective effect against the catabolic actions of IL-1. In the current study, we examine whether the long-term (42 days) application of dynamic deformational loading on chondrocyte-seeded agarose constructs can mitigate these catabolic effects. Three studies were carried out using two IL-1 isoforms (IL-1α and IL-1β) in chemically defined medium supplemented with a broad range of cytokine concentrations and durations. Physiologic loading was unable to counteract the long-term catabolic effects of IL-1 under any of the conditions tested, and in some cases led to further degeneration over unloaded controls.

1. Introduction

Articular cartilage is a specialized connective tissue that bears load and reduces friction across moving joints. It is composed of an extracellular matrix that contains no nerves or blood vessels and relatively few cells. Once injured, articular cartilage does not heal well, but often degenerates further, leading to pain and loss of function (Hangody and Modis, 2006). Tissue engineering offers great hope for expanding the range of treatment options by generating healthy replacement cartilage from a combination of isolated, living cells embedded in a scaffold carrier (Cima et al., 1991; Capito and Spector, 2003; Hung et al., 2004; Giannoudis and Pountos, 2005; Giannoni and Cancedda, 2006; Habibovic et al., 2006; Raghunath et al., 2007; Schulz and Bader, 2007).

In order to function within a defect site an engineered implant must have both the mechanical competency and the chemical fortitude to survive and flourish within an environment that is likely to contain potent catabolic mediators stemming from chronic inflammation (van den Berg and Bresnihan, 1999; Schiff, 2000; Lotz, 2001; Smeets et al., 2003). Interleukin-1 (IL-1) is a pro-inflammatory cytokine that has been shown to be elevated in osteoarthritis (Towle et al., 1997) and leads to cartilage degradation in *in vitro* tests (Ratcliffe et al., 1986; Morales and Hascall, 1989; Temple et al., 2006). The catabolic effects of IL-1 may be especially pronounced in underdeveloped engineered cartilage (Xu et al., 1996; Cook et al., 2000; Rotter et al., 2005; Lima et al., 2008), whose chondrocytes are not yet fully embedded in a dense chondroprotective cartilaginous extracellular matrix (Li et al., 2003).

As the interplay of mechanical and chemical factors is integral to cartilage maintenance and/or degeneration, it motivates researchers to examine the combined effects of chemical and mechanical stimuli (Mauck et al., 2003a, b). The chondrocyte-seeded agarose system has clear basic science and tissue-engineering applications in which both chemical and mechanical stimuli can be carefully controlled. Several short-term studies using an agarose culture model have suggested that applied loading may have a protective effect against the catabolic actions of IL-1 (Gassner et al., 1999; Honda et al., 2000; Xu et al., 2000; Agarwal et al., 2001; Chowdhury et al., 2001).

Chowdhury et al. (2001, 2003) have shown that dynamic loading counteracts IL-1-induced increase of nitric oxide (NO) and PGE_2 in chondrocyte-seeded agarose constructs. Mio and co-workers have reported that RNA expression of anabolic factors (aggrecan and type II collagen) in chondrocyte-seeded agarose constructs increases with application of dynamic loading for 24 h.

* Corresponding author. Tel.: +1 212 854 6542; fax: +1 212 854 8725.
E-mail address: cth6@columbia.edu (C.T. Hung).

0021-9290/$ - see front matter © 2008 Published by Elsevier Ltd.
doi:10.1016/j.jbiomech.2008.06.015

Long-term culture of chondrocytes in agarose results in the formation of a functional matrix (Buschmann et al., 1992, 1995) and applied deformational loading can enhance development of tissue properties (Mauck et al., 2000, 2003a, b; Lima et al., 2007). The culture system preserves the chondrocyte phenotype by maintaining a physiologic three-dimensional environment and produces extracellular matrix components with a proteoglycan composition and corresponding Young's modulus similar to that of native cartilage (Mouw et al., 2005).

In the current *in vitro* study, we examine the effects of IL-1 on the mechanical and biochemical properties of engineered tissue and explore whether the long-term application of physiological levels of dynamic deformational loading on chondrocyte-seeded agarose constructs can mitigate these effects.

2. Materials and methods

2.1. Experimental design

Three studies were carried out in this set of experiments. In Study 1 ($n = 5$–7/group), we establish a broad range of response by culturing constructs for 28 days with or without dynamic deformational loading in a chemically defined (CD) medium with one of two IL-1 isoforms (IL-1α and IL-1β, 10 ng/mL). Based on these results, we selected the most potent isoform (IL-1α) for the remaining two studies. In Study 2 ($n = 6$–9/group), we examined the dependence on cytokine concentration by testing a logarithmic range from 0.01 to 10 ng/mL over 42 days in culture. In Study 3 ($n = 8$/group), we repeat the logarithmic range of concentrations; however, we restrict IL-1 exposure to periods of deformational loading only. Thus, in Study 3 IL-1 is present for 3 h/day (for both loaded and unloaded groups), while in Studies 1 and 2 IL-1 is present 24 h/day. The timelines of the studies are detailed in Fig. 1. Each study was performed independently, using individual cell isolations pooled from different animals, and repeated twice. Values reported were averaged across repeat studies.

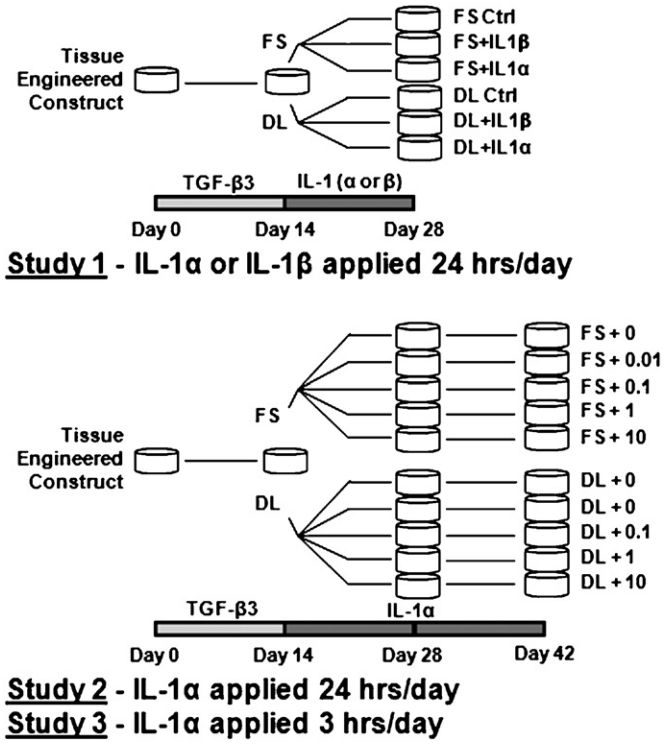

Fig. 1. Study 1: (testing IL-1 isoform dependence) tissue-engineered constructs were cultured for 14 days in a CD medium supplemented with TGF-β3. For the subsequent 14 days constructs were exposed to either IL-1α or IL-1β and either DL 3 h/day or maintained in FS without TGF-β3. Study 2: (testing IL-1 concentration): constructs were cultured for 14 days in CD medium with TGF-β3 and for the next 28 days were exposed to IL-1α in a logarithmic range of concentrations (0, 0.01, 0.1, 1, or 10 ng/mL) with or without loading. Study 3 (testing IL-1 exposure time): constructs were cultured as in Study 2, with the exception that IL-1α was added only during loading periods (3 h/day).

2.2. Cell isolation

Articular cartilage was harvested from bovine carpo-metacarpal (CMC) joints of freshly slaughtered 1–3-month-old calves. The cartilage tissue was digested in high-glucose Dulbecco's Modified Eagle's Medium (hgDMEM, 7.5 mL/g) with collagenase type IV (390 activity units/mL, Sigma, St. Louis, MO) for 11 h at 37 °C with stirring. The resulting cell suspension was filtered, combined, and cast into slabs with a final cell concentration of 30×10^6 in 2% agarose (Type VII, Sigma). The slabs were cored to final construct dimensions ($\varnothing 0.4 \times 0.23$ cm) and maintained in culture in one of the two medium formulations (described below) for up to 42 days depending on the study (Fig. 1).

2.3. Growth medium

CD medium consisted of hgDMEM supplemented with $1 \times$ PSF, 0.1 μM dexamethasone, 50 μg/mL ascorbate 2-phosphate, 40 μg/mL L-proline, 100 μg/mL sodium pyruvate, and 1X ITS+premix (insulin, human transferrin, and selenous acid, Becton Dickinson, Franklin Lakes, NJ). CD medium was further supplemented with 10 ng/mL of TGF-β3 (R&D Systems, Minneapolis, MN) for the first 14 days of culture. All culture media was changed every other day. This protocol has been shown to promote significant matrix elaboration that results in engineered tissue with native equilibrium modulus and proteoglycan content (Lima et al., 2007). The final mechanical and biochemical properties attained within the culture period can vary depending on the cell isolation, as is typical of the native tissue.

2.4. Interleukin supplementation

In Study 1, cell-seeded agarose constructs were cultured for 14 days in CD medium without IL-1. For the subsequent 14 days, constructs were exposed to either IL-1α or IL-1β at 10 ng/mL and either dynamically loaded (DL) 3 h/day or maintained in free swelling (FS). Mechanical testing and biochemical analysis was carried out as described below on days 0, 14, and 28.

In Studies 2 and 3, constructs were cultured for 14 days in CD medium without IL-1 as above. In Study 2, for the subsequent 28 days, the culture medium was supplemented with 0.01, 0.1, 1, or 10 ng/mL IL-1α and constructs were loaded or remained in FS. In Study 3, for the subsequent 28 days the constructs were exposed to 0.1, 1, or 10 ng/mL IL-1α during loading times only (for 3 h/day both FS and DL constructs were transferred to Petri dishes with new IL-1α-supplemented medium). For concentrations and time-courses see Fig. 1.

2.5. Loading protocol

Dynamic sinusoidal strain was applied at 1 Hz, with a nominal amplitude of 5% (10% peak-to-peak deformation) above a 10% tare strain, in unconfined compression with impermeable platens. Loading was applied continuously for 3 h/day, 5 days/week, beginning on day 14 (previously found to be optimal CD medium formulations (Lima et al., 2007)). Built-in compliance in the loading devices compensated for increasing stiffness in developing constructs, altering the load and displacement profiles and circumventing platen lift-off through the entire culture period as described previously (Lima et al., 2007).

2.6. Material testing

Cylindrical constructs were tested in unconfined compression using a custom computer-controlled testing system (Soltz and Ateshian, 1998). Samples were loaded to 10% strain at a strain rate of 0.05% strain/s, after an initial 0.02 N tare load. After achieving stress–relaxation equilibrium, the unconfined compression dynamic modulus G^* was measured by superimposing 2% peak-to-peak sinusoidal strain at 1 Hz.

2.7. Biochemical content

The biochemical content of each sample was assessed according to wet weight. Samples were digested in proteinase-K overnight at 56 °C and analyzed for either glycosaminoglycan (GAG) content using the 1,9-dimethylmethylene blue dye-binding assay (Farndale et al., 1982) or ortho-hydroxyproline (OHP) content via a colorimetric assay by reaction with chloramine-T and dimethylaminobenzaldehyde (Stegemann and Stalder, 1967), as described previously (Kelly et al., 2005). Cell viability (not shown) was measured via Live/Dead assay (Invitrogen, Carlsbad, CA).

Please cite this article as: Lima, E.G., et al., Physiologic deformational loading does not counteract the catabolic effects of interleukin-1 in long-term culture of chondrocyte-seeded agarose constructs. Journal of Biomechanics (2008), doi:10.1016/j.jbiomech.2008.06.015

2.8. Histological analysis

Samples were fixed in acid formalin ethanol (Lin et al., 1997), paraffin embedded, sectioned (8 μm thick), and stained with safranin-O (1% in dH_2O, pH 6.7) to view proteoglycan distribution. To ensure consistency, all time points and experimental groups were stained at the same time in a single batch, with native explant groups serving as controls. Distribution of intensity across a section was quantified using ImageJ (NIH). Gray scale intensity was normalized to mean intensity at center of histological section for the ordinate and percentage across the cross-section for the abscissa and averaged for all samples in each group.

2.9. Statistics

Statistics were performed with the Statistica (Statsoft, Tulsa, OK) software package. Groups were examined for significant differences by two-way analysis of variance ($\alpha = 0.05$) using Tukey's honest significant difference test (HSD) with E_Y, G^*, GAG, or OHP as the dependent variable, and time in culture and loading condition as the independent variables.

3. Results

3.1. Study 1 (testing medium and IL-1 isoform dependency)

All experimental groups cultured in CD medium without the addition of IL-1 grew in culture, developing significant differences in E_Y, G^*, and GAG by day 28 when compared to day 14 (Fig. 2A–C).

The application of dynamic loading resulted in significantly increased mechanical properties (Fig. 2A and B) by day 28 compared to FS controls, but with no significant differences in GAG (Fig. 2C) or collagen (not shown).

The presence of interleukin resulted in lower E_Y, G^*, and GAG when compared to IL-1 free controls, regardless of the isoform used (Fig. 2A and B). The application of dynamic loading did not mitigate this effect; both the DL+IL-1α and the DL+IL-1β groups developed no significant mechanical or biochemical differences compared to the FS+IL-1α or the FS+IL-1β groups.

Between the two isoforms, IL-1α was the more potent; both FS+IL-1α and DL+IL-1α were significantly lower in E_Y, G^*, and GAG compared to FS+IL-1β and DL+IL-1β, but there were no significant differences in collagen values between the two groups (not shown).

Safranin-O staining indicated clear differences between the control groups and the cytokine-treated groups: whereas both FS and DL control groups had a largely uniform distribution of staining across their cross-sections, constructs that had been treated with IL-1α or IL-1β had an uneven distribution of staining, with the majority of GAG loss occurring at the periphery (Fig. 3).

3.2. Study 2 (testing the effect of IL-1α concentration)

All experimental groups cultured in CD medium without the addition of IL-1 grew in culture, developing significant differences in E_Y, G^*, and GAG at each time point tested (Fig. 4A–C).

The application of dynamic loading resulted in significantly increased mechanical properties (Fig. 4A and B) compared to FS controls by day 28. There continued to be a significant increase in E_Y for the DL control by day 42, but with no further significant changes in G^*, GAG (Fig. 4B, C). Collagen values were unaffected by supplementation with IL-1α (not shown).

Exposure to the cytokine seemed to have an all or nothing effect. At concentrations above 0.01 ng/mL constructs did not develop mechanical or biochemical properties above their day 14 values, with no significant differences between the treated groups. This result was true regardless of whether constructs were maintained in DL or FS culture. Exposure at the lowest dosage tested (0.01 ng/mL) did not inhibit development, with no significant differences from untreated controls on day 28 or 42 (Fig. 4). There were no detrimental effects on cell viability (not shown) with any of the concentrations tested.

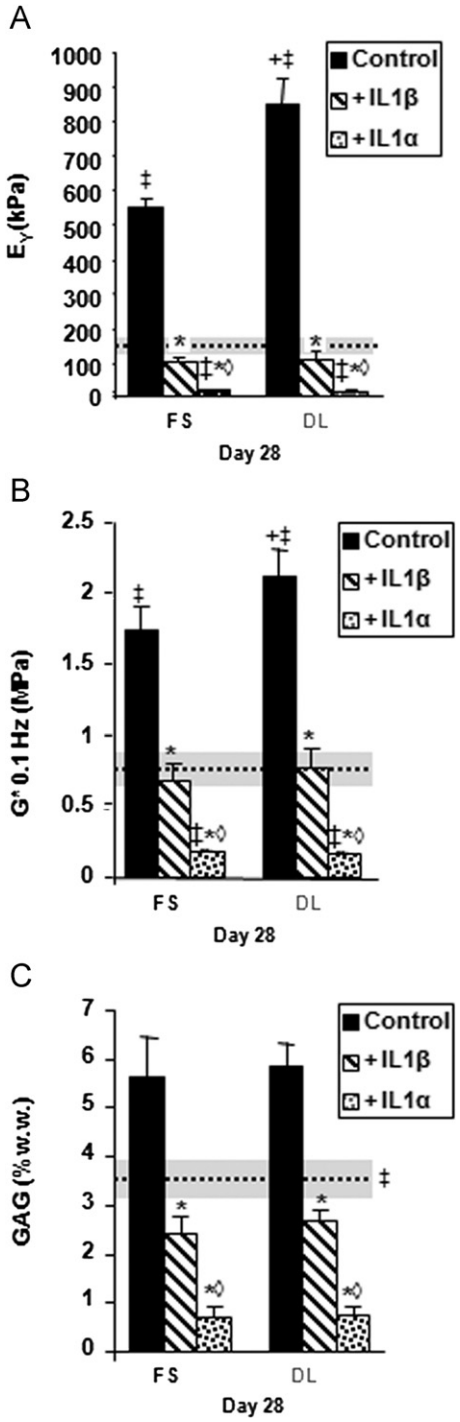

Fig. 2. (A) Equilibrium Young's modulus, (B) dynamic modulus at 0.1 Hz and (C) GAG (% wet weight) for tissue-engineered (TE) constructs cultured first in FS culture (14 days) and then an additional 14 days in either FS or DL culture in CD medium with IL-1α or IL-1β. Dotted line indicates day 14 time point. Horizontal shaded bar indicates standard deviation. ‡$p<0.05$ vs. day 14, *$p<0.01$ vs. FS or DL control, +$p<0.03$ for DL control vs. FS control, ◇$p<0.01$ vs. IL-1β.

3.3. Study 3 (IL-1 added only during loading)

Similarly to Study 2, all experimental groups grew and developed significant higher E_Y, G^* and GAG at each time point

Please cite this article as: Lima, E.G., et al., Physiologic deformational loading does not counteract the catabolic effects of interleukin-1 in long-term culture of chondrocyte-seeded agarose constructs. Journal of Biomechanics (2008), doi:10.1016/j.jbiomech.2008.06.015

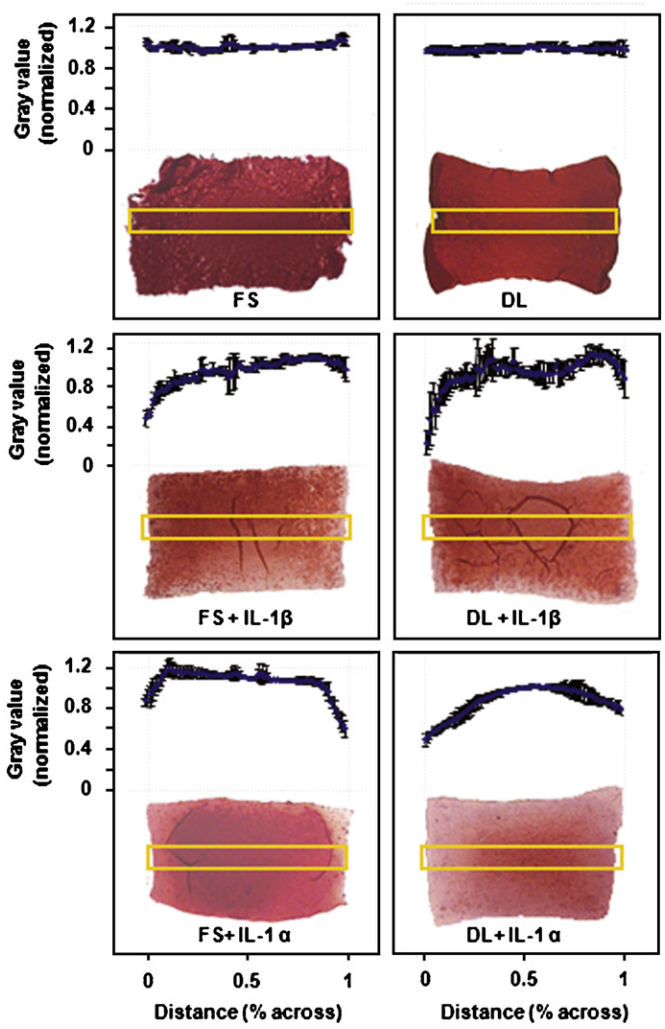

Fig. 3. Safranin-O staining for GAG comparing FS and DL constructs with IL-1α, IL-1β, or as untreated control (Study 1, day 35, CD medium). Graph indicates gray scale intensity normalized to mean intensity at the center of histological section for the ordinate and percentage across the cross-section for the abscissa (each data point represents 1% across). Boxes indicate the region used for quantification. Graphs represent the average of four samples within each group.

tested during the 42-day culture period, and the application of dynamic loading significantly increased E_Y and G^* compared to FS controls by day 42 (not shown). The 3 h daily exposure to IL-1α at 0.1 and 1 ng/mL, however, did not result in significant mechanical or biochemical differences from controls regardless of the dosage. At the highest concentration (10 ng/mL), IL-1α did result in significantly lower GAG and this was not counteracted by the application of dynamic loading.

4. Discussion

The findings of the current set of studies suggest that physiological loading is unable to counteract the long-term catabolic effects of IL-1 in chondrocyte-seeded agarose constructs. Under the conditions of this study, interleukin-induced tissue degradation was apparent from the decreased material and biochemical properties (but with no loss of cell viability) after tissue treatment irrespective of the application of loading. Conversely, the stimulatory effects of mechanical loading, in the absence of IL-1, were noted by the significantly increased stiffness of dynamically loaded constructs compared to FS constructs.

It was our goal to establish a controlled, long-term *in vitro* model that approximates both the chemical and mechanical environment within the joint. In Study 1, we attempted to establish a broad foundation for this model by examining the effect of dynamic deformational loading on constructs cultured in a CD medium formulation and exposed to one of the two cytokine conditions.

We adopted a dynamic deformational loading tissue culture protocol that we have demonstrated to foster development of functional tissue engineered (TE) cartilage (Lima et al., 2007). This protocol is based on the sequential application of growth factor (TGF-β3) followed by physiologic deformational loading (i.e. loading is introduced starting at day 14 in culture when TGF-β3 is discontinued). As such, we chose to introduce interleukin treatment coincident with applied loading, either during the 3 h-loading period (Study 3) or continuously in culture (Study 1 and 2).

Similarly, both IL-1α and IL-1β isoforms have been widely used as inducers of inflammation and degradation in experimental models of osteoarthritis (Smith et al., 1991; Pattoli et al., 2005). We found that IL-1α induced a stronger response than IL-1β in our bovine chondrocytes-seeded agarose constructs; however, the application of dynamic deformational loading did not ameliorate these catabolic effects over the long-term with either isoform.

Interestingly, the decrease in GAG content seemed greatest at the periphery of the dynamically loaded and interleukin (DL+IL-1α) group, indicating that dynamic loading may not only fail to protect against degenerative effects, but also increase the rate of matrix loss. There are a number of experimental parameters to consider that together will modulate the degree of cellular exposure to the inflammatory cytokine. These include the concentration of IL-1, the day in culture that IL-1 was first introduced, the total number of days of IL-1 treatment, and the amount of time per day of IL-1 treatment. The application of dynamic deformational loading may be yet another way to modulate the degree of cellular exposure to the cytokine.

Theoretical analysis of dynamic deformational loading of neutrally charged gels (such as agarose) predicts that loading can lead to enhanced transport of solutes such as growth factors and cytokines (Mauck et al., 2003a, b; Chahine et al., 2005). The transient concentration of these solutes within the gel during loading can even be enhanced to values many times above the surrounding bathing solution. Thus, although the application of dynamic deformational loading has clearly been shown to reduce the catabolic response of chondrocytes in the short term—reducing or abolishing IL-1β-induced release of NO and PGE_2 (Chowdhury et al., 2001, 2006), we speculated that long-term development may be inhibited by higher concentrations of the cytokine within the gel.

We indirectly examined this possibility in Studies 2 and 3 by modulating the dosage and exposure time of IL-1α. We anticipated that the application of dynamic deformational loading at lower concentrations would result in increased degradation of the dynamically loaded group over the FS group, as these DL constructs would be exposed to transitory spikes in the concentration of IL-1 above that of FS. This was not the case. In Study 2, modulating the concentration of IL-1 did not result in a gradient of mechanical and biochemical properties, but instead had an equal degradative effect at 0.1, 1, and 10 ng/mL and no effect at a 0.01 ng/mL concentration. Thus, exposure to the cytokine seemed to have an all or nothing effect once the cytokine dosage was above an activation threshold.

We were interested to see if there was evidence in the literature of an activation threshold beyond which further increases in IL-1 concentration would not lead to further

Please cite this article as: Lima, E.G., et al., Physiologic deformational loading does not counteract the catabolic effects of interleukin-1 in long-term culture of chondrocyte-seeded agarose constructs. Journal of Biomechanics (2008), doi:10.1016/j.jbiomech.2008.06.015

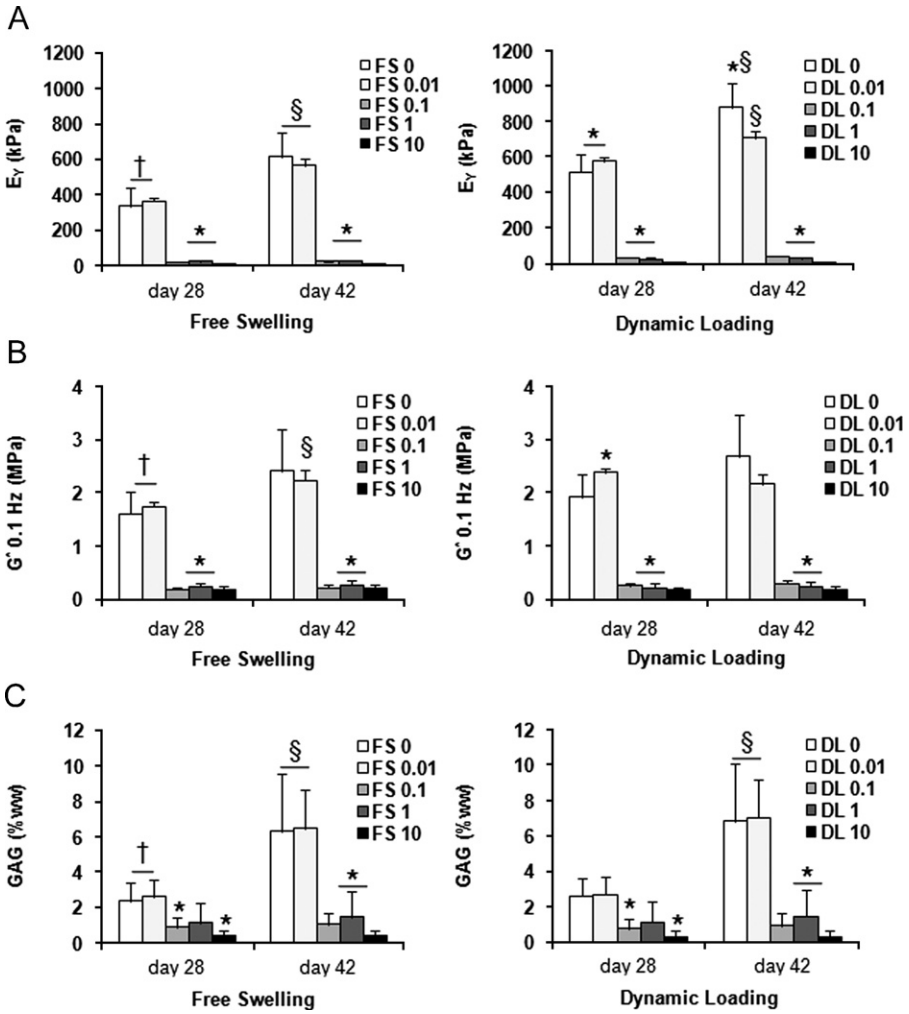

Fig. 4. (A) Equilibrium Young's modulus, (B) dynamic modulus at 0.1 Hz and (C) GAG (% wet weight) for constructs cultured first for 14 days in FS culture and then an additional 14 days in either FS or DL culture in CD medium. DL groups were additionally exposed to IL-1α in a logarithmic range of concentrations (0, 0.01, 0.1, 1, or 10 ng/mL). *$p<0.01$ for vs. FS 0 and FS 0.01 on same day. †$p<0.05$ for FS on day 28 vs. DL on day 42. §$p<0.05$ for day 42 groups vs. same groups on day 28.

degradative response. In a study by Kuroki et al. (2005), canine chondrocytes were cultured in agarose for 9 days in a serum-free medium with a gradient of IL-1α and IL-1β concentrations (20, 50 and 100 ng/mL). They found all concentrations were equally inhibitory as measured by RNA expression. Chowdhury et al. (2001, 2006) also examined the short-term IL-1β response in both bovine and human chondrocytes in agarose with a range (0.1–100 ng/mL) of concentrations. They found that nitrite and PGE_2 production by bovine chondrocytes increased in a step-like manner with increasing IL-1β concentrations, but that the human response increased rapidly at 0.1 ng/mL with no further significant increases at higher concentrations of cytokine. Thus, although the evidence in the literature is somewhat mixed, the results of the current investigation lead us to believe that transient increases in IL-1α concentration due to loading are not in themselves responsible for further cell-mediated catabolic degradation.

The transient concentration of cytokine may also be critical in interpreting the results of Study 3, where IL-1α was included for 3 h/day. In this study there was little or no effect of the cytokine regardless of the bathing concentration. Since the solutes take time to diffuse through the scaffold, it is likely that the actual cellular exposure to IL-1α was at a significantly lower concentration than the bathing medium due to the relatively short treatment duration (3 h). This limited concentration and transient exposure to the cytokine could account for the lack of cytokine-induced tissue degradation. In an arthritic patient, exposure to pro-inflammatory IL-1α within the joint is likely to be of a near constant duration (as in Study 2) rather than transitory in nature (as in Study 3) and at an average concentration of 0.17 ng/mL (Marks and Donaldson, 2005; Pattoli et al., 2005).

It is important to note that results of the current experiments differ from those in the literature that have reported protective effects of applied loading on IL-1-treated chondrocyte constructs (Chowdhury et al., 2001). In these earlier studies, experiments were performed on agarose-encapsulated chondrocytes before significant matrix was elaborated and for short culture durations, whereas our study examined cultures grown as long as 42 days with concomitant matrix elaboration and a much longer duration of interleukin exposure. Differences in matrix composition between engineered constructs can lead to disparities in the manner in which IL-1, physical stimuli, or the combination of both is presented to chondrocytes. At early time points in culture, chondrocyte deformation is similar to that which is applied to the agarose matrix, but in as little as 6 days cells can elaborate a pericellular matrix that is stiffer than the surrounding hydrogel matrix, shielding the chondrocytes from full deformation (Lee and Bader, 1995). At later culture times, coalescence of an elaborated matrix re-establishes loading-induced cell deformation in the culture system (Guilak et al., 1995; Chahine et al., 2007). The results of the current study suggest the application of dynamic

Please cite this article as: Lima, E.G., et al., Physiologic deformational loading does not counteract the catabolic effects of interleukin-1 in long-term culture of chondrocyte-seeded agarose constructs. Journal of Biomechanics (2008), doi:10.1016/j.jbiomech.2008.06.015

deformational loading is insufficient to protect against degradation over the long term.

A greater understanding of the potential interplay between mechanical stimuli and cytokines may help to elucidate mechanisms that underlie cartilage degeneration in OA, including the effects of load, pro-inflammatory cytokines, and their combination on both intact articular cartilage and on developing engineered tissue. The findings of this study reject the hypothesis that physiologic loading counteracts the catabolic effects of IL-1 in chondrocyte-seeded agarose constructs.

Conflict of interest statement

There were no financial and personal relationships that could have inappropriately influenced the work presented herein.

Acknowledgment

The research presented in this manuscript was funded in part by the National Institutes of Health grants: AR46568 and AR53530.

References

Agarwal, S., Long, P., Gassner, R., Piesco, N.P., Buckley, M.J., 2001. Cyclic tensile strain suppresses catabolic effects of interleukin-1beta in fibrochondrocytes from the temporomandibular joint. Arthritis and Rheumatism 44 (3), 608–617.

Buschmann, M.D., Gluzband, Y.A., Grodzinsky, A.J., Kimura, J.H., Hunziker, E.B., 1992. Chondrocytes in agarose culture synthesize a mechanically functional extracellular matrix. Journal of Orthopaedic Research 10 (6), 745–758.

Buschmann, M.D., Gluzband, Y.A., Grodzinsky, A.J., Hunziker, E.B., 1995. Mechanical compression modulates matrix biosynthesis in chondrocyte/agarose culture. Journal of Cell Science 108 (Pt 4), 1497–1508.

Capito, R.M., Spector, M., 2003. Scaffold-based articular cartilage repair. IEEE Engineering in Medicine and Biology Magazine 22 (5), 42–50.

Chahine, N.O., Lima, E.G., Wei, V., Hung, C.T., Ateshian, G.A., 2005. Dynamic Deformational Loading Significantly Enhances the Transport of Dextran Molecules into Agarose Hydrogels. ORS, Washington, DC.

Chahine, N.O., Hung, C.T., Ateshian, G.A., 2007. In-situ measurements of chondrocyte deformation under transient loading. European Cells and Materials 13, 100–111 (discussion 111).

Chowdhury, T.T., Bader, D.L., Lee, D.A., 2001. Dynamic compression inhibits the synthesis of nitric oxide and PGE(2) by IL-1beta-stimulated chondrocytes cultured in agarose constructs. Biochemical and Biophysical Research Communications 285 (5), 1168–1174.

Chowdhury, T.T., Bader, D.L., Lee, D.A., 2003. Dynamic compression counteracts IL-1 beta-induced release of nitric oxide and PGE2 by superficial zone chondrocytes cultured in agarose constructs. Osteoarthritis Cartilage 11 (9), 688–696.

Chowdhury, T.T., Bader, D.L., Lee, D.A., 2006. Dynamic compression counteracts IL-1beta induced iNOS and COX-2 activity by human chondrocytes cultured in agarose constructs. Biorheology 43 (3–4), 413–429.

Cima, L.G., Vacanti, J.P., Vacanti, C., Ingber, D., Mooney, D., Langer, R., 1991. Tissue engineering by cell transplantation using degradable polymer substrates. Journal of Biomechanical Engineering 113 (2), 143–151.

Cook, J.L., Anderson, C.C., Kreeger, J.M., Tomlinson, J.L., 2000. Effects of human recombinant interleukin-1beta on canine articular chondrocytes in three-dimensional culture. American Journal of Veterinary Research 61 (7), 766–770.

Farndale, R.W., Sayers, C.A., Barrett, A.J., 1982. A direct spectrophotometric microassay for sulfated glycosaminoglycans in cartilage cultures. Connective Tissue Research 9 (4), 247–248.

Gassner, R., Buckley, M.J., Georgescu, H., Studer, R., Stefanovich-Racic, M., Piesco, N.P., Evans, C.H., Agarwal, S., 1999. Cyclic tensile stress exerts anti-inflammatory actions on chondrocytes by inhibiting inducible nitric oxide synthase. Journal of Immunology 163 (4), 2187–2192.

Giannoni, P., Cancedda, R., 2006. Articular chondrocyte culturing for cell-based cartilage repair: Needs and perspectives. Cells Tissues Organs 184 (1), 1–15.

Giannoudis, P.V., Pountos, I., 2005. Tissue regeneration. The past, the present and the future. Injury 36 (Suppl 4), S2–S5.

Guilak, F., Ratcliffe, A., Mow, V.C., 1995. Chondrocyte deformation and local tissue strain in articular cartilage: A confocal microscopy study. Journal of Orthopaedic Research 13 (3), 410–421.

Habibovic, P., Woodfield, T., de Groot, K., van Blitterswijk, C., 2006. Predictive value of in vitro and in vivo assays in bone and cartilage repair—what do they really tell us about the clinical performance? Advances in Experimental Medicine and Biology 585, 327–360.

Hangody, L., Modis, L., 2006. Surgical treatment options for weight bearing articular surface defect. Orvosi Hetilap 147 (46), 2203–2212.

Honda, K., Ohno, S., Tanimoto, K., Ijuin, C., Tanaka, N., Doi, T., Kato, Y., Tanne, K., 2000. The effects of high magnitude cyclic tensile load on cartilage matrix metabolism in cultured chondrocytes. European Journal of Cell Biology 79 (9), 601–609.

Hung, C.T., Mauck, R.L., Wang, C.C., Lima, E.G., Ateshian, G.A., 2004. A paradigm for functional tissue engineering of articular cartilage via applied physiologic deformational loading. Annals of Biomedical Engineering 32 (1), 35–49.

Kelly, T.A., Ng, K.W., Wang, C.C., Ateshian, G.A., Hung, C.T., 2005. Spatial and temporal development of chondrocyte-seeded agarose constructs in free-swelling and dynamically loaded cultures. Journal of Biomechanics 39, 1489–1497.

Kuroki, K., Stoker, A.M., Cook, J.L., 2005. Effects of pro-inflammatory cytokines on canine articular chondrocytes in a three-dimensional culture. American Journal of Veterinary Research 66 (7), 1187–1196.

Lee, D.A., Bader, D.L., 1995. The development and characterization of an in vitro system to study strain-induced cell deformation in isolated chondrocytes. In Vitro Cellular Developmental Biology. Animal 31 (11), 828–835.

Li, K.W., Wang, A.S., Sah, R.L., 2003. Microenvironment regulation of extracellular signal-regulated kinase activity in chondrocytes: effects of culture configuration, interleukin-1, and compressive stress. Arthritis and Rheumatism 48 (3), 689–699.

Lima, E.G., Bian, L., Ng, K.W., Mauck, R.L., Byers, B.A., Tuan, R.S., Ateshian, G.A., Hung, C.T., 2007. The beneficial effect of delayed compressive loading on tissue-engineered cartilage constructs cultured with tgf-β3. Osteoarthritis Cartilage 15 (9), 1025–1033.

Lima, E.G., Tan, A.R., Tai, T., Bian, L., Stoker, A.M., Ateshian, G.A., Cook, J.L., Hung, C.T., 2008. Differences in interleukin-1 response between engineered and native cartilage. Tissue Engineering (ISSN:1937-3341).

Lin, W., Shuster, S., Maibach, H.I., Stern, R., 1997. Patterns of hyaluronan staining are modified by fixation techniques. Journal of Histochemistry and Cytochemistry 45 (8), 1157–1163.

Lotz, M., 2001. Cytokines in cartilage injury and repair. Clinical Orthopaedics and Related Research 391 (Suppl), S108–S115.

Marks, P.H., Donaldson, M.L., 2005. Inflammatory cytokine profiles associated with chondral damage in the anterior cruciate ligament-deficient knee. Arthroscopy 21 (11), 1342–1347.

Mauck, R.L., Soltz, M.A., Wang, C.C., Wong, D.D., Chao, P.H., Valhmu, W.B., Hung, C.T., Ateshian, G.A., 2000. Functional tissue engineering of articular cartilage through dynamic loading of chondrocyte-seeded agarose gels. Journal of Biomechanical Engineering 122 (3), 252–260.

Mauck, R.L., Hung, C.T., Ateshian, G.A., 2003a. Modeling of neutral solute transport in a dynamically loaded porous permeable gel: implications for articular cartilage biosynthesis and tissue engineering. Journal of Biomechanical Engineering 125 (5), 602–614.

Mauck, R.L., Nicoll, S.B., Seyhan, S.L., Ateshian, G.A., Hung, C.T., 2003b. Synergistic action of growth factors and dynamic loading for articular cartilage tissue engineering. Tissue Engineering 9 (4), 597–611.

Morales, T.I., Hascall, V.C., 1989. Effects of interleukin-1 and lipopolysaccharides on protein and carbohydrate metabolism in bovine articular cartilage organ cultures. Connective Tissue Research 19 (2–4), 255–275.

Mouw, J.K., Case, N.D., Guldberg, R.E., Plaas, A.H., Levenston, M.E., 2005. Variations in matrix composition and gag fine structure among scaffolds for cartilage tissue engineering. Osteoarthritis Cartilage 13 (9), 828–836.

Pattoli, M.A., MacMaster, J.F., Gregor, K.R., Burke, J.R., 2005. Collagen and aggrecan degradation is blocked in interleukin-1-treated cartilage explants by an inhibitor of ikappab kinase through suppression of metalloproteinase expression. Journal of Pharmacology and Experimental Therapeutics 315 (1), 382–388.

Raghunath, J., Rollo, J., Sales, K.M., Butler, P.E., Seifalian, A.M., 2007. Biomaterials and scaffold design: key to tissue-engineering cartilage. Biotechnology and Applied Biochemistry 46, 73–84.

Ratcliffe, A., Tyler, J.A., Hardingham, T.E., 1986. Articular cartilage cultured with interleukin 1. Increased release of link protein, hyaluronate-binding region and other proteoglycan fragments. Biochemical Journal 238 (2), 571–580.

Rotter, N., Ung, F., Roy, A.K., Vacanti, M., Eavey, R.D., Vacanti, C.A., Bonassar, L.J., 2005. Role for interleukin 1alpha in the inhibition of chondrogenesis in autologous implants using polyglycolic acid-polylactic acid scaffolds. Tissue Engineering 11 (1–2), 192–200.

Schiff, M.H., 2000. Role of interleukin 1 and interleukin 1 receptor antagonist in the mediation of rheumatoid arthritis. Annals of the Rheumatic Diseases 59 (Suppl 1), i103–i108.

Schulz, R.M., Bader, A., 2007. Cartilage tissue engineering and bioreactor systems for the cultivation and stimulation of chondrocytes. European Biophysics Journal 36 (4–5), 539–568.

Smeets, T.J., Barg, E.C., Kraan, M.C., Smith, M.D., Breedveld, F.C., Tak, P.P., 2003. Analysis of the cell infiltrate and expression of proinflammatory cytokines and matrix metalloproteinases in arthroscopic synovial biopsies: Comparison with synovial samples from patients with end stage, destructive rheumatoid arthritis. Annals of the Rheumatic Diseases 62 (7), 635–638.

Smith, R.J., Chin, J.E., Sam, L.M., Justen, J.M., 1991. Biologic effects of an interleukin-1 receptor antagonist protein on interleukin-1-stimulated cartilage erosion and chondrocyte responsiveness. Arthritis and Rheumatism 34 (1), 78–83.

Soltz, M.A., Ateshian, G.A., 1998. Experimental verification and theoretical prediction of cartilage interstitial fluid pressurization at an impermeable

contact interface in confined compression. Journal of Biomechanics 31 (10), 927–934.
Stegemann, H., Stalder, K., 1967. Determination of hydroxyproline. Clinica Chimica Acta 18 (2), 267–273.
Temple, M.M., Xue, Y., Chen, M.Q., Sah, R.L., 2006. Interleukin-1alpha induction of tensile weakening associated with collagen degradation in bovine articular cartilage. Arthritis and Rheumatism 54 (10), 3267–3276.
Towle, C.A., Hung, H.H., Bonassar, L.J., Treadwell, B.V., Mangham, D.C., 1997. Detection of interleukin-1 in the cartilage of patients with osteoarthritis: A possible autocrine/paracrine role in pathogenesis. Osteoarthritis Cartilage 5 (5), 293–300.
van den Berg, W.B., Bresnihan, B., 1999. Pathogenesis of joint damage in rheumatoid arthritis: Evidence of a dominant role for interleukin-i. Baillieres Best Practice and Research Clinical Rheumatology 13 (4), 577–597.
Xu, C., Oyajobi, B.O., Frazer, A., Kozaci, L.D., Russell, R.G., Hollander, A.P., 1996. Effects of growth factors and interleukin-1 alpha on proteoglycan and type ii collagen turnover in bovine nasal and articular chondrocyte pellet cultures. Endocrinology 137 (8), 3557–3565.
Xu, Z., Buckley, M.J., Evans, C.H., Agarwal, S., 2000. Cyclic tensile strain acts as an antagonist of IL-1 beta actions in chondrocytes. Journal of Immunology 165 (1), 453–460.

Please cite this article as: Lima, E.G., et al., Physiologic deformational loading does not counteract the catabolic effects of interleukin-1 in long-term culture of chondrocyte-seeded agarose constructs. Journal of Biomechanics (2008), doi:10.1016/j.jbiomech.2008.06.015

A.3 Genipin enhances the mechanical properties of tissue-engineered cartilage and protects against inflammatory degradation when used as a medium supplement

Eric G. Lima, Andrea R. Tan, Timon Tai, Kacey G. Marra, Alicia DeFail, Gerard A. Ateshian, Clark T. Hung

Genipin enhances the mechanical properties of tissue-engineered cartilage and protects against inflammatory degradation when used as a medium supplement

Eric G. Lima,[1,2] Andrea R. Tan,[1] Timon Tai,[1] Kacey G. Marra,[3,4] Alicia DeFail,[3,4] Gerard A. Ateshian,[1] Clark T. Hung[1]

[1]*Department of Biomedical Engineering, Columbia University, New York, New York*
[2]*Department of Mechanical Engineering, Cooper Union, New York, New York*
[3]*Department of Surgery, University of Pittsburgh, Pittsburgh, Pennsylvania*
[4]*Department of Bioengineering, University of Pittsburgh, Pittsburgh, Pennsylvania*

Received 23 April 2008; revised 18 July 2008; accepted 27 August 2008
Published online 24 November 2008 in Wiley InterScience (www.interscience.wiley.com). DOI: 10.1002/jbm.a.32305

Abstract: Genipin is a naturally-derived biocompatible cross-linking agent commonly used to generate three dimensional tissue-engineered scaffolds or to fix biologically derived scaffolds prior to implantation. Here we propose a novel use for genipin as a long-term culture medium supplement to promote cross-linking of *de novo* cell products that are produced in engineered cartilage. We hypothesize that the application of genipin will stabilize the extracellular matrix components and increase the mechanical properties of developing engineered cartilage. Chondrocytes encapsulated in agarose hydrogel (a neutrally charged polysaccharide scaffold that is unaffected by genipin cross-linking) were cultured in a chemically-defined growth medium that was supplemented with varying concentrations of genipin (22 μM, 220 μM, 2200 μM) for various durations (continuous or intermittent). Tissues developed significantly higher mechanical properties (+28% dynamic modulus and +20% Young's modulus) by day 42 with genipin treatment compared to untreated controls. These increases were not immediate, but presented over culture time after genipin treatment. The genipin treated groups were also more resistant to cytokine-induced degradation with interleukin-1α; maintaining an E_Y (+218%), G* (+390%) and glycosaminoglycan (GAG) content (+477%) over genipin-untreated constructs subjected to interleukin. We hypothesize two mechanisms through which the physical enhancement of tissue properties may be fostered: (1) by cross-link mediated reorganization and enhanced retention of cell-elaborated extracellular matrix components, and (2) through reduction of the loss of extracellular matrix components by increasing their resilience to catabolic degradation. These studies demonstrate a potential use of genipin as a medium supplement to develop enhanced engineered cartilage. © 2008 Wiley Periodicals, Inc. J Biomed Mater Res 91A: 692–700, 2009

Key words: cartilage tissue engineering; mechanical properties; cross-linking; ECM (extracellular matrix); cell culture

INTRODUCTION

Osteoarthritis (OA) is a common and painful disorder characterized by the degeneration of the articular surfaces of diarthrodial joints. One of the most promising approaches to treat OA is the design of engineered tissue that reproduces the functional properties of healthy cartilage. This tissue engineering approach typically entails the use of living cells embedded in a three-dimensional scaffold that is cultured over time in a growth medium supplemented with various physical or biological stimulants to encourage development.

Recently, our laboratory has been able to cultivate engineered cartilage with an equilibrium modulus (E_Y) and an glycosaminoglycan (GAG) content that match the native tissue, using the temporal application of growth factors over a 6-week culture period.[1] While these findings are encouraging, the dynamic modulus (G^*) and the collagen content for these con-

Correspondence to: C. T. Hung, Department of Biomedical Engineering, Columbia University, 351 Engineering Terrace, MC8904, 1210 Amsterdam Avenue, New York, NY 10027, USA; e-mail: cth6@columbia.edu

Contract grant sponsor: NIH; contract grant number: AR46568
Contract grant sponsor: Musculoskeletal Transplant Foundation; contract grant number: CU07-194

structs amount to less than a quarter of those of native articular cartilage. Of the two mechanical measurements, G^*, which is correlated with the collagen content, is considered to be more physiologically relevant as it measures the behavior of the tissue during the application of cyclic loads and better captures fluid pressurization within the biphasic tissue. No group has currently been able to reproduce native values of collagen regardless of the tissue engineering strategy employed. Obtaining native values of G^* and collagen therefore remains an important but elusive challenge.

Cross-linking agents such as glutaraldehyde, formaldehyde, or epoxy are typically used to chemically treat (or fix) devitalized xenografts and allografts to reduce the immune rejection or the enzymatic degradation that is typical of transplanted bioprostheses.[2,3] Typically, however, cross-linking agents are lethal to cells. The use of genipin, a naturally occurring cross-linker with toxicity levels 10,000-fold less than glutaraldehyde,[4] as a biocompatible and stable cross-linker has been established by other groups[5,6] and this provides a promising new avenue to explore for tissue engineering.

Genipin cross-linking works by forming intra- and intermolecular cross-links of the amino residues on tropocollagen or proteoglycan molecules. A modified cyclic form of genipin can reside stably within the extracellular network, adding bridges across adjacent fibers. As such, previous groups have explored the use of genipin as a onetime treatment to fix tissue prior to implantation,[7] for the assembly of tissue engineering scaffolds prior to cell seeding,[8,9] or to modulate the release of growth factors from degradable scaffolds or beads.[5] Genipin has also been studied for its anti-inflammatory effects, administered either directly to different cell lines[10,11] or orally to animals.[12,13] Moreover, genipin cross-linking has been shown to affect the mechanical properties of biological tissues, increasing the tensile strength of bovine pericardium,[14] porcine tendon,[15] and type I collagen gels.[16]

Our laboratory uses agarose hydrogel as a scaffold system for cartilage tissue engineering. This gel has been used extensively in chondrocyte biology studies and has shown some promise for tissue engineering applications. Agarose is a neutrally charged polysaccharide and as such is unaffected by genipin. However, the chondrocytes embedded in the gel elaborate an extracellular matrix over time in culture which exhibits amine groups that are subject to genipin cross-linking. In this set of studies, we propose a novel use for genipin: not as a scaffold cross-linker, but as a medium supplement to promote cross-linking of *de novo* cell products, as they are produced. We hypothesize that the application of genipin will stabilize the extracellular matrix components and increase the mechanical properties of developing cartilaginous tissue in our agarose hydrogels. We hypothesize two mechanisms through which the physical enhancement of tissue properties is fostered: (1) by reorganization and enhanced retention of cell synthesized extracellular matrix components, and (2) through reduction of the loss of extracellular matrix components by increasing their resilience to catabolic degradation.

MATERIALS AND METHODS

Both the concentration and duration of genipin were modulated as variables in the current set of studies. In a preliminary study, three concentrations of genipin were examined to establish cell toxicity. Based on these results the two most promising concentrations were selected for use in long-term culture. In study 1, genipin was applied to the culture medium continuously throughout the culture duration. In study 2, genipin was applied to the culture medium briefly (24 h) on selected days only. Finally, we examined one of our hypotheses for the mechanisms behind the accumulated benefits in study 3 by perturbing the system with the inflammatory cytokine interleukin-1α (IL-1α).

Cell isolation

Articular cartilage was harvested from bovine carpometacarpal joints of freshly slaughtered 1–3-month-old calves. Three to five joints were used for each study, and cells were pooled from all joints. Each study was repeated at least once with different cell isolations and the results were combined and averaged. The sample size stated before each study represents the combined number of samples for all repeated studies. The cartilage tissue was combined, weighed, and digested with type IV collagenase (Sigma Chemicals, St. Louis, MO) for 11 h at 37°C, with stirring in high-glucose Dulbecco's modified Eagle's medium (hgDMEM). Collagenase-supplemented medium mixture was added at 7.5 mL/g of tissue, with the collagenase concentration normalized to 390 activity units/mL. The resulting cell suspension was filtered through a 70-μm pore size mesh and sedimented in a bench-top centrifuge for 10 min at 1000*g*. Viable cells were counted using hemacytometer and trypan blue. One volume of chondrocyte suspension (at 60×10^6 cells/mL) was then mixed with an equal volume of 4% low-melt agarose (type VII; Sigma) at 37°C to yield a final cell concentration of 30×10^6 in 2% agarose. The chondrocyte/agarose mixture was cast into slabs and cored using a sterile disposable punch (Miltex, York, PA) to final dimensions of 0.4 cm diameter and 0.23 cm thickness (0.029 cm^3). Some bovine explants (used in the preliminary study) were also cored from the original undigested tissue and cut to the same dimensions (resulting in midzone cartilage only).

Chemically defined cell culture

Constructs were maintained in serum-free growth medium for up to 52 days (with variable genipin concentra-

tions and time courses as illustrated in Fig. 1). The serum-free growth medium for studies 1 and 2 consisted of hgDMEM supplemented with 1× PSF (100 units/mL penicillin, 100 μg/mL streptomycin, 0.25 μg/mL fungizone), 0.1 μ*M* dexamethasone, 50 μg/mL ascorbate 2-phosphate, 40 μg/mL L-proline, 100 μg/mL sodium pyruvate, and 1× ITS + premix (insulin, human transferrin, and selenous acid; Becton Dickinson, Franklin Lakes, NJ). The growth medium for study 3 was identical to the previous two studies with the exception that beginning on day 42 dexamethasone supplementation was discontinued (it is a known anti-inflammatory agent that interferes with IL-1α). For all studies, growth medium was changed every 3 days and supplemented additionally with 10 ng/mL TGF-β3 (R&D Systems, Minneapolis, MN) for the first 2 weeks of culture.

Genipin supplementation

In the preliminary study, cell-seeded agarose constructs, cell-free controls, and freshly harvested bovine explant cartilage were incubated in culture media supplemented with 0, 22, 220, 2200 μ*M* of sterile genipin (Sigma-Aldrich) for 7 days. Mechanical testing and cell viability (using the molecular probes live/dead viability/cytotoxicity kit) was carried out on days 0, 3, and 7. Based on these results, three additional studies were performed. In study 1, constructs were exposed to 0, 22, or 220 μ*M* genipin continuously throughout the 42-day culture period and tested on days 0, 14, and 42. In study 2, on days 13 and 41 a subset of the genipin-free controls were isolated and exposed to genipin for 24 h at the same concentrations as study 1. These constructs were tested immediately after 24 h of exposure (days 14 and 42) and also 7 days after exposure (days 21 and 49). In study 3, constructs were exposed to 22 μ*M* of genipin (the low range reported in the literature[14]) from days 42 to 49, after which genipin supplementation was discontinued and the cross-linked constructs were challenged with IL-1α (10 ng/mL) for 3 days (until day 52). For concentrations and time courses see Figure 1.

Material testing

Cylindrical constructs were tested for both their equilibrium Young's modulus (E_Y) and their dynamic modulus (G^*) in unconfined compression using a custom computer-controlled testing system.[17] To measure E_Y an initial 0.02*N* tare load was applied, followed by a compression to 10% strain, at a strain rate of 0.05%/s. E_Y was calculated from the equilibrium stress at 10% strain. Previous studies have shown E_Y to remain invariant across strain magnitudes ranging from 0 to 20% for cartilage explants. G^* was measured after achieving stress-relaxation equilibrium by superimposing a 2% peak to peak sinusoidal strain at 0.1 Hz.

Biochemical content

The biochemical content of each sample was assessed by first measuring the sample wet weight, lyophilizing overnight, and measuring dry weight. Gross water content was then determined from the difference. Once dried, the samples were digested in proteinase-K overnight at 56°C, as described previously.[18] Aliquots of the digest were analyzed for GAG content using the 1,9-dimethylmethylene blue dye-binding assay.[19,20] Additional aliquots were analyzed for DNA content using the PicoGreen assay. A further aliquot was acid hydrolyzed in 12*N* HCl at 110°C for 16 h, dried over NaOH, and resuspended in assay buffer (24 m*M* citric acid monohydrate, 0.012 v/v glacial acetic acid, 85 m*M* sodium acetate trihydrate, 85 m*M* sodium hydroxide, pH 6.0). Ortho-hydroxyproline (OHP) content was then determined via a colorimetric assay by reaction with chloramine T and dimethylaminobenzaldehyde,[21] scaled for microplates. OHP content was converted to total collagen content using the conversion of 1:10 ratio of OHP:Collagen. Each biochemical constituent (DNA, GAG, and collagen) was then normalized to the tissue wet weight to correct for differences in construct size.

Statistical analysis

Statistics were performed with the Statistica (Statsoft, Tulsa, OK) software package. Each data point represents the mean and standard deviation. Groups were examined for significant differences by analysis of variance ($\alpha = 0.05$), with E_Y, G^*, GAG, or OHP as the dependent variable. Tukey's Honest Significant Difference Test for unequal *n post hoc* tests were carried out with a statistical significance set at $p = 0.05$.

RESULTS

For the preliminary study, live/dead assays established that after 7 days of continuous supplementation there were no differences in cell mortality from the genipin-free control for both the 22 and 220 μ*M* genipin groups (>98% cells vital); however, there was complete cell death in the same period for the 2200 μ*M* group (Fig. 2). There were no differences in the mechanical properties (E_Y, G^*) of these tissue-engineered constructs at any concentration tested ($E_Y = 11 \pm 1$ kPa, G^* at 0.1 Hz = 0.07 ± 0.01 MPa). Likewise there were no changes in the mechanical properties or visual appearance of the cell-free agarose scaffolds.

Explant cartilage treated with genipin became dark purple over a 24-h period, but just as in the case of tissue-engineered constructs, the mechanical properties of genipin-treated explants were found to be identical to untreated controls ($E_Y = 1011 \pm 97$ kPa, G^* at 0.1 Hz = 13 ± 1.3 MPa). From these results, only the 22 and 220 μ*M* concentrations were deemed suitable for long-term culture and the highest concentration (2200 μ*M*) was eliminated.

In study 1, live/dead assays carried out after 42 days of continuous incubation in genipin confirmed no change in cell viability compared with

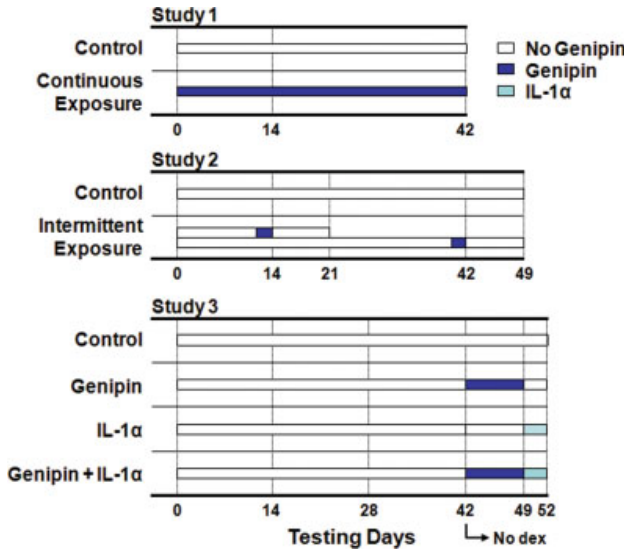

Figure 1. Schematic of genipin exposure over culture period. Control groups were not exposed to genipin. Study 1: Constructs were exposed to genipin continuously (continuous exposure) in the culture medium. Study 2: Constructs were exposed to genipin for 24 h only (brief exposure) and tested 1 and 7 days later. Study 3: On day 42, dexamethasone was removed from the culture medium and constructs were exposed to genipin continuously for 1 week prior to a 3-day interleukin-1α (IL-1α) challenge. [Color figure can be viewed in the online issue, which is available at www.interscience.wiley.com.]

untreated controls using these concentrations (data not shown). The mechanical properties and the physical appearance of the constructs treated with genipin were significantly different from controls. Engineered constructs turned purple with the addition of genipin, with higher concentrations of genipin yielding greater intensities of purple (Fig. 3). This change in color is characteristic of genipin as it spontaneously reacts with the amine groups and indicates cross-linking. In study 2, BE groups (constructs were removed from genipin 24 h after exposure and cultured in genipin-free growth medium) visually maintained the intensity of color for the 7 days tested (data not shown). Genipin-supplemented culture medium also turned purple, even when there were no constructs present, suggesting that constituents within the aqueous formulation were being cross-linked.

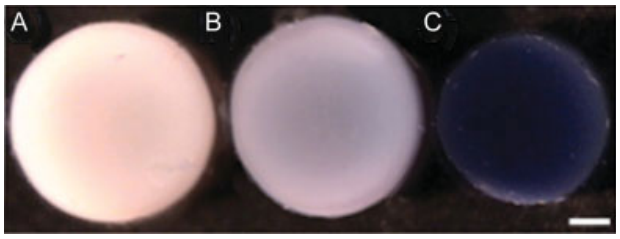

Figure 3. Gross morphology of tissue engineered cylindrical constructs on day 42 after continuous incubation in genipin-supplemented media at three concentrations: (A) 0 μ*M*, (B) 22 μ*M*, and (C) 220 μ*M*. The tissue volume at the lower concentrations has increased by 20–30% compared with the 220 μ*M* concentration which remained at the original volume. Scale bar = 1 mm. [Color figure can be viewed in the online issue, which is available at www.interscience.wiley.com.]

By day 42 in culture the mechanical properties of the continuous exposure (CE) groups were as follows: both CE controls (E_Y = 788 ± 63 kPa, G^* = 2.5 ± 0.5 MPa) and CE 22 μM (E_Y = 873 ± 92 kPa, G^* = 3.2 ± 0.2 MPa) developed significantly higher mechanical properties over time in culture (study 1, Fig. 4). The G^*, in particular, was significantly higher for the CE 22 μ*M* group than the control group, but the CE 220 μ*M* group, in contrast, remained at day 0 mechanical properties (E_Y = 23 ± 22 kPa, G^* = 0.3 ± 0.03 MPa). Cell viability assays of this group indicated the cells remained alive while PicoGreen assays indicated no differences in cell proliferation over other groups. GAG and collagen levels increased significantly over time in culture for all groups; however, total GAG values for the CE 220 μ*M* group was significantly less than the CE 22 μ*M* and control groups.

For brief exposure (BE) groups (24-h duration, study 2), there were no significant differences in mechanical properties from controls immediately after 24-h incubation (day 42: BE 22 μ*M*: E_Y = 790 ± 60 kPa, G^* = 2.7 ± 0.2 MPa; BE 220 μ*M*: E_Y = 739 ± 69 kPa, G^* = 2.6 ± 0.3 MPa); however, after 7 days of culture without genipin these groups developed significantly higher mechanical properties compared with

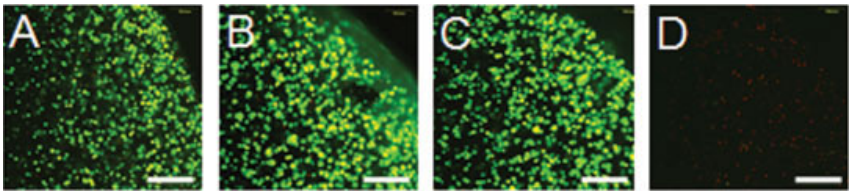

Figure 2. Cell viability staining after 7-day continuous incubation in genipin-supplemented media at four genipin concentrations: (A) 0 μ*M*, (B) 22 μ*M*, (C) 220 μ*M*, and (D) 2200 μ*M*. Bright green indicates living cells. Dim red indicates dead cells. Scale bar = 250 μm. [Color figure can be viewed in the online issue, which is available at www.interscience.wiley.com.]

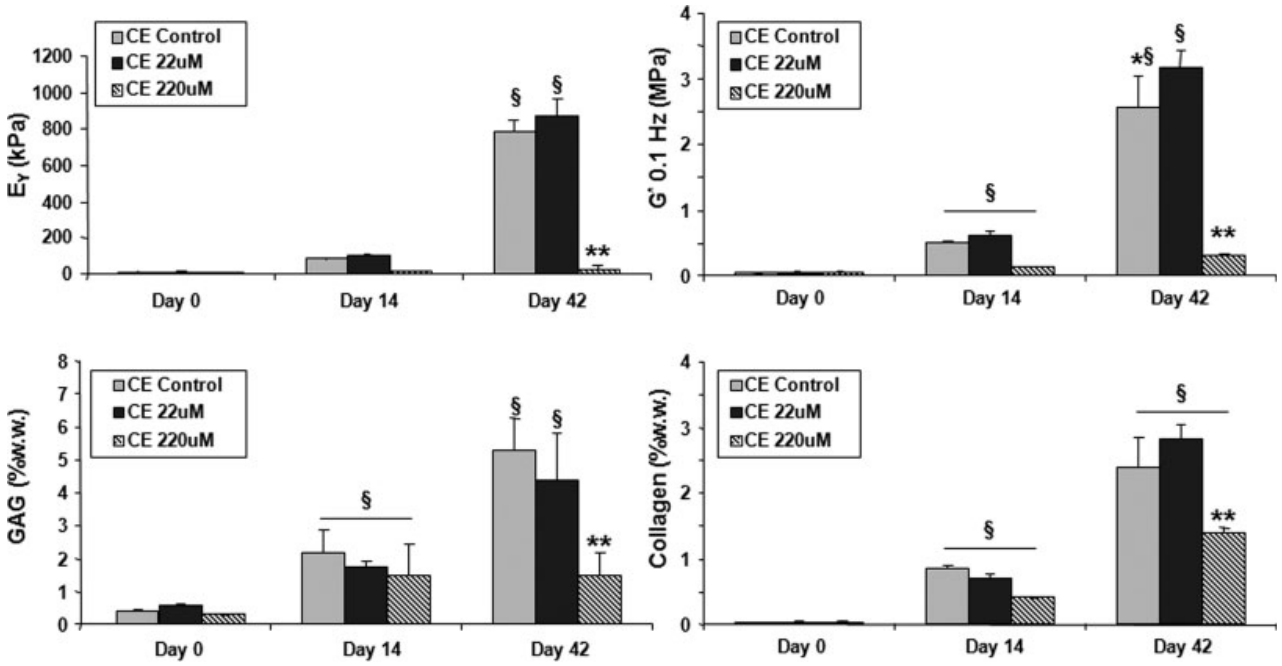

Figure 4. Equilibrium Young's modulus (E_Y), dynamic modulus at 0.1 Hz (G^*), GAG (%ww), and collagen (%ww) of constructs incubated in genipin continuously throughout the culture period. CE, continuous exposure. $^*p < 0.05$ for control versus genipin groups. $^{\S}p < 0.05$ against all groups in the previous time points. $^{**}p < 0.05$ for 220 μM versus other day 42 groups.

controls (day 49: BE Control: $E_Y = 1068 \pm 123$ kPa, $G^* = 3.4 \pm 0.43$ MPa; BE 22 μM: $E_Y = 1279 \pm 214$ kPa, $G^* = 4.02 \pm 0.9$ MPa; BE 220 μM: $E_Y = 1200 \pm 128$ kPa, $G^* = 3.5 \pm 0.5$ MPa). There were no differences in GAG and collagen between the day 42 and day 49 groups (Fig. 5).

Since the culture medium itself changed colors when exposed to genipin it is possible that genipin cross-links constituents within the culture medium and diluted the dose that was delivered to the constructs. To account for this possibility, a separate study (not shown) was carried out in which constructs were bathed briefly (1–3 h) in genipin-supplemented phosphate-buffered saline (PBS) and subsequently returned to genipin-free culture medium. The results using this protocol were consistent with those observed in study 2 with direct medium supplementation for 24 h.

In study 3, constructs treated with IL-1α (and not genipin) dropped significantly in E_Y (−69%), G^* (−86%), and GAG (−81%), but not collagen (Fig. 6). The genipin + IL-1α group also developed significantly lower E_Y (−33%), G^* (−44%), but interestingly GAG values did not measurably change compared with controls. Collagen values, similarly, did not change significantly. When compared with the IL-1α group, the genipin + IL-1α group maintained significantly higher E_Y (+218%), G^* (+390%), and GAG (+477%). Figure 6 presents these values normalized to controls for comparison; the actual values obtained on day 52 were as follows: Control: $E_Y = 640 \pm 88$ kPa, $G^* = 2.90 \pm 0.35$ MPa, GAG = 6.6% ± 0.2% (ww), Col = 2.33% ± 0.2% (ww); Genipin-treated control: $E_Y = 731 \pm 134$ kPa, $G^* = 2.74 \pm 0.41$ MPa, GAG = 6.8% ± 0.3% (ww), Col = 2.3% ± 0.3% (ww); IL-1α treated: $E_Y = 197 \pm 10$ kPa, $G^* = 0.34 \pm 0.01$ MPa, GAG = 1.3% ± 0.5% (ww), Col = 3.1% ± 0.5% (ww); and genipin + IL-1α treated: $E_Y = 431 \pm 47$ kPa, $G^* = 1.34 \pm 0.07$ MPa, GAG = 6.1% ± 0.8% (ww), Col = 3.8% ± 0.4% (ww).

DISCUSSION

The hypothesis governing this set of studies was that genipin would cross-link the extracellular matrix within the developing engineered constructs as the extracellular matrix proteins are produced and would thereby increase the mechanical properties of the constructs over time. The fundamental premise of the hypothesis was supported: there were increases in mechanical properties without significant changes in cell viability or biochemical quantities of GAG or collagen, suggesting a genipin-induced enhancement of tissue stiffness.

There is no established concentration for the use of genipin; therefore in the current set of studies we used values that span both the low (22 μM[14]) and high (2000 μM[16]) range reported in the literature.

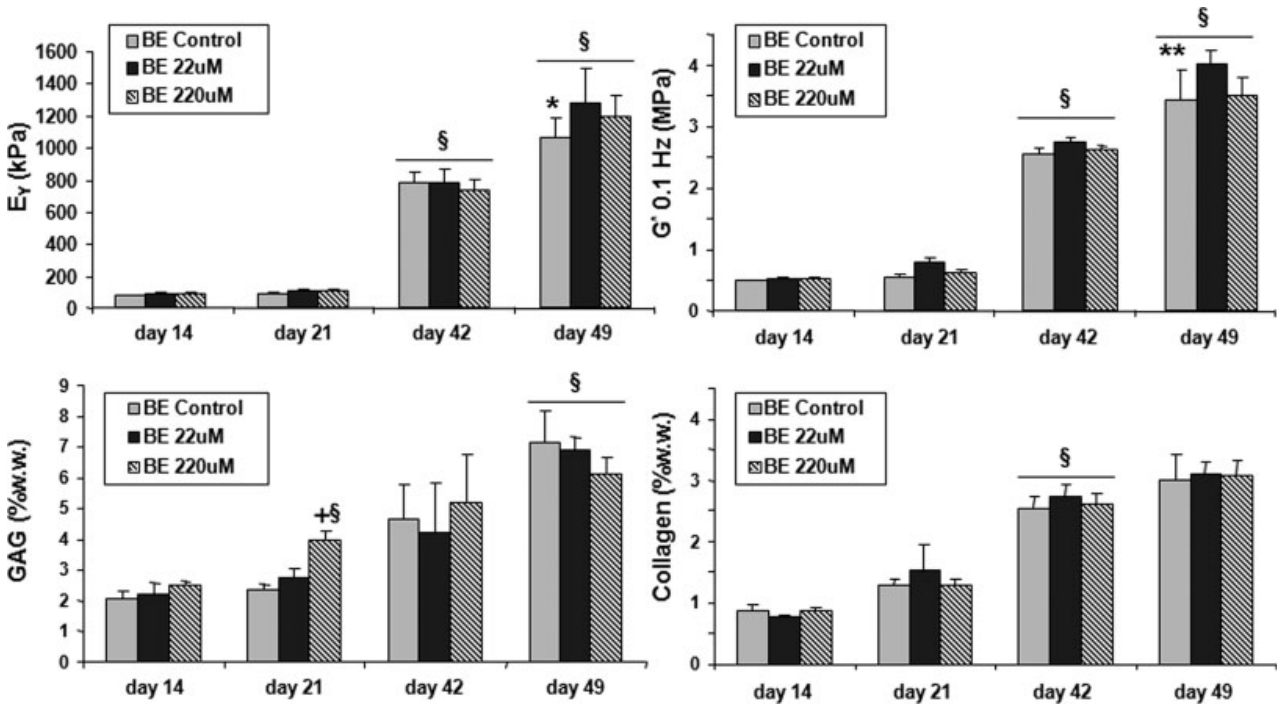

Figure 5. Equilibrium Young's modulus (E_Y), dynamic modulus at 0.1 Hz (G^*), GAG (%ww), and collagen (%ww) of constructs incubated for 24 h in genipin (on days 13 and 41). A subset of untreated control was used at each treatment point. BE, brief exposure. $^{\S}p < 0.05$ against all groups in the previous time points. $^{*}p < 0.05$ for control versus genipin groups. $^{**}p < 0.05$ for control versus 22 μM group. $^{+}p < 0.05$ for BE 220 μM versus other day 21 groups.

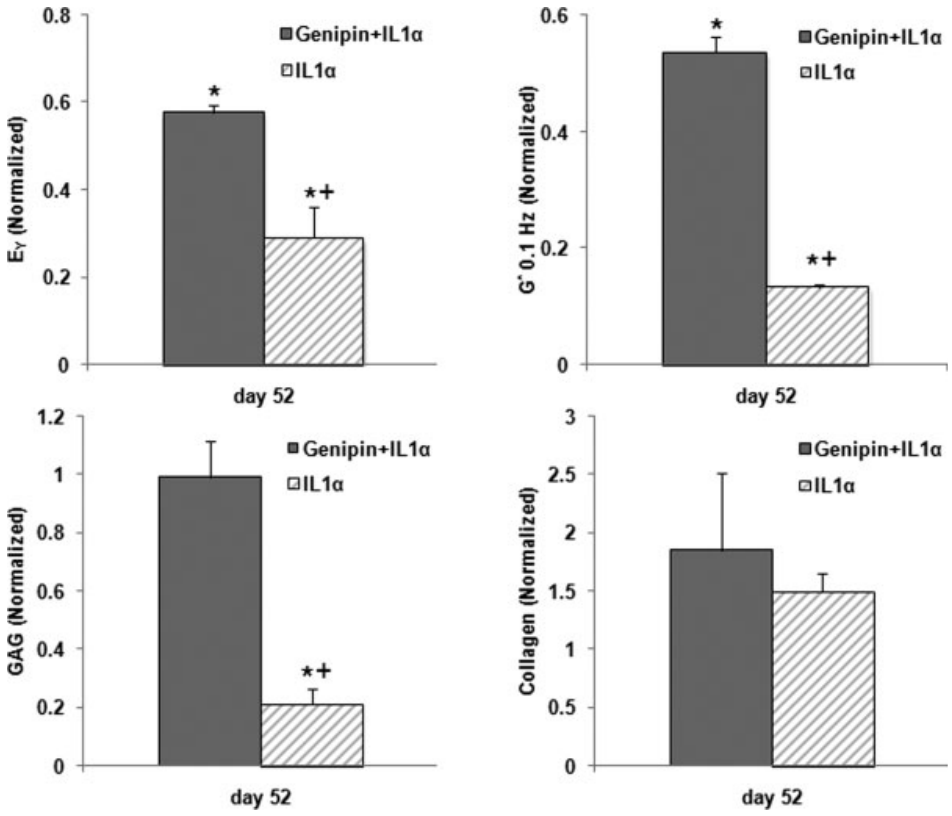

Figure 6. Equilibrium Young's modulus (E_Y), dynamic modulus at 0.1 Hz (G^*), GAG (%ww), and collagen (%ww) of constructs challenged with IL-1α for 3 days. Values are normalized to day 49 controls. $^{*}p < 0.05$ against either control group. $^{+}p < 0.05$ for Genipin + IL-1α versus IL-1α group.

Additionally, we adopted two durations for medium supplementation—continuous and intermittent supplementation of genipin. The toxicity of genipin when supplemented directly to the culture medium was found to be dependent on both dose and duration of exposure. Long-term CE (study 1) was lethal at 2200 μ*M*, detrimental (but not lethal) at 220 μ*M*, and beneficial at 22 μ*M*. Short-term exposure (study 2) at 220 and 22 μ*M* on the other hand was sufficient to obtain the benefits on the tissue level without the detrimental effects on the cellular level.

In both long-term and short-term exposure protocols we observed similar increases in mechanical properties over time in culture, but in both cases these benefits did not occur until later time points. This suggests that the tissue must reach some degree of extracellular maturity prior to genipin treatment. It also suggests that prolonged medium supplementation is probably unnecessary, but that BE, in growth medium or in PBS, followed by continuing cultivation may be the best method to realize the benefits of biocompatible cross-linking.

It is notable that genipin-induced changes did not occur immediately but took several days to manifest (Fig. 5). Initially we believed this was due to the nature of the agarose hydrogel scaffold. However, we found that there were similarly no immediate changes to native cartilage explant mechanical properties when exposed to the same concentrations of genipin. Together these observations indicate that the increased stiffness of the constructs is not due directly to physical strengthening of the extracellular network via genipin cross-links, but it is attributable to other mechanisms that lead to a cumulative increase of tissue properties over time.

One possibility is that genipin directly affected cell metabolism in addition to cross-linking the extracellular matrix. There have been no studies reported on the effect of genipin on chondrocytes specifically, but there is evidence that genipin suppresses cell proliferation and alters RNA activity in subconjunctival fibroblast[10] and some epithelial cell lines.[11] There was no decrease in cell proliferation in the current set of studies as confirmed by PicoGreen DNA quantification (not shown). Likewise, there were no significant differences in matrix accumulation of GAG or collagen over time. Additionally, we examined the effect of genipin on chondrocytes cultured on tissue culture plates and found no significant differences on cell proliferation and cell morphology after 14 days of CE at 22 μ*M* (results not shown); therefore, we do not believe that alterations in cell metabolism were the main cause for the increased mechanical properties observed.

Instead, we speculate that the presence of cross-links may have modulated the nature of subsequent matrix deposition by the chondrocytes, either by leading to a more consistent fiber alignment for genipin-treated constructs relative to untreated controls, or by reducing the catabolic loss of matrix components as suggested by study 3.

Chondrocytes in culture balance catabolic and anabolic activities to remodel their surrounding extracellular matrix. By challenging the chondrocytes with IL-1α (study 3) we artificially amplified the catabolic process. Cross-linking has been shown to increase resistance to enzymatic degradation through collagenase digestion.[2,4,22,23] We have previously observed that in our culture system IL-1α triggers a rapid loss in GAG content, along with higher matrix metalloproteinase-3 levels, but with no significant changes in collagen content within the first 14 days of treatment.[24,25] Here we observed that indeed the extracellular matrix degraded less after pretreatment with genipin, demonstrating an increased resilience to degradation through cell-mediated processes. Genipin cross-linking may have led to mechanical benefits over time by increasing the chemical resistance of a variety of extracellular matrix components, such as GAG, to catabolism associated with normal matrix remodeling. Interestingly, although the mechanical properties of these genipin treated tissues dropped with exposure to IL-1α, their GAG values remained unchanged. This suggests that some other, as of yet unmeasured matrix constituent was affected by the cytokine and responsible for the decreased construct stiffness. Alternatively, as we have not analyzed the size of GAGs that are retained in genipin-treated constructs subjected to interleukin (and compared to control) we could speculate that GAGs were indeed broken down and their interrelationship with the collagen network disrupted, leading to the observed significant decrease in functional material properties. In this scenario, GAG and collagen content may not have changed because the genipin cross-links entrapped the degradative products within the construct rather than permit them to diffuse into the culture medium.

As a corollary to study 3, genipin treatments, as described in this article, may be useful to reduce the inflammatory response of the engineered tissue upon implantation. Implanting allogenic tissue in the body generally invokes an immune reaction except for certain immunologically privileged area[26] such as the eye and the brain. Allogenic chondrocytes are considered to be to some degree immunoprivileged,[27,28] because they reside within a dense extracellular matrix that is not vascularized and, therefore, has less interaction with blood born leukocytes. Even so, the presence of extracellular matrix constituents, such as collagen, can themselves invoke an immune reaction[29] and can lead to the rejection and degradation of the allograft within the joint.[30,31] The immunologic reactivity and susceptibility of grafts

appear to be inversely related to the amount and maturity of cartilage-specific extracellular matrix present.[32] Reducing the number of free amino residues in the collagen through various cross-linking methods, such as genipin, has been shown to reduce the antigenicity of the resulting tissue.[33,34]

Inflammatory cytokines, such as interleukin-1α, are often present in the joint, either as preexisting chronic condition or as a result of the surgical intervention itself.[35–38] Previously we have shown that engineered cartilage can be more susceptible to degradation by these cytokines than mature endogenous cartilage.[24] In those studies, engineered tissue that was exposed temporarily to IL-1α stopped growing, catabolically degraded the surrounding extracellular matrix, and did not recover. In study 3 genipin modification of the tissue resulted in increased resistance to IL-1α degradation. This result suggests a mechanism by which the tissue developed higher mechanical properties over time and that it might provide a means to protect the tissue from transient insults of inflammatory cytokines during or after surgery.

In summary, genipin supplementation of the culture medium as described here led to significant increases over control in both the dynamic (+28%) and Young's (+20%) modulus. This demonstrates the potential for long-term gains in mechanical properties using biocompatible cross-linking agents as direct medium supplements. However, considering that the magnitude of the findings were relatively incremental in the context of the dynamic modulus value for native articular cartilage (4 MPa vs. 20–40 MPa for explants[25]) the most clinically relevant finding may be the potential reduction in antigenicity and the increased resistance to enzymatic degradation with genipin treatment. This approach warrants further investigation toward optimizing effects of genipin on engineered constructs used *in vivo*.

References

1. Lima EG, Bian L, Ng KW, Mauck RL, Byers BA, Tuan RS, Ateshian GA, Hung CT. The beneficial effect of delayed compressive loading on tissue-engineered cartilage constructs cultured with TGF-beta3. Osteoarthritis Cartilage 2007;15:1025–1033.
2. Sung HW, Huang RN, Huang LL, Tsai CC, Chiu CT. Feasibility study of a natural crosslinking reagent for biological tissue fixation. J Biomed Mater Res 1998;42:560–567.
3. Liang HC, Chang Y, Hsu CK, Lee MH, Sung HW. Effects of crosslinking degree of an acellular biological tissue on its tissue regeneration pattern. Biomaterials 2004;25:3541–3552.
4. Sung HW, Chang WH, Ma CY, Lee MH. Crosslinking of biological tissues using genipin and/or carbodiimide. J Biomed Mater Res A 2003;64:427–438.
5. Ferretti M, Marra KG, Kobayashi K, Defail AJ, Chu CR. Controlled in vivo degradation of genipin crosslinked polyethylene glycol hydrogels within osteochondral defects. Tissue Eng 2006;12:2657–2663.
6. Huang LL, Sung HW, Tsai CC, Huang DM. Biocompatibility study of a biological tissue fixed with a naturally occurring crosslinking reagent. J Biomed Mater Res 1998;42:568–576.
7. Englert C, Blunk T, Muller R, von Glasser SS, Baumer J, Fierlbeck J, Heid IM, Nerlich M, Hammer J. Bonding of articular cartilage using a combination of biochemical degradation and surface cross-linking. Arthritis Res Ther 2007;9:R47.
8. Kuo YC, Ku IN. Effects of gel concentration, human fibronectin, and cation supplement on the tissue-engineered cartilage. Biotechnol Prog 2007;23:238–245.
9. Moffat KL, Marra KG. Biodegradable poly(ethylene glycol) hydrogels crosslinked with genipin for tissue engineering applications. J Biomed Mater Res B Appl Biomater 2004;71:181–187.
10. Kitano A, Saika S, Yamanaka O, Ikeda K, Reinach PS, Nakajima Y, Okada Y, Shirai K, Ohnishi Y. Genipin suppresses subconjunctival fibroblast migration, proliferation and myofibroblast transdifferentiation. Ophthalmic Res 2006;38:355–360.
11. Kitano A, Saika S, Yamanaka O, Reinach PS, Ikeda K, Okada Y, Shirai K, Ohnishi Y. Genipin suppression of fibrogenic behaviors of the α-TN4 lens epithelial cell line. J Cataract Refract Surg 2006;32:1727–1735.
12. Koo HJ, Song YS, Kim HJ, Lee YH, Hong SM, Kim SJ, Kim BC, Jin C, Lim CJ, Park EH. Antiinflammatory effects of genipin, an active principle of gardenia. Eur J Pharmacol 2004;495:201–208.
13. Koo HJ, Lim KH, Jung HJ, Park EH. Anti-inflammatory evaluation of gardenia extract, geniposide and genipin. J Ethnopharmacol 2006;103:496–500.
14. Sung HW, Chang Y, Chiu CT, Chen CN, Liang HC. Crosslinking characteristics and mechanical properties of a bovine pericardium fixed with a naturally occurring crosslinking agent. J Biomed Mater Res 1999;47:116–126.
15. Sung HW, Hsu CS, Lee YS, Lin DS. Crosslinking characteristics of an epoxy-fixed porcine tendon: Effects of pH, temperature, and fixative concentration. J Biomed Mater Res 1996;31:511–518.
16. Sundararaghavan HG, Monteiro GA, Lapin NA, Chabal YJ, Miksan JR, Shreiber DI. Genipin-induced changes in collagen gels: Correlation of mechanical properties to fluorescence. J Biomed Mater Res A 2008;87:308–320.
17. Soltz MA, Ateshian GA. Experimental verification and theoretical prediction of cartilage interstitial fluid pressurization at an impermeable contact interface in confined compression. J Biomech 1998;31:927–934.
18. Kelly TA, Ng KW, Wang CC, Ateshian GA, Hung CT. Spatial and temporal development of chondrocyte-seeded agarose constructs in free-swelling and dynamically loaded cultures. J Biomech 2006;39:1489–1497.
19. Farndale RW, Sayers CA, Barrett AJ. A direct spectrophotometric microassay for sulfated glycosaminoglycans in cartilage cultures. Connect Tissue Res 1982;9:247–248.
20. Farndale RW, Buttle DJ, Barrett AJ. Improved quantitation and discrimination of sulphated glycosaminoglycans by use of dimethylmethylene blue. Biochim Biophys Acta 1986;883:173–177.
21. Stegemann H, Stalder K. Determination of hydroxyproline. Clin Chim Acta 1967;18:267–273.
22. Chen CN, Sung HW, Liang HF, Chang WH. Feasibility study using a natural compound (reuterin) produced by *Lactobacillus reuteri* in sterilizing and crosslinking biological tissues. J Biomed Mater Res 2002;61:360–369.
23. Sung HW, Chen CN, Chang Y, Liang HF. Biocompatibility study of biological tissues fixed by a natural compound (reuterin) produced by *Lactobacillus reuteri*. Biomaterials 2002;23:3203–3214.
24. Lima EG, Tan AR, Tai T, Bian L, Stoker AM, Ateshian GA, Cook JL, Hung CT. Differences in interleukin-1 response between engineered and native cartilage. Tissue Eng 2008;14:1721–1730.

25. Bian L, Lima EG, Angione SL, Ng KW, Williams DY, Xu D, Stoker AM, Cook JL, Ateshian GA, Hung CT. Mechanical and biochemical characterization of cartilage explants in serum-free culture. J Biomech 2008;41:1153–1159.
26. Streilein JW, Stein-Streilein J. Does innate immune privilege exist? J Leukoc Biol 2000;67:479–487.
27. Garrett JC, Steensen RN. Meniscal transplantation in the human knee: A preliminary report. Arthroscopy 1991;7:57–62.
28. Rodeo SA, Seneviratne A, Suzuki K, Felker K, Wickiewicz TL, Warren RF. Histological analysis of human meniscal allografts. A preliminary report. J Bone Joint Surg Am 2000;82A: 1071–1082.
29. Lynn AK, Yannas IV, Bonfield W. Antigenicity and immunogenicity of collagen. J Biomed Mater Res B Appl Biomater 2004;71:343–354.
30. Galili U, LaTemple DC, Walgenbach AW, Stone KR. Porcine and bovine cartilage transplants in cynomolgus monkey. II. Changes in anti-Gal response during chronic rejection. Transplantation 1997;63:646–651.
31. Stone KR, Walgenbach AW, Abrams JT, Nelson J, Gillett N, Galili U. Porcine and bovine cartilage transplants in cynomolgus monkey. I. A model for chronic xenograft rejection. Transplantation 1997;63:640–645.
32. Arnoczky SP. The biology of allograft incorporation. J Knee Surg 2006;19:207–214.
33. Murayama Y, Satoh S, Oka T, Imanishi J, Noishiki Y. Reduction of the antigenicity and immunogenicity of xenografts by a new cross-linking reagent. ASAIO Trans 1988;34:546–549.
34. Paul RG, Bailey AJ. Chemical stabilisation of collagen as a biomimetic. Scientific World J 2003;3:138–155.
35. Lotz M. Cytokines in cartilage injury and repair. Clin Orthop Relat Res 2001(391, Suppl):S108–S115.
36. Schiff MH. Role of interleukin 1 and interleukin 1 receptor antagonist in the mediation of rheumatoid arthritis. Ann Rheum Dis 2000;59(Suppl 1):i103–i108.
37. Smeets TJ, Barg EC, Kraan MC, Smith MD, Breedveld FC, Tak PP. Analysis of the cell infiltrate and expression of proinflammatory cytokines and matrix metalloproteinases in arthroscopic synovial biopsies: Comparison with synovial samples from patients with end stage, destructive rheumatoid arthritis. Ann Rheum Dis 2003;62:635–638.
38. van den Berg WB, Bresnihan B. Pathogenesis of joint damage in rheumatoid arthritis: Evidence of a dominant role for interleukin-I. Baillieres Best Pract Res Clin Rheumatol 1999;13:577–597.

Appendix B

Thesis Publications

B.1 Full Length Manuscripts

Lima EG, Tan AR, Tai T, Bian L, Stoker AM, Ateshian GA, Cook JL, Hung CT, "Differences in Interleukin-1 Response between Engineered and Native Cartilage." Tissue Eng Part A, 2008. 14(10): p. 1721-30.

Lima EG, Tan AR, Tai T, Bian L, Ateshian GA, Cook JL, Hung CT. "Physiologic deformational loading does not counteract the catabolic effects of interleukin-1 in long-term culture of chondrocyte-seeded agarose constructs." J Biomech, 2008. 41(15): p. 3253-9.

Lima EG, Tan AR, Tai T, Marra KG, Defail A, Ateshian GA, Hung CT. "Genipin enhances the mechanical properties of tissue-engineered cartilage and protects against inflammatory degradation when used as a medium supplement." J Biomed Mater Res A, 2009. 91(3): p. 692-700.

Tan AR, Dong EY, Ateshian GA, Hung CT. "Response of engineered cartilage to mechanical insult depends on construct maturity." Osteoarthritis Cartilage, 2010. 18(12): p. 1577-85.

Tan AR, Dong EY, Andry JP, Ateshian GA, Hung CT. "Co-Culture of Engineered Cartilage With Primary Chondrocytes Induces Expedited Growth." Clin Orthop Relat Res, 2011. 469(10): p. 2735-43.

Jayabalan P, Tan AR, Rahaman MN, Bal BS, Hung CT, Cook JL. "Bioactive Glass 13-93 as a Subchondral Substrate for Tissue-engineered Osteochondral Constructs: A Pilot Study." Clin Orthop Relat Res, 2011. 469(10): p. 2754-63.

Tan AR, Alegre-Aguaron E, O'Connell GD, VandenBerg CD, Aaron RK, Vunjak-Novakovic G, Bulinski JC, Ateshian GA, Hung CT. "Passage-Dependent Relationship between Mesenchymal

Stem Cell Mobilization and Chondrogenic Potential." *Submitted to Osteoarthritis and Rheumatism.*

O'Connell GD*, Tan AR*, Cui V, Bulinski JC, Attur M, Abramson SB, Ateshian GA, Hung CT. "Human Chondrocyte Migration Behavior to Guide Biofabrication of Engineered Cartilage." *Submitted to Biofabrication.*

Tan AR, VandenBerg CD, Bulinski JC, Ateshian GA, Cook JL, Hung CT. "Chondroprotective Effects of Cytokine Preconditioning on Engineered Cartilage Response to Interleukin-1." *In preparation.*

Chao PH, Tan AR, Hung CT. "Chondrocyte Migration is Modulated by it's Osmotic Environment." *In preparation.*

B.2 Book Chapters

Tan, A.R. Hung, C.T. (2011). Engineering Functional Cartilage Grafts. In H.S. Bernstein, Tissue Engineering in Regenerative Medicine (p. 237-250). New York: Springer.

B.3 Conference Abstracts

Tan AR, Lima EG, Marra KG, Hung CT: "Genipin protects engineered cartilage against IL-1alpha induced degradation." Proceedings of the 2008 Summer Bioengineering Conference, Marco Island, FL, June 25-29, poster. 3rd place in master's student competition.

Tan AR, Barsi JM, Jayabalan PS, Rahaman MN, Bal BS, Ateshian GA, Cook JL, Hung CT: "Bioactive Glass (13-93) as a Medium Supplement for Culturing Tissue-Engineered Cartilage." 55th Annual Meeting of the Orthopaedic Research Society, Las Vegas, NV, February 22-25, 2009.

Tan AR, Ateshian GA, Hung CT: "Chondrocyte Death in Overloaded Engineered Cartilage Depends on Construct Maturity." 55th Annual Meeting of the Orthopaedic Research Society, Las Vegas, NV, February 22-25, 2009.

Tan AR, Dinh AR, Albro MB, Ateshian GA, Hung CT: "Type IX Agarose Gel Produces Better Tissue Engineered Cartilage Constructs than Type VII Agarose." 55th Annual Meeting of the Orthopaedic Research Society, Las Vegas, NV, February 22-25, 2009.

P. Jayabalan, Tan AR, J.M. Barsi, M.N. Rahaman, B.S. Bal, G.A. Ateshian, C.T. Hung, J.L. Cook: "Bioactive Glass (13-93) as a subchondral substrate and culture media supplement for tissue engineered cartilage." 8th World Congress of the International Cartilage Repair Society, Miami, FL, May 23-26, 2009.

Tan AR, Rajan V, Ateshian GA, Hung CT: "Immediate and Long-Term Response of Engineered Cartilage to Injury." Proceedings of the 2009 Summer Bioengineering Conference, Lake Tahoe, CA, June 17-21, 2009.

Dong EY, Tan AR, Hung CT: "Tissue Engineered Cartilage Exhibits Increased Mechanical and Biochemical Properties When Co-Cultured with a Sub-confluent Chondrocyte Feeder Layer." 2009 Biomedical Engineering Society Annual Meeting, Pittsburgh, PA, October 8-11.

Tan AR, Dong EY, Ateshian GA, Hung CT: "Tissue Engineered Cartilage Growth is Expedited when Co-Cultured with a Chondrocyte Feeder Layer." 56th Annual Meeting of the Orthopaedic Research Society, New Orleans, LA, March 6-9, 2010.

Tan AR, Rajan V, Ateshian GA, Hung CT: "Reparative Capacity of Engineered Cartilage to Overload-Induced Cracking or Cutting Injury in Culture." 56th Annual Meeting of the Orthopaedic Research Society, New Orleans, LA, March 6-9, 2010.

Jayabalan PS, Tan AR, Rahaman MN, Bal BS, Sims HJ, Hung CT, Cook JL: "Bioactive Glass (13-93) as a Subchondral Substrate for Tissue-Engineered Osteochondral Constructs." 56th Annual Meeting of the Orthopaedic Research Society, New Orleans, LA, March 6-9, 2010.

Tan AR, Dong EY, Rho B, Sampat SR, Bulinski, JC, Ateshian GA, Hung CT: "Co-Culture of a Chondrocyte Monolayer with Engineered Cartilage Constructs Immediately Increases Tissue Properties." Proceedings of the 2010 Summer Bioengineering Conference, Naples, FL, June 16-19, 2010.

Gunja N, Fong J, Tan AR, Moy M, Xu D, O'Connell G, Bulinski JC, Ateshian GA, Hung CT: "Priming of Synovium-Derived Mesenchymal Stem Cells for Cartilage Tissue Engineering." Proceedings of the 2010 Summer Bioengineering Conference, Naples, FL, June 16-19, 2010.

Tan AR, Andry JP, Ateshian GA, Hung CT: "Chondrogenic Media (CM) Protects Native and Engineered Cartilage Constructs From Cell Death After Injury." 2010 Congress of International Cartilage Repair Society, Sitges, Spain, September 26-29, 2010.

Tan AR, Andry JP, Bulinski JC, Ateshian GA, Hung CT: "Time-Dependence of Co-Culture Setup for Expedited Tissue Engineered Cartilage Formation." 57th Annual Meeting of the Orthopaedic Research Society, Long Beach, CA, January 13-16, 2011.

Tan AR, Dowling RM, Andry JP, Yeager K, Ateshian GA, Cook JL, Hung CT: "Optimizing Osteochondral Graft Harvesting Techniques to Reduce Cell Death in Surrounding Tissue." 57th Annual Meeting of the Orthopaedic Research Society, Long Beach, CA, January 13-16, 2011.

Tan AR, Oswald ES, Hampilos PJ, Li VJ, Dowling RM, Bulinski JC, Liao JC, Hung CT: "Reprogramming Adult Bovine Chondrocytes for Cartilage Tissue Engineering." 57th Annual Meeting of the Orthopaedic Research Society, Long Beach, CA, January 13-16, 2011.

Jayabalan P, Tan AR, Rahaman MN, Bal BS, Hung CT, Cook JL: "The Relationship Between the Constituents of the Media, Mineralization of Bioactive Glass (13-93) and Chondrocyte

Metabolism in the Tissue Engineering of Cartilage." 57th Annual Meeting of the Orthopaedic Research Society, Long Beach, CA, January 13-16, 2011.

Tan AR, Alegre-Aguaron E, Dujari DN, Sampat SR, Bulinski JC, Ateshian GA, Hung CT: "Effects of Passaging on the Migration Response of Synovium-Derived Stem Cells to an Applied DC Electric Field." Proceedings of the 2011 Summer Bioengineering Conference, Nemacolin, PA, June 22-25, 2011.

Tan AR, Ackerman GP, VandenBerg CD, Dermksian MV, Bulinski JC, Hung CT: "Response of Synovium Derived Stem Cells to an Applied DC Electric Field After Passage with Growth Factors." 58th Annual Meeting of the Orthopaedic Research Society, San Francisco, CA, February 4-7, 2012.

Tan AR, VandenBerg CD, Ateshian GA, Hung CT: "Preexposure of Engineered Cartilage to Interleukin-1α Affords Protection against Subsequent Cytokine Exposure." 58th Annual Meeting of the Orthopaedic Research Society, San Francisco, CA, February 4-7, 2012.

Tan AR, Alegre-Aguaron E, Bulinski JC, Ateshian GA, Hung CT: "Co-Culture of Synovium Derived Stem Cells Induces Cell Migration into Adjacent Wound Sites within Chondrocyte-Seeded Engineered Cartilage." 58th Annual Meeting of the Orthopaedic Research Society, San Francisco, CA, February 4-7, 2012.

Alegre-Aguaron E, Tan AR, Mei A, Cook JL, Ateshian GA, Hung CT: "Strategies for Enhancing Cartilage Properties Using Adult Cells: Cell Seeding Density and Coculture with Synovium Derived Stem Cells." 58th Annual Meeting of the Orthopaedic Research Society, San Francisco, CA, February 4-7, 2012.

Wen SM, Tan AR, Hung CT, Chao PG: "Chondrocyte Migration is Modulated by Osmotic Environment." 58th Annual Meeting of the Orthopaedic Research Society, San Francisco, CA, February 4-7, 2012.

Tan AR, Langford TF, Chao PG, Aaron RK, Bulinski JC, Ateshian GA, Hung CT: "Role of AQP1 Water Channel During Chondrocyte Migration in an Applied DC Electric Field." 59th Annual Meeting of the Orthopaedic Research Society, San Antonio, TX, January 26-29, 2013.

Tan AR, Langford TF, Aaron RK, Bulinski JC, Hung CT: "Response of Staphylococcus Aureus Biofilm to an Applied DC Electric Field." 59th Annual Meeting of the Orthopaedic Research Society, San Antonio, TX, January 26-29, 2013.

Tan AR, Langford TF, Aaron RK, Bulinski JC, Ateshian GA, Hung CT: "Differing Effects of Interleukin-1α on the Response of Chondrocytes and Synovium Derived Stem Cells in Response to an Applied DC Electric Field." 59th Annual Meeting of the Orthopaedic Research Society, San Antonio, TX, January 26-29, 2013.

Roach BL, Tan AR, Stoker AM, Cook JL, Yeager KJ, Ateshian GA, Hung CT: "Fabrication of Tissue-Engineered Cartilage Grafts with Anatomic Surface Contours for Repair of Large Focal

Defects." Proceedings of the 2013 Summer Bioengineering Conference, Sunriver, OR, June 26-29, 2013.

Tan AR, Bulinski JC, Aaron RK, Hung CT: "Upregulation of HIF-1α Enhances Cell Migration Response to Applied DC Electric Field." 60th Annual Meeting of the Orthopaedic Research Society, New Orleans, LA, March 15-18, 2014.

Tan AR, Ateshian GA, Hung CT: "Early Physiologic Dynamic Loading Mitigates Catabolic Glycosaminoglycan Degradation by IL-1α in Tissue Engineered Constructs." 60th Annual Meeting of the Orthopaedic Research Society, New Orleans, LA, March 15-18, 2014.

Appendix C

List of Abbreviations

Cartilage Biology

OA	osteoarthritis
PG	proteoglycan
GAG	glycosaminoglycan
ECM	extracellular matrix
PCM	pericellular matrix
MMP	matrix metalloproteinases
MSC	mesenchymal stem cell
SDSC	synovium-derived stem cell
bMSC	bone marrow-derived stem cell
AQP	aquaporin
HIF	hypoxia-inducible factor

Cytokines and Growth Factors

IL	interleukin
TNF	tumor necrosis factor
TGF	transforming growth factor
FGF	fibroblast growth factor

PDGF	platelet derived growth factor

Medium Components

DMEM	Dulbecco's Modified Eagle's Medium
CM	chondrogenic Medium
FBS	fetal bovine serum